



Selective Oxidation of Alkyl Aromatics by Bimetallic Heterogeneous Catalysts

Thesis submitted in accordance with the requirements of
Cardiff University for the degree of

Doctor of Philosophy

Cicely Giles

March 2018

DECLARATION

This work has not been submitted in substance for any other degree or award at this or any other university or place of learning, nor is being submitted concurrently in candidature for any degree or other award.

Signed (candidate)

Date

STATEMENT 1

This thesis is being submitted in partial fulfilment of the requirements for the degree of Doctor of Philosophy.

Signed (candidate)

Date

STATEMENT 2

This thesis is the result of my own independent work/investigation, except where otherwise stated, and the thesis has not been edited by a third party beyond what is permitted by Cardiff University's Policy on the Use of Third Party Editors by Research Degree Students. Other sources are acknowledged by explicit references. The views expressed are my own.

Signed (candidate)

Date

STATEMENT 3

I hereby give consent for my thesis, if accepted, to be available online in the University's Open Access repository and for inter-library loan, and for the title and summary to be made available to outside organisations.

Signed (candidate)

Date

Acknowledgements

This thesis was made possible by the hard work and effort of many people.

Firstly, I must thank Professor Graham Hutchings and Cardiff University for the opportunity to undertake this PhD, and Professor David Knight and Dr Alison Paul for their advice and support throughout graduate and postgraduate study.

Secondly, I am grateful to my supervisors; Professor Graham Hutchings, Dr Ewa Nowicka, Dr Meenakshisundaram Sankar and Dr James Carter for patient guidance and tutelage throughout this work.

My thanks also go to Dr Chris Morgan and Dr Greg Shaw for their efforts keeping the laboratories running, Dr David Morgan and Simon Waller for their analytical expertise, and Steven Morris, Alun Davies and Lee Wescombe for going above and beyond as technicians.

I owe particular thanks to those who supported me in difficult circumstances. These include my loving family and friends, both from the university and beyond. Special gratitude goes to my parents; to Drs James Hayward, Oliver Burrows, and Keith Bugler; and to Nathan Allen, Ben Brain, Angharad Thomas and Emma Humphries. Thank you for your encouragement, understanding and many shared cups of tea over the years.

Finally, I must thank my husband Roger Glanville, without whom I could never have made it to the end.

Abstract

This thesis reports the selective oxidation of alkyl aromatic substrates under mild 'green' conditions, with a particular emphasis on developing alternatives to established gold-based catalysts. Three alkyl aromatics were chosen for investigation: toluene, ethylbenzene and 2-ethylnaphthalene; so differences due to increased alkyl chain length and extended aromaticity could be explored.

The oxidation of toluene using tertiary-butyl hydroperoxide (tBHP) was carried out with a ruthenium-palladium catalyst. This catalyst was found to be highly active, more so than a gold-palladium equivalent, and further optimised in terms of molar ratio of Ru : Pd, wt.% metal loading, reducing temperature and support material. The resulting catalyst was found to be reusable with little loss of conversion, though selectivity changed significantly. This was the case despite notable metal leaching. Finally, the catalyst was explored via experiments varying substrate : metal molar ratio and time-on-line studies, revealing unusual behaviour.

The ruthenium-palladium catalyst was also applied to the oxidation of 2-ethylnaphthalene with tBHP. Extensive comparisons were drawn between this catalyst and gold-palladium equivalents. Sol immobilisation, conventional impregnation and modified impregnation were tested as preparation methods. Once again, the ruthenium-palladium bimetallic catalyst proved to be more active than the gold-palladium, even at very low wt.% loadings.

Finally, an iron-palladium catalyst was applied to the oxidation of ethylbenzene with molecular oxygen. High molar ratios of substrate : metal were explored, and conversion found to be highly dependent on this factor. The catalyst was optimised in terms of molar ratio of Fe : Pd, wt.% metal loading, preparation method and reducing temperature. The resulting iron-palladium catalyst achieved activity exceeding that of gold-palladium in similar conditions. This activity was attributed to radical chemistry, explored via studies with initiators and scavengers.

Contents

Chapter One – Introduction

1.1.	Catalysis	8
1.2.	Heterogeneous Catalysis	9
1.3.	Catalyst Design and Preparation	12
1.4.	Catalytic Oxidation Reactions	13
1.5.	Oxidation of Alkyl Aromatics	15
1.5.1.	Toluene Oxidation	17
1.5.2.	2-Ethyl-naphthalene Oxidation	23
1.5.3.	Ethylbenzene Oxidation	24
1.5.4.	Summary	32
1.6.	Aims of the Thesis	32
1.6.1.	Toluene Oxidation	33
1.6.2.	2-Ethyl-naphthalene Oxidation	33
1.6.3.	Ethylbenzene Oxidation	33
1.7.	References	34

Chapter Two – Experimental

2.1.	Introduction	38
2.2.	Chemicals	38
2.3.	Definitions	38
2.4.	Methods of Catalyst Preparation	39
2.4.1.	Sol Immobilisation	39
2.4.2.	Impregnation	39
2.4.3.	Modified Impregnation	39
2.5.	Reactors	40
2.5.1.	Radleys multi-pot 'Starfish' reactor	40
2.5.2.	Glass reactors	40
2.5.3.	Autoclave	41
2.6.	Oxidation Reactions	42
2.6.1.	Ethylbenzene oxidation	42

2.6.2.	Toluene oxidation	42
2.6.3.	2-Ethyl-naphthalene oxidation	43
2.7.	Product Analysis	43
2.7.1.	Gas chromatography	43
2.7.2.	Gas chromatography – mass spectrometry	47
2.7.3.	Nuclear magnetic resonance spectroscopy	50
2.8.	Catalyst Characterisation	52
2.8.1.	Microwave-plasma atomic emissions spectroscopy	52
2.8.2.	Inductively coupled plasma atomic emission spectroscopy	53
2.8.3.	Temperature programmed reduction	53
2.8.4.	CO chemisorption	55
2.8.5.	X-ray powder diffraction	56
2.8.6.	X-ray photoelectron spectroscopy	57
2.9.	References	58

Chapter Three – Toluene Oxidation

3.1.	Introduction	60
3.2.	Oxidation reactions in the glass reactor	61
3.2.1.	Blank reactions	61
3.2.2.	Oxidation reactions with AuPd, PtPd and RuPd	62
3.3.	Oxidation reactions in the Radleys reactor	69
3.3.1.	Blank reactions	69
3.3.2.	Oxidation reactions with AuPd, PtPd and RuPd	70
3.3.3.	Comparison of heterogeneous catalyst with catalyst precursors	75
3.3.4.	Comparison RuPd and monometallic Ru and Pd catalysts	78
3.3.5.	Influence of metal molar ratio	80
3.3.6.	Investigating metal leaching	81
3.3.7.	Catalyst reusability	84
3.3.8.	Influence of metal loading	86
3.3.9.	Influence of substrate:metal ratio	89
3.3.10.	Influence of reduction temperature	91
3.3.11.	Influence of support material	92

3.3.12.	Role of tBHP and air	94
3.3.13.	Influence of reaction temperature	97
3.3.14.	Time-on-line studies	98
3.4.	Conclusions	101
3.4.1.	Comparing the glass and Radleys reactors	101
3.4.2.	Catalyst investigation and optimisation	102
3.5.	References	104

Chapter Four – 2-Ethyl-naphthalene Oxidation

4.1.	Introduction	106
4.2.	Oxidation reactions in the Radleys reactor	107
4.2.1.	Blank reactions	107
4.2.2.	Oxidation reactions with RuPd/TiO ₂ and AuPd/TiO ₂	108
4.2.3.	Comparison of activity of bimetallic and monometallic catalysts	112
4.2.4.	Influence of metal molar ratio	116
4.2.5.	Influence of substrate:metal ratio	119
4.2.6.	Influence of tBHP:metal ratio	120
4.2.7.	Influence of tBHP:substrate ratio	124
4.2.8.	Influence of oxidant solvent	125
4.2.9.	Influence of temperature	127
4.3.	Conclusions	128
4.4.	References	130

Chapter Five – Ethylbenzene oxidation

5.1.	Introduction	132
5.2.	Oxidation reactions in the Radleys Reactor	133
5.2.1.	Blank reactions	133
5.2.2.	AuPd catalysts	135
5.2.3.	FePd catalysts	137
5.2.4.	Comparison of bimetallic and monometallic catalysts	141
5.2.5.	Influence of metal molar ratio	143
5.2.6.	Influence of metal loading	147

5.2.7.	Influence of reducing temperature	149
5.2.8.	Influence of preparation method and catalyst precursors	153
5.2.9.	Influence of radical initiators	159
5.2.10.	Influence of radical scavengers	162
5.3.	Conclusions	166
5.4.	References	167
Chapter Six – Conclusions		
6.1.	Conclusions	169
6.1.1.	1 wt.% Ru _{0.50} Pd _{0.50} / TiO ₂	169
6.1.2.	1 wt.% Fe _{0.35} Pd _{0.65} / TiO ₂	172
6.2.	Future work	173
6.2.1.	1 wt.% Ru _{0.50} Pd _{0.50} / TiO ₂	173
6.2.2.	1 wt.% Fe _{0.35} Pd _{0.65} / TiO ₂	174
6.3.	References	175

Chapter One – Introduction

1.1. Catalysis

Catalytic reactions have been known throughout human history, but the term ‘catalysis’ was first defined by Berzelius in 1835^{1,2}. Recognising that solid platinum accelerated the decomposition of hydrogen peroxide but was itself unchanged by the process, he dubbed platinum a ‘catalyst’. Since this time, catalysis has grown into a vast area of study, and the definition of a catalyst widely discussed³⁻⁶. Today, the *Oxford English Dictionary* defines a catalyst as a “substance that increases the rate of a chemical reaction without itself undergoing any permanent chemical change”⁷.

A catalyst achieves this increase in rate by providing an alternative, less energetically demanding reaction pathway. The catalyst stabilises reaction intermediates or transition states, and therefore decreases the activation energy required for reaction. A greater proportion of the available reactants meet the lower energy barrier, and the net result is an increase in rate. Therefore a catalyst influences the reaction kinetics, but the thermodynamics of the process are unchanged.

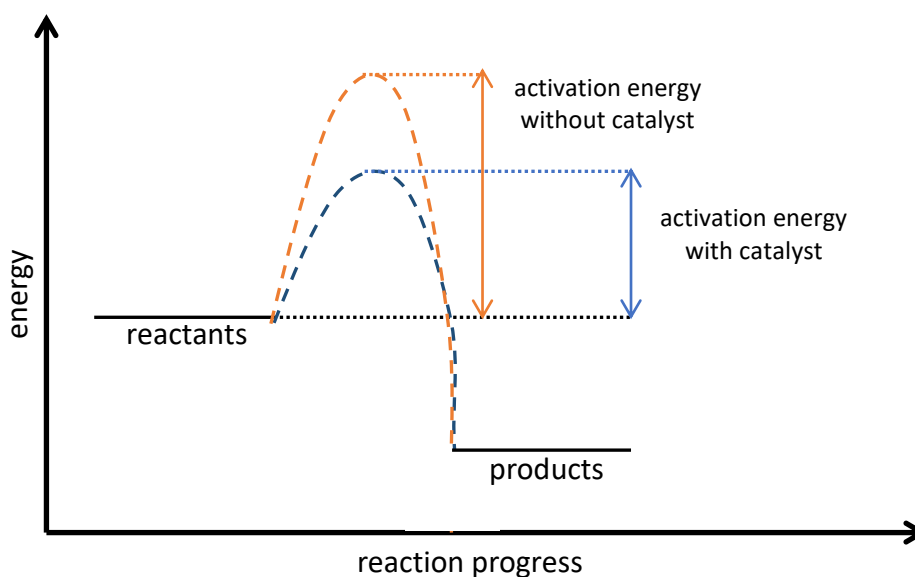


Figure 1. Energy profile of a reaction with and without catalyst

All catalysts operate according to this basic principle. There are three main classes: homogenous, heterogeneous and enzymatic.

Homogeneous catalysts exist in the same state as the reactants. For example, the manufacture of ethylene glycol from water and epoxyethane takes place in aqueous media, catalysed by sulphuric acid^{8,9}. Homogeneous catalysts often exhibit very high activity; however, it can be difficult and expensive to remove them from the reactant and product mixture after the reaction. This is particularly important when the catalyst itself is costly or contains toxic or environmentally harmful materials such as heavy metals^{10,11}.

Heterogeneous catalysts are in a different state or phase to the reactants. For instance, a solid catalyst may operate on liquid or gaseous chemicals. Heterogeneous catalysts are therefore usually much easier to separate from the reaction mixture than homogeneous catalysts. This helps prevent catalyst loss and removes the need for expensive and complex separation procedures. Once separated, the heterogeneous catalyst can be regenerated, if necessary, and used again. Examples of heterogeneous catalysts used in industry include the porous iron-based catalyst used in the Haber-Bosch process for synthesis of ammonia^{12,13}, and the nickel catalysts used in the manufacture of synthesis gas from carbon dioxide and hydrogen¹⁴.

Enzymatic catalysis is a form of biological catalysis upon which all living things depend. Enzymes are biological molecules that frequently exhibit extremely high selectivity to specific substrates and products; often exceeding anything that can be achieved in a laboratory. In most cases (excluding enzymes found in extremophiles or modified in the laboratory) enzymes operate in the mild conditions typical of living cells. However, this can be limiting, and it is difficult to use enzymatic catalysis at the scale and under the conditions required for industrial processes.

1.2. Heterogeneous catalysis

Heterogeneous catalysis offers significant advantages over homogeneous or enzymatic catalysis. Principally, there is the ease of catalyst recovery. This is

essential so the catalyst can be reused, and to prevent contamination of products. It also helps to prevent loss of catalyst, which is often expensive, and would in turn lead to loss of productivity.

Heterogeneous catalysts also offer high 'tunability'. This means catalysts can be tailored to particular reactions, conditions, products and even reactors. Optimising the catalyst to suit specific circumstances can result in very high activity and selectivity.

Heterogeneous catalytic reactions take place at the phase boundary. In the majority of cases, this boundary is the interface between a solid catalyst and liquid or gaseous reactants, and so the surface of the catalyst plays a crucial role in its activity. Understanding the nature of the surface *via* proper characterisation can provide important insights into the associated reaction mechanism. There are various models for this; most significantly the Langmuir-Hinshelwood¹⁵, Eley-Rideal¹⁶ and Mars-van-Krevelen mechanisms^{17,18}.

The Langmuir-Hinshelwood mechanism (illustrated in **Figure 2**) operates when two or more reactants adsorb to the surface of the catalyst; bringing them into proximity with each other *via* surface diffusion. Adsorbing to the surface may also weaken or break bonds within the molecules, or force them to adopt particular conformations. The adsorbed species then react with one another to form the product or products, which desorb from the catalyst surface, leaving it available for more reactant molecules.

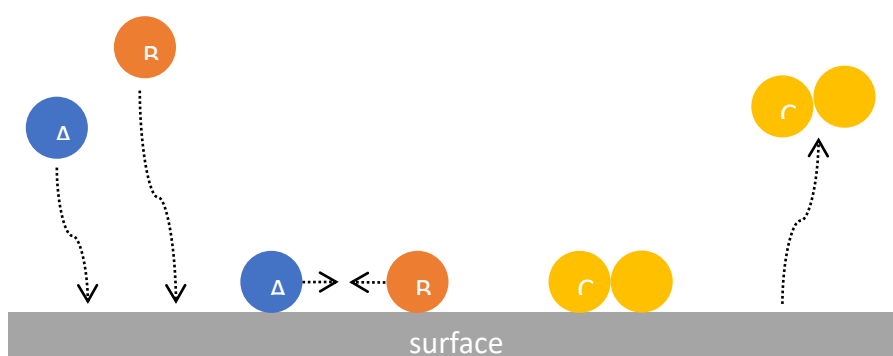


Figure 2. Langmuir-Hinshelwood mechanism

The Eley-Rideal mechanism (**Figure 3**) proceeds with one of the required reactants adsorbing to the catalyst surface. As before, this may weaken bonds within the molecule, or promote a specific conformation. The other reactant or reactants interact with this component without themselves being adsorbed to the catalyst. The resulting product then desorbs, allowing further reactants to adsorb.

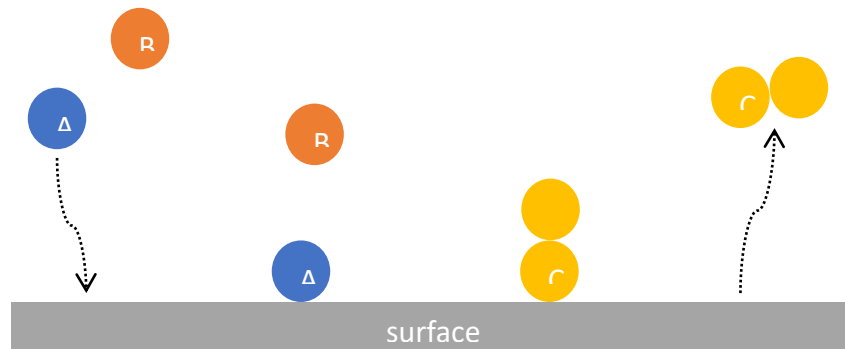


Figure 3. Eley-Rideal mechanism

The Mars-van-Krevelen mechanism (**Figure 4**) involves the catalyst more intimately. In this case, the reactant interacts with the surface of the catalyst directly; for instance with lattice oxygen. This forms the product species, which desorbs. Post-reaction, any vacancies left in the catalyst surface must be refilled to maintain catalyst activity. This may occur by diffusion of gas from the bulk of the catalyst to the surface, or by treating the surface with gas. Carbon monoxide oxidation by gold supported on ZnO surfaces is thought to occur *via* a Mars-van-Krevelen mechanism¹⁹.

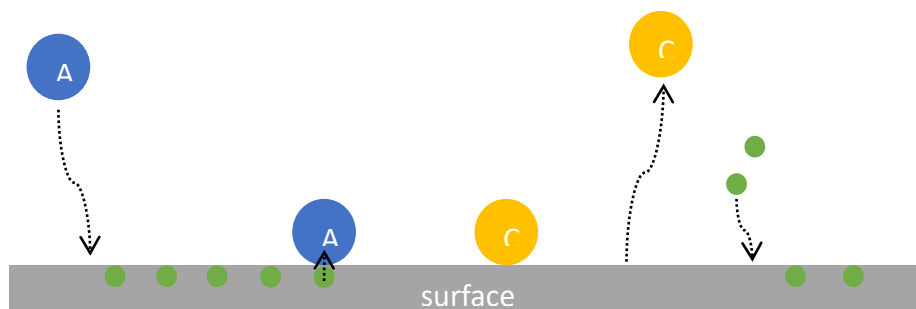


Figure 4. Mars-van-Krevelen mechanism

Understanding the mechanism or combination of mechanisms a heterogeneous catalyst operates by can help inform the design process.

1.3. Catalyst design and preparation

As briefly discussed in section 1.2., heterogeneous catalysts offer the advantage of high ‘tunability’: a huge number of factors can be adjusted and manipulated to improve performance and durability or reduce cost. The sheer variation possible allows catalysts to be designed and prepared to meet the particular requirements of the reaction and application.

This work focusses chiefly on supported metal-nanoparticle catalysts. These have a long history of study and vary widely. The choice of an appropriate metal or metals is the first step in the process, and different metals or groups of metals are favoured for different types of reaction. For instance, gold is well-established for selective oxidation reactions^{20, 21}, and platinum and palladium are used as oxidation catalysts in catalytic converters^{22,23}.

A combination of two or more metals in the same catalyst can modify its properties^{24,25}. Alloying changes the electronic structure of the particle²⁶, and can result in effects such as improved stability and reduced sintering. The metals do not necessarily have to form an alloy to produce an effect, however. Addition of another metal to the catalyst may produce changes to the surface or active site that promote reactivity or selectivity in a similar manner to a dopant. For example, it has recently been reported that Co_3O_4 nanorods doped with indium are far more active for CO oxidation than their non-doped counterparts²⁷. Core-shell structures of different compositions may lead to differences in product distribution, stability and activity^{28,29, 30}.

The selection of an appropriate support material is equally as important as the choice of metal. Notable support materials include metal oxides such as TiO_2 , zeolites including ZSM-5, and the cordierite monolith used in catalytic converters²². A suitable support must not only be stable under the required working conditions for long periods; it must also be rendered into a form appropriate for use; for

example as a mesh or pellets, and it cannot be so costly as to make the resulting catalyst unmarketable.

Furthermore, the nature of the support influences or dictates key properties of the catalyst such as thermal stability, surface area, porosity and the morphology of metal nanoparticles. Metal-support interactions can have profound effects on the electronic structure of the nanoparticle, and consequently their reactivity³¹. In some cases, the structure of the support material also plays a significant role in selectivity. For example, the pore and channel sizes of a zeolite may determine the shape of the product, such as in the isomerisation of alkanes³².

The choice of support must also be considered in conjunction with preparation method. Certain supports may necessitate or disallow certain procedures or processes. The preparation method and choice of precursors used will also influence catalyst activity. For instance, impregnation methods that differ in apparently only minor ways may generate nanoparticles of an entirely different average size, or composition^{33,34}. Any pre-treatment procedures, such as reduction or calcination, may also have significant consequences for the activity of the resulting catalyst³⁵.

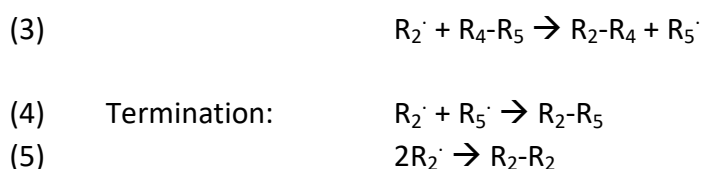
1.4. Catalytic oxidation reactions

In 1991, R. A. Sheldon described three mechanisms of oxidation³⁶⁻³⁸:

- i) Auto-oxidation by a free radical chain reaction.
- ii) Oxidation of substrate coordinated to a metal ion and subsequent re-oxidation of the reduced metal.
- iii) Catalytic transfer of oxygen.

The first case, auto-oxidation by a free-radical chain reaction, is not a catalytic process. This mechanism can be split into three stages; initiation, propagation and termination; as described by the equations below.





In the initiation step, homolytic cleavage of substrate or a radical initiator produces a free radical species. This radical species undergoes subsequent reactions with more substrate or initiator, producing further radicals which allow the reaction to propagate. When oxidative radicals form, an oxidation reaction occurs.

While the auto-oxidation mechanism is not in itself catalytic, the formation of radicals by homolytic cleavage can be catalysed with appropriate radical initiators. Many radical initiators, such as alkyl peroxides, are oxygen sources. Oxygen can also be incorporated from sacrificial oxidants or even O_2 in the atmosphere. The exact nature of the process is determined by the species present.

The second mechanism requires the presence of a metal species that is oxidised, then oxidises the substrate and is thus reduced, ready to repeat the cycle again. Homogeneous palladium-catalysed oxidation of alkanes with hydrogen peroxide as oxidant³⁹ is a good example of this, as described in **Figure 5**.

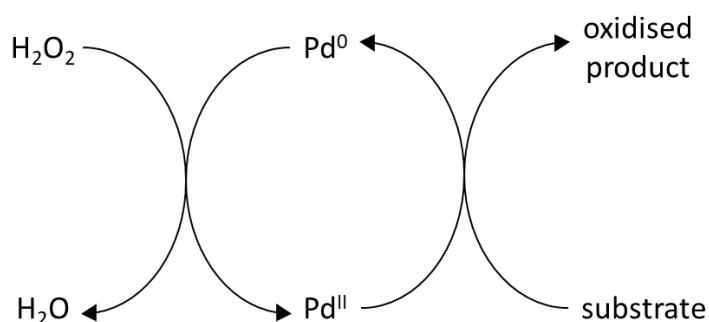


Figure 5. Catalytic cycle of Pd-catalysed oxidation of alkane with H_2O_2

The catalytic transfer of oxygen involves the transfer of oxygen atoms from one part of a molecule to another via interaction with a catalyst. Reactions of this type can be used to carry out cyclisation and alkyne group functionalisation, and has

been reported for gold, iridium, rhodium and ruthenium based catalysts among others⁴⁰.

In the third case, oxygen is sourced from the substrate. In the case of the other two mechanisms, an external source of oxygen is required to form products such as alcohols, aldehydes, ketones or carboxylic acids. Traditionally, this was usually a sacrificial oxidant, such as KMnO_4 . Oxidants of this kind have significant disadvantages. They are frequently extremely harmful to the environment, necessitating extensive and complex clean-up processes. They are also often toxic and expensive. As such, the use of more benign oxidants is increasingly preferred.

Perhaps the most obvious choice for an eco-friendly oxidant is oxygen gas itself. However, it can be difficult to utilise in this form, due to the triplet ground state and high bond strength. Noble metal catalysts, such as those based on Au, Pd and Pt, are notable for their ability to use O_2 as oxidant.

Peroxides provide a good alternative to O_2 gas, being both oxygen-rich and reactive, without the heavy metal content of historical oxidants. They are readily available. However, peroxides require careful handling, being both flammable and explosive. Alkyl peroxides such as tertiary-butylhydrogenperoxide are typically less hazardous than the more widely used hydrogen peroxide. Established catalytic oxidation reactions utilising peroxides include procedures for treating waste-water⁴¹.

1.5. Oxidation of alkyl aromatics

The alkyl aromatics are a broad family of chemicals. Many alkyl aromatics can be obtained as by-products of the petrochemical industry, and are therefore both abundant and relatively cheap. As such, they are an attractive feedstock⁴². Partial oxidation of alkyl aromatics can produce versatile activated compounds with applications in the pharmaceutical, agricultural and fine chemical industries.

However, partial oxidation is particularly challenging. There are several reasons for this, and the problem is both thermodynamic and kinetic.

Like the alkanes, alkyl aromatics are stable and unreactive. This is because reaction requires cleavage of strong C-H bonds. The strength of this bond varies depending on its location and environment. A C-H bond on a CH₂ group in the alkyl chain portion of an alkyl aromatic may have a bond strength of around 411 kJmol⁻¹. C-H bonds in a CH₃ group have a higher bond strength of around 423 kJmol⁻¹, making oxidation at the terminal position particularly difficult. The strength of C-H bonds on the aromatic portion of the molecule will vary slightly according to their position relative to the alkyl chain and any adjoining rings. For instance, in naphthalene the C-H bonds on alpha carbons have a bond strength of approximately 465 kJmol⁻¹, and C-H bonds on the beta carbons have a bond strength of approximately 464 kJmol⁻¹.

The energetic demands for cleaving these bonds can be met by increasing reaction temperature, but that often leads to a significant loss in selectivity. Once activated, the bond is susceptible to further oxidation, as this is thermodynamically favourable. Products can be over-oxidised. Complete combustion leads to CO₂ and water, and therefore loss of yield.

As described in section 1.1, a catalyst does not influence the thermodynamics of a reaction, only its kinetics. Therefore the presence of a catalyst cannot make complete combustion less thermodynamically favourable, but could, for example, facilitate a reaction at a lower temperature, at which the rate of over-oxidation is lower. A catalyst that allows the partially oxidised product to desorb prior to any further oxidation would be ideal. Even so, it may still be necessary to restrict conversion to ensure high selectivity.

Reaction selectivity may also be subject to steric hindrance; especially when dealing with a polyaromatic or branched alkyl chain.

This work will focus on the oxidation of three model alkyl aromatics: toluene, 2-ethylnaphthalene and ethylbenzene.

1.5.1. Toluene oxidation

Toluene is the simplest alkyl aromatic, and an industrially significant chemical in its own right, particularly as a fuel additive and a precursor to benzene. Toluene is typically produced from fuel sources by the petrochemical industry.

Toluene can be partially oxidised to a number of value-added products, most significantly benzyl alcohol, benzaldehyde, benzoic acid and benzyl benzoate, as shown in **Figure 6**. These compounds are widely used in paints, varnishes, dyes, cosmetics, perfumes, flame retardants and pharmaceuticals.

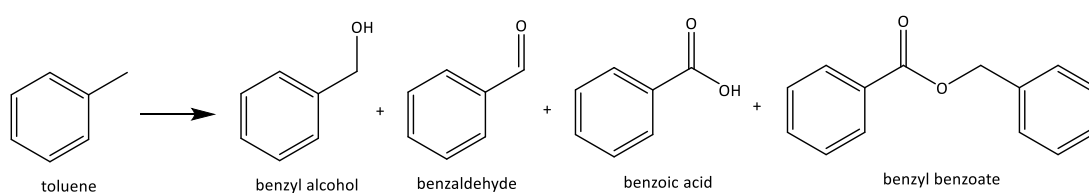


Figure 6. Toluene oxidation scheme

Currently, these partially oxidised products are produced using homogeneous processes with restricted conversions. For example, benzoic acid is produced from toluene using homogeneous cobalt salts and air as an oxidant⁴⁴. In the Snia-Viscosa process, this reaction takes place at 165 °C under 10.13 bar air, in aqueous acetic acid and in the presence of bromide as a promoter⁴⁵. These conditions result in 15% conversion of toluene with 90% selectivity to benzoic acid, which can then be separated from the reaction mixture *via* fractional distillation⁴⁶. However, the acidic media and bromide species present causes damage to the reaction vessel over time. The Dow and Rhodia processes for toluene oxidation to benzoic acid utilise similar conditions, with similar drawbacks⁴⁷.

J.A. Alonso *et al.*⁴⁸ achieved high conversion of toluene to benzoic acid using a heterogeneous catalyst. An oxygen-deficient perovskite was used in conjunction with n-hydroxyphthalimide, known as NHPI, as a means of producing carbon-based radicals⁴⁹. Under acidic conditions, the perovskite (La,Sr)_{0.5}(Mn,Co)_{0.5}O_{3-δ} activates the NHPI, and when supplied with 20 bar O₂ at 90 °C for 3 h, 99.7% conversion of toluene was achieved, with 98% selectivity to benzoic acid and 2% selectivity to

benzaldehyde. The same system was applied to ethylbenzene oxidation, and will be discussed in section 1.5.3. Unfortunately, the reaction was not tested in other solvents, so it is unclear how active the system would be in non-acidic conditions.

The heterogeneous commercial catalyst EnviroCAT EPAC can be used for toluene oxidation to benzoic acid⁵⁰ but requires a promoter. The reaction is promoted by catalytic amounts of trimethylacetic acid but occurs in solvent-free conditions in refluxing toluene over 22 h with O₂ supplied at 400 mL/min. After 22 h, typical yields of benzoic acid reached 85%. The authors note that the reaction seemed to proceed through oxidation of toluene to benzyl alcohol, subsequent oxidation of benzyl alcohol to benzaldehyde and finally oxidation of benzaldehyde to benzoic acid. This suggests that increasing reaction times could increase yields of benzoic acid but decrease yields of other products.

Sadiq and Ilyas⁵¹ developed another solvent-free system for heterogeneous toluene oxidation that does not require acid promotion. A ~1 wt.% Pt/ZrO₂ catalyst was prepared *via* the incipient wetness technique. This catalyst was then stirred with toluene at a range of temperatures with O₂ bubbled through as oxidant. The products formed varied with reaction time and temperature. When the experiment was run for under 3 h, benzoic acid, benzyl alcohol and benzaldehyde were observed, with benzoic acid being the major product. At reaction times of greater than 3 h, benzoic acid was still the major product, with over 60% selectivity, but the other products were benzaldehyde, benzyl benzoate, trans-stilbene and methyl biphenyl carboxylic acid. This supports the theory that benzyl alcohol and benzaldehyde are ultimately converted to benzoic acid. The effect of changing the temperature of this reaction is shown in **Table 1**.

Table 1. Oxidation of toluene with Pt/ZrO₂ at different reaction temperatures⁵¹

Temperature (°C)	Conversion (%)	Selectivity (%)		
		<i>Benzyl alcohol</i>	<i>Benzaldehyde</i>	<i>Benzoic acid</i>
60	9.6	45.8	17.7	24.0
70	15.4	22.1	18.2	53.9
80	23.9	12.1	21.8	62.3
90	37.2	6.5	19.6	70.4

Reaction conditions: 0.2 g 1 wt.% Pt/ZrO₂, 10 mL toluene, 40 mL/min O₂ flow.

These results clearly demonstrate one of the chief challenges of selective toluene oxidation. Increasing reaction temperature improves conversion, but also increases selectivity to benzoic acid. This is reflected in the reactions discussed previously, which achieve high conversion and form benzoic acid almost exclusively. Therefore selectively forming benzyl alcohol or benzaldehyde may require restricted conversions.

This was observed for a homogeneous catalyst by Seddon and Stark⁵². The authors utilised two catalysts, one cobalt-based and the other palladium-based, to carry out reactions in ionic liquid at 80 °C and under 10.13 bar O₂ pressure for 48 h. Using the Pd-based catalyst, 4.5% yield of benzyl alcohol and 1% yield of benzaldehyde was observed. Using the Co-based catalyst in otherwise similar conditions, a maximum 4.7% yield of benzaldehyde was achieved. The authors note that the use of ionic liquids (in this case [C₄dmim][BF₄] or [C₄mim][BF₄]) as a solvent appears to protect the benzaldehyde from further oxidation.

Cobalt has also been used as a homogeneous catalyst for toluene oxidation in the form of cobalt tetraphenylporphyrin, with some success⁴⁷.

Tilley *et al.*⁵³ successfully 'heterogenized' a cobalt catalyst for selective toluene oxidation to benzaldehyde. A cobalt complex was immobilised on the surface of SBA-15 to produce CoSBA-15 as catalyst. This was used with toluene in acetonitrile as the solvent for 24 h at 80 °C in the presence of a large excess of TBHP. The authors suspected that the catalyst generates free radical species from TBHP that then carry out the reaction. This results in 7.97% conversion of toluene with 63.8% selectivity to benzaldehyde. This catalyst was also explored for ethylbenzene oxidation and will be discussed further in section 1.5.3.

The success of cobalt as a catalyst for toluene oxidation caused Xu *et al.*⁴⁵ to investigate it as a nanoparticle catalyst supported on γ -Al₂O₃. Initial results revealed that Co/ γ -Al₂O₃ was selective to benzaldehyde and benzyl alcohol, with selectivities of 77.8% and 20.6% respectively, but conversion was low at 2%. An equivalent Cu/ γ -Al₂O₃ catalyst provided a slightly improved conversion of 2.5% and 85.7% and

13.0% selectivity to the same two products, prompting the investigators to examine bimetallic copper-based catalysts. Some of these results are reproduced in **Table 2**.

Table 2. Oxidation of toluene with γ -Al₂O₃ supported Cu-based bimetallic catalysts⁴⁵

Catalyst	Conversion (%)	Selectivity (%)			
		<i>Benzyl alcohol</i>	<i>Benzaldehyde</i>	<i>Benzoic acid</i>	<i>Other</i>
CuCo	0.7	36.7	12.4	29.9	21.0
CuZn	1.1	13.4	86.6	0	0
CuMn	1.9	19.1	74.9	3.2	2.8
CuFe	7.4	23.8	45.6	27.1	3.5

Reaction conditions: 50 mL toluene, 1.0 g catalyst, 190 °C, 10 bar O₂, 2 h. 10 wt.% metal catalysts, molar ratio Cu:other metal = 1:0.3.

Table 2 clearly demonstrates that the species of the second metal in the catalyst can have a significant effect on its activity. Of the bimetallic catalysts tested, only the 10 wt.% Cu₁Fe_{0.3}/γ-Al₂O₃ catalyst improves on the activity of the monometallic. It is, however, not the most selective to benzaldehyde: 10 wt.% Cu₁Zn_{0.3}/γ-Al₂O₃ exhibits the highest selectivity at 86.6%, and very low conversion of 2%. However, the authors were able to improve the selectivity to benzaldehyde of the Fe containing catalyst by adding pyridine to the system. When supplied in a toluene:pyridine molar ratio of 100:1, selectivity to benzaldehyde was increased from 45.6% to 85.9% without changing conversion. The authors attribute this to pyridine adsorbing to surface sites more strongly than benzaldehyde, effectively assisting with removing benzaldehyde from the catalyst before further oxidation takes place.

The catalyst developed by Xu *et al.*⁴⁵ is significant because it avoids the use of the platinum group metals, or PGMs, in favour of cheaper alternatives. For some reactions, gold is also a viable alternative, despite its expense, as typically only small quantities are needed. Gold nanoparticle catalysts are particularly well known due to their high activity in a range of redox reactions and especially notable for their ability to utilise O₂ as an oxidant⁵⁴⁻⁵⁶. AuPd nanoparticles in particular have been shown to be active for oxidation, as widely explored for a number of primary alcohols^{28,57}.

Goumin *et al.*⁵⁸ applied a monometallic Au catalyst to toluene oxidation. After 8 h reaction at 160 °C under 10 bar O₂, the Au/ γ -MnO₂ catalyst achieved 13.5% conversion and 64.1% selectivity to benzaldehyde. Other products were small amounts of benzyl alcohol (3.5% selectivity), benzoic acid (16.8%) and benzyl benzoate (15.6%). α -MnO₂ and δ -MnO₂ supported catalysts were found to be less effective. Activity was found to increase with decreasing particle size. The relationship between gold nanoparticle size and activity is well known^{54, 56}.

Li *et al.*⁵⁹ achieved high selectivity to benzaldehyde using a AuPd bimetallic catalyst. 1 wt.% AuPd/MIL-101 was prepared using a sol-gel method with a 1.4:1 Au:Pd ratio. Oxidation was carried out in acetonitrile for 4 h at 150 °C, under 10 bar O₂. This resulted in only 4% conversion of toluene but a remarkable 95.2% selectivity to benzaldehyde. This catalyst was also applied to ethylbenzene oxidation, as discussed in section 1.5.3.

AuPd bimetallic nanoparticles supported on carbon and titania have been extensively investigated by Hutchings' group⁶⁰ and compared with monometallic equivalents. The 1 wt.% catalysts were prepared in a range of different molar ratios using the sol immobilisation method. Testing was carried out in an autoclave reactor for 7 h or 48 h, under 10 bar O₂ and at a range of temperatures. A selection of the results are reproduced in **Tables 3, 4 and 5**.

Table 3. Oxidation of toluene by 1 wt.% metal catalysts⁶⁰

Catalyst	Au:Pd ratio	Conversion (%)	Selectivity (%)			
			<i>Benzyl alcohol</i>	<i>Benzaldehyde</i>	<i>Benzoic acid</i>	<i>Benzyl benzoate</i>
Au/C	1:0	0.2	9.0	81.9	0.0	8.1
Pd/C	0:1	1.6	3.9	56.4	3.3	36.4
AuPd/C	7:1	0.3	28.4	57.6	6.2	7.8
AuPd/C	3:1	1.5	1.8	63.4	3.1	31.4
AuPd/C	1:1.85	4.8	0.9	12.7	10.3	76.1
AuPd/C	1:2	5.3	1.2	8.3	11.1	79.3
AuPd/C	1:3	5.2	1.9	8.5	10.3	79.3
AuPd/C	1:7	4.3	9.6	13.6	7.3	69.5

Reaction conditions: 20 mL toluene, 6500:1 substrate:metal molar ratio, 160 °C, 10 bar O₂, 7 h, 1500 rpm stirring.

In **Table 3**, a very clear relationship between conversion and selectivity was observed. The monometallic catalysts and AuPd catalysts with more Au than Pd content were selective to benzaldehyde. For each of these catalysts, conversion after 7 h was extremely low, at <2%. When conversion exceeds 2% there is a very noticeable decrease in selectivity to benzaldehyde and benzyl alcohol and increase in selectivity to benzyl benzoate, which forms from the other products *via* a condensation reaction. This appears to be more likely when the proportion of Pd present exceeds the proportion of Au.

Longer reaction times also favour a shift towards benzyl benzoate as product, but allow for far greater conversions, as seen in **Table 4**. This is somewhat similar to the trend observed for benzoic acid discussed earlier.

Table 4. Oxidation of toluene by 1 wt.% metal catalysts⁶⁰

Catalyst	Time (h)	Conversion (%)	Selectivity (%)			
			<i>Benzyl alcohol</i>	<i>Benzaldehyde</i>	<i>Benzoic acid</i>	<i>Benzyl benzoate</i>
AuPd/C	7	4.8	0.9	12.7	10.3	76.1
AuPd/C	48	50.8	0.1	1.1	4.5	94.3
AuPd/TiO ₂	7	2.1	2.9	6.6	1.0	89.5
AuPd/TiO ₂	7	2.2	2.2	6.5	2.3	89.0
AuPd/TiO ₂	48	24.1	0.5	1.2	2.8	95.5

Reaction conditions: 20 mL toluene, 6500:1 substrate:metal molar ratio, 1:1.85 molar ratio Au:Pd, 160 °C, 10 bar O₂, 1500 rpm stirring.

Similarly, increasing temperature leads to an increase in conversion and decreasing selectivity to benzyl alcohol and benzaldehyde in favour of benzyl benzoate. This is shown in **Table 5**.

Table 5. Oxidation of toluene by 1 wt.% metal catalysts⁶⁰

Catalyst	Temp. (°C)	Conversion (%)	Selectivity (%)			
			<i>Benzyl alcohol</i>	<i>Benzaldehyde</i>	<i>Benzoic acid</i>	<i>Benzyl benzoate</i>
AuPd/C	80	0.9	8.6	34.2	0.1	57.2
AuPd/C	120	10.6	0.2	7.1	13.1	79.7
AuPd/C	160	50.8	0.1	1.1	4.5	94.3
AuPd/TiO ₂	120	4.0	1.1	6.0	4.8	88.1
AuPd/TiO ₂	160	24.1	0.5	1.2	2.8	95.5

Reaction conditions: 20 mL toluene, 6500:1 substrate:metal molar ratio, 1:1.85 molar ratio Au:Pd, 48 h, 10 bar O₂, 1500 rpm stirring.

Throughout the investigation, catalysts supported on TiO₂ displayed approximately half the activity of equivalent catalysts supported on C. Despite this, it displays slightly increased selectivity to benzyl benzoate as product. This is potentially related to the acidity of the support, the stabilisation of intermediates or radicals.

It has been established that in some forms, carbon itself can be catalytic⁶¹. This has fuelled investigation of graphene and carbon-nanotubes as catalysts and catalyst supports^{62, 63}. Ma *et al.*⁶⁴ investigated what they call 'Layered Carbon' as a catalyst for oxidation of a variety of alkyl aromatic oxidations, including toluene, 2-ethylnaphthalene (discussed in section 1.5.2.) and ethylbenzene (discussed in section 1.5.3.).

The authors explored layered carbon, LC, (which contains graphene) doped with nitrogen. A catalyst containing approximately 7.8% N determined by XPS analysis was applied for toluene oxidation in water with TBHP as oxidant. The reaction was run for 24 h at 80 °C, and achieved 67.5% conversion and a 67.0% yield of benzoic acid. This represents a significant improvement on yields from the Snia-Viscosa process. Further studies indicated the catalyst was recoverable and reusable with very little loss of catalytic activity.

1.5.2. 2-ethylnaphthalene oxidation

2-ethylnaphthalene is a speciality chemical that can be oxidised to many different products, including 2-acetylnaphthalene and α -methyl-2-naphthalenemethanol, shown in **Figure 7**. In cases where C-C bond cleavage is feasible, products such as 2-naphthoic acid, 1-indanone, phthalide and phthalic acid may be produced, also shown in **Figure 7**. Selective oxidation of 2-ethylnaphthalene at the terminal end of the alkyl chain is particularly challenging, due to the superior bond strength of the CH₃ group over the CH₂. Therefore the products of this reaction, 2-naphthaleneacetaldehyde, 2-naphthaleneethanol and 2-naphthaleneacetic acid, shown in **Figure 8**, are seldom observed.

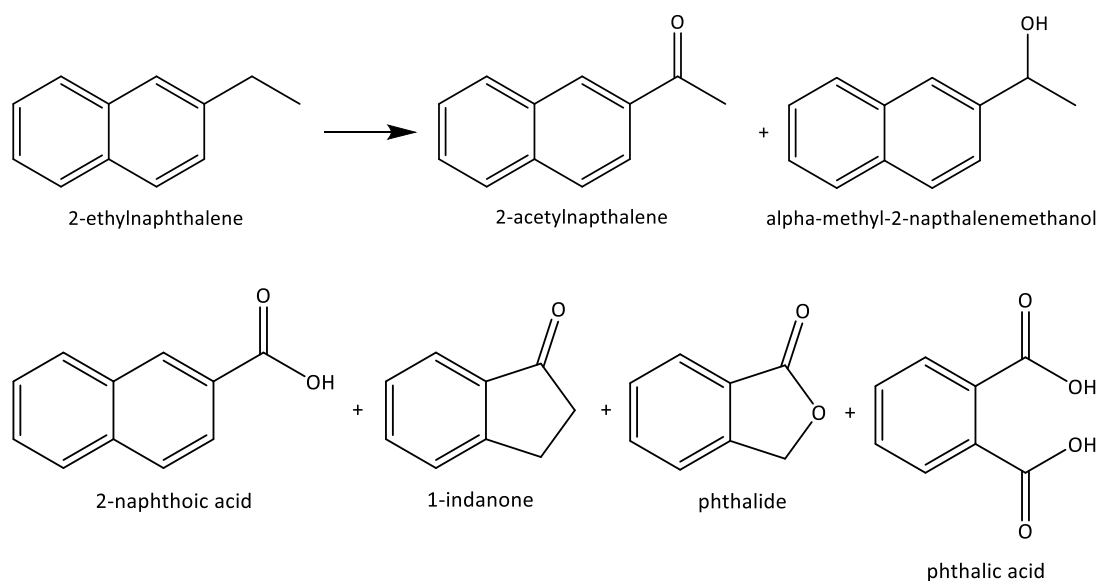


Figure 7. Possible products of 2-ethylnaphthalene oxidation

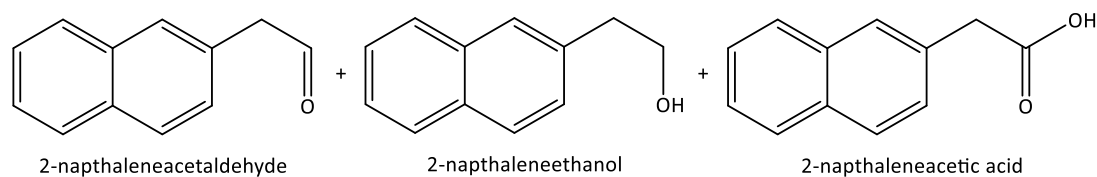


Figure 8. Products of terminal oxidation of the alkyl chain in 2-ethylnaphthalene

The partially oxidised products of 2-ethylnaphthalene have applications in the food, cosmetics and pharmaceutical industries⁶⁵; therefore a heterogeneous route to them is desirable.

Ma *et al.*⁶⁴ explored nitrogen-doped Layered Carbon catalysts for oxidation of 2-ethylnaphthalene. Under the experimental conditions of 1mmol 2-ethylnaphthalene, 3 mmol tBHP and 3 mL water at 80 °C for 24 h, 0.01 g of the Layered Carbon catalyst containing 7.8% N (according to XPS) achieved a remarkable <99% conversion and 95.9% yield of 2-acetylnaphthalene.

1.5.3. Ethylbenzene oxidation

Ethylbenzene is obtained by the catalytic combination of benzene and ethane over zeolites, such as the 6.8 wt.% Pt/H-ZSM5 catalyst reported by Suzuki *et al.*⁶⁶.

Ethylbenzene can be oxidised to a number of oxidised products, but most significantly to acetophenone and 1-phenylethanol, shown in **Figure 9**. Selective oxidation of the terminal carbon of the alkyl chain is difficult, given the comparative ease of oxidising the CH₂ group. Therefore the products of terminal oxidation, shown in **Figure 10**, are not commonly observed.

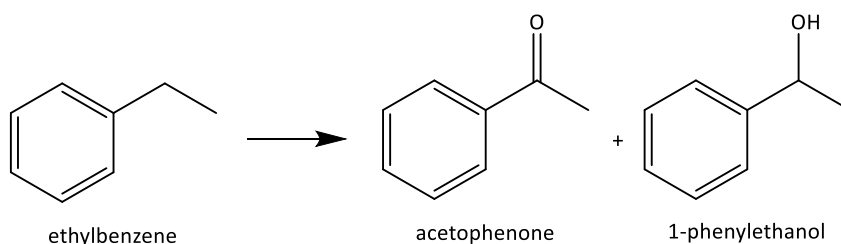


Figure 9. Products of ethylbenzene oxidation

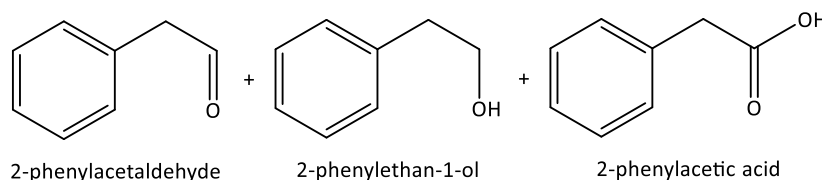


Figure 10. Products of terminal oxidation of alkyl chain in ethylbenzene

Acetophenone is a value-added compound used extensively in paints, inks, resins, perfumes and food products. At present acetophenone is obtained as a side-product of ethylbenzene dehydrogenation, or alternatively from a homogeneous process in acidic conditions^{67, 68}. Acetophenone is relatively stable under typical conditions^{52, 69} but over-oxidation can lead to formation of benzoic acid.

Benzoic acid was the major product when J.A. Alonso *et al.*⁴⁸ utilised acid conditions for ethylbenzene oxidation reactions with a (La,Sr)_{0.5}(Mn,Co)_{0.5}O_{3-δ}/NHPI system, (as discussed in section 1.5.1. for toluene oxidation). Nearly 100% conversion was achieved under the reaction conditions of 20 bar O₂ at 90 °C for 3 h. This reaction

was 67% selective to benzoic acid, with the remainder being towards acetophenone.

H. Garcia and co-workers⁷⁰ also applied NHPI to ethylbenzene oxidation. In this case, NHPI was encapsulated in commercial Fe(BTC) (BTC = 1,3,5-benzenetricarboxylate). The resulting heterogenized catalyst contained a high proportion of Fe^{III}. At 120 °C, in an O₂ atmosphere, this catalyst achieved only 3% conversion of ethylbenzene and 98% selectivity to acetophenone and phenylethanol after 2 h and 17% conversion and 92% selectivity to the same two major products after 18 h.

Tilley *et al.*⁵³ also explored a heterogenized catalyst for the oxidation of ethylbenzene. The CoSBA-15 catalyst (also shown to be active for toluene oxidation, see section 1.5.1.) was shown to be capable of selective oxidation of ethylbenzene to acetophenone at temperatures as low as 25 °C. At this temperature, 14.3% conversion and 96.6% selectivity to acetophenone was achieved after 24 h. Running the reaction at 80 °C decreased selectivity to 82.5% but increased conversion to 38.0%.

Like Tilley and co-workers, Ma *et al.*⁶⁴ utilised tBHP as an oxidant and achieved conversion at extremely low temperatures. Layered Carbon catalysts doped with nitrogen were investigated. Increasing the percentage nitrogen present in the catalyst appeared to encourage N atoms to occupy graphitic sites in the catalyst and leads to a substantial increase in selectivity to acetophenone, as seen in **Table 6**.

Table 6. Oxidation of ethylbenzene with N-doped Layered Carbon catalysts⁶⁴

N content (%)	Conversion (%)	Yield (%)			
		Acetophenone	1-phenylethanol	Benzaldehyde	Benzoic acid
1.4	63.7	36.0	2.4	3.3	1.4
3.4	95.4	84.4	0.1	1.6	0
4.9	97.9	86.4	0	0	5.2
7.8	98.6	91.3	0	0	5.0

Reaction conditions: 0.01 g LC catalyst, 1 mmol ethylbenzene, 3 mmol tBHP (30% in H₂O), 3 mL H₂O, 80 °C, 24 h.

The result for the most heavily N-doped catalyst above represents extremely high conversion and selectivity in very mild conditions. In fact, this catalyst was shown to be so active, conversions of 94.0% could be achieved when running the reaction at only 30 °C for 96 h.

The work by J.A. Alonso *et al.*, H. Garcia *et al.*, Tilley and coworkers and Ma *et al.* relies on radical activity stimulated by the involvement of NHPI or tBHP. However, these are not always necessary. MnCO_3 has been investigated as a heterogeneous catalyst independently of a radical source⁷¹. When applied to ethylbenzene oxidation at 190 °C under 10 bar O_2 for 2 h, MnCO_3 achieved 34.4% conversion, with 75.4% selectivity to acetophenone and 20.9% selectivity to 1-phenylethanol. It was important to establish that the observed activity was not the result of leached manganese rather than the solid catalyst. The authors established that Mn(II) ions were less active than the MnCO_3 catalyst for oxidation of toluene under the reaction conditions, but did not investigate this for ethylbenzene oxidation. Nor did they report reusability studies, though they did note little difference between fresh and used catalyst was observed by XRD.

Choudhary *et al.*⁷² investigated a Mg-Al hydrotalcite catalyst exchanged with MnO_4^- anions. Different ratios of Mg:Al were explored, with a Mg:Al ratio of 10:1 found to be the most active of those tested. When refluxed in the absence of solvent at 130 °C and 1.48 bar O_2 for 5 h, this catalyst achieved 22.7% conversion with 98.0% selectivity to acetophenone. The catalyst demonstrated stability and reusability in further reactions, and no leaching of MnO_4^- was detected. If achievable on a larger scale, this suggests that immobilising permanganates in hydrotalcite structures could allow their oxidising properties to be exploited without incurring their drawbacks as stoichiometric oxidants. The success of the catalyst with a Mg:Al ratio of 10:1 over others tested was attributed to this metal ratio producing the highest number of basic sites, which the authors propose are key for reactivity.

Tatsumi *et al.*⁷³ also emphasised the vital role of basicity. Ni-Al hydrotalcites were prepared in a variety of different molar Ni:Al ratios, shown in **Table 7**, and with a variety of different guest anions, shown in **Table 8**.

Table 7. Activity of Ni-Al hydrotalcites with varying Ni:Al ratios for ethylbenzene oxidation⁷³

molar ratio Ni:Al	Conversion (%)	Selectivity to acetophenone (%)
2:1	28	99.5
3:1	31	99.8
4:1	32	99.4
5:1	47	99.3

Reaction conditions: 2.45 g catalyst, 122.5 mmol ethylbenzene, 5 mL min⁻¹ O₂ flow, 135 °C, 5 h. Hydrotalcite catalysts prepared with CO₃²⁻ as guest anion.

Table 8. Activity of Ni-Al hydrotalcites with different guest anions for ethylbenzene oxidation⁷³

Guest anion	Conversion (%)	Selectivity to acetophenone (%)	pH of catalyst suspension
CO ₃ ²⁻	47	99.3	9.4
Cl ⁻	28	79.5	8.0
NO ₃ ⁻	24	74.2	7.8
SO ₄ ²⁻	23	64.0	7.1

Reaction conditions: 2.45 g catalyst, 122.5 mmol ethylbenzene, 5 mL min⁻¹ O₂ flow, 135 °C, 5 h. Molar ratio Ni:Al 5:1. Catalyst suspensions prepared from 0.3 g catalyst in 20 mL H₂O.

The choice of guest anion was shown to affect selectivity to acetophenone, with the most basic, CO₃²⁻, proving the most selective of the guest anions tested. A Ni:Al ratio of 5:1 was found to be most effective, with increasing conversion observed with increasing Ni content. The optimised catalyst prepared with these parameters achieved 47% conversion and 99.3% selectivity to acetophenone when used under atmospheric pressure with O₂ bubbled through the substrate at 135 °C for 5 h. The catalyst was shown to be reusable with no detectable leaching of Ni. The suggested reaction scheme for this is shown in **Figure 11**. The presence of a radical mechanism is supported by a drastic decrease in conversion when the radical scavenger hydroquinone was present.

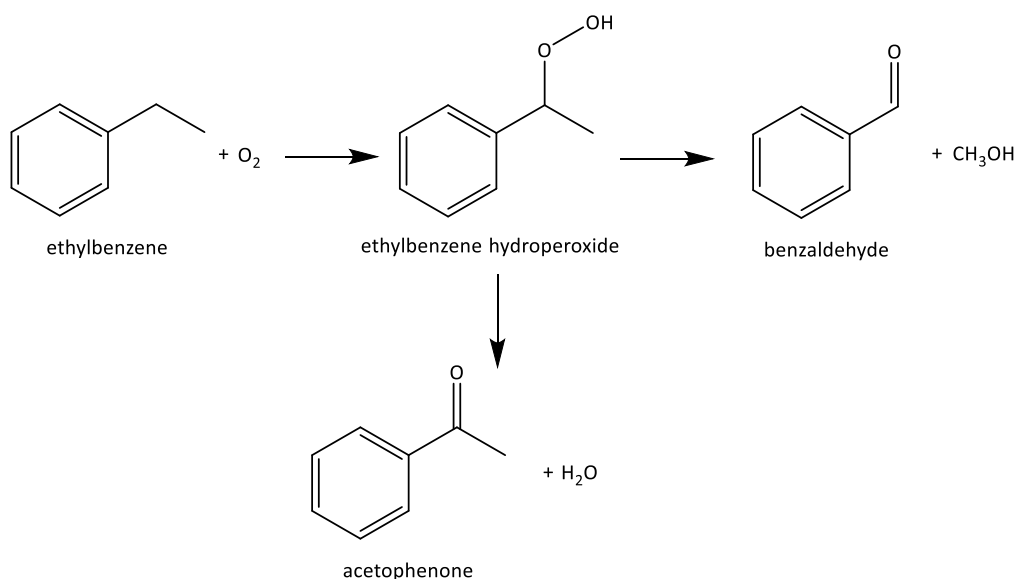


Figure 11. Mechanism proposed by T. Tatsumi *et al.*

Tatsumi *et al.* suggest that the high selectivity observed is the result of basic sites on the Ni-Al hydrotalcite selectively converting the intermediate ethylbenzene hydroperoxide to acetophenone.

The activity of Ni for the oxidation of ethylbenzene has been explored by a number of researchers. Yusuff *et al.*⁷⁴ compared Ni(II) complexes encapsulated in zeolite Y to similar catalysts containing Co(II) and Cu(II) complexes. These catalysts were prepared by ion-exchange of zeolite Y with chloride solutions of the appropriate metal and subsequent treatment with excess dimethylglyoxime ($dmgH_2$) or *N,N'*-ethylenebis(7-methylsalicylideneamine) (Me_2salen). The resulting catalysts were reacted with ethylbenzene for 8 h in benzene as solvent and in the presence of 30% H_2O_2 as oxidant. The molar ratio H_2O_2 :substrate was 2:1.

In these conditions, all of the prepared catalysts were found to be active. The most active were the copper catalysts, and so these were studied further at varying reaction temperatures, and with O_2 rather than H_2O_2 as an oxidant, as shown in **Table 9**.

Table 9. Oxidation of ethylbenzene by Cu-complexes encapsulated in zeolite⁷⁴

Catalyst	Oxidant	Reaction temp. (°C)	Conversion (wt.%)
Cu/zeolite Y exchanged with (dmgH ₂)	O ₂	50	16.8
	H ₂ O ₂	50	24.0
		60	33.6
		70	46.3
Cu/zeolite Y exchanged with (Me ₂ salen)	O ₂	50	11.1
	H ₂ O ₂	50	23.1
		60	29.4
		70	39.2

Reaction conditions: 0.03 mol ethylbenzene, 10 mL benzene, 50 mg catalyst, 8 h. Where applicable, 0.06 mol H₂O₂ supplied as 30% solution.

The results reproduced in **Table 9** demonstrate that oxidation with O₂ rather than H₂O₂ is possible, though at lower conversion. As expected, increasing reaction temperature increases conversion. Acetophenone was the sole product. The authors also found that the prepared catalysts were reusable without loss of activity, and attributed this to the metal complexes being effectively immobilised in cavities within the zeolite, unable to leach out.

Leaching can present a significant problem in supported metal nanoparticle catalysts. Sometimes, it can be prevented by modifying surface or nanoparticle properties and improving metal-support interaction. Choice of support can also play a vital role in determining activity and product distribution.

Grunwaldt *et al.*⁷⁵ encountered leaching during the investigation of silver nanoparticles supported on SiO₂ modified with Ce. In this work, the oxidation of *p*-xylene, cumene, toluene and ethylbenzene was investigated. Initial studies on the oxidation of *p*-xylene by a 10 wt.% Ag/SiO₂ catalyst prepared by impregnation suggested that the reaction could be promoted by the addition of CeO₂ and a carboxylic acid to the mixture. When this methodology was applied to ethylbenzene oxidation by the same catalyst, the presence of CeO₂ hindered the reaction, though the addition of acid increased selectivity to acetophenone. Furthermore, it was also found that the presence of acid, either as an additive or reaction products, encouraged leaching of silver into solution.

It was found that catalysts prepared by flame spray pyrolysis did not significantly leach, even in the presence of carboxylic acid. In these catalysts, the SiO₂ support material was modified with Ce, which the authors believe prevented the formation of large silver nanoparticles such as those found on the equivalent catalyst without Ce, 1 wt.% Ag/SiO₂. Results for ethylbenzene oxidation by Ce-modified 1 wt.% Ag/Ce-SiO₂ catalysts are reproduced in **Table 10**.

Table 10. Oxidation of ethylbenzene by 1 wt.% Ag/ Ce/SiO₂ catalysts⁷⁵

Catalyst	Yield (%)			TON
	<i>1-phenylethanol</i>	<i>Acetophenone</i>	<i>Ethylbenzene hydroperoxide</i>	
1 wt.% Ag 10% Ce/SiO ₂	4.0	6.8	4.2	2000
1 wt.% Ag 30% Ce/SiO ₂	2.0	3.8	6.0	1600
1 wt.% Ag 50% Ce/SiO ₂	1.7	3.2	1.8	890

Reaction conditions: 122 mmol ethylbenzene, 100 mg biphenyl, 100 mg catalyst, 3 mol% benzoic acid, refluxing in O₂ atmosphere, 136 °C, 3 h.

Increasing amounts of Ce decreases the product yield. In fact, none of these catalysts outperform the 10 wt.% Ag/SiO₂ catalyst prepared by impregnation, but nevertheless present a significant advantage in terms of the lack of leaching and reduced metal loading, corresponding to higher turnover numbers. This serves as an excellent example of how support choice and tailoring can have a significant impact on the outcome.

Venugopal *et al.*⁷⁶ investigated Ni nanoparticles on various supports for ethylbenzene oxidation. 10 wt.% Ni catalysts were prepared by incipient wetness impregnation, with SiO₂, hydroxyapatite (HAp), SBA-15, 4USY and 13USY utilised as supports. Catalysts were tested in solvent-free conditions in the presence of O₂ at 150 °C for 6 h. Under these conditions, Ni/13USY achieved the highest conversion of 21.4%, with 76.5% selectivity to acetophenone. Ni/HAp achieved a higher selectivity of 80.9% and a similar conversion of 20.4%. Of the remaining catalysts, only Ni/SBA-15 achieved a conversion >10%, but with poor selectivity. The investigation concludes that in this system, a higher concentration of acidic centres

on the support material promotes selectivity to byproducts such as benzaldehyde and 1-phenylethanol.

Li *et al.*⁵⁹ applied an AuPd/MIL-101 catalyst found to be highly selective for toluene oxidation to ethylbenzene oxidation. Conversion of ethylbenzene was higher than that of toluene in the same conditions (150 °C, 15 bar O₂, 4 h), at 38.5%. Acetophenone and 1-phenylethanol were the primary products, formed in 65.3% selectivity and 21.9% selectivity respectively.

1.5.4. Summary

Significant challenges remain for selective oxidation in mild conditions.

Heterogeneous oxidation catalysts typically contain expensive platinum group metals and often require acid conditions or promoters. Even then, in many cases conversions are low. This can be a deliberate choice to ensure selectivity: particularly to products such as alcohols and aldehydes, which can be converted to the corresponding carboxylic acids by secondary oxidation. However, even when conversions are not restricted for this reason, yields of product are generally low.

Improving upon reported catalysts to achieve higher yields of product and greater TOFs is of interest. This will likely require some elucidation of the mechanism, particularly with respect to radical chemistry.

1.6. Aims of the thesis

This work was supported by an ERC Advanced Grant as part of the ‘Addressing global sustainability challenges by changing perceptions in catalyst design: After the Gold Rush’ project. This project involves the investigation and development of efficient catalytic solutions to key environmental and sustainability issues; with a particular emphasis on developing gold-free bimetallic catalysts.

This thesis concerns the oxidation of alkyl aromatics in the liquid phase. Three substrates were chosen for investigation: toluene, ethylbenzene and 2-ethylnaphthalene. These compounds are both commercially relevant and good

model compounds to inform future work. When considered together, the effect of increased alkyl chain-length and increased conjugation can be examined.

The key objectives in each case were:

- The development of a stable, active catalyst for oxidation in mild conditions.
- Developing alternatives to gold catalysts that achieve comparable or better results.
- The elucidation of the reaction mechanism to inform catalyst design.

1.6.1. Toluene oxidation

Liquid-phase oxidation of toluene with gold-containing bimetallic catalysts has been studied previously. This investigation builds on reported work, exploring AuPd and PtPd catalysts before moving on to an alternative, gold-free bimetallic catalyst: RuPd/TiO₂. RuPd/TiO₂ was found to be capable of oxidation in mild conditions. This work is discussed in Chapter Three.

1.6.2. 2-ethylnaphthalene oxidation

2-ethylnaphthalene can be partially oxidised to a number of different products, most significantly 2-acetylnaphthalene. The RuPd/TiO₂ catalyst explored throughout Chapter Three for selective oxidation of toluene is applied to 2-ethylnaphthalene oxidation in the same conditions. Additionally, the previously reported AuPd/TiO₂ catalyst is investigated and the results compared to its ruthenium counterpart. This work is detailed in Chapter Four.

1.6.3. Ethylbenzene oxidation

A FePd/TiO₂ catalyst was explored for ethylbenzene oxidation in mild conditions. Attempts were made to optimise this catalyst and explore the role of radicals in the reaction. Unusual behaviour dependent of molar ratios of substrate:metal was observed. This work is reported in Chapter Six.

1.7. References

1. B. Lindstrom and L. J. Pettersson, *Cattech*, 2003, **7**, 130-138.
2. J. Wisniak, 2010, **21**, 60-69.
3. M. Boudart and T. Kwan, *Industrial and Engineering Chemistry*, 1956, **48**, 562-569.
4. P. B. Weisz, *Annual Review of Physical Chemistry*, 1970, **21**, 175-&.
5. R. L. Burwell, *Abstracts of Papers of the American Chemical Society*, 1982, **183**, 11-HIST.
6. R. Schlogl, *Angewandte Chemie-International Edition*, 2015, **54**, 3465-3520.
7. *Journal*.
8. S. Rebsdat and D. Mayer, in *Ullmann's Encyclopedia of Industrial Chemistry*, Wiley-VCH Verlag GmbH & Co. KGaA, 2000.
9. S. Rebsdat and D. Mayer, in *Ullmann's Encyclopedia of Industrial Chemistry*, Wiley-VCH Verlag GmbH & Co. KGaA, 2000.
10. M. A. Barakat, 2011, **4**, 361-377.
11. P. A. Kobielska, A. J. Howarth, O. K. Farha and S. Nayak, 2018, **358**, 92-107.
12. F. Haber and G. van Oordt, *Zeitschrift Fur Anorganische Chemie*, 1905, **44**, 341-378.
13. J. W. Erisman, M. A. Sutton, J. Galloway, Z. Klimont and W. Winiwarter, 2008, **1**, 636.
14. R. Schlögl, *Chemical Energy Storage*, 2012.
15. Z. Belohlav and P. Zamostny, 2000, **78**, 513-521.
16. W. H. Weinberg, *Accounts of Chemical Research*, 1996, **29**, 479-487.
17. *Chemical Engineering Science*, 1954, **3**, 41 - 59.
18. C. Doornkamp and V. Ponec, *Journal of Molecular Catalysis a-Chemical*, 2000, **162**, 19-32.
19. *Computational and Theoretical Chemistry*, 2017, **1100**, 28 - 33.
20. G. Bond, *Gold Bulletin*, 2008, **41**, 235-241.
21. H. Wu, L. Wang, J. Zhang, Z. Shen and J. Zhao, 2011, **12**, 859-865.
22. J. Kašpar, P. Fornasiero and N. Hickey, *Fundamentals of Catalysis and Applications to Environmental Problems*, 2003, **77**, 419-449.

23. J. A. Lupescu, J. W. Schwank, G. B. Fisher, J. Hangan, S. L. Peczonczyk and W. A. Paxton, *9th International Conference on Environmental Catalysis (ICEC2016), Newcastle, Australia, 2018*, **223**, 76-90.
24. G. J. Hutchings, *Catalysis Today*, 2014, **238**, 69-73.
25. R. Ferrando, J. Jellinek and R. L. Johnston, *Chemical Reviews*, 2008, **108**, 845-910.
26. B. Coq and F. Figueras, *Journal of Molecular Catalysis a-Chemical*, 2001, **173**, 117-134.
27. L. Ma, C. Y. Seo, X. Chen, K. Sun and J. W. Schwank, 2018, **222**, 44-58.
28. D. I. Enache, J. K. Edwards, P. Landon, B. Solsona-Espriu, A. F. Carley, A. A. Herzing, M. Watanabe, C. J. Kiely, D. W. Knight and G. J. Hutchings, *Science*, 2006, **311**, 362-365.
29. S. S. Li, D. D. Gong, H. G. Tang, Z. Ma, Z. T. Liu and Y. Liu, *Chemical Engineering Journal*, 2018, **334**, 2167-2178.
30. Z. Z. Yang, X. X. Lin, X. F. Zhang, A. J. Wang, X. Y. Zhu and J. J. Feng, *Journal of Alloys and Compounds*, 2018, **735**, 2123-2132.
31. F. Solymosi, *Catalysis Reviews*, 1968, **1**, 233-255.
32. G. Sastre, A. Chica and A. Corma, *Journal of Catalysis*, 2000, **195**, 227-236.
33. M. Sankar, Q. He, M. Morad, J. Pritchard, S. J. Freakley, J. K. Edwards, S. H. Taylor, D. J. Morgan, A. F. Carley, D. W. Knight, C. J. Kiely and G. J. Hutchings, *Acs Nano*, 2012, **6**, 6600-6613.
34. G. J. Hutchings and C. J. Kiely, *Accounts of Chemical Research*, 2013, **46**, 1759-1772.
35. C. He, X. Zhang, S. Gao, J. Chen and Z. Hao, *Journal of Industrial and Engineering Chemistry*, 2012, **18**, 1598-1605.
36. R. A. Sheldon, *Chemtech*, 1991, **21**, 566-576.
37. R. A. Sheldon, *HETEROGENEOUS CATALYTIC-OXIDATION AND FINE CHEMICALS*, 1991.
38. I. Arends and R. A. Sheldon, *Applied Catalysis a-General*, 2001, **212**, 175-187.
39. E. V. Gusevskaya, *Quimica Nova*, **26**, 242-248.
40. J. Xiao and X. Li, *Angewandte Chemie International Edition*, 2011, **50**, 7226-7236.

41. S. Perathoner and G. Centi, *Topics in Catalysis*, 2005, **33**, 207-224.
42. 1976.
43. C. Barckholtz, T. A. Barckholtz and C. M. Hadad, *Journal of the American Chemical Society*, 1999, **121**, 491-500.
44. X. Li, J. Xu, L. Zhou, F. Wang, J. Gao, C. Chen, J. Ning and H. Ma, *Catalysis Letters*, 2006, **110**, 255-260.
45. F. Wang, J. Xu, X. Q. Li, J. Gao, L. P. Zhou and R. Ohnishi, *Advanced Synthesis & Catalysis*, 2005, **347**, 1987-1992.
46. **1975**.
47. T. G. Carrell, S. Cohen and G. C. Dismukes, *Journal of Molecular Catalysis A: Chemical*, 2002, **187**, 3-15.
48. A. Aguadero, H. Falcon, J. M. Campos-Martin, S. M. Al-Zahrani, J. L. G. Fierro and J. A. Alonso, *Angewandte Chemie-International Edition*, 2011, **50**, 6557-6561.
49. Y. Ishii, S. Sakaguchi and T. Iwahama, *Advanced Synthesis & Catalysis*, 2001, **343**, 393-427.
50. T. W. Bastock, J. H. Clark, K. Martin and B. W. Trenbith, *Green Chemistry*, 2002, **4**, 615-617.
51. M. Ilyas and M. Sadiq, *Catalysis Letters*, 2009, **128**, 337-342.
52. K. R. Seddon and A. Stark, *Green Chemistry*, 2002, **4**, 119-123.
53. R. L. Brutchey, I. J. Drake, A. T. Bell and T. D. Tilley, *Chemical Communications*, 2005, 3736-3738.
54. A. Corma and H. Garcia, *Chemical Society Reviews*, 2008, **37**, 2096-2126.
55. N. Lopez and J. K. Nørskov, *Journal of the American Chemical Society*, 2002, **124**, 11262-11263.
56. M.-C. Daniel and D. Astruc, *Chemical Reviews*, 2004, **104**, 293-346.
57. N. Dimitratos, J. A. Lopez-Sanchez, D. Morgan, A. F. Carley, R. Tiruvalam, C. J. Kiely, D. Bethell and G. J. Hutchings, *Physical Chemistry Chemical Physics*, 2009, **11**, 5142-5153.
58. F. Jiang, X. Zhu, B. Fu, J. Huang and G. Xiao, *Chinese Journal of Catalysis*, 2013, **34**, 1683-1689.
59. J. Long, H. Liu, S. Wu, S. Liao and Y. Li, *Acs Catalysis*, 2013, **3**, 647-654.

60. L. Kesavan, R. Tiruvalam, M. H. Ab Rahim, M. I. bin Saiman, D. I. Enache, R. L. Jenkins, N. Dimitratos, J. A. Lopez-Sanchez, S. H. Taylor, D. W. Knight, C. J. Kiely and G. J. Hutchings, *Science*, 2011, **331**, 195-199.
61. X. Liu and L. Dai, 2016, **1**, 16064.
62. J. Luo, H. Yu, H. Wang and F. Peng, *Catalysis Communications*, 2014, **51**, 77-81.
63. K.-P. Lee, S.-H. Lee, K. S. Sundaram and G. A. Iyengar, *Radiation Physics and Chemistry*, 2012, **81**, 1422-1425.
64. Y. Gao, G. Hu, J. Zhong, Z. Shi, Y. Zhu, D. S. Su, J. Wang, X. Bao and D. Ma, *Angewandte Chemie-International Edition*, 2013, **52**, 2109-2113.
65. L. Červený, K. Mikulcová and J. Čejka, 2002, **223**, 65-72.
66. S. Kato, K. Nakagawa, N.-o. Ikenaga and T. Suzuki, 2001, **73**, 175-180.
67. B. Gutmann, P. Elsner, D. Roberge and C. O. K. Kappe, *Journal*, 2013, 2669-2676.
68. T. Liu, H. Cheng, L. Sun, F. Liang, C. Zhang, Z. Ying, W. Lin and F. Zhao, 2016, **512**, 9-14.
69. T. Mallat and A. Baiker, *Chemical Reviews*, 2004, **104**, 3037-3058.
70. A. Dhakshinamoorthy, M. Alvaro and H. Garcia, *Chemistry-a European Journal*, 2011, **17**, 6256-6262.
71. J. Gao, X. Tong, X. Li, H. Miao and J. Xu, *Journal of Chemical Technology and Biotechnology*, 2007, **82**, 620-625.
72. V. R. Choudhary, J. R. Indurkar, V. S. Narkhede and R. Jha, *Journal of Catalysis*, 2004, **227**, 257-261.
73. S. K. Jana, P. Wu and T. Tatsumi, *Journal of Catalysis*, 2006.
74. K. O. Xavier, J. Chacko and K. K. M. Yusuff, *Applied Catalysis a-General*, 2004, **258**, 251-259.
75. M. J. Beier, B. Schimmoeller, T. W. Hansen, J. E. T. Andersen, S. E. Pratsinis and J.-D. Grunwaldt, *Journal of Molecular Catalysis a-Chemical*, 2010, **331**, 40-49.
76. G. Raju, P. S. Reddy, J. Ashok, B. M. Reddy and A. Venugopal, *Journal of Natural Gas Chemistry*, 2008, **17**, 293-297.

Chapter Two – Experimental

2.1. Introduction

This chapter will introduce the equipment, methods and analytical techniques used throughout this work.

2.2. Chemicals

All chemicals were purchased from commercial sources and used as received, without further purification^{77, 78}.

Table 1. Chemicals used

Chemical	Supplier	Purity
toluene	Alfa-Aesar	≥99.5%
n-decane	Alfa-Aesar	≥99.0%
2-ethylnaphthalene	Sigma-Aldrich	≥99.0%
Luperox TBH70X: tertiary-butyl hydroperoxide (tBHP) solution	Sigma-Aldrich	70 wt.% in H ₂ O
tertiary-butyl hydroperoxide solution in decane	Sigma-Aldrich	5.0 - 6.0 M in decane
σ-xylene	Sigma-Aldrich	≥98.0%
ethylbenzene	Sigma-Aldrich	≥99.8%
HCl 37% in H ₂ O	Sigma-Aldrich	≤5ppm organic impurities ≤1ppm free Cl ⁻
polyvinylalcohol	Sigma-Aldrich	≥99.0%
PdCl ₂	Sigma-Aldrich	≥99.0%
HAuCl ₄ .3H ₂ O	Sigma-Aldrich	≥99.9%
RuCl ₃ .xH ₂ O	Sigma-Aldrich	40.0-49.0% Ru content
FeCl ₂	Sigma-Aldrich	≥98.0%
NaOH (pellets)	Sigma-Aldrich	≥97.0%
NaBH ₄	Sigma-Aldrich	≥96.0%

2.3. Definitions

$$\text{Conversion (\%)} = \frac{\text{total mols product(s)}}{\text{initial mols substrate}} * 100\%$$

$$\text{Selectivity (\%)} = \frac{\text{mols product}}{\text{total mols product(s)}} * 100\%$$

$$\text{Product yield (\%)} = \frac{\text{mols product}}{\text{initial mols substrate}} * 100\%$$

$$\text{Turnover number (TON)} = \frac{\text{total mols product(s)}}{\text{mols metal in catalyst}}$$

$$\text{Turnover frequency (TOF)} = \frac{\text{TON}}{\text{reaction time}}$$

2.4. Methods of catalyst preparation

2.4.1. Sol immobilisation³⁴

2 M PdCl₂, 2 M FeCl₃, 2 M Fe(NO₂)₃ and 2 M HAuCl₄ were prepared as aqueous solutions and appropriate volumes of the required metals taken and placed in 800 mL of rapidly stirring H₂O. A 1 wt% aqueous solution of polyvinylalcohol (PVA) was prepared, and added to the solution in a ratio of 2 mols PVA to every 1 mol of metal, to control particle size via encapsulation. This produced a dark brown sol. The metals in the stirring sol were then reduced by addition of NaBH₄, supplied as a 0.1 M solution in a ratio of 5 mols NaBH₄ for every mol metal. The solid support was added directly to the stirring mixture. Finally, the pH of the solution was decreased to 2 by dropwise addition of H₂SO₄ to remove PVA from the surface. The catalyst was retrieved by filtration under vacuum and washed with 1 L H₂O. The catalyst was then dried for 18 h at 120°C.

2.4.2. Impregnation³⁴

2 M PdCl₂, 2 M FeCl₃, 2 M Fe(NO₂)₃ and 2 M HAuCl₄ were prepared as aqueous solutions and appropriate volumes of the required metals stirred together. The solid support was added slowly to ensure homogeneous mixing. The temperature was then increased to evaporate all solvent. This produced a dry paste. The resulting paste was retrieved, ground and calcined at 400°C for 3 h in air.

2.4.3. Modified impregnation³³

2 M PdCl₂, 2 M FeCl₃, 2 M Fe(NO₂)₃ and 2 M HAuCl₄ were prepared as aqueous solutions and mixed together in the appropriate combination. The solution was

further acidified with HCl to form a 0.5 M solution. This mixture was stirred and the solid support added slowly to ensure homogeneous mixing. The temperature was increased to evaporate the solvent and this resulted in a dry paste. The paste was retrieved, ground and reduced for 3 h at 400°C in 5% H₂ in Ar.

2.5. Reactors

2.5.1. Radleys multi-pot 'Starfish' reactor

The Radleys 'Starfish' reactor consisted of an aluminium heating block, with five ports, mounted on a heating and stirring plate. The temperature was monitored and controlled *via* a thermocouple positioned in the block. Stirring was controlled by a dial on the heating and stirring plate body. A central pole supported a gas manifold with five ports. This was supplied with nitrogen or oxygen *via* a wall-mounted regulator and delivered into the glass round-bottomed reactor vessels *via* tubing ending in glass plungers, secured into the vessels by screw-top caps.

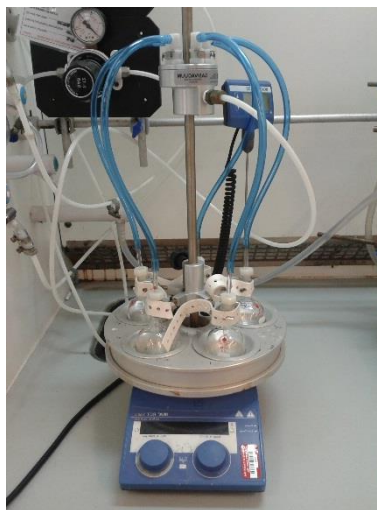


Figure 1. Radleys multi-pot 'Starfish' reactor

2.5.2. Glass reactors

The glass reactor set-up consisted of 50 mL glass round-bottomed flasks fitted with condensers, heated by oil-baths mounted on heating and stirring plates. The rate of stirring was controlled by a dial on the heating and stirring plate body, the

temperature monitored and controlled by a thermocouple positioned in the oil-bath. The oil in the bath was kept circulating using a stirrer bar.



Figure 2. Glass reactors with condensers

2.5.3. Autoclave

A Parr autoclave fitted with a 100 mL volume PTFE liner was used. To ensure safety, the autoclave was fitted with a vent line and 1000-psi (~70 bar) bursting disc. Gas was supplied to the autoclave *via* a non-return gas tap. Gas pressure was controlled *via* a wall-mounted regulator and monitored by a sensor within the autoclave. The temperature within the autoclave was monitored by a thermocouple. The reaction vessel was heated by a heating jacket that fitted around the stainless steel autoclave body, controlled by an external PC. Samples were extracted via sample valve.

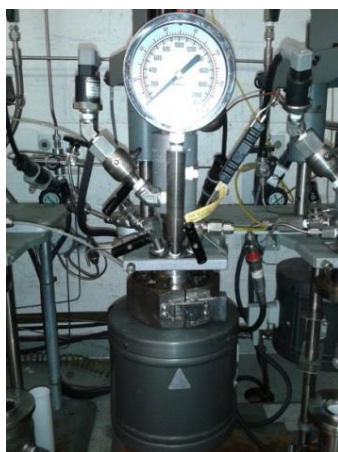


Figure 3. Autoclave reactor in heating jacket

2.6. Oxidation reactions

2.6.1. Ethylbenzene oxidation

Reactions were carried out in Radleys multi-pot reactor (2.5.1.).

Catalyst and stirrer bars were loaded into the reaction flasks prior to the ethylbenzene. The vessels were then flushed with O₂ for two minutes before being sealed at atmospheric pressure. The O₂ supply was kept open throughout the experiment. When sealed, the flasks were loaded into the aluminium heating block, heated to 140°C. The stirring was then set to 1000 rpm to encourage thorough mixing. After the reaction time had elapsed, the pressurised flasks were removed from the heating block and gas manifold and cooled in an ice bath for ten minutes. The cooled vessels were then opened and the reaction mixture filtered under gravity to remove solid.

2.6.2. Toluene oxidation

Reactions were carried out in the Radleys multi-pot reactor (2.5.1.), the glass reactor setup (2.5.2.) and in the autoclave (2.5.3.).

In the Radleys multi-pot reactor, toluene and tBHP solution were loaded into vessel, followed by catalyst and stirrer bars. For reactions under air, the flask was then sealed with the connecting gas tubes locked into manifold. For reactions with pressurised O₂ or He, the flask was flushed for two minutes prior to being sealed and the gas supply kept open throughout the experiment. Flasks were then loaded into the aluminium heating plate, which was heated to 80°C and stirring set to 1000 rpm. After the reaction time had elapsed, the sealed flasks were cooled in an ice bath for ten minutes prior to being depressurised. The biphasic reaction mixture was then centrifuged to separate the layers and solid catalyst.

In the glass reactor setup, oil baths were heated to 80°C with 1000 rpm stirring and 7°C water circulated through condensers. Catalyst and stirrer bars were loaded into flasks, followed by toluene and finally tBHP. The flask was then placed in the oil bath and the condenser fitted. After the reaction time had elapsed, the flasks were

cooled in an ice bath for ten minutes. The biphasic reaction mixture was then centrifuged to separate the layers and the solid catalyst.

In the autoclave, catalyst, toluene and tBHP were loaded into the PTFE liner, the liner placed in the autoclave body and the reactor sealed. For reactions with O₂ or N₂, the autoclave was then flushed three times with the appropriate gas and the supply kept open throughout the experiment. The heating jacket was then fitted around the autoclave, and the heating and 1000 rpm stirring started *via* the controlling PC. After the reaction time had elapsed, the heating jacket was removed and the autoclave cooled in an ice bath for twenty minutes. The autoclave was then opened and the biphasic mixture centrifuged to separate the layers and remove solid catalyst.

2.6.3. 2-ethylnaphthalene oxidation

Reactions were carried out in the Radleys multi-pot reactor (2.5.1).

2-ethylnaphthalene and tBHP were loaded into a vessel fitted with a stirrer bar. 2-10 mg catalyst was then loaded into the vessel. For reactions under air, the flask was then sealed with the connecting gas tubes locked into manifold. For reactions with pressurised O₂ or He, the flask was flushed for two minutes prior to being sealed and the gas supply kept open throughout the experiment. Experiments were carried out at 1-3 bar. Flasks were then loaded into the aluminium heating plate, which was heated to 80°C and stirring set to 1000 rpm. After the reaction time had elapsed, the sealed flasks were cooled in an ice bath for ten minutes prior to being opened. The biphasic reaction mixture was then centrifuged to separate the layers and solid catalyst.

2.7. Product analysis

2.7.1. Gas chromatography⁷⁹⁻⁸¹

Gas chromatography (GC) is an analytical technique for the separation and quantification of products in a gaseous or liquid mixture. A basic schematic of a GC apparatus for the analysis of liquid samples is given in **Figure 4**.

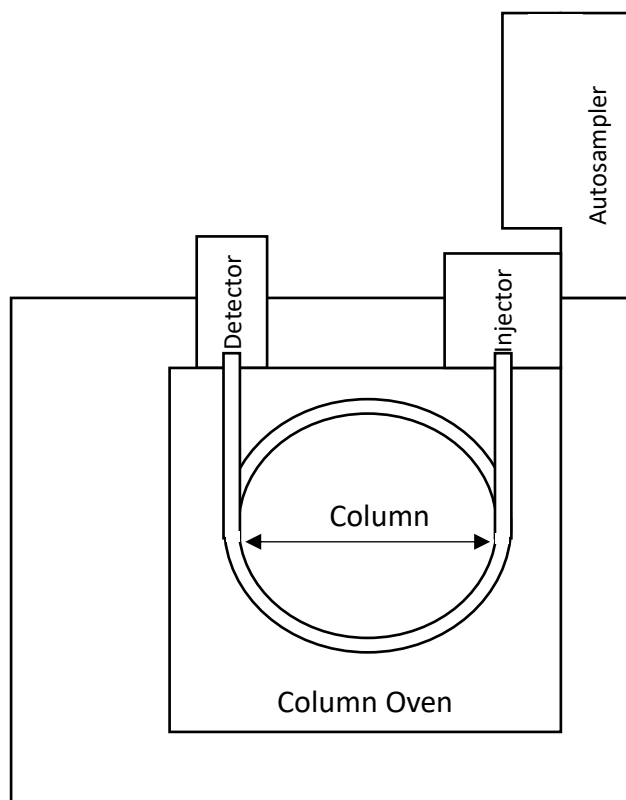


Figure 4. Schematic of a gas chromatogram

In the first step, a small quantity of liquid sample is collected by a syringe; operated by hand or by an autosampler. Using an autosampler allows for automation of analysis and helps to ensure a consistent injection volume.

The sample is then delivered through a septum into the injector, shown in **Figure 5**. The injector is heated and supplied with an inert carrier gas such as He or N₂. This vaporises the liquid sample and homogenises it with the carrier. Manipulating the flow of gas causes the sample to be 'split'; with some being vented and the rest passing through the inlet sleeve. This split is essential when using capillary columns, which have a very low sample capacity. The inlet sleeve may contain an inert packing substance such as glass wool; this helps to trap any solid contaminants (such as fragments of septum). The reduced volume of sample then passes into the column.

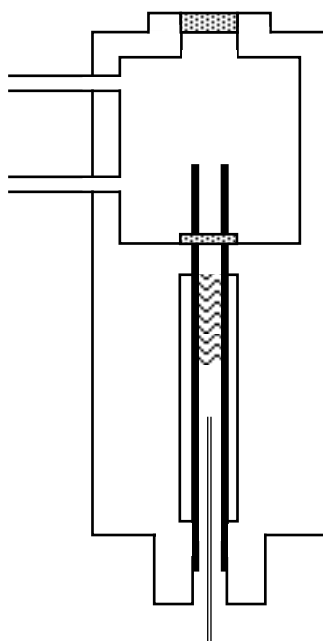


Figure 5. GC injector schematic

The column is responsible for the separation of components. The column is lined with an inert substance, known as the stationary phase, and has the carrier gas flowing through it, known as the mobile phase. The mixture components are separated according to their affinity for the stationary phase. Compounds with a strong affinity for the stationary phase pass through the column slowly; those with little affinity for the stationary phase are more associated with the mobile phase, and pass through the column more quickly. Therefore the choice of an appropriate stationary phase for the application is essential. The separation process can be further tuned by adjusting the column length and diameter, the thickness of the column lining, the pressure and flow rate of carrier gas and the temperature of the column. For this reason, the column is in a programmable oven and the pressure and flow rate is monitored and controlled.

After elution from the column, each component in turn passes into the detector. Many kinds of detector are available, but one of the most inexpensive and common is the flame ionisation detector (FID), which offers high sensitivity but cannot be used to detect CO, CO₂, N₂ or H₂O. A schematic of an FID is shown in **Figure 6**.

The compound elutes from the column into a hydrogen flame, which combusts and ionises the sample. The flame is placed on an anode, with a 'collector' cathode

above. This detects the ionised particles and relays the resulting electrical response to a controlling PC. The electrical signal, usually measured in pico-amps, is plotted (y-axis) against time since injection (x-axis) to produce a chromatogram.

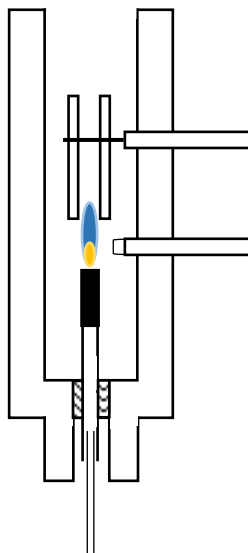


Figure 6. GC flame ionisation detector (FID) schematic

Each peak on the chromatogram corresponds to one of the components of the sample mixture. The area of each peak is proportional to the number of moles of the product in the injected sample; and therefore can be used to quantify the product present when compared to known values. To counteract any variation in injected volume, peaks are often normalised to a standard. To do this, a fixed amount of a compound not present in the reaction mixture) can be added to the analytical sample post-reaction (external standard) or present throughout the reaction (internal standard), if stable and nonreactive.

For the analysis of ethylbenzene oxidation samples, 0.500 mL reaction sample was analysed with 0.500 mL of toluene as external standard. Analysis was carried out on a Varian-450 gas chromatograph fitted with a CP 3800 autosampler equipped with a 10 μ L syringe. The column used was a CP-Wax 52 CB with a polyethylene glycol stationary phase and the following dimensions: 25 m length x 0.53 mm diameter x 2 μ m lining.

For analysis of toluene and 2-ethylnaphthalene oxidation samples, 0.250 mL of reaction sample was analysed with 0.100 mL of o-xylene as external standard. Analysis was carried out on an Agilent 7820A gas chromatograph, fitted with a 7650A automatic liquid sampler equipped with a 10 μ L syringe. The column used was a CP-Sil 5 CB with a dimethylpolysiloxane stationary phase and the following dimensions: 15 m length x 0.53 mm diameter x 2 μ m lining.

2.7.2. Gas chromatography - mass spectrometry^{80, 82, 83}

Gas chromatography mass spectrometry (GCMS) couples a gas chromatograph with a mass spectrometer to allow separation and identification of compounds in a liquid or gaseous mixture.

Firstly, the components are separated *via* gas chromatography (as described in section 2.7.1.). The separated components then pass into a mass spectrometer for analysis. A simple schematic of a mass spectrometer is presented in **Figure 7**.

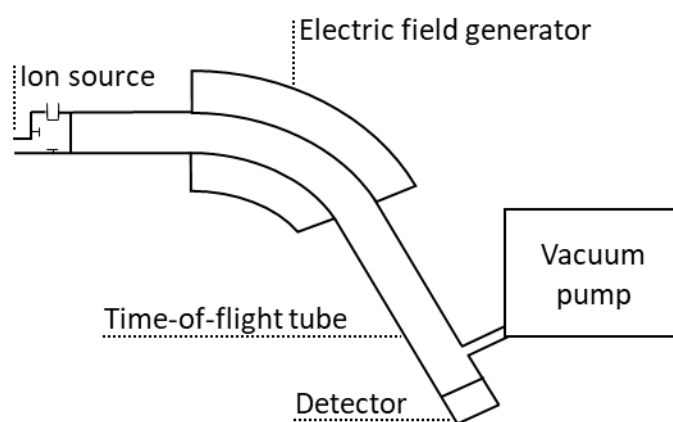


Figure 7. Schematic of a mass spectrometer

The ion source is responsible for ionising the analyte. There are multiple techniques that can be used for this, depending on the nature of the sample to be analysed and the operating conditions. In GC-MS systems, electron ionisation (EI) is typically used; EI offers a high degree of fragmentation and therefore detailed spectra, but requires a vacuum to operate.

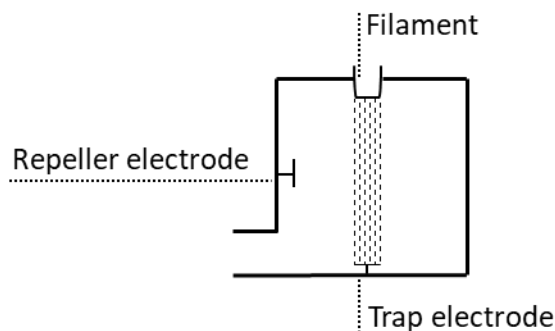


Figure 8. Schematic of an electron ionisation source

In an EI source, a heated filament is supplied with an electric current, liberating excited electrons. These are accelerated towards a trap electrode, creating a beam. The sample to be analysed is passed through this beam at a 90° degree angle, causing it to fragment and ionise. The ionised particles are then repelled towards a mass analyser by a repeller electrode.

The mass analyser separates ions according to their mass-to-charge ratio. There are many types of mass analyser; one of the most common being time-of-flight (TOF).

When the sample ions pass into the TOF analyser, they are subjected to an electric field of known strength. This results in all ions with the same charge possessing the same kinetic energy. Therefore the velocity of these ions is dependent on mass-to-charge ratio alone. More massive ions take longer to travel through the system to the detector: thus they spend longer 'in flight'.

Two types of detector are used in TOF mass spectrometers; microchannel plate detectors (MPD) or secondary emission multipliers (SEM).

The time each fragment spends 'in flight' is recorded, and from this and the known instrumental parameters, mass-to-charge ratio can be calculated. This can be plotted against relative ion intensity expressed as a percentage, producing a fragmentation pattern unique to the compound. A simplified diagram of a mass spectrum is shown in **Figure 10**.

The sum totals of peak intensities in the observed mass spectra are combined to generate a total ion chromatogram (TIC). Each peak in the TIC therefore

corresponds to one compound, which can be identified by comparing the fragmentation pattern to a database of known compounds.

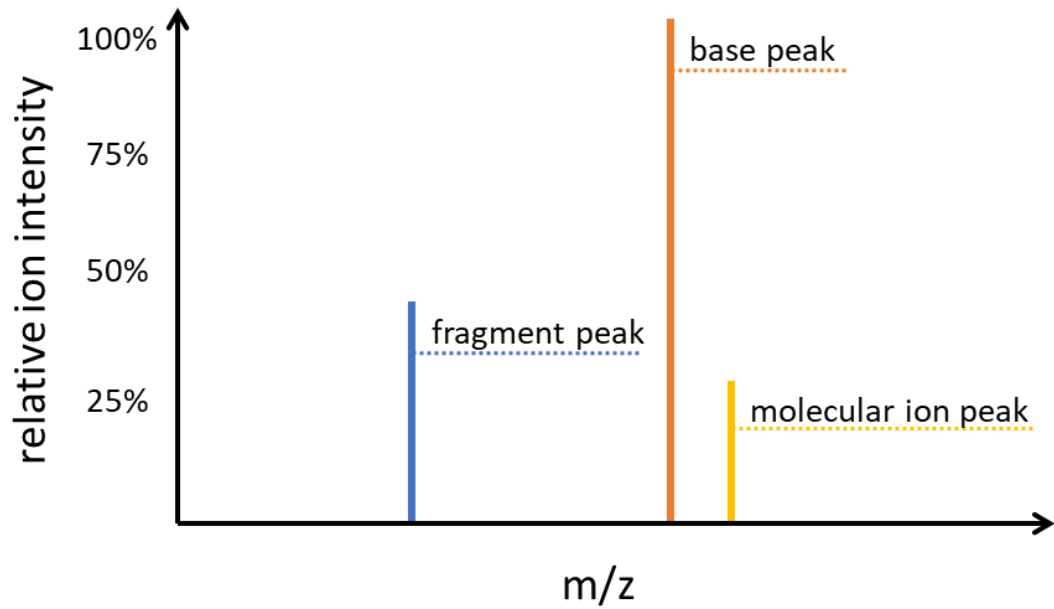


Figure 10. A diagram of the components of a mass spectrum

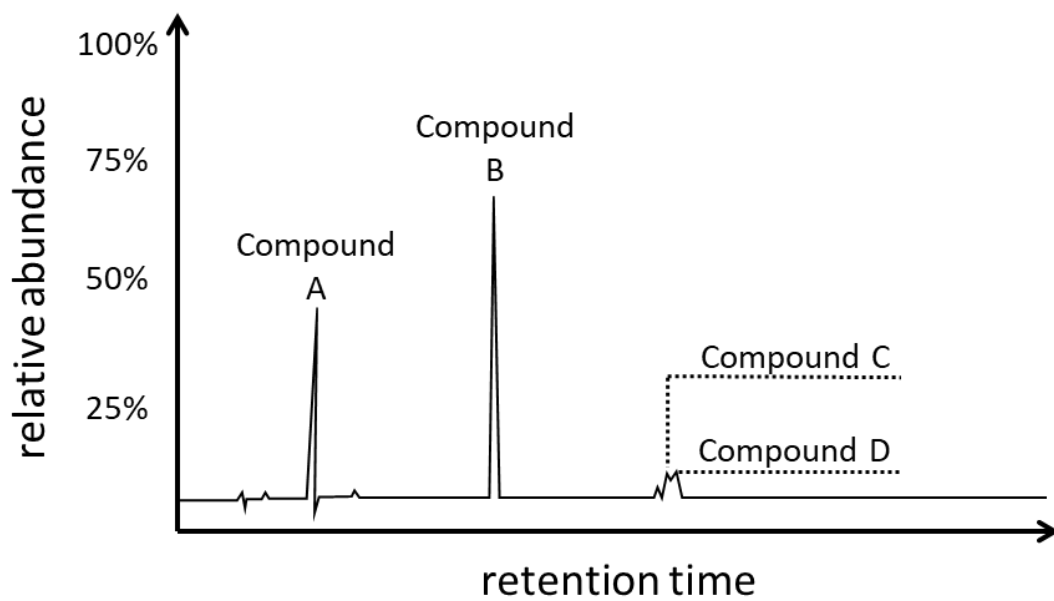


Figure 11. A diagram of a total ion chromatograph

GCMS analysis was carried out on a Waters GCT Premier instrument fitted with a VF-5HT column with the following dimensions: 30 m length x 0.25mm diameter x 0.10 μ m lining.

2.7.3. Nuclear magnetic resonance spectroscopy⁸⁴⁻⁸⁶

Nuclear magnetic resonance spectroscopy (NMR spectroscopy) exploits the magnetic properties of nuclei to investigate the structure and dynamics of the molecules to which they belong. NMR analysis can be carried out on gaseous, liquid or solid samples, provided that some of the atoms present have an angular momentum, P , known as 'spin', that is not equal to zero. The most commonly used types of NMR are ^1H NMR and C^{13} NMR.

In a typical ^1H NMR experiment, a small amount of sample is placed in a glass tube. For liquid or solid samples, a deuterated solvent is sometimes added. Deuterium has a nuclear spin of zero, and therefore will not be observed in the resulting spectra. An internal standard can also be added. The accepted standard for organic samples is trimethylsilane (TMS), which gives a distinct signal against which all others can be normalised.

The glass tube containing the sample is placed in a holder and subjected to a magnetic field. The 'spin active' nuclei (those with $P \neq 0$) align with (+) or against (-) this field. This puts them in a higher (-) or lower (+) energy state; described as $-\frac{1}{2}$ and $+\frac{1}{2}$ respectively. The energy difference between these states is termed ΔE , as described in **Figure 12**.

ΔE is dependent on the magnetic environment of the nucleus and proportional to the strength of the applied magnetic field. When radiated with energy equal to ΔE , the nuclei are excited to the $-\frac{1}{2}$ state. They then undergo relaxation back into the $+\frac{1}{2}$ state, emitting energy to other nuclei in the molecule (spin-spin relaxation), or to the surroundings (spin-lattice relaxation). This produces an electromagnetic signal with a characteristic frequency (resonance). Nuclei in the same magnetic environment produce signals of the same frequency, and appear together on the resulting spectrum. Therefore the number of signals seen in an NMR spectrum is

equivalent to the number of magnetic environments present (for the nuclei in question). A ^1H NMR spectrum of toluene can be seen in **Figure 13**.

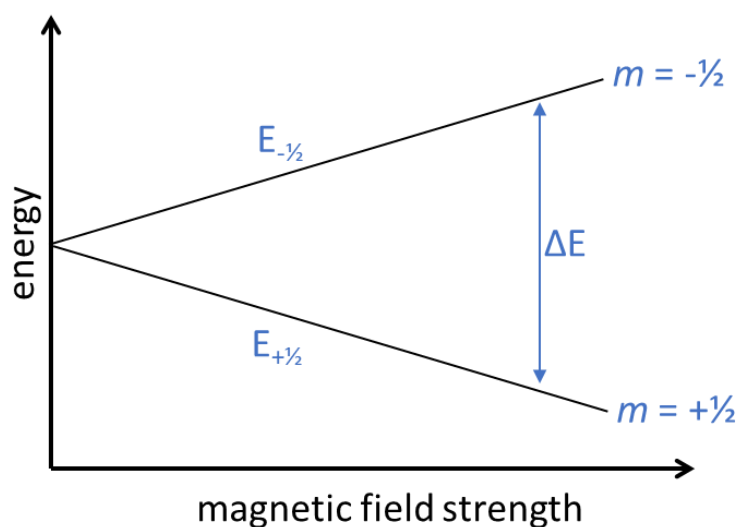


Figure 12. Increasing energy gap between spin states in the presence of increasing magnetic field

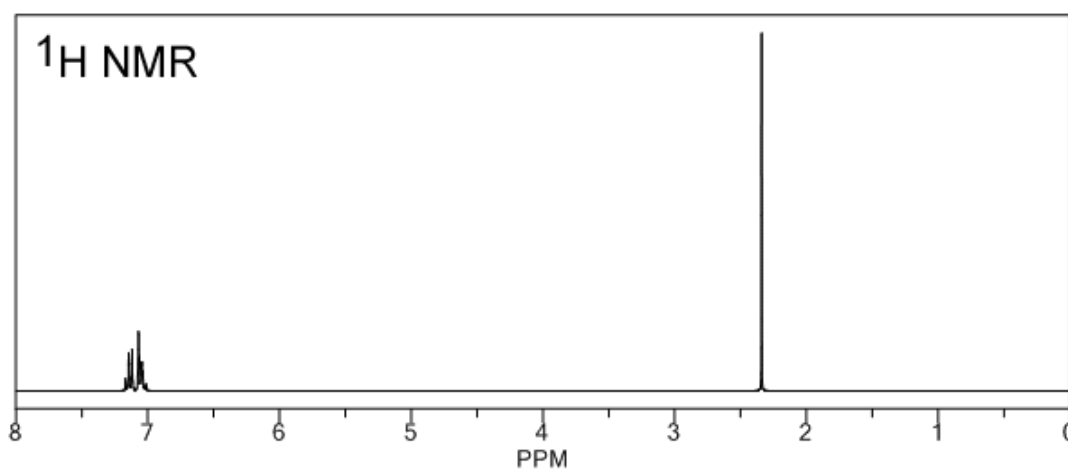


Figure 13. Example of a ^1H NMR spectrum of toluene

The chemical shift, plotted on the x-axis, is a relative value derived from the difference between the signal frequency of the analyte and the frequency of the signal from a known standard (usually TMS). It is expressed in ppm. Different functional groups produce signals with characteristic chemical shifts, allowing them to be identified.

The integration of the signals indicates the proportion of nuclei present in each environment. The signal for each magnetic environment can be split into multiple lines. This occurs as a result of multiple magnetic nuclei interacting with and influencing the magnetic field of others in the vicinity. The splitting is described in terms of *J*, the spin-spin coupling constant, given in Hz. Analysing the *J* values for nuclei therefore gives information about their closest neighbours.

Splitting can be seen in **Figure 13**, where the signal from the protons on the equivalent carbons *meta* to the CH₃ group is split by the neighbouring *para* and *ortho* environments.

When chemical shift, the integration of peaks and the *J* values are considered in conjunction with each other, it is possible to determine a great deal about the structure of the molecule (or molecules) present in a sample. For this reason, NMR spectroscopy is used extensively in organic synthesis; particularly when dealing with new compounds.

Analytical samples were run on a Bruker 'Avance' 400 Hz DPX NMR spectrometer, using d₆-DMSO as a solvent. Results were analysed using MestReNova software version 6.0.2-5475.

2.8. Catalyst characterisation

2.8.1. Microwave-plasma atomic emission spectroscopy^{87, 88}

Microwave-plasma atomic emission spectroscopy (MP-AES) is used to determine the concentration of an element or elements in a liquid sample. When used to analyse reaction mixtures, or solutions made from digested catalysts, it can be used to quantify leaching from supported metal catalysts.

In the MP-AES device a gas stream, typically argon or nitrogen, is excited by an external source (such as a magnetron) to generate a plasma. The liquid sample is then sprayed into this plasma, and microwave energy is conferred to the atoms present. This excites electrons in the sample which, on relaxing, emit energy of a characteristic frequency. This is recorded by a detector, and can be used to identify

the atoms present. The intensity of the signal is also recorded. When this data is compared to that obtained from standard solutions of known concentration, the concentration of the element in an unknown sample can be calculated.

MP-AES analysis was carried out on an Agilent 4100 MP-AES system. Catalyst samples were digested in *aqua regia* for 18 h. After this time, high purity H₂O was added to produce appropriately concentrated solutions. All sample solutions were filtered through 0.45 µM PTFE syringe filters to remove particulates prior to analysis.

2.8.2. Inductively coupled plasma atomic emission spectroscopy⁸⁹

Similar in principle to MP-AES (described in section 2.8.1) inductively coupled plasma atomic emission spectroscopy (ICP-AES, commonly referred to as ICP or ICP analysis) also provides information on the concentration of an element or elements in a sample.

In this case, a plasma is generated by exposure to an intense electromagnetic field. As in the case of MP-AES, the liquid sample is then sprayed through the plasma and resulting atomic emissions recorded by the detector. ICP-AES is considerably more sensitive than MP-AES, but more costly to run.

ICP analysis was carried out on an Agilent 7900 ICP-MS system.

2.8.3. Temperature programmed reduction^{90,91}

Temperature programmed reduction (TPR) can be used to assess the reduction temperatures of metal oxides and alloys, and when applied in conjunction with other techniques may help identify surface species.

A simple TPR apparatus consists of a sample loop, connected to a controlled gas supply and placed inside a heating jacket or furnace. The sample, in this case the dry powdered catalyst prior to any reduction or heat treatment procedure, is placed in the sample loop and secured there using quartz wool. A thermocouple is placed inside the loop to allow the temperature to be monitored. The loop is then placed in the furnace or heating jacket, secured into the gas line and checked for any leaks.

To carry out temperature programmed reduction, a reducing gas or gas mixture must be used, e.g. 10% H₂ in Ar. The similar techniques of temperature programmed desorption and temperature programmed oxidation utilise gases that will adsorb and then desorb from the surface and oxidise the surface respectively.

The gas supply is typically controlled accurately *via* an electronic flow controller (EFC). Prior to analysis, air is removed from the sample loop by passing an inert gas through it. The sample is then prepared for analysis by a pre-treatment step. This usually involves passing an inert gas over the sample at a fixed temperature for a set time, to scrub physisorbed species such as water from the surface. The reducing gas or gas mixture is then supplied. While the catalyst is exposed to the reducing gas, the temperature inside the sample loop is steadily increased by heating the furnace. When the unreduced metal species in the sample reaches the required temperature, hydrogen is consumed and the metal reduced. The temperature at which this happens is characteristic of the species; but may be reduced or increased as a result of alloying or interactions with the support.

The consumption of hydrogen changes the composition of the gas feed. This in turn alters the thermal conductivity of the feed, and so a thermal conductivity detector (TCD) can be used.

In the TCD, the thermal conductivity of a reference sample of carrier gas is measured. This is compared against the thermal conductivity of the sample gas stream. When an analyte compound elutes, the thermal conductivity of the gas stream typically decreases, causing a measurable difference in the values for reference gas and sample. This produces a signal which can be plotted (y-axis) against temperature (x-axis).

Alternatively, a mass spectrometer can be used as a detector.

Temperature programmed reduction was carried out on a Quantachrome ChemBET PULSAR TPR/TPD with a TCD. Samples were scrubbed with nitrogen prior to reduction.

2.8.4. CO chemisorption^{92, 93}

Chemisorption analysis involves probing nanoparticle structures by exploiting the adsorption properties of different kinds of site. CO chemisorption is one of the most commonly utilised methods, due to the well-defined binding behaviour of CO to some metals.

CO molecules can bind in two ways; linearly, in which the CO molecule binds to one metal atom *via* the σ orbital of the carbon atom; or in a bridging fashion, which can occur between two, three or (rarely) four metal atoms by π bonding. The manner in which CO binds to the metal is determined by the nature of the sites available on the nanoparticle, the temperature, and the degree of CO coverage.

When the amount of metal present in a sample is known, the surface can be titrated using CO gas. In this case, a known quantity of catalyst sample would be placed in a sample loop and connected to a gas supply. The sample loop is often located in a furnace or heating jacket, as temperature can also affect CO binding behaviour. Prior to analysis, the sample must be 'scrubbed' to remove surface bound species. This can be done simply by passing inert carrier gas over the sample. When this is complete, CO can be delivered into the system from a gas sampling loop of known volume. Therefore a known amount of CO passes over the sample, where some adsorbs to relevant metal sites. The remainder passes with the carrier gas out to the detector. A TCD is typically used (described in section 2.8.3.). For each subsequent injection of CO, the amount absorbed decreases as the surface becomes saturated. When fully saturated, all CO passes through the sample loop to the detector, resulting in concurrent signals.

The size of the metal nanoparticles can then be calculated, based on the adsorbed volume of CO, the metal species present, the quantity of each metal species, and the temperature. This can further be used to calculate dispersion of nanoparticles on the surface. However, certain assumptions have to be made to do this. For instance, it is assumed that the metal present is entirely reduced, and that all CO present binds linearly.

CO chemisorption was carried out on a Quantachrome ChemBET PULSAR TPR/TPD. Samples were scrubbed with nitrogen prior to reduction in situ and subsequent analysis.

2.8.5. X-ray powder diffraction⁹⁴

Powder X-ray diffraction or x-ray diffraction (XRD) is an analytical technique that utilises x-ray radiation to provide information on the bulk properties of crystalline powder samples. The information obtained is an averaged result of all signals, and therefore it is vitally important that the sample be homogenised prior to analysis; usually by grinding.

The homogenised powder sample is loaded into a holder, taking care to ensure an even, unbroken surface. X-ray radiation is generated in an x-ray tube, typically by heating a filament in a cathode ray tube apparatus, and passed through a filter to ensure the beam is monochromatic. The beam is incident upon the sample surface, and is reflected off it to the detector. The sample or x-ray source is then rotated to change the angle of incidence and the process repeated.

At particular incident angles, depending on the unit cell geometry of the sample, the Bragg equation, given below, is satisfied. When the Bragg condition is fulfilled, the waves incident on the sample undergo constructive interference, and this produces a more intense signal. This produces a peak in the resulting x-ray diffraction pattern.

$$2d\sin\theta = n\lambda$$

Where d is the separation between layers, θ is the angle of incident radiation, n is the order and λ is wavelength.

The patterns obtained by this analysis are characteristic of particular crystalline phases of materials, allowing them to be identified by reference to existing databases.

X-ray powder diffraction was carried out on a Panalytical X'pert Pro diffractometer using Ni filtered CuK α radiation.

2.8.6. X-ray photoelectron spectroscopy⁹⁵

X-ray photoelectron spectroscopy (XPS) is used to study the elemental composition of surfaces. When applied to heterogeneous catalysts, it is often used to determine the electronic state of metals supported on the surface, and identify surface species.

For analysis, the sample must be under ultra-high vacuum. When in position and under vacuum, the sample is exposed to monochromatic x-ray radiation. This excites and liberates electrons from the surface of the analyte. The electrons are collected by a lens and relayed to an electron detector, which counts them and determines their kinetic energy. From this, the binding energy can be determined using the equation:

$$BE = h\nu - KE$$

Where BE is binding energy, KE is kinetic energy of the electrons, and $h\nu$ is the energy of the photon, consisting of h , Planck's constant, and ν frequency.

This binding energy is characteristic of the particular element, and the electronic configuration from which the electron was liberated. The number of electrons detected from each element is proportional to the amount of that element present in the scanned area.

The number of electrons detected is plotted (y-axis) against their binding energy (x-axis) to give an XPS spectrum. This pattern is characteristic of the elements involved.

X-ray photoelectron spectroscopy was carried out on a Kratos Axis Ultra DLD spectrometer using monochromatic AlK α radiation.

2.9. References

1. Manufacturer's information, Alfa Aesar, <https://www.alfa.com/en/>).
2. Manufacturer's information, Sigma-Aldrich, <https://www.sigmaaldrich.com/united-kingdom.html>).
3. G. J. Hutchings and C. J. Kiely, *Accounts of Chemical Research*, 2013, **46**, 1759-1772.
4. M. Sankar, Q. He, M. Morad, J. Pritchard, S. J. Freakley, J. K. Edwards, S. H. Taylor, D. J. Morgan, A. F. Carley, D. W. Knight, C. J. Kiely and G. J. Hutchings, *Acs Nano*, 2012, **6**, 6600-6613.
5. Gas Chromatography, <http://www.gas-chromatography.net/gas-chromatography.php>, (accessed 25/03/18).
6. Gas Chromatography, https://chem.libretexts.org/Core/Analytical_Chemistry/Instrumental_Analysis/Chromatography/Gas_Chromatography, 25/03/18).
7. Gas Chromatography, <https://www.agilent.com/en-us/products/gas-chromatography>, (accessed 25/03/18).
8. Gas Chromatography Mass Spectrometry (GC/MS), <http://www.bris.ac.uk/nerclsmf/techniques/gcms.html>, (accessed 25/03/18).
9. Gas Chromatography Mass Spectrometry (GC/MS) Information, <https://www.thermofisher.com/uk/en/home/industrial/mass-spectrometry/mass-spectrometry-learning-center/gas-chromatography-mass-spectrometry-gc-ms-information.html>, (accessed 25/03/18).
10. Nuclear Magnetic Resonance, <https://www.cardiff.ac.uk/chemistry/research/facilities/nuclear-magnetic-resonance>).
11. Nuclear Magnetic Resonance, <https://www.bruker.com/products/mr/nmr.html>, (accessed 25/03/18).
12. J. D. Roberts, *Journal of Chemical Education*, 1961, **38**, 581.
13. *Journal*.

14. 4100 MP-AES, <https://www.agilent.com/en/products/mp-aes/mp-aes-systems/4100-mp-aes>, 25/03/18).
15. 7900 ICP-MS, <https://www.agilent.com/en/products/icp-ms/icp-ms-systems/7900-icp-ms>, (accessed 25/03/18).
16. N. W. Hurst, S. J. Gentry, A. Jones and B. D. McNicol, *Catalysis Reviews*, 1982, **24**, 233-309.
17. S. Subramanian, *Platinum Metals Review*, 1992.
18. Carrying Out Dispersion Measurements by CO Pulse Chemisorption, <https://www.azom.com/article.aspx?ArticleID=12246>, (accessed 25/03/18).
19. C.-H. Yang and J. G. Goodwin, 1982, **20**, 13-18.
20. Powder X-ray Diffraction, https://chem.libretexts.org/Core/Analytical_Chemistry/Instrumental_Analysis/Diffraction_Scattering_Techniques/Powder_X-ray_Diffraction, (accessed 25/03/18).
21. What is X-ray Photoelectron Spectroscopy (XPS)?, <https://xpssimplified.com/whatisxps.php>, (accessed 20/03/18).

Chapter Three – Toluene Oxidation

3.1. Introduction

In this chapter, results for the investigation into partial oxidation of toluene are presented.

Per the project aims described in Chapter One, section 1.6., the focus of this work was selective oxidation under mild conditions. Experimental conditions were chosen based on previously reported results with supported precious metal catalysts. Tertiary-butylhydroperoxide (tBHP) was selected as an oxidant due to its high activity, radical initiation properties and environmental friendliness^{96, 97}.

Initial studies were carried out in the glass reactor setup described in Chapter 2, section 2.5.2. It was quickly established that this arrangement was not suitable and subsequent work was carried out in the Radleys reactor. The reasons for this are described in more detail in section 3.2.2.

Preliminary work concentrated on the previously reported catalysts AuPd/TiO₂ and PtPd/TiO₂. These catalysts were tested in both the glass reactor and Radleys reactor setup, establishing the viability of the chosen conditions and apparatus. These results also served as a useful benchmark against which other catalysts could be compared.

The study was then extended to another palladium alloy catalyst, RuPd/TiO₂. This catalyst proved not only to be active, but to display some highly unusual behaviour that warranted further investigation.

All results reported are an averaged value of three or more runs with mass balances $\geq 94\%$.

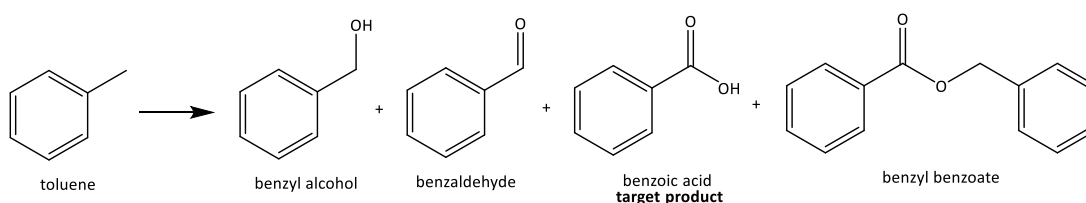


Figure 9. Toluene oxidation scheme

3.2. Oxidation reactions in the glass reactor

3.2.1. Blank reactions

Reactions were run in the absence of a catalyst to ensure no auto-oxidation occurred under the reaction conditions. The results are shown in **Figure 2**. Conditions and reactor setup are described in Chapter 2, section 2.6.2. Carbon balances for these reactions were >98%.

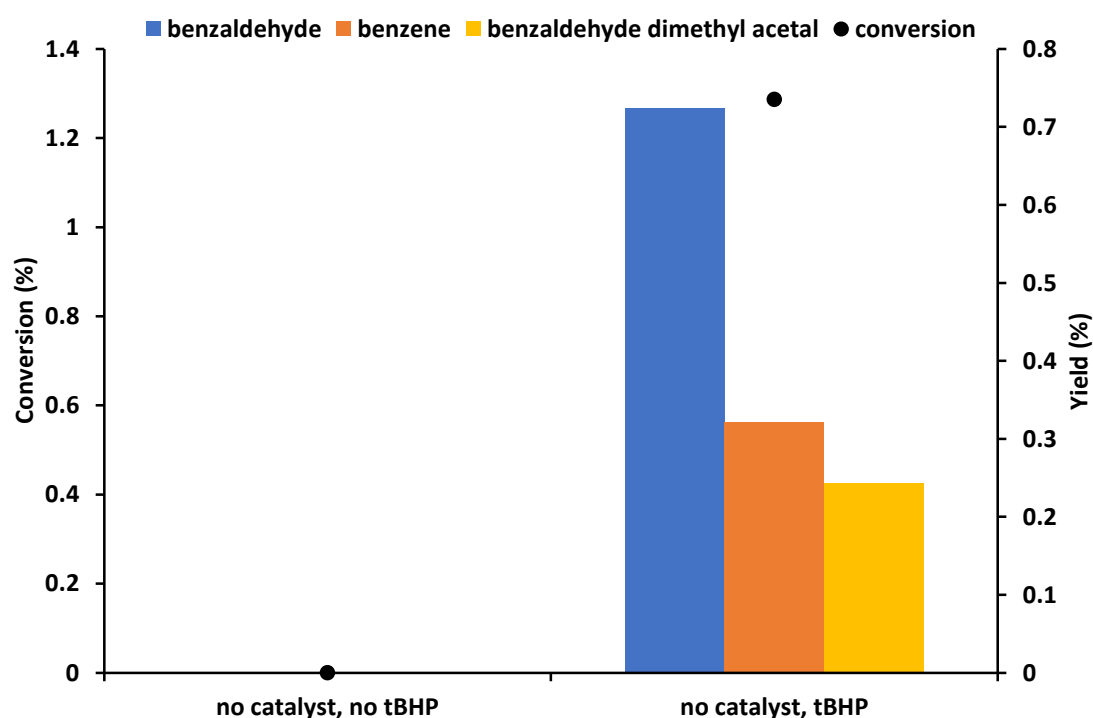


Figure 2. Oxidation of toluene in the absence of catalyst

Reaction conditions: 47 mmol toluene, 47 mmol tBHP supplied as 70 wt% solution in water (where applicable), 80°C, 24 h, 1000 rpm stirring.

In the absence of catalyst and tBHP, no oxidation occurs. When tBHP is present, there is low conversion of 1.3%. This is likely the result of auto-oxidation of toluene triggered by radical species generated by the breakdown of tBHP³⁶. Approximately 6% of the supplied tBHP was converted to t-BuOH during the reaction. The products of the auto-oxidation reaction were benzaldehyde, benzene and benzaldehyde dimethyl acetal, with benzaldehyde being the preferred product.

3.2.2. Oxidation reactions with AuPd, PtPd and RuPd

AuPd/TiO₂ and PtPd/TiO₂ catalysts prepared by the sol immobilisation technique have been found to be active for the oxidation of several alkyl aromatic species, including toluene⁹⁸⁻¹⁰⁰. This activity can be attributed to the high activity and selectivity displayed by Au and Pt for oxidation chemistry, the beneficial effects of alloying with palladium and the small particle size achieved by preparing the catalysts *via* the sol immobilisation method³⁴ (described in Chapter Two, section 2.4.1.), which is beneficial for catalyst activity and presents a high number of active sites.

The viability of the glass reactor system and the selected reaction conditions were tested by applying 1 wt.% Au_{0.36}Pd_{0.64}/TiO₂ and 1 wt.% Pt_{0.35}Pd_{0.65}/TiO₂ catalysts prepared by sol immobilisation for toluene oxidation. Results are presented in **Figure 3a**, and the breakdown of other products in **Figure 3b**. Carbon balances for these reactions were >96%; the loss is potentially due to cracked products not detected by the GC.

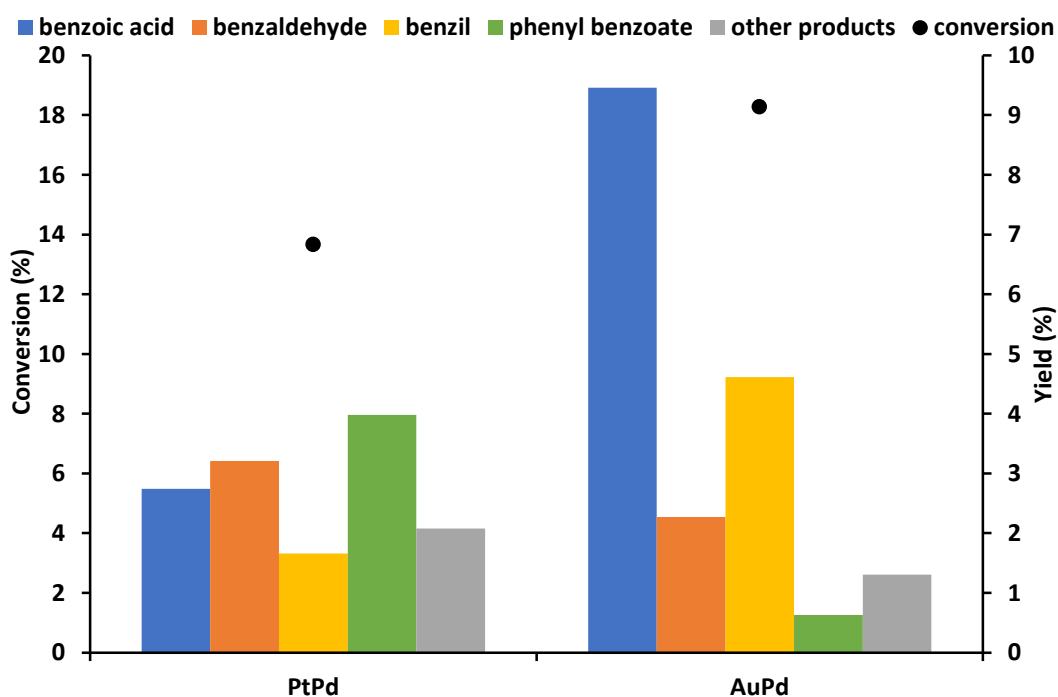


Figure 3a. Comparison of sol immobilisation catalysts in glass reactor

Reaction conditions: *Molar ratio substrate:metal 6500:1, 47 mmol toluene, 47 mmol tBHP supplied as 70 wt.% solution in water, 80°C, 24 h, 1000 rpm stirring.*

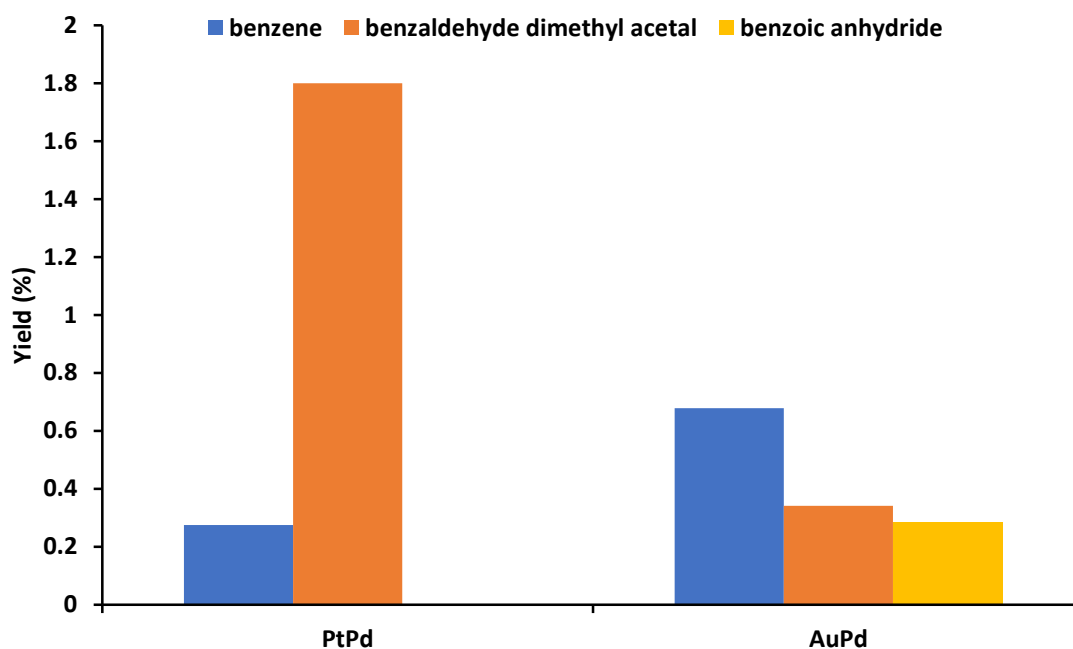


Figure 3b. Distribution of 'other products' obtained from sol immobilisation catalysts in glass reactor

Reaction conditions: *Molar ratio substrate:metal 6500:1, 47 mmol toluene, 47 mmol tBHP supplied as 70 wt.% solution in water, 80°C, 24 h, 1000 rpm stirring.*

Both catalysts demonstrate toluene oxidation far in excess of the tBHP only reaction under these conditions, thus indicating that the testing method is valid. The 1 wt.% Au_{0.36}Pd_{0.64}/TiO₂ catalyst achieves higher conversion than the platinum equivalent, 1 wt.% Pt_{0.35}Pd_{0.65}/TiO₂. The gold catalyst is also far more selective to benzoic acid. This is consistent with the literature for toluene oxidation (discussed in Chapter One, section 1.5.1.) which describes the tendency of the reaction to be more selective to benzoic acid at higher conversions, as benzaldehyde is oxidised to the acid. Both catalysts produce products tentatively identified as benzil and phenyl benzoate (based on retention time, solubility, polarity and colour), in significant amounts. The AuPd catalyst also produced very small quantities of benzoic anhydride, which was not detected in blank reactions. The absence of benzyl alcohol as a product is also notable, suggesting this product has undergone a secondary oxidation.

A scheme of reaction products is shown in **Figure 4**.

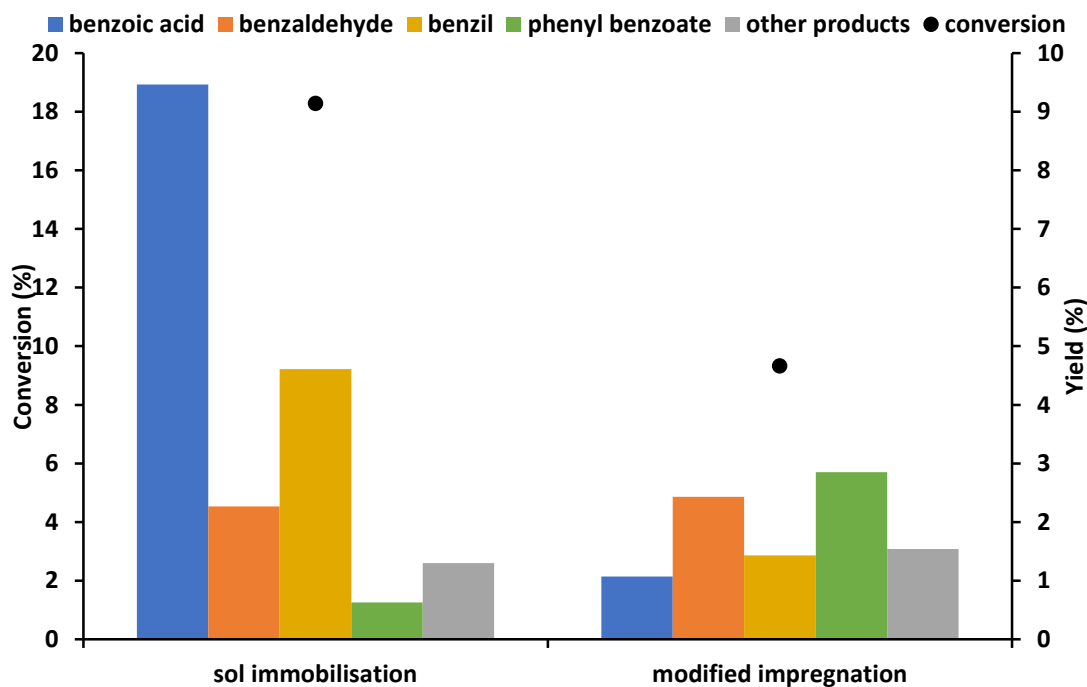


Figure 5a. Activity of 1 wt.% Au_{0.36}Pd_{0.64}/TiO₂ catalysts prepared by different methods

Reaction conditions: *Molar ratio substrate:metal 6500:1, 47 mmol toluene, 47 mmol tBHP supplied as 70 wt.% solution in water, 80°C, 24 h, 1000 rpm stirring.*

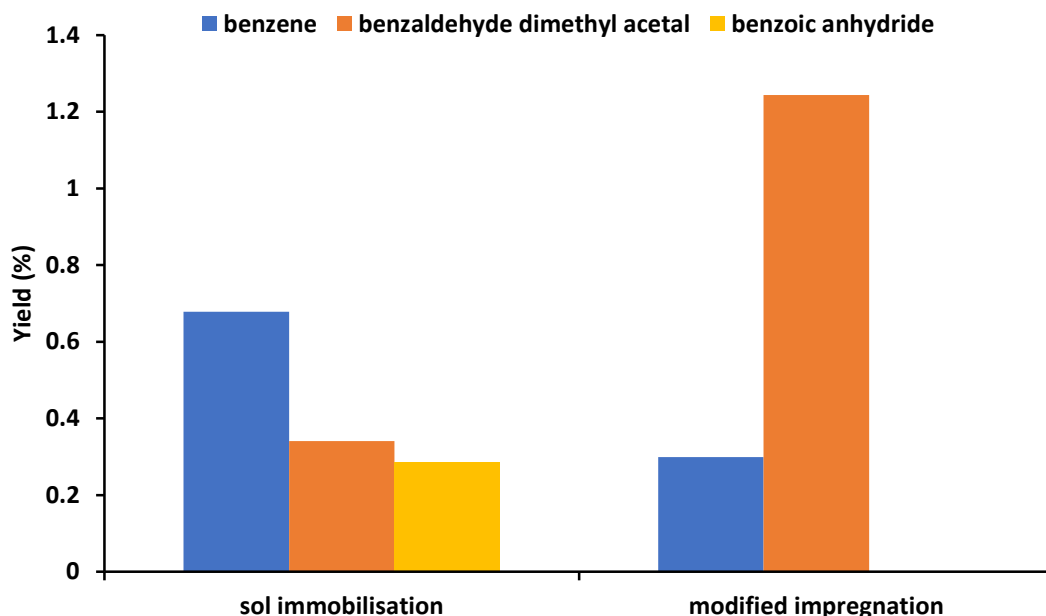


Figure 5b. 'Other products' of 1 wt.% Au_{0.36}Pd_{0.64}/TiO₂ catalysts

Reaction conditions: *Molar ratio substrate:metal 6500:1, 47 mmol toluene, 47 mmol tBHP supplied as 70 wt.% solution in water, 80°C, 24 h, 1000 rpm stirring.*

As it was the purpose of this study to replace gold with an alternative metal, other palladium alloys were considered. The results obtained with the sol immobilised 1 wt.% Pt_{0.35}Pd_{0.65}/TiO₂ catalyst were not encouraging, and so attention was given to ruthenium-palladium alloys. 1 wt.% RuPd/TiO₂ has been reported for catalytic hydrogenation of levulinic acid, a reaction for which 1 wt.% AuPd/TiO₂ is also active¹⁰¹. For that reaction, 1 wt.% RuPd/TiO₂ was found to offer high stability and very high activity, superior to that of the 1 wt.% AuPd/TiO₂ catalyst prepared by the same modified impregnation method.

1 wt.% Ru_{0.50}Pd_{0.50}/TiO₂ was prepared by modified impregnation and tested for toluene oxidation. 1 wt.% Au_{0.50}Pd_{0.50}/TiO₂ was prepared by the same method and also tested for the sake of comparison. Results are shown in **Figure 6a** and **Figure 6b**. Carbon balances for these reactions were >95%.

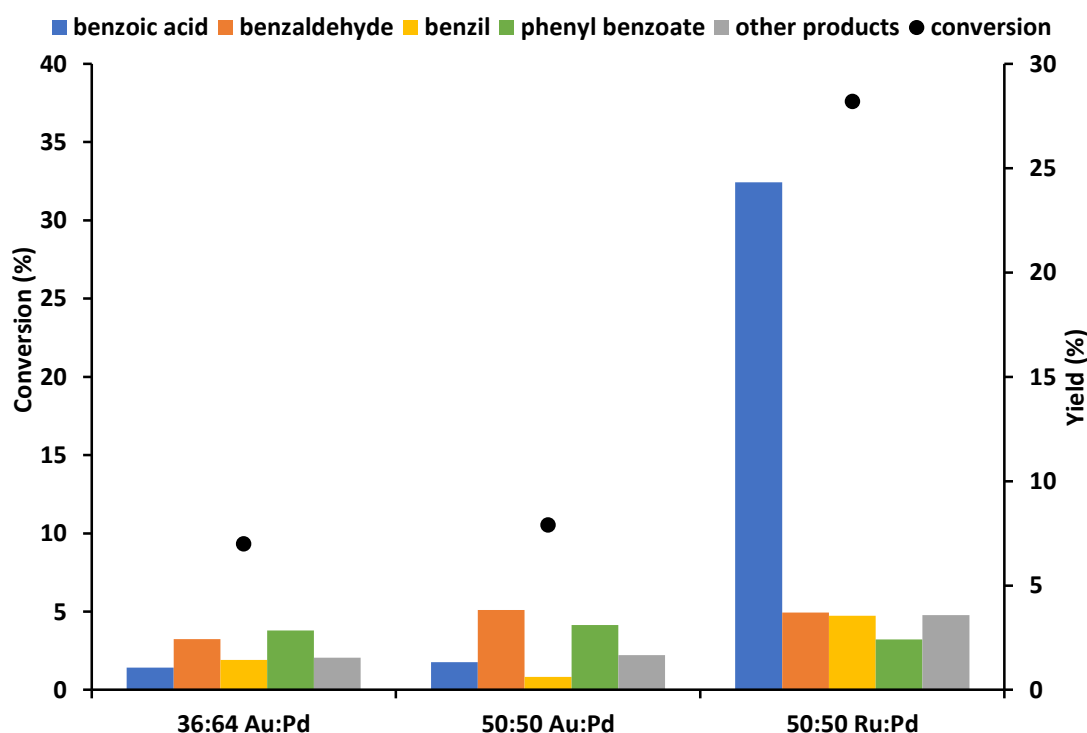


Figure 6a. Activity of catalysts prepared by modified impregnation method

Reaction conditions: *Molar ratio substrate:metal 6500:1, 47 mmol toluene, 47 mmol tBHP supplied as 70 wt.% solution in water, 80°C, 24 h, 1000 rpm stirring.*

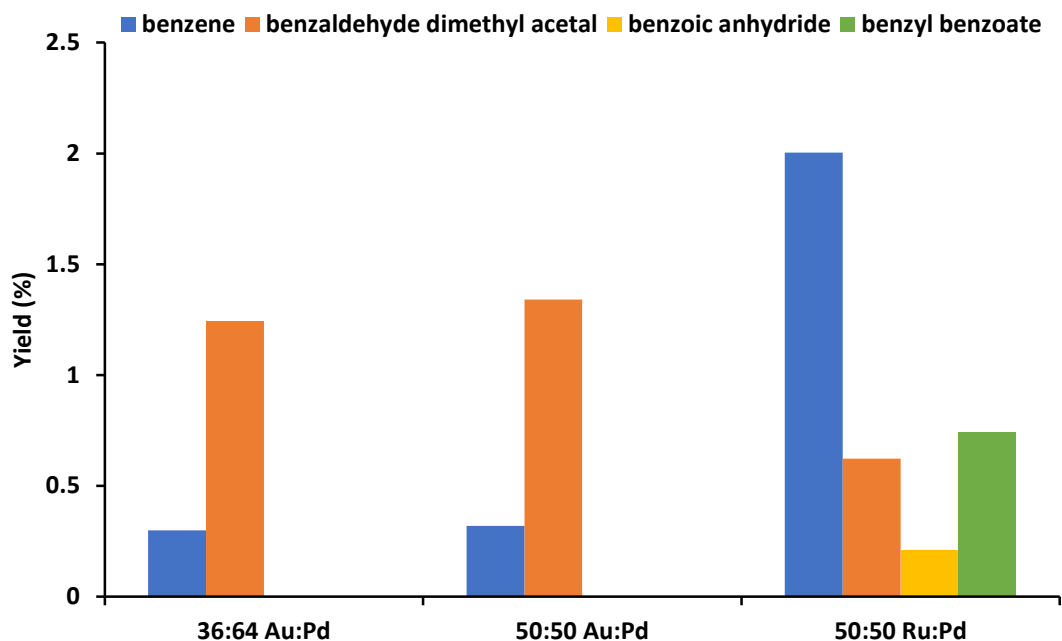


Figure 6b. 'Other products' of modified impregnation catalysts

Reaction conditions: *Molar ratio substrate:metal 6500:1, 47 mmol toluene, 47 mmol tBHP supplied as 70 wt.% solution in water, 80°C, 24 h, 1000 rpm stirring.*

It is evident from **Figure 6a** that the ruthenium-palladium catalyst demonstrates superior activity to the gold-palladium catalysts made by the same method. In fact, the 1 wt.% Ru_{0.50}Pd_{0.50}/TiO₂ catalyst also significantly improves on the results obtained with the 1 wt.% Au_{0.36}Pd_{0.64}/TiO₂ catalyst prepared by sol immobilisation. Once again, a corresponding improvement in selectivity to benzoic acid is observed at the improved conversion. The TOF reflects this: the gold palladium catalysts have TOF values of approximately 18 h⁻¹, whereas the TOF of the ruthenium-palladium catalyst is approximately 50 h⁻¹. This compares favourably with the 1.5 wt.% Au/γ-MnO₂ catalyst reported by Guomin *et al.*⁵⁸ which achieves a TOF value of 62.7 h⁻¹ when used at 160 °C and 10 bar O₂ in the presence of solvent.

Given the high activity of 1 wt.% Ru_{0.50}Pd_{0.50}/TiO₂, this catalyst was selected for further investigation.

However, it became apparent that carbon balances varied greatly for subsequent reactions. Multiple repeats of the same reaction – with all conditions being kept the same – could result in mass balances ranging from as little as 40% to 98%.

Reactions with a poor carbon balance correlated with a visible decrease in the liquid volume of the reaction, leading to the conclusion that product or substrate was lost from the reactor; most likely *via* evaporation. Decreasing the temperature of the water circulated through the condensers from room temperature to 7°C offered no improvement.

Further investigation suggested that the extraction rate of the fumehood in which the reactors were located was the controlling factor. This rate was not directly controllable from the hood itself, being part of a larger laboratory system. Observation indicated that the extraction rate varied greatly over time, even within as little as 24 h.

Several identical experiments were carried out with the 1 wt.% Ru_{0.50}Pd_{0.50}/TiO₂ catalyst on different days. The extraction rate of the fumehood was noted when the reaction was started. A poor mass balance and visible loss of liquid volume was found to correlate with an increased rate of extraction, as shown in **Figure 7**.

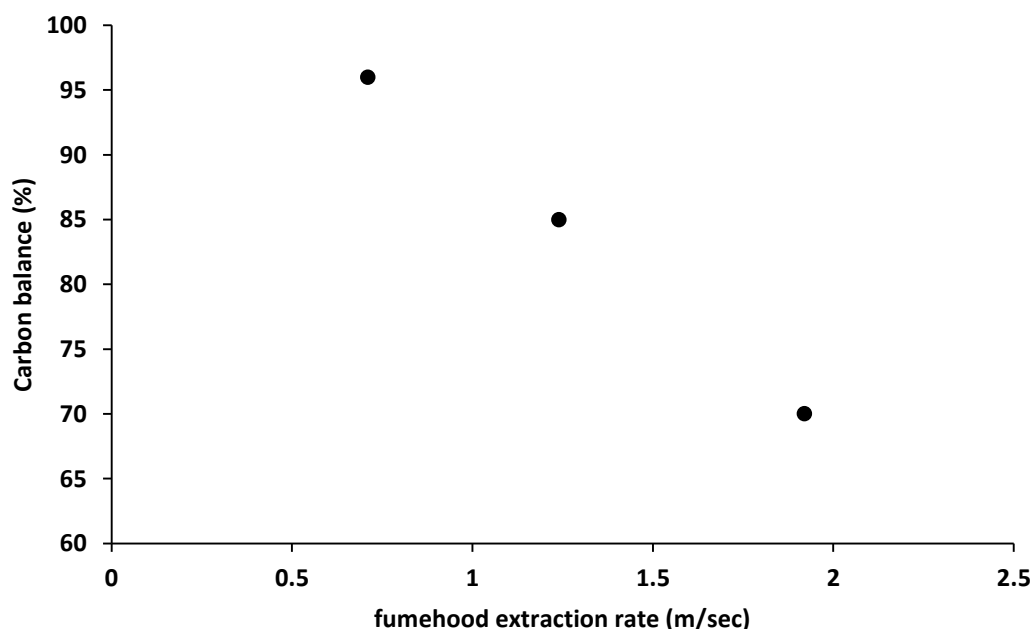


Figure 7. Relationship between fumehood extraction and carbon balance

Reaction conditions: *Molar ratio substrate:metal 6500:1, 47 mmol toluene, 47 mmol tBHP supplied as 70 wt.% solution in water, 80°C, 24 h, 1000 rpm stirring.*

As the fumehood extraction rate could not be adequately controlled, it was necessary to move to an isolated system. For this reason, the investigation was moved into the Radleys Multipot 'Starfish' Reactor, described in Chapter Two, section 2.5.1.

3.3. Oxidation reactions in the Radleys reactor

3.3.1. Blank reactions

To ensure that no auto-oxidation takes place under the selected conditions in this reactor, reactions were run in the absence of catalyst. This is particularly important in the Radleys reactor rather than the glass reactor setup, as in this case the reactants are under slight pressure. Results are shown in **Figure 8**. Carbon balances for these reactions were >97%.

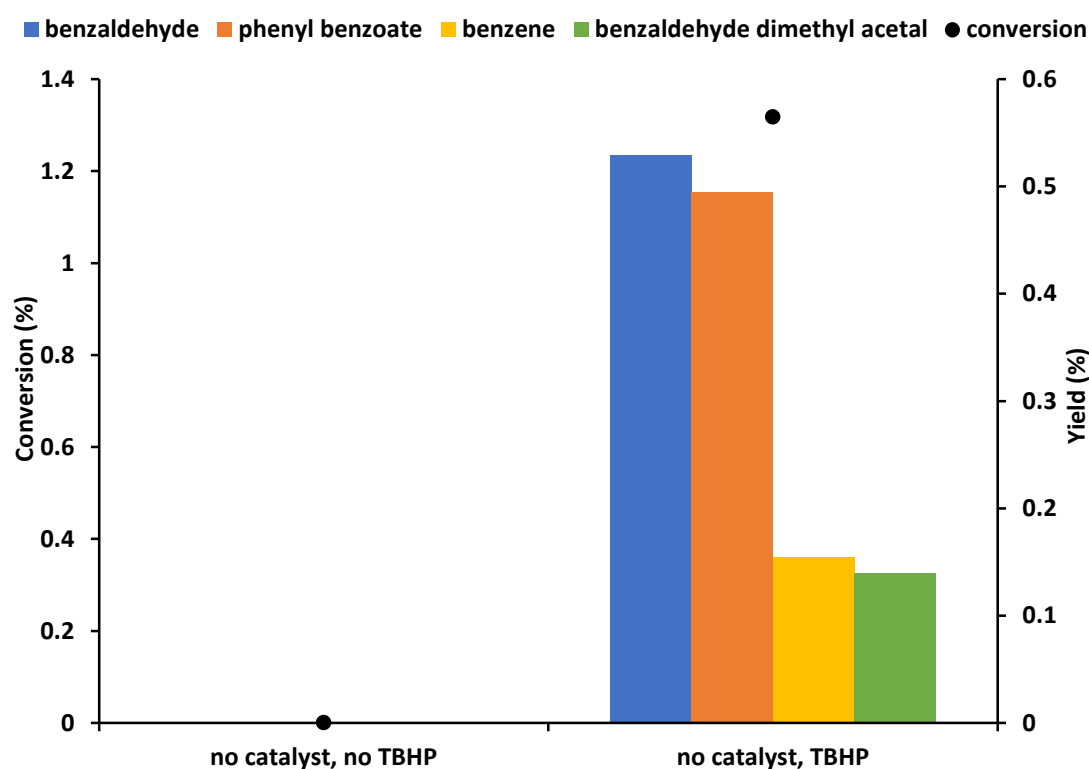


Figure 8. Blank reactions in the Radleys reactor

Reaction conditions: 24 mmol toluene, 24 mmol tBHP supplied as 70 wt.% solution in water (where applicable), 80 °C, 24 h, 1000 rpm stirring.

The results of the blank reactions in the Radleys reactor are consistent with those obtained in the glass reactor system. When only toluene is present, no conversion is observed, i.e. auto-oxidation is insignificant. When tBHP is present, but no catalyst, 1.1% conversion is observed from the auto-oxidation reaction catalysed by radicals derived from tBHP. This reaction is unselective, forming benzaldehyde and phenyl benzoate in around 0.5% yield (yield calculated using an estimated response factor). The other products in this case were benzene and benzaldehyde dimethyl acetal, obtained in yields of 0.15% and 0.14% respectively in the presence of tBHP.

3.3.2. Oxidation reactions with AuPd, PtPd and RuPd

The glass and Radleys systems differ in several ways, and do not necessarily produce the same results. This is discussed in detail in section 3.4.1. Briefly: reactions in the Radleys reactor are at half the scale of those in the glass reactor, the reactors use different heating methods, may have different stirring rates, and the glass reactor is open to air while the Radleys reactor vessels are sealed and at slight pressure. As such, the two reactors are not directly comparable, so it was appropriate to retest the catalysts investigated in section 3.2.2.

Therefore, 1 wt.% Pt_{0.35}Pd_{0.65}/TiO₂ and 1 wt.% Au_{0.36}Pd_{0.64}/TiO₂ catalysts prepared by the sol immobilisation technique were applied to toluene oxidation in the Radleys reactor. The results for both catalysts are presented in **Figure 9a**, and the distribution of other products in **Figure 9b**. Carbon balances for these reactions were >94%.

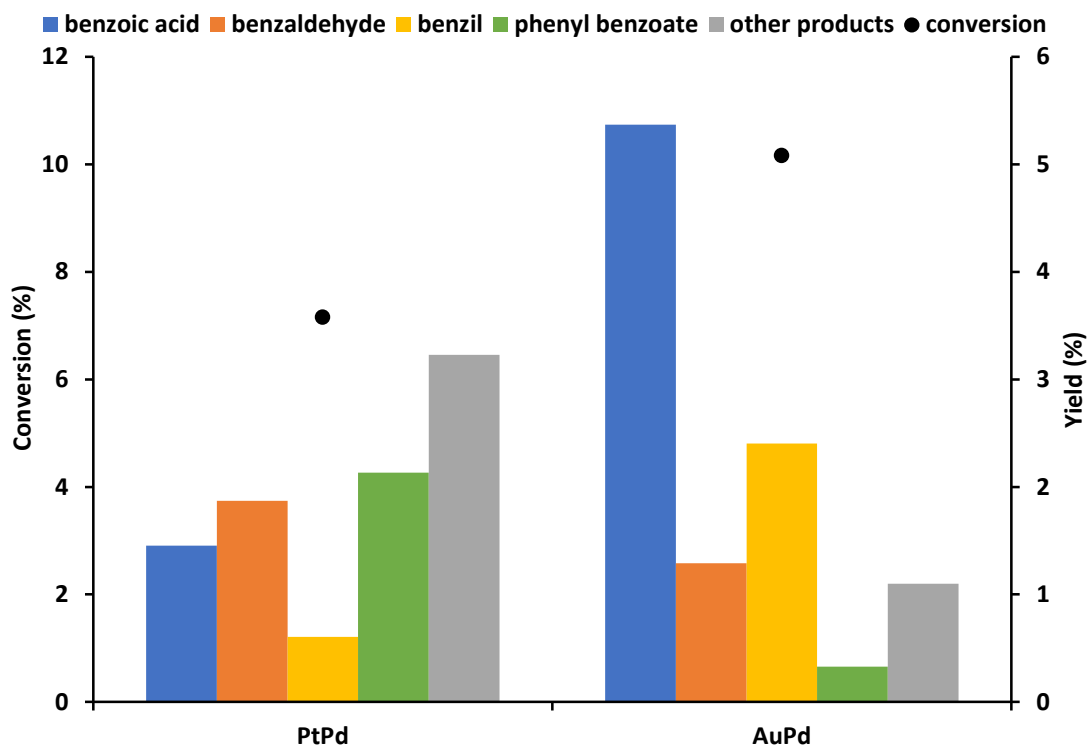


Figure 9a. Activity of sol immobilised catalysts in the Radleys reactor

Reaction conditions: *Molar ratio substrate:metal 6500:1, 24 mmol toluene, 24 mmol tBHP supplied as 70 wt.% solution in water, 80 °C, 24 h, 1000 rpm stirring.*

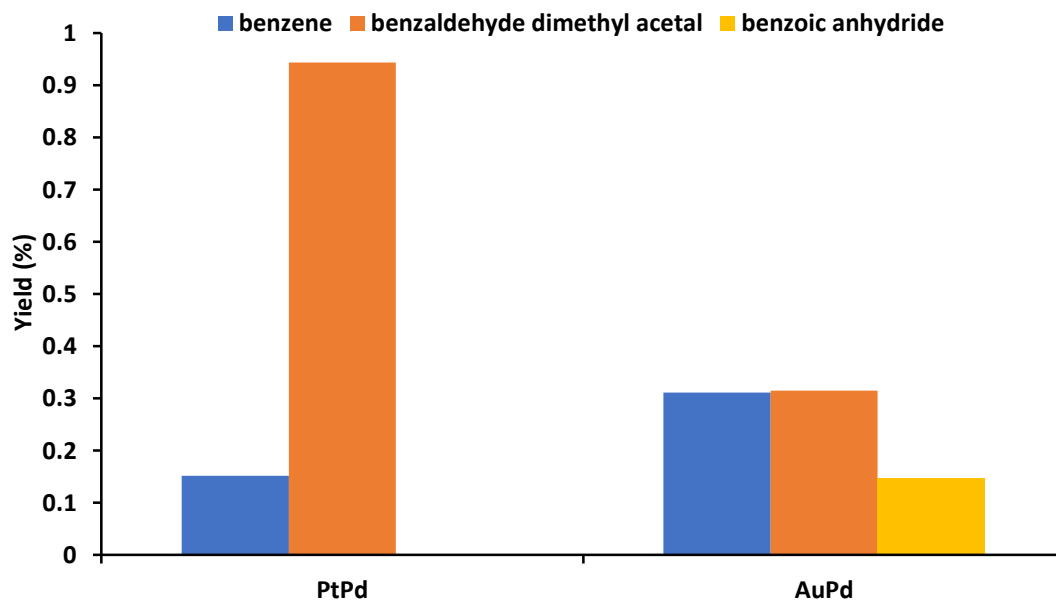


Figure 9b. Yields of 'other products' from sol immobilised catalysts in the Radleys reactor

Reaction conditions: *Molar ratio substrate:metal 6500:1, 24 mmol toluene, 24 mmol tBHP supplied as 70 wt.% solution in water, 80 °C, 24 h, 1000 rpm stirring.*

The sol immobilised catalysts achieve approximately half the conversion in the Radleys reactor that they achieved in the glass reactor system. However, the trends in activity and product distribution are consistent. In both cases, the gold-palladium catalyst is the more active and therefore selective to the target benzoic acid, though overall product yields are low.

The activity of the 1 wt.% Au_{0.36}Pd_{0.64}/TiO₂ catalyst prepared by sol immobilisation was compared to an equivalent catalyst prepared by modified impregnation. Results are presented in **Figure 10a**, and the distribution of other products in **Figure 10b**. Carbon balances for these reactions were >97%.

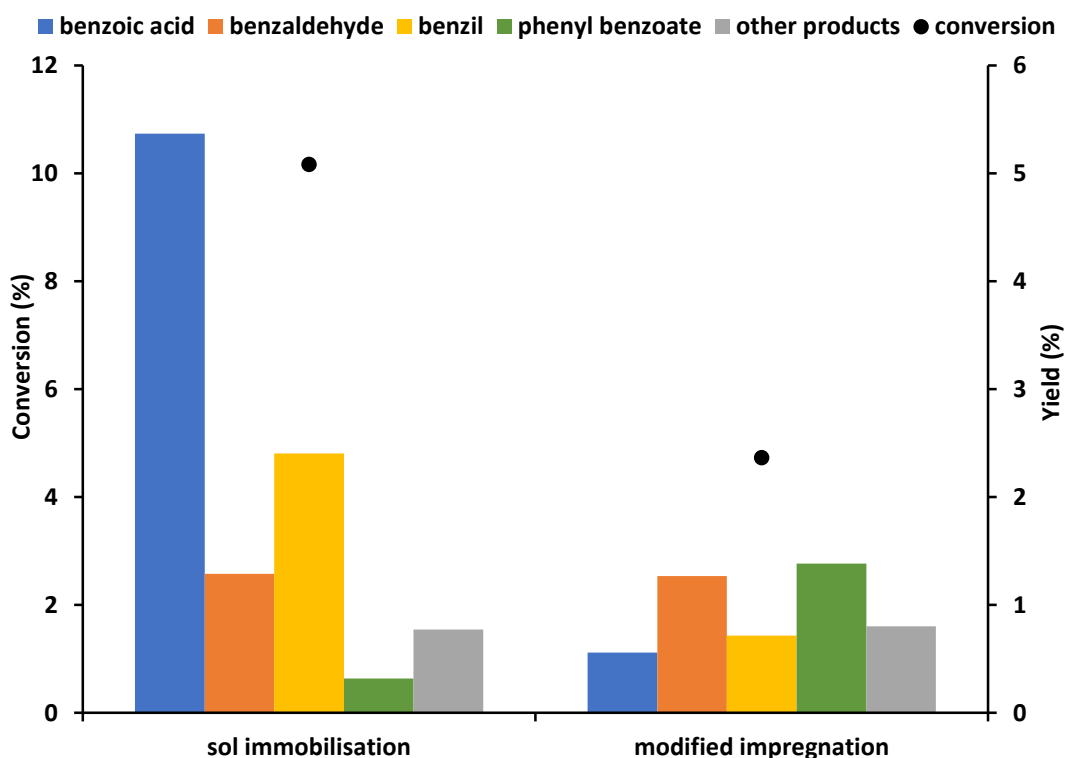


Figure 10a. Activity of 1 wt.% Au_{0.36}Pd_{0.64}/TiO₂ catalysts prepared by different methods

Reaction conditions: *Molar ratio substrate:metal 6500:1, 24 mmol toluene, 24 mmol tBHP supplied as 70 wt.% solution in water, 80 °C, 24 h, 1000 rpm stirring.*

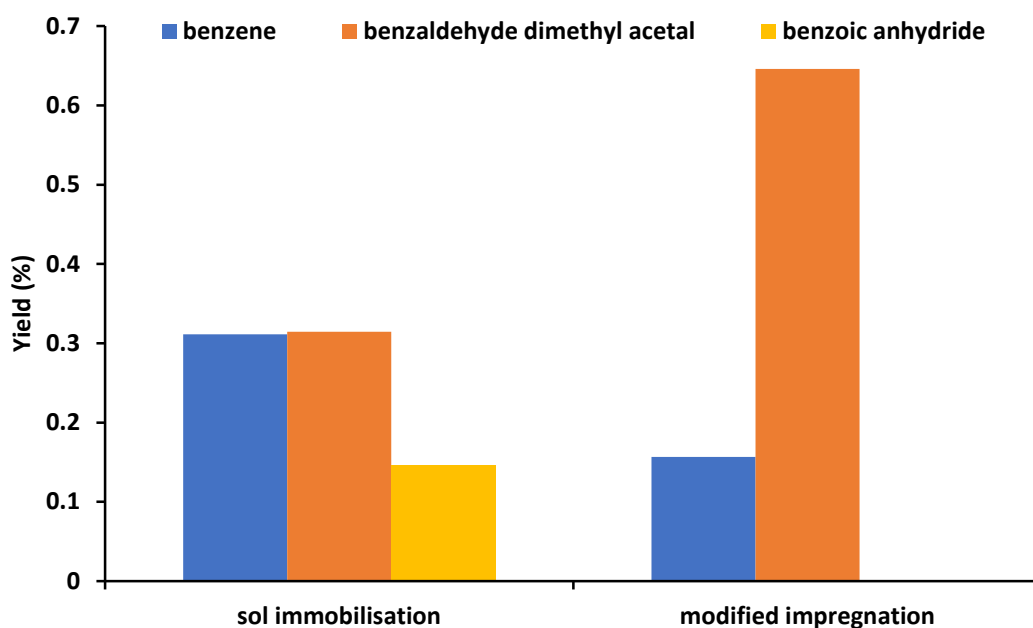


Figure 10b. Yields of 'other products' of 1 wt.% Au_{0.36}Pd_{0.64}/TiO₂ catalysts

Reaction conditions: *Molar ratio substrate:metal 6500:1, 24 mmol toluene, 24 mmol tBHP supplied as 70 wt.% solution in water, 80°C, 24 h, 1000 rpm stirring.*

Once again, the conversions achieved are approximately half that observed in the glass reactor, but trends remain the same. The sol immobilisation method is the more effective choice, achieving substantially greater conversion than the modified impregnation equivalent. Consequently, the selectivity to benzoic acid is significantly higher as well.

However, in the glass reactor it was shown that a ruthenium-palladium catalyst prepared in this manner was very active for toluene oxidation, and so modified impregnation catalysts were tested in the Radleys setup.

Results for 1 wt.% Au_{0.36}Pd_{0.64}/TiO₂, 1 wt.% Au_{0.50}Pd_{0.50}/TiO₂ and 1 wt.% Ru_{0.50}Pd_{0.50}/TiO₂ catalysts prepared by modified impregnation are compared in **Figure 11a**, and the distribution of other products in **Figure 11b**. Carbon balances for these reactions were >93%.

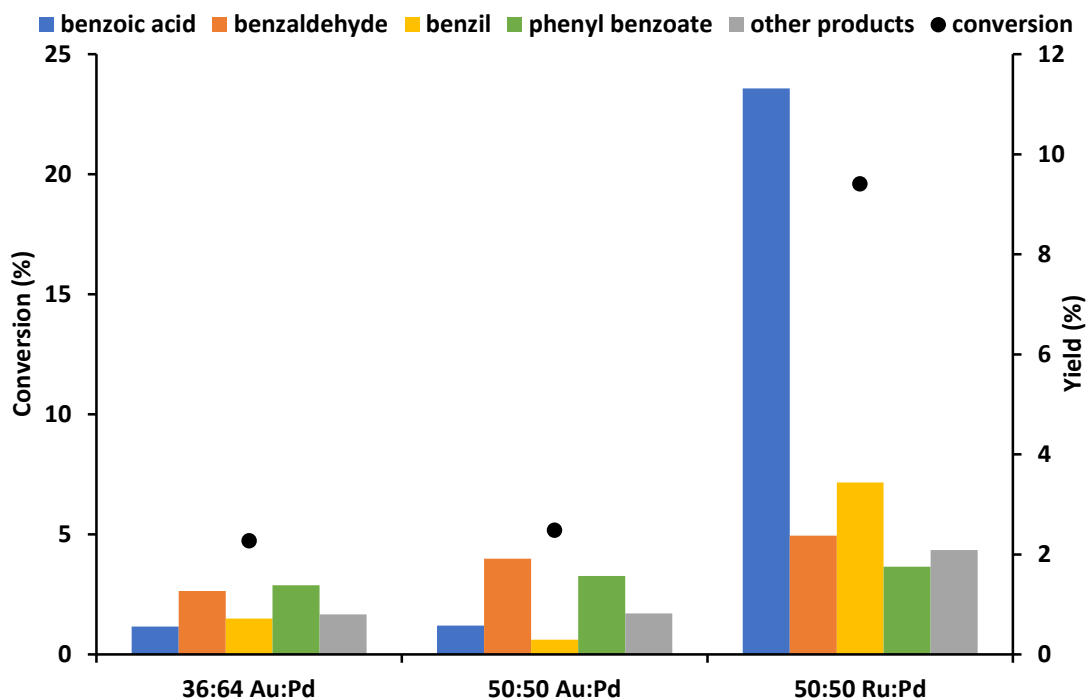


Figure 11a. Activity of 1 wt.% catalysts prepared by modified impregnation

Reaction conditions: *Molar ratio substrate:metal 6500:1, 24 mmol toluene, 24 mmol tBHP supplied as 70 wt.% solution in water, 80°C, 24 h, 1000 rpm stirring.*

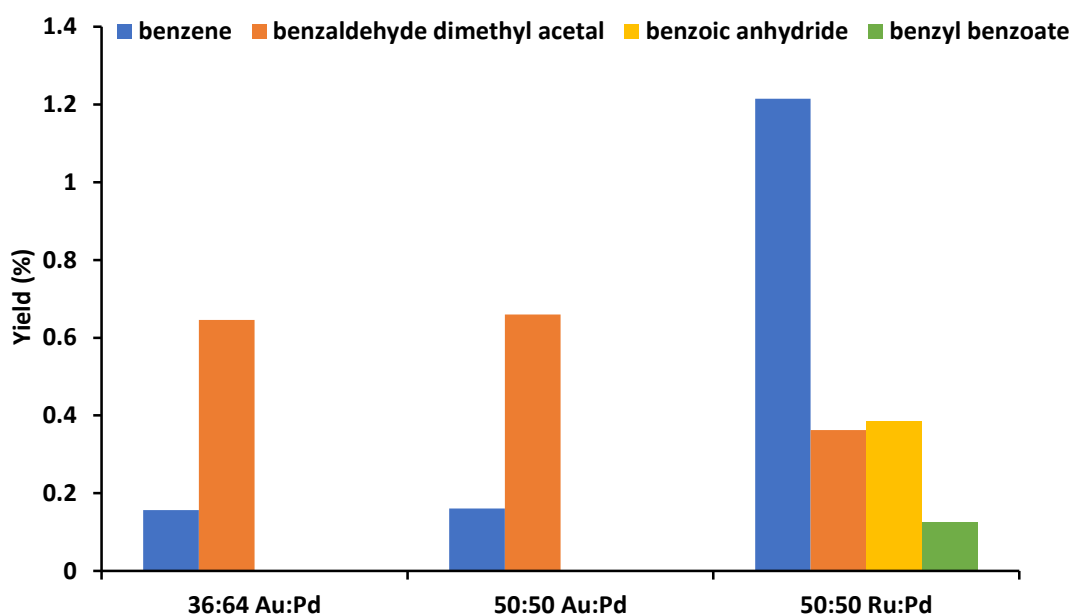


Figure 11b. Yields of 'other products' of 1 wt.% catalysts prepared by modified impregnation

Reaction conditions: *Molar ratio substrate:metal 6500:1, 24 mmol toluene, 24 mmol tBHP supplied as 70 wt.% solution in water, 80°C, 24 h, 1000 rpm stirring.*

The 1 wt.% RuPd/TiO₂ modified impregnation catalyst displays superior activity to the 1 wt.% AuPd/TiO₂ catalysts prepared by the same method, producing a higher conversion and thus yield of benzoic acid. The yield presented corresponds to 58% selectivity to benzoic acid. This indicates that ruthenium may be a suitable replacement for gold in catalysts for this reaction in this reactor, and thus this catalyst was investigated further.

The RuPd modified impregnation catalyst also produces small quantities of benzene, benzaldehyde dimethyl acetal, benzoic anhydride and benzyl benzoate as products. Neither benzoic anhydride or benzyl benzoate were observed when using AuPd modified impregnation catalysts, but benzyl benzoate has previously been reported for a AuPd catalyst⁶⁰.

3.3.3. Comparison of heterogeneous catalyst with catalyst precursors

It is known that in some cases, metal nanoparticles may leach from the support material into solution. This can occur in both aqueous and organic media. The homogeneous metal may then act as a catalyst for certain reactions, giving a false impression of an active heterogeneous catalyst.

To establish whether the precursors of the homogeneous metals or the support material, TiO₂, was responsible for the observed activity of the 1 wt.% Ru_{0.50}Pd_{0.50}/TiO₂ catalyst, the catalyst precursors were tested. The precursors of the 1 wt.% Ru_{0.50}Pd_{0.50}/TiO₂ catalyst are PdCl₂, RuCl₃ and TiO₂. These were assessed for toluene oxidation under the same conditions, singly and in combination. The moles of PdCl₂, RuCl₃ and TiO₂ used in each case were equivalent to the moles present in the reaction with the 1 wt.% Ru_{0.50}Pd_{0.50}/TiO₂ heterogeneous catalyst. The TiO₂ tested underwent the modified impregnation procedure (in the absence of any metal) to ensure similarity to the support of the finished catalyst. Results are shown in **Figure 12a**, and the distribution of the other products in **Figure 12b**.

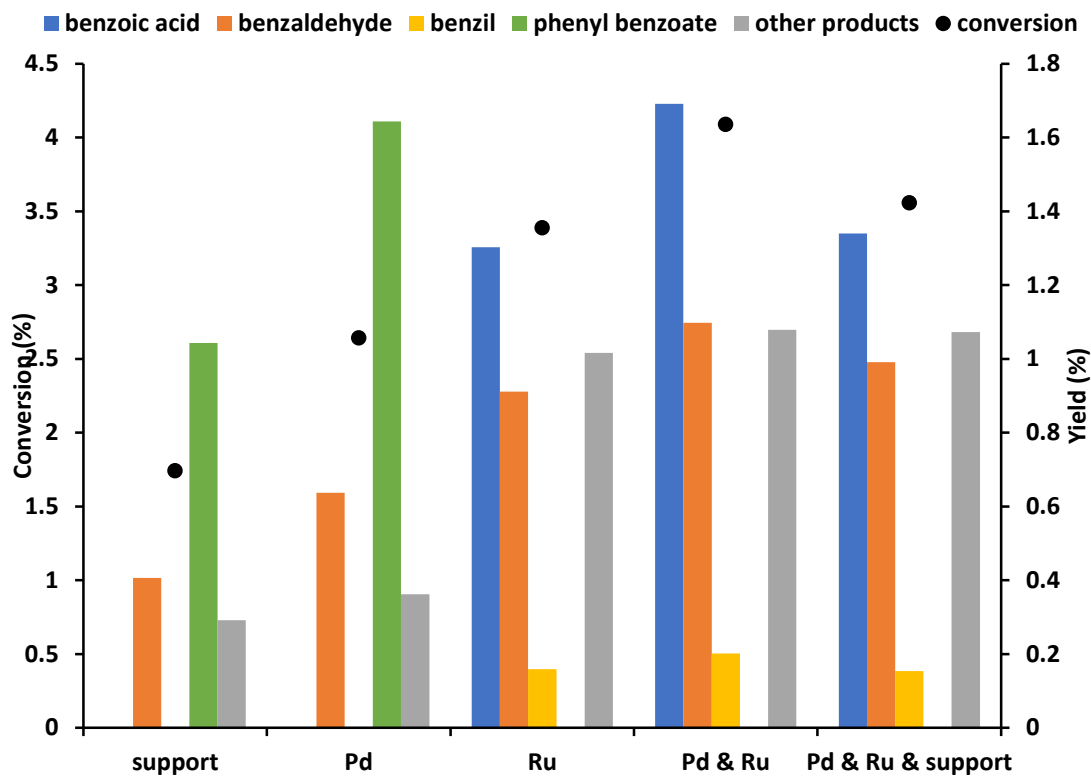


Figure 12a. Toluene oxidation by precursors of the 1 wt.% Ru_{0.50}Pd_{0.50}/TiO₂ catalyst

Reaction conditions: 24 mmol toluene, 24 mmol tBHP supplied as 70 wt.% solution in water, 80°C, 24 h, 1000 rpm stirring.

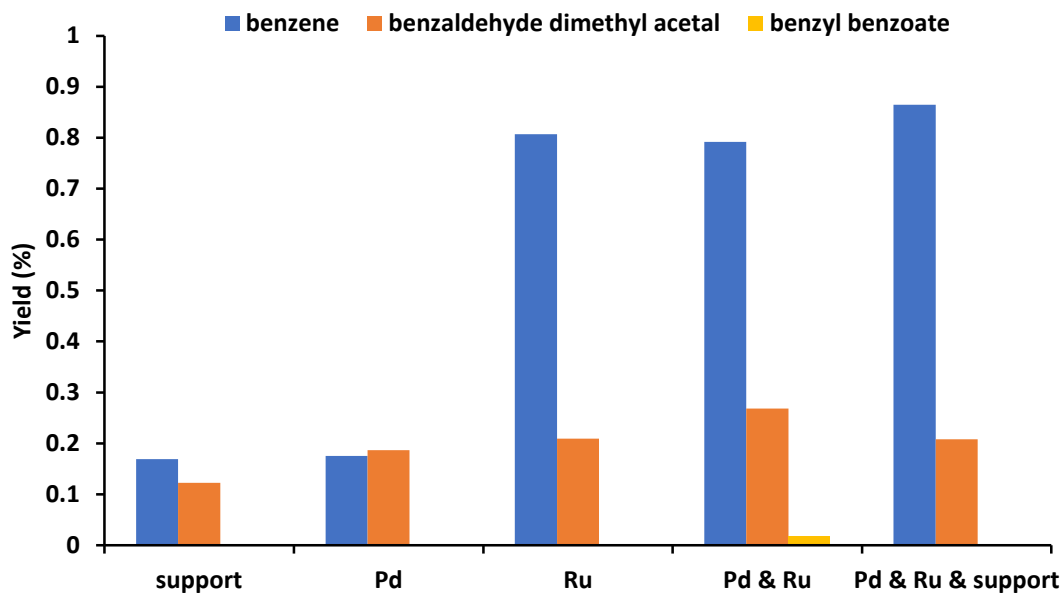


Figure 12b. Yields of 'other products' produced by precursors of the 1 wt.% Ru_{0.50}Pd_{0.50}/TiO₂ catalyst

Reaction conditions: 24 mmol toluene, 24 mmol tBHP supplied as 70 wt.% solution in water, 80°C, 24 h, 1000 rpm stirring.

All of the catalyst precursors display very low activity under reaction conditions. None approach the activity achieved by the prepared catalyst, even when used in combination. To understand why, we must consider several factors.

Firstly we must consider the oxidation state of the metals, as oxidation state plays an important role in activity. The 1 wt.% Ru_{0.50}Pd_{0.50}/TiO₂ modified impregnation catalyst is treated in 5% H₂ in Ar for 4h at 400°C; this is intended to reduce the Ru and Pd present to the metallic state. In PdCl₂ and RuCl₃, the metals exist in the +2 and +3 states respectively. This may explain the comparatively low activity of the metal salts in comparison. However, we must also consider the solubility of these precursors in toluene; if insoluble, the poor activity may be attributable to mass transport limitations.

To determine the effectiveness of the catalyst treatment, samples of the dried and untreated catalyst and of the dried and treated catalyst were examined by XPS. It should be noted that the treatment step was not carried out in situ with the analysis, and so it is possible that some re-oxidation could occur during the transfer. Results are shown in **Table 1**.

catalyst	species present (% metal content)			
	<i>Pd-O</i>	<i>Pd metal</i>	<i>Ru-O</i>	<i>Ru metal</i>
untreated	37.5	0.0	62.5	0.0
treated	30.3	9.1	24.2	36.4

By this analysis, none of the metal present on the untreated sample is in the 0 oxidation state. After treatment, 23% of the detected palladium (9.1% of detected metal) is in the metallic state, as is 60% of the ruthenium (36.4% of detected metal). It is unclear from this data alone if the treatment procedure is simply insufficient to reduce all the metal present or if re-oxidation occurred between treatment and analysis. It does, however, confirm that different oxidation states are present in the heterogeneous catalyst than in the homogeneous salts, which may help explain the difference in activity.

The XPS analysis also indicated the presence of a Cl species in the untreated catalyst. No Cl was detected in the treated sample: this is encouraging as one of the primary purposes of the treatment step is to remove Cl impurities, which may act as catalyst poisons or influence the oxidation state of the metals present. The presence of chlorine, as in the chloride salts, may drastically inhibit reaction, again possibly explaining the low homogeneous activity.

Finally, any alloying of the metals in the heterogeneous catalyst also affects electronic structure; no alloying is possible when using the catalyst precursors. The heterogeneous catalyst may also benefit from metal-support interactions and the formation of certain site morphologies on the metal nanoparticle.

TiO₂ and PdCl₂ display similar selectivity, comparable to that of the reaction with toluene and tBHP in the absence of catalyst; no benzoic acid is observed in either case. Reactions containing ruthenium produce benzoic acid as the preferred product; observed yields corresponding to approximately 40% selectivity. This behaviour is likely linked to the tendency of the reaction to form benzoic acid at higher conversions as a result of benzaldehyde oxidation. The AuPd and PtPd catalysts, which achieve lower conversions, are correspondingly less selective to benzoic acid.

3.3.4. Comparison of RuPd and monometallic Ru and Pd catalysts

The high selectivity to benzoic acid observed with the RuPd/TiO₂ catalyst and the results achieved by the other catalysts and catalyst precursors, discussed in sections 3.3.2. and 3.3.3., suggest that a monometallic Ru/TiO₂ catalyst might be highly active. Due to the relationship between conversion and formation of benzoic acid, if this catalyst is active it can also be expected to be selective. Conversely, a Pd/TiO₂ catalyst might be expected to achieve low conversion and produce no benzoic acid.

Monometallic 1 wt.% Ru/TiO₂ and 1 wt.% Pd/TiO₂ were prepared by modified impregnation and tested. It should be noted that previous reports with this catalyst attribute the success of the modified impregnation method to the formation of small nanoparticles of random alloys³³. In the case of monometallic catalysts, the small nanoparticle size may still be beneficial, but there is no alloying effect to

consider. Results for these monometallics, compared to the result for the 1 wt.% Ru_{0.50}Pd_{0.50}/TiO₂, are shown in **Figure 13**. Carbon balances were >95% for these reactions.

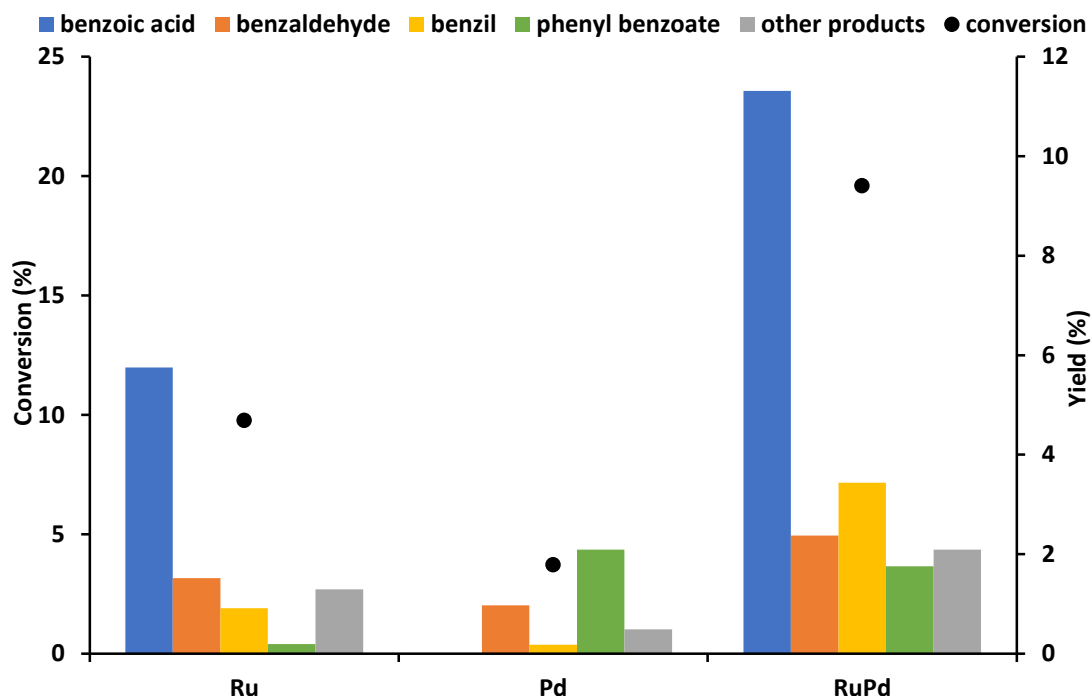


Figure 13. Comparison of bimetallic RuPd catalyst with Pd and Ru monometallic catalysts

Reaction conditions: *Molar ratio substrate:metal 6500:1, 24 mmol toluene, 24 mmol tBHP supplied as 70 wt.% solution in water, 80°C, 24 h, 1000 rpm stirring.*

As predicted, the Ru monometallic catalyst achieves higher conversion than the Pd monometallic catalyst, and thus is also more selective to benzoic acid. Both the Ru monometallic and the RuPd catalyst achieve 58% selectivity to benzoic acid. Like the blank reactions performed with tBHP, no benzoic acid is formed in the reaction with the Pd monometallic catalyst.

The superior activity of bimetallic RuPd over monometallic Ru strongly suggests that the addition of palladium causes beneficial alloying, or other changes that enhance the activity of the ruthenium component. These could include beneficial changes in nanoparticle size or dispersion. To investigate this, the catalysts were analysed by CO chemisorption. Results are shown in **Table 2**.

Table 2. Nanoparticle size and dispersion of different 1 wt.% catalysts

	catalyst		
	<i>Ru</i>	<i>Pd</i>	<i>Ru_{0.50}Pd_{0.50}</i>
dispersion (%)	51.70	45.18	41.56
average particle size (Å)	8.60	8.26	8.98
metal surface area (m ² /g)	1.89	2.01	1.85

The nanoparticle characteristics of the three catalysts are broadly similar. This might suggest that the electronic changes in the nanoparticle due to alloying or interaction between the two metals are responsible for the enhanced activity. The Ru_{0.50}Pd_{0.50} catalyst possesses the lowest dispersion and metal surface area, and the largest average particle size, of the catalysts tested. The differences are only slight, however, and fall within error for this instrument.

3.3.5. Influence of metal molar ratio

In section 3.3.4. it was established that bimetallic RuPd is more active than either 1 wt.% Ru/TiO₂ or 1 wt.% Pd/TiO₂ prepared by the same method. 1 wt.% Ru_{0.75}Pd_{0.25}/TiO₂ and 1 wt.% Ru_{0.25}Pd_{0.75}/TiO₂ catalysts were prepared by modified impregnation to explore the most effective molar ratio of metals. Results are shown in **Figure 14**. Carbon balances were >93%.

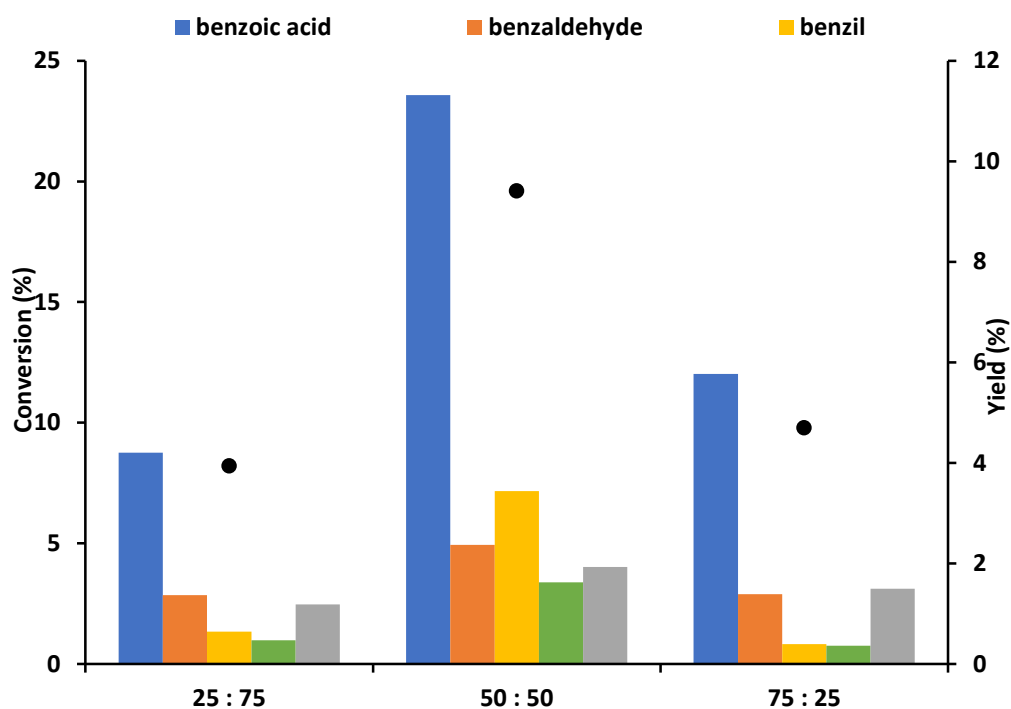


Figure14. Comparison of bimetallic RuPd catalysts with different metal ratios

Reaction conditions: *Molar ratio substrate:metal 6500:1, 24 mmol toluene, 24 mmol tBHP supplied as 70 wt.% solution in water, 80°C, 24 h, 1000 rpm stirring.*

The 1 wt.% Ru_{0.25}Pd_{0.75}/TiO₂ catalyst achieves around double the conversion of the 1 wt.% Pd/TiO₂ monometallic catalyst; further evidence that ruthenium is inherently active for this oxidation. However, the 1 wt.% Ru_{0.75}Pd_{0.25}/TiO₂ catalyst achieves a similar conversion and yield to the 1 wt.% Ru/TiO₂ monometallic, despite the lower ruthenium content. This strongly implies that modification of the catalyst by the addition of palladium enhances activity, or else that the particle morphology is greatly influenced by metal ratio. The best proof of this is that the bimetallic catalyst with an equimolar ratio of ruthenium and palladium is the most effective by a wide margin.

The selectivity of the 1 wt.% Ru_{0.75}Pd_{0.25}/TiO₂ and 1 wt.% Ru_{0.50}Pd_{0.50}/TiO₂ catalysts to benzoic acid is very similar, at approximately 58%. The palladium rich catalyst exhibits a slightly reduced selectivity to benzoic acid of 54%.

The 1 wt.% Ru_{0.25}Pd_{0.75}/TiO₂ and 1 wt.% Ru_{0.75}Pd_{0.25}/TiO₂ catalysts were also examined by CO chemisorption. Results are given in **Table 3**.

	catalyst		
	<i>Ru_{0.25}Pd_{0.75}</i>	<i>Ru_{0.50}Pd_{0.50}</i>	<i>Ru_{0.75}Pd_{0.25}</i>
dispersion (%)	6.52	41.56	30.47
average particle size (Å)	41.10	8.98	14.60
metal surface area (m ² /g)	0.38	1.85	1.11

The bimetallic catalyst with the equimolar ratio features the smallest average nanoparticle size and the highest particle dispersion and metal surface area. Increased metal surface area often increases catalyst activity due to the increased availability of active sites.

3.3.6. Investigating metal leaching

In section 3.3.3. it was shown that the homogeneous catalyst precursors achieve very low conversions, and thus cannot be responsible for the high activity of the 1 wt.% Ru_{0.50}Pd_{0.50}/TiO₂ catalyst. However, this does not indicate leaching is not taking place. It is possible that either Ru or Pd or both leach from the catalyst surface. This could affect the observed activity and influence the particle morphology and the available reaction sites.

To determine the degree of any leaching, MP-AES analysis was carried out on solutions prepared from digested 1 wt.% Ru_{0.50}Pd_{0.50}/TiO₂ catalyst. A used catalyst was compared to an unused catalyst from the same batch. The process is described in Chapter Two, section 2.8.1. Results are shown in **Table 4**.

catalyst	Ru		Pd	
	<i>maximum (ppm)</i>	<i>observed (ppm)</i>	<i>maximum (ppm)</i>	<i>observed (ppm)</i>
unused	23.18	1.64	24.40	21.43
used	22.98	0.13	24.19	4.01
<i>metal loading % difference</i>	7		71	

Catalyst digested for 18 h in aqua regia. 'used' catalyst reaction conditions: Molar ratio substrate:metal 6500:1, 24 mmol toluene, 24 mmol tBHP supplied as 70 wt.% solution in water, 80°C, 24 h, 1000 rpm stirring.

The results of MP-AES analysis suggest extremely high leaching of palladium from the catalyst. 87% of the total Pd content (determined by calculation from catalyst mass and loading) is observed in the analysis of the unused catalyst, compared to only 17% in the analysis of the used catalyst. This leaves 71% of Pd unaccounted for, apparently having been leached into solution during the reaction.

Only 7% of the total Ru content (determined by calculation from the catalyst mass and loading) is observed in the analysis of the unused catalyst. This indicates that the digestion method used (18 h submersion in aqua regia) is insufficient to remove ruthenium from the catalyst surface. Therefore we cannot draw any conclusions regarding ruthenium leaching from this data.

Given the difficulty in digesting ruthenium, it was appropriate to examine the reaction mixture itself for metal content, rather than digested catalyst. This was not possible on the MP-AES system due to the intolerance to organic solvents.

Instead, both the aqueous and organic layers of the reaction mixture were examined by ICP analysis. To do this, the layers were separated and evaporated to dryness, then the flask washed thoroughly with either 30 wt.% HCl or 10 M NaOH and analytical solutions made from the washings. Results are shown in **Table 5**.

	HCl wash		NaOH wash	
	<i>Ru (mg/L)</i>	<i>Pd (mg/L)</i>	<i>Ru (mg/L)</i>	<i>Pd (mg/L)</i>
aqueous layer	0.0040	0.3300	0.0585	0.9135
organic layer	0.0130	1.0600	0.0310	0.0310
% metal leached	0.20	16.52	0.78	23.29

Layers analysed post reaction under the following conditions: Molar ratio substrate:metal 6500:1, 24 mmol toluene, 24 mmol tBHP supplied as 70 wt.% solution in water, 80°C, 24 h, 1000 rpm stirring.

The results of ICP analysis indicate very little leaching of ruthenium: <1% of the metal present. However, palladium leaches to a considerable extent, though the results presented here suggest far less Pd loss than those obtained by MP-AES. The reasons for this disparity are unknown, but may relate to poor recovery of

palladium by this method, or potentially to Pd complexing with products and subsequently being filtered out of the sample prior to MP-AES analysis.

As it was established that metal leaches from the catalyst, a hot filtration experiment was performed to determine if the homogeneous metal was active.

A standard reaction was performed with the 1 wt.% Ru_{0.50}Pd_{0.50}/TiO₂ catalyst. After the reaction time, the solid catalyst was filtered from the reaction mixture and the mixture placed back in the reactor for a further 24 h. No additional tBHP was added. Progress of the reaction was monitored by taking samples at 25 h, 26 h, 28 h, 32 h and 48 h.

Conversion increased after the removal of solid catalyst, indicating that homogeneous metal is active. 8 h after the filtration, (total reaction time 32 h) total conversion had increased from 19.6% to 33.2%, with a 21.74% yield of benzoic acid. This corresponds to an increase in selectivity to benzoic acid from 58% to 66%; a product of the increased conversion. No further increase was observed from the 32 h to 48 h total reaction time. This may be due to the reduced amount of tBHP available by this point.

Leached metal is detrimental in terms of waste and expense. It may also have an adverse effect on catalyst reusability, discussed in section 3.3.7. To reduce the degree of leaching and improve metal-support interaction, catalysts with lower metal loadings were prepared. These are discussed in section 3.3.8. Treatment procedures such as reduction can also minimise leaching. The effect of reducing temperature is explored in section 3.3.10.

3.3.7. Catalyst reusability

Industrial catalysts must not only be active but stable. Ideal catalysts are long-lasting and/or can be regenerated (cheaply) with no loss of activity. In a laboratory batch process, the 'reusability' of the catalyst is assessed by recovering the catalyst after reaction and then using it again. This is repeated as many times as necessary.

The 1 wt.% Ru_{0.50}Pd_{0.50}/TiO₂ catalyst was recovered after reaction, washed with acetone, dried in air and then retested. Results for multiple re-uses of the same

catalyst are shown in **Figure 15a**. The distribution of other products is shown in **Figure 15b**.

The conversion achieved with the reused catalyst remains broadly stable, with a slight decrease observed on the fifth use. The 1 wt.% Au_{0.36}Pd_{0.64}/TiO₂ catalyst⁹⁸ was also found to be stable over multiple uses with no loss of conversion, which was attributed to the lack of sintering.

However, unlike the reported 1 wt.% Au_{0.36}Pd_{0.64}/TiO₂ catalyst, the selectivity and resulting product yields of the 1 wt.% Ru_{0.50}Pd_{0.50}/TiO₂ catalyst change significantly with catalyst reuse. Selectivity to the acid decreases from 58% during the first use, to 38% during the fifth. There is a corresponding increase in selectivity to benzaldehyde from 12% to 17% and in selectivity to benzil, from 17% in the first use to 34% in the fifth.

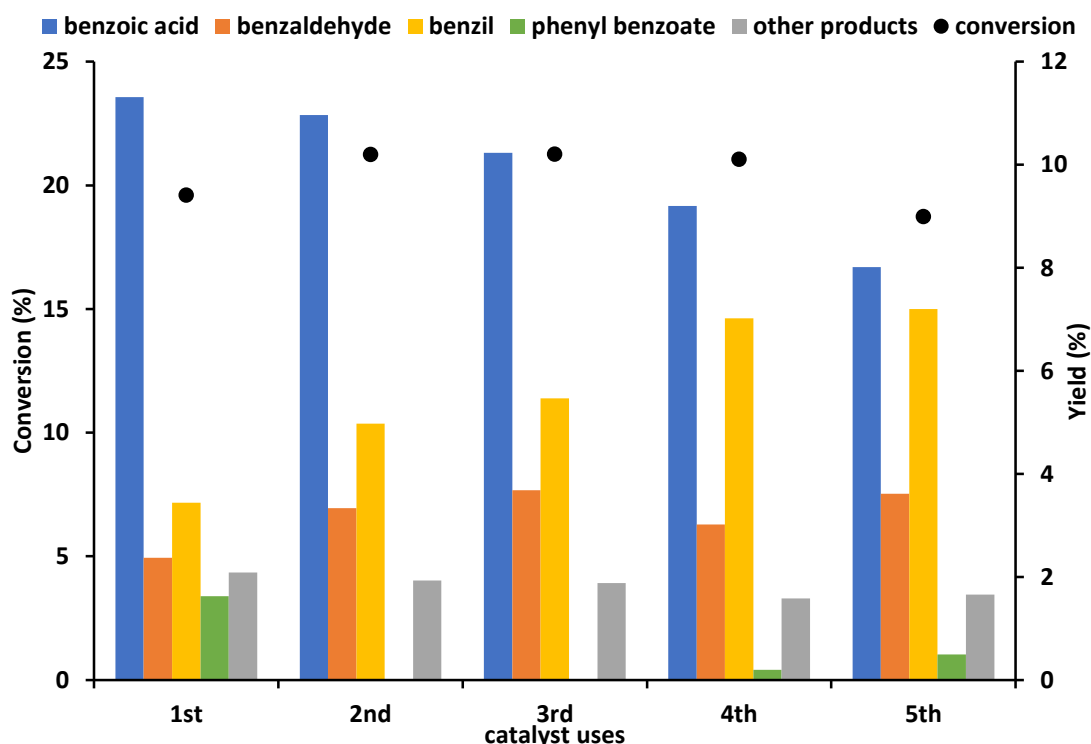


Figure 15a. The reusability of the catalyst recovered and washed with acetone

Reaction conditions: *Molar ratio substrate:metal 6500:1, 24 mmol toluene, 24 mmol tBHP supplied as 70 wt.% solution in water, 80 °C, 24 h, 1000 rpm stirring.*

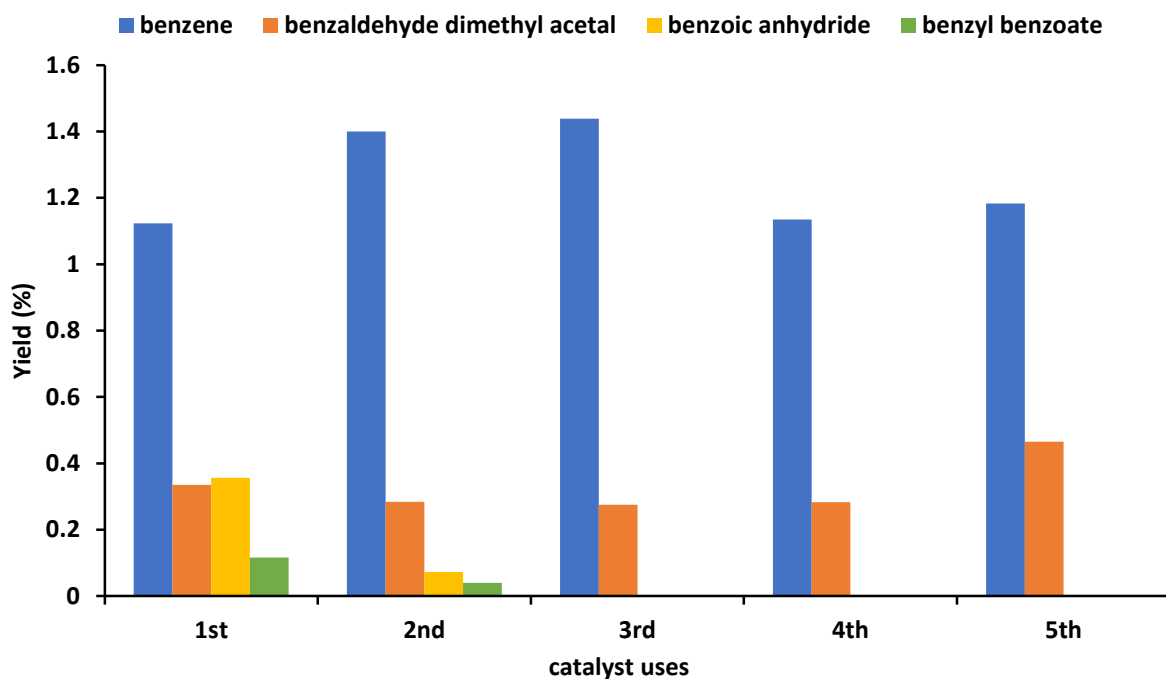


Figure 15b The reusability of the catalyst recovered and washed with acetone

Reaction conditions: *Molar ratio substrate:metal 6500:1, 24 mmol toluene, 24 mmol tBHP supplied as 70 wt.% solution in water, 80 °C, 24 h, 1000 rpm stirring.*

In **Figure 15b**, it is shown that benzoic anhydride and benzyl benzoate are not observed as products when the catalyst is used for the third time onwards. This absence may be explained by the decreasing yield of benzoic acid, as they form from this product.

The loss of selectivity may be attributable to changing nanoparticles as palladium leaches from the catalyst. Alternatively, it may be connected to a build-up of product on the catalyst surface which is not removed by washing with acetone. However, no products were detected on the surface of the washed catalyst by FTIR. If the reason for this change could be established, it would be potentially useful in the development of benzaldehyde selective catalysts.

3.3.8. Influence of metal loading

High metal loadings often lead to larger particle sizes, decreased metal-support interaction and consequently increased metal leaching^{102, 103}. Lowering the metal loading can improve metal-support interaction and reduce leaching, and is also

beneficial in terms of cost. Furthermore, lowering metal loading does not necessarily decrease activity, as smaller nanoparticles can be more active than larger ones.

0.10 wt.% and 0.01 wt.% Ru_{0.50}Pd_{0.50}/TiO₂ catalysts were prepared by modified impregnation and compared with the equivalent 1.00 wt.% catalyst previously studied. The same mass catalyst, substrate and tBHP was used in all reactions; therefore the tenfold and hundredfold reduction in metal loading is reflected in a tenfold and hundredfold increase in substrate:metal ratio. Results are shown in **Figure 16a**, with the distribution of other products in **Figure 16b**.

As the weight loading of metal on the catalyst decreases, so does the conversion of toluene. However, this decrease is far from linear, as might be expected. In fact, a tenfold reduction in metal loading from 1.00 wt.% to 0.10 wt.% produces only an approximate 1.5% decrease in conversion. To understand this, we must consider that the decrease in weight loading of metal is not the sole change taking place.

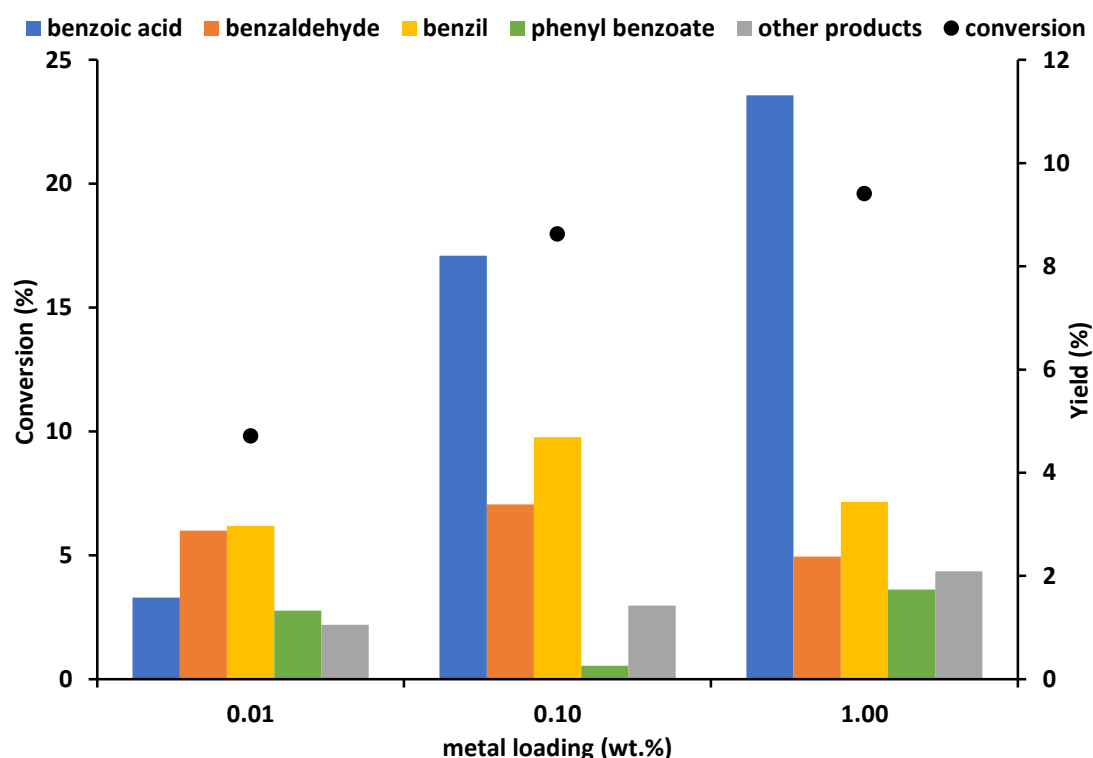


Figure 16a. Effect of decreasing % metal loading using RuPd/TiO₂ catalysts

Reaction conditions: 38 mg catalyst, 24 mmol toluene, 24 mmol tBHP supplied as 70 wt.% solution in water, 80°C, 24 h, 1000 rpm stirring.

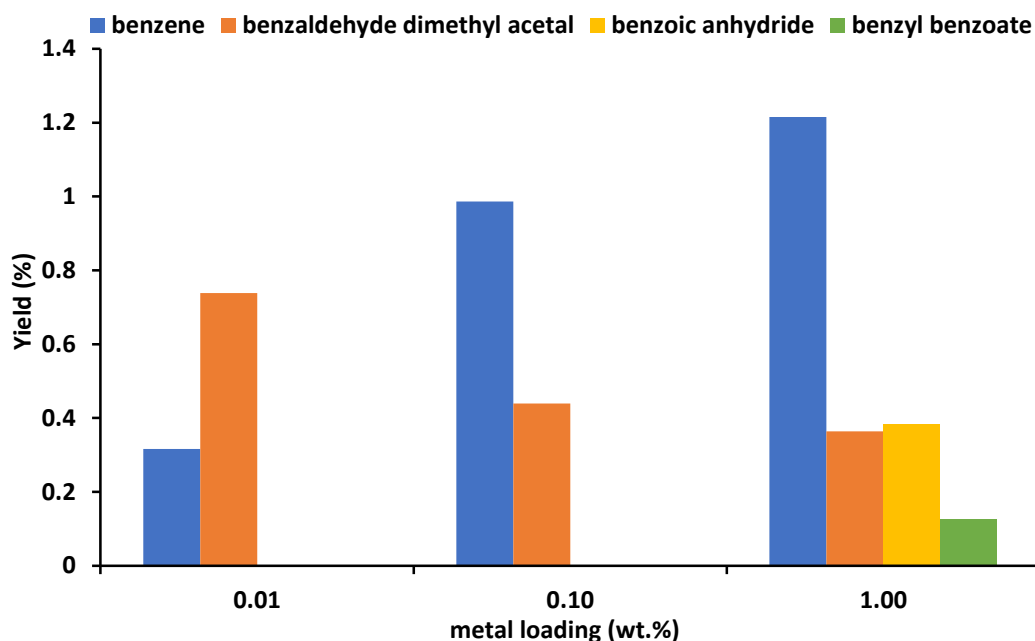


Figure 16b. Effect of decreasing % metal loading using RuPd/TiO₂ catalysts

Reaction conditions: 38 mg catalyst, 24 mmol toluene, 24 mmol tBHP supplied as 70 wt.% solution in water, 80 °C, 24 h, 1000 rpm stirring.

Each catalyst was prepared by the same modified impregnation method, but the resulting nanoparticles on each do not necessarily share the same morphology or average nanoparticle size. The reduction in metal loading may lead to the formation of particles of different sizes, with significant changes in particle dispersion. Both of these factors will influence the activity of the catalyst in addition to the reduced metal loading. Therefore the catalysts with reduced metal loadings were examined by CO chemisorption, as shown in **Table 6**. Dispersion and particle size could not be reliably calculated for the 0.01 wt. % catalyst

Table 6. Nanoparticle size and dispersion of different wt.% catalysts			
	wt.% Ru_{0.50}Pd_{0.50}		
	0.01	0.10	1.00
dispersion (%)	-	60.54	41.56
average particle size (Å)	-	6.17	8.98
metal surface area (m ² /g)	0.18	0.27	1.85

As metal loading decreases there is a substantial decrease in metal surface area, as expected. The reduction in metal loading also leads to a decrease in particle size.

This is far more pronounced for the 0.01 wt.% catalyst than the 0.10 wt.%, and may be partially responsible for the loss of catalyst activity.

These results can also be assessed in terms of TOF. This relates conversion to mols of metal directly, and is therefore a useful measure by which catalysts can be compared. The TOF achieved by each catalyst is shown in **Table 7**.

metal loading (wt. %)	conversion (%)	TOF (h^{-1})
1.00	19.6	50
0.10	18.0	480
0.01	9.8	2730

Reaction conditions: 38 mg catalyst, 24 mmol toluene, 24 mmol tBHP supplied as 70 wt.% solution in water, 80°C, 24 h, 1000 rpm stirring.

TOF values reported in the literature for heterogeneously catalysed toluene oxidation do not frequently exceed 100. Reported sol immobilised 1 wt.% AuPd/TiO₂⁹⁸ has a TOF of 72 h^{-1} . The AuPd/MIL-101 catalyst reported by Li *et al.*⁵⁹ is considered a prominent catalyst with a TOF of 100 h^{-1} . Both the 0.10 wt.% and 0.01 wt.% Ru_{0.50}Pd_{0.50}/TiO₂ catalysts significantly improve on this, despite achieving relatively low % conversion. With further optimisation of catalyst, conditions and reactor system it may be possible to exploit this.

3.3.9. Influence of substrate:metal ratio

In section 3.3.8. it was established that catalysts with very low metal loadings achieved significant TOFs. As the same mass catalyst was used in all cases, the decrease in metal loading corresponds to an increase in substrate:metal ratio (among other factors, discussed further in section 3.3.6.). This can also be achieved by varying the mass catalyst applied to the reaction. Given the high TOF h^{-1} achieved previously, this was investigated further.

The mass of 1 wt.% Ru_{0.50}Pd_{0.50}/TiO₂ supplied to the reaction was varied to produce metal:substrate ratios in the range of 3,000 to 30,000. Results are shown in **Figure 17**.

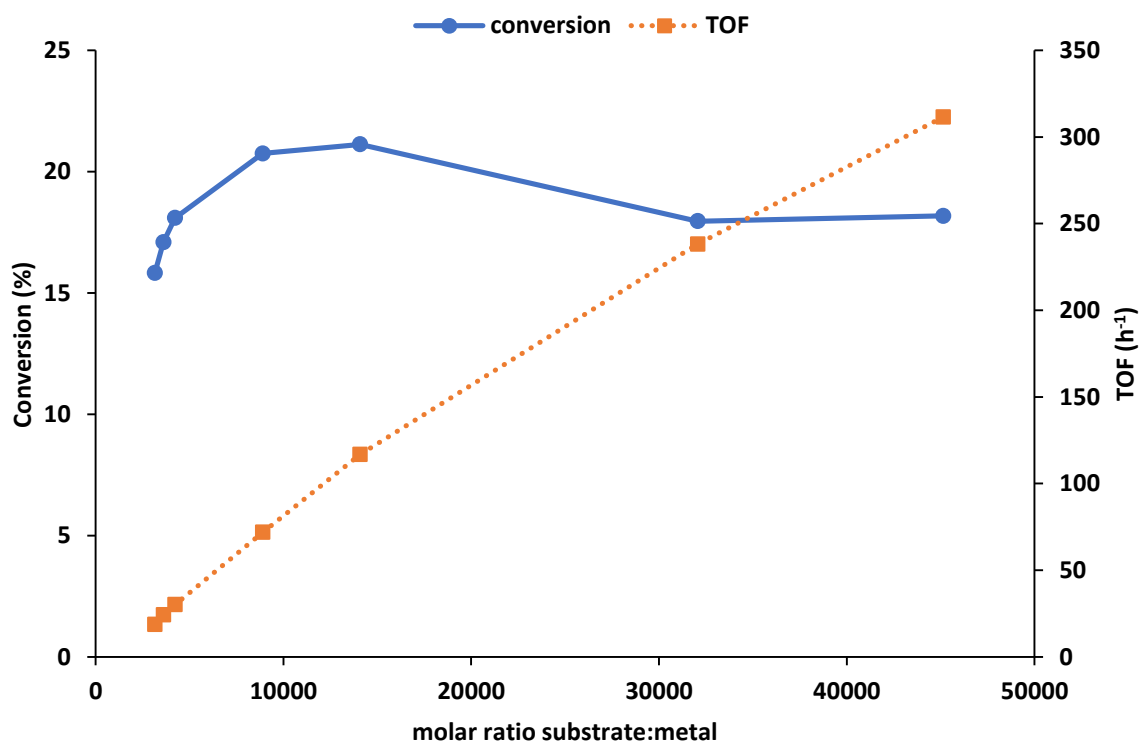


Figure 17. Effect of varying molar ratio of substrate:metal on conversion and TOF

Reaction conditions: 24 mmol toluene, 24 mmol tBHP supplied as 70 wt.% solution in water, 80°C, 24 h, 1000 rpm stirring.

It is evident from this data that some unusual behaviour is taking place. It is generally expected that increasing the mass catalyst applied (thus decreasing the substrate:metal ratio) would result in an increase in conversion, due to the greater availability of catalyst for reaction. This trend should continue until mass transport limitations come into effect.

Here, increasing the mass of catalyst applied actually leads to a decrease in conversion. This could, in part, be due to mass transport limitations and inefficient stirring. As the mass catalyst used increases, it may encourage agglomeration into particles, effectively decreasing the available catalyst surface area and possibly leading to a net decrease in conversion.

As shown previously, a decrease in conversion leads to a decrease in selectivity to benzoic acid and corresponding increase in selectivity to benzaldehyde and benzil. This is reflected in the yields shown in **Figure 18**.

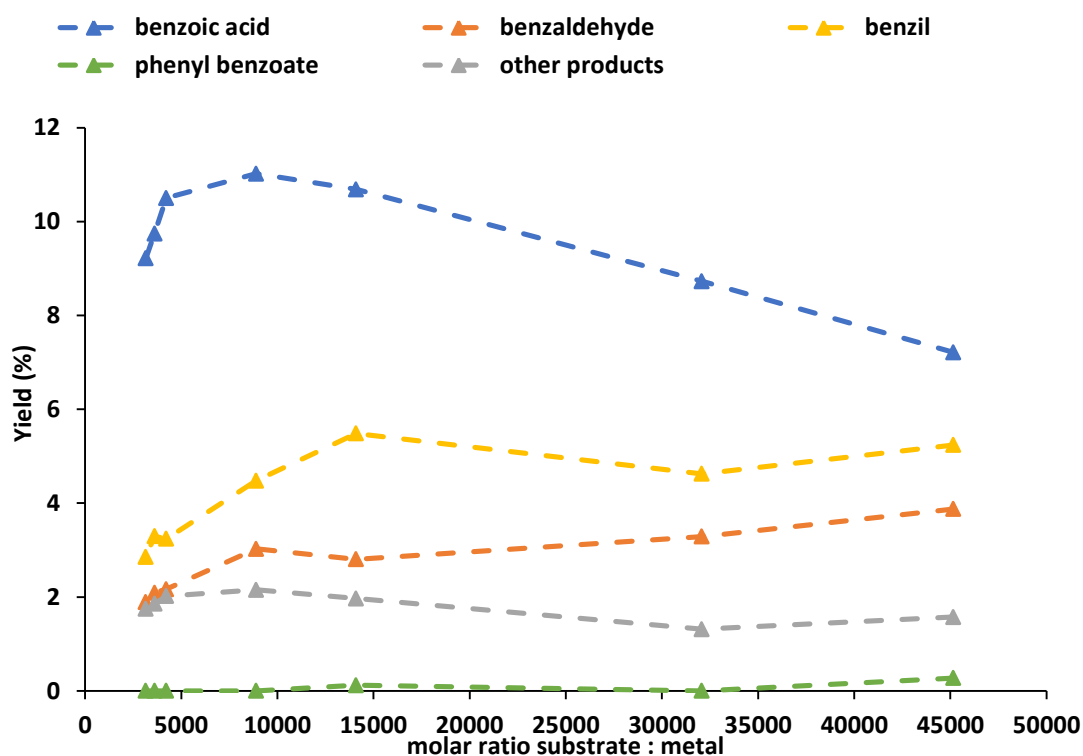


Figure 18. Effect of varying substrate:metal ratio on product yields

Reaction conditions: 24 mmol toluene, 24 mmol tBHP supplied as 70 wt.% solution in water, 80°C, 24 h, 1000 rpm stirring.

3.3.10. Influence of reduction temperature

The reduction of the catalyst is a key part of the modified impregnation procedure, as it is responsible for removing remaining chloride species which could otherwise act as poisons, and ensuring the metal present is reduced to the 0 oxidation state. The temperature, time and gas feed used for the reduction step can also have a significant effect on the size and morphology of the metal nanoparticles, and thus on any leaching. 1 wt.% Ru_{0.50}Pd_{0.50}/TiO₂ prepared by modified impregnation was separated into portions and each reduced at a different temperature: 200°C, 300°C, 400°C and 500°C. All of these catalysts were tested under the standard reaction conditions and the results are presented in **Figure 19**.

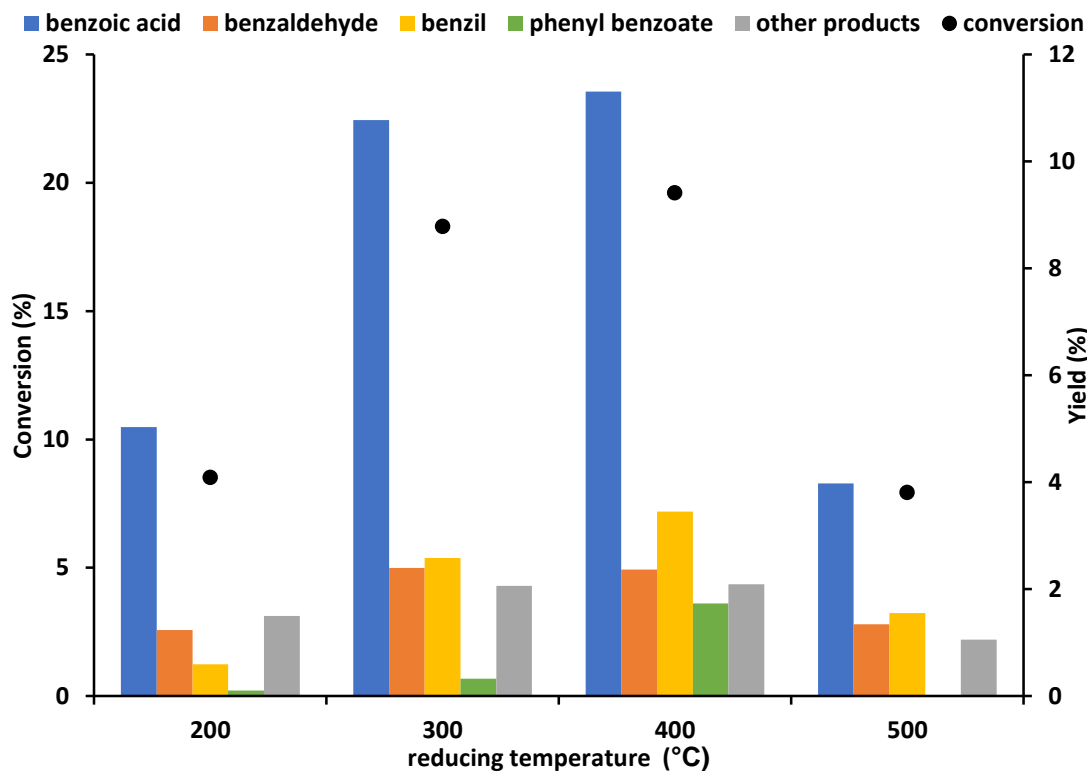


Figure 19. Influence of reducing temperature on catalyst activity

Reaction conditions: *Molar ratio substrate:metal 6500:1, 24 mmol toluene, 24 mmol tBHP supplied as 70 wt.% solution in water, 80 °C, 24 h, 1000 rpm stirring.*

The catalysts reduced at 300°C and 400°C display significantly superior activity to those reduced at either 200°C or 500°C.

At 200°C, it is possible that the metals present on the catalyst are not properly reduced, and therefore in the wrong electronic state for catalysis. Alternatively, 200°C may simply be too low a temperature to ensure the removal of chloride species from the surface, which instead remain and potentially act as poisons¹⁰⁴.

At 500°C, the small metal nanoparticles generated by the modified impregnation method may sinter into larger particles; reducing the total metal surface area and therefore the number of available active sites.

3.3.11. Influence of support material

The choice of support material is a key part of catalyst design. This investigation has focussed on TiO_2 (p25 Degussa, a mix of 15% anatase and 85% rutile titania) as a support, as this is a well characterised and commercially available material, and has previously been found suitable in the oxidation of similar compounds using similar bimetallic catalysts. TiO_2 is thought to prolong the half-life of oxygen-based radicals¹⁰⁵. This may not be beneficial in this case, as a greater concentration of radicals on the surface may increase rates of termination. TiO_2 is also acidic, and the presence of acid sites on the support may also play a role in the reaction.

Several alternate support materials are available, and many have previously been investigated in conjunction with palladium alloys such as AuPd and PtPd. Such supports include C^{60} and CeO_2 ⁷⁵. Carbon may undergo many different treatments, the carbon support used here was pH neutral Darco G-60. CeO_2 is a basic support.

1 wt.% $\text{Ru}_{0.5}\text{Pd}_{0.5}$ catalysts supported on Darco G-60 neutral carbon and CeO_2 were prepared. The carbon supported catalyst was prepared *via* the modified impregnation method, as described in Chapter 2, section 2.4.3. The CeO_2 supported catalyst was prepared from a PdCl_2 solution that was not additionally acidified with HCl, as the acid solution could react with the basic CeO_2 . This and the inherent differences between the supports means the nanoparticles formed on each catalyst are not necessarily similar; for example having different nanoparticle sizes, compositions and dispersion.

The carbon and ceria supported catalysts were tested and their activity compared to that of 1 wt.% $\text{Ru}_{0.50}\text{Pd}_{0.50}/\text{TiO}_2$. Results are shown in **Figure 20**.

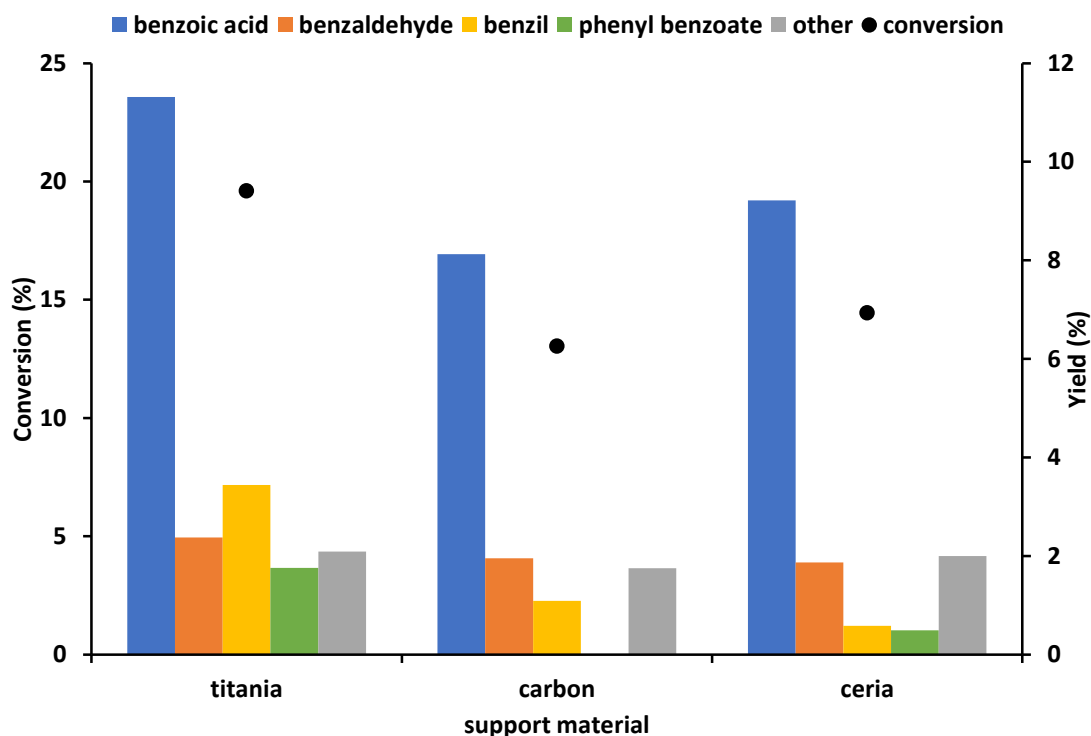


Figure 20. Influence of catalyst support material

Reaction conditions: *Molar ratio substrate:metal 6500:1, 24 mmol toluene, 24 mmol tBHP supplied as 70 wt.% solution in water, 80°C, 24 h, 1000 rpm stirring.*

The TiO₂ supported catalyst achieves the greatest activity, resulting in the highest product yield. The % selectivity towards each product remains similar across all three supports; approximately 60% to the acid and 13% to benzaldehyde. This similarity in product distribution suggests that selectivity may be entirely determined by the metal nanoparticles present, or is not significantly influenced by the presence of acidic or basic sites on the catalyst support.

The relative pH of the support may, however, have a significant role to play in promoting conversion. The data presented above might suggest that acidic sites on TiO₂ are beneficial, but this would not explain the difference in activity observed between the C and CeO₂ supported catalysts. We must also consider the effect played by surface area, as this differs in each case, and of the particle size that forms on each support, as this may also vary.

3.3.12. Role of tBHP and air

Reactions in the glass and Radleys reactor were carried out in air in the presence of tBHP. To determine if air or tBHP was acting as the oxidant, the reaction was carried out in the Radleys reactor under a helium atmosphere, thus removing the potential for air to be the oxidant. Results are presented in **Figure 21**.

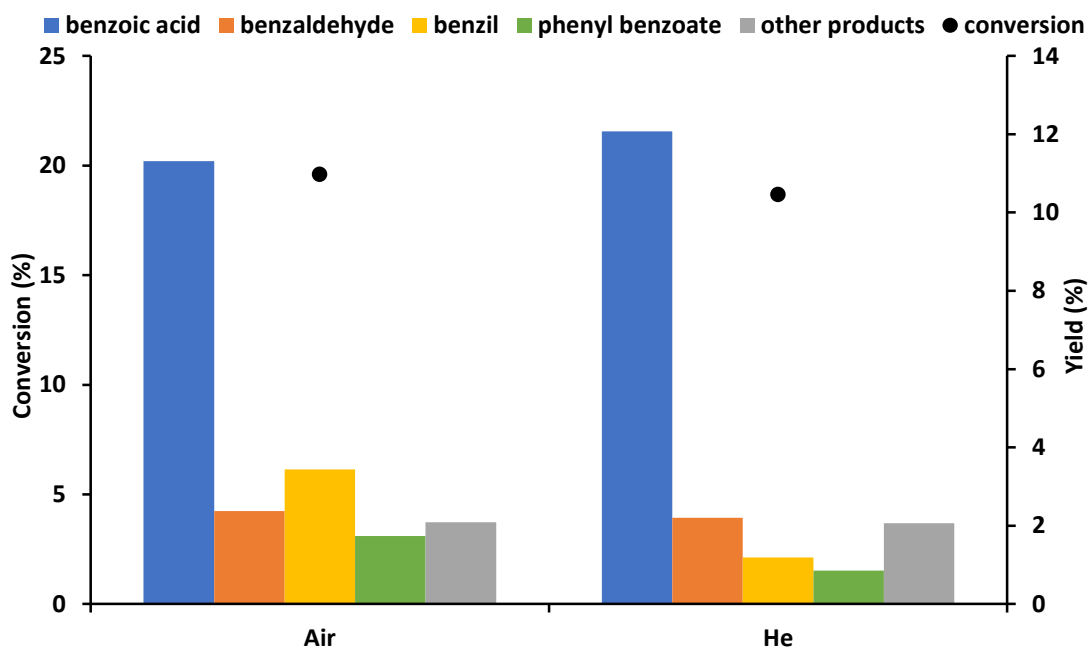


Figure 21. Average results for reactions carried out under 1 bar air or 1 bar He

Reaction conditions: *Molar ratio substrate:metal 6500:1, 24 mmol toluene, 24 mmol tBHP supplied as 70 wt.% solution in water, 80 °C, 24 h, 1000 rpm stirring.*

The activity of the 1 wt.% Ru_{0.50}Pd_{0.50}/TiO₂ catalyst under the different gases at the same pressure is comparable. This indicates that air is not required for the reaction; tBHP can serve as the oxidant. This does not conclusively prove that air *cannot* act as an oxidant, however.

If tBHP is the oxidant even when air is present, decreasing the amount of tBHP supplied should lead to a decrease in conversion. To investigate this, a series of reactions were carried out in which the mmols of tBHP used was varied. The resulting conversion was plotted against the molar ratio of substrate:tBHP in **Figures 22a** and **22b**.

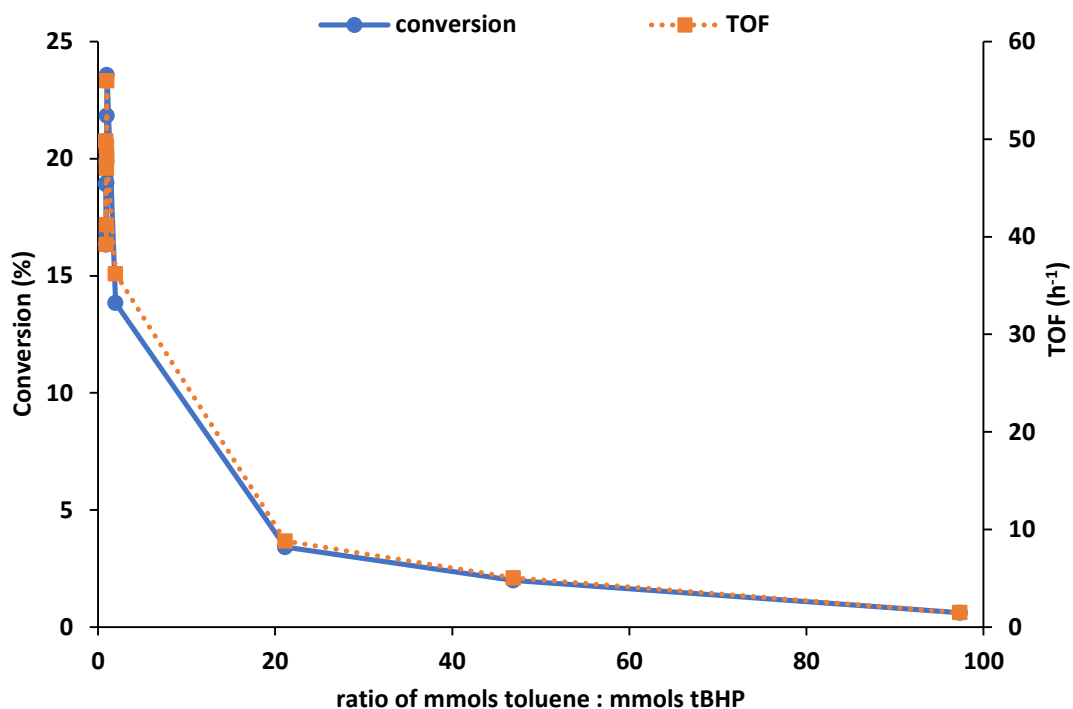


Figure 22a. The effect of varying substrate:tBHP molar ratio on conversion and TOF

Reaction conditions: *Molar ratio substrate:metal 6500:1, 24 mmol toluene, tBHP supplied as 70 wt.% solution in water, 80°C, 24 h, 1000 rpm stirring.*

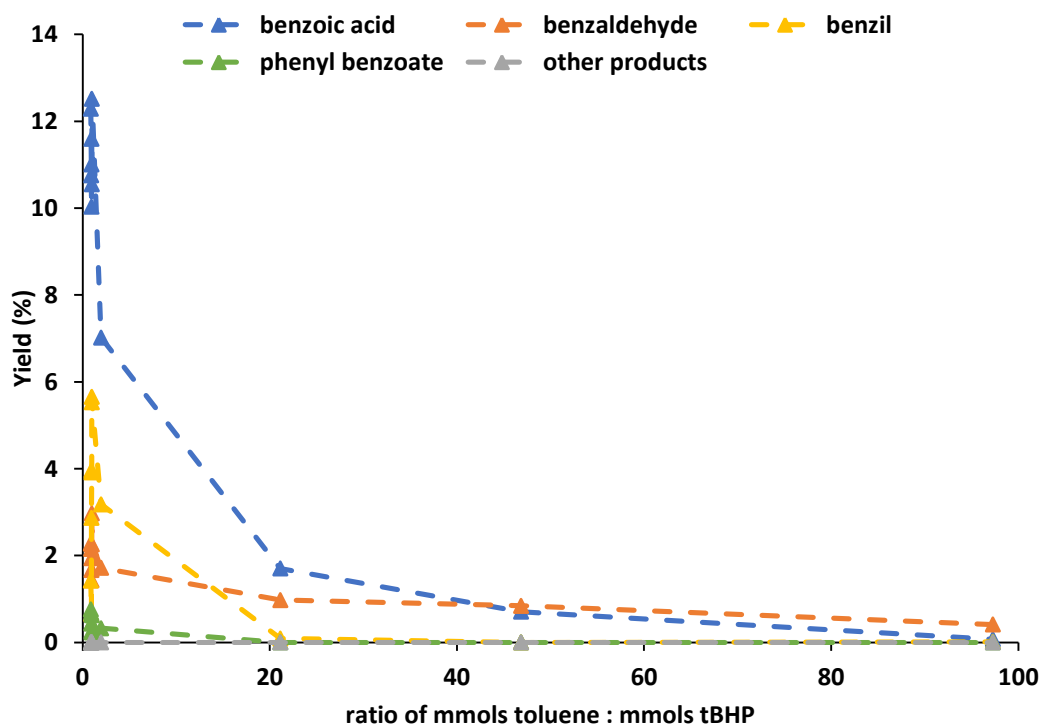


Figure 22b. The effect of varying substrate:tBHP molar ratio on product yield

Reaction conditions: *Molar ratio substrate:metal 6500:1, 24 mmol toluene, tBHP supplied as 70 wt.% solution in water, 80°C, 24 h, 1000 rpm stirring.*

Decreasing the amount of tBHP supplied under 24 mmols, resulting in a greater than 1:1 molar ratio of substrate:tBHP, results in a drastic decrease in conversion and therefore yield. This is as expected for tBHP acting as an oxidant. However, the decrease is not a simple linear decrease, as might be expected if the reaction was first order with respect to tBHP. This may be the result of mass transport limitations, particularly due to the complications arising from the biphasic system.

The change in conversion is accompanied by a significant shift in selectivity, shown in **Figures 22c and 22d** for clarity. As the mmols tBHP supplied is reduced, increasing the toluene:tBHP molar ratio, the reaction becomes increasingly selective to benzaldehyde and increasingly less selective to benzoic acid. The reaction favours benzaldehyde as the major product at toluene:tBHP molar ratios greater than 42. This is likely the result of there simply being insufficient oxidant present for the further oxidation of benzaldehyde.

Selectivity to benzil and phenyl benzoate decreases with increasing mmols toluene:tBHP, formation of these products becoming effectively negligible. Benzaldehyde dimethyl acetal represents almost all the other products shown.

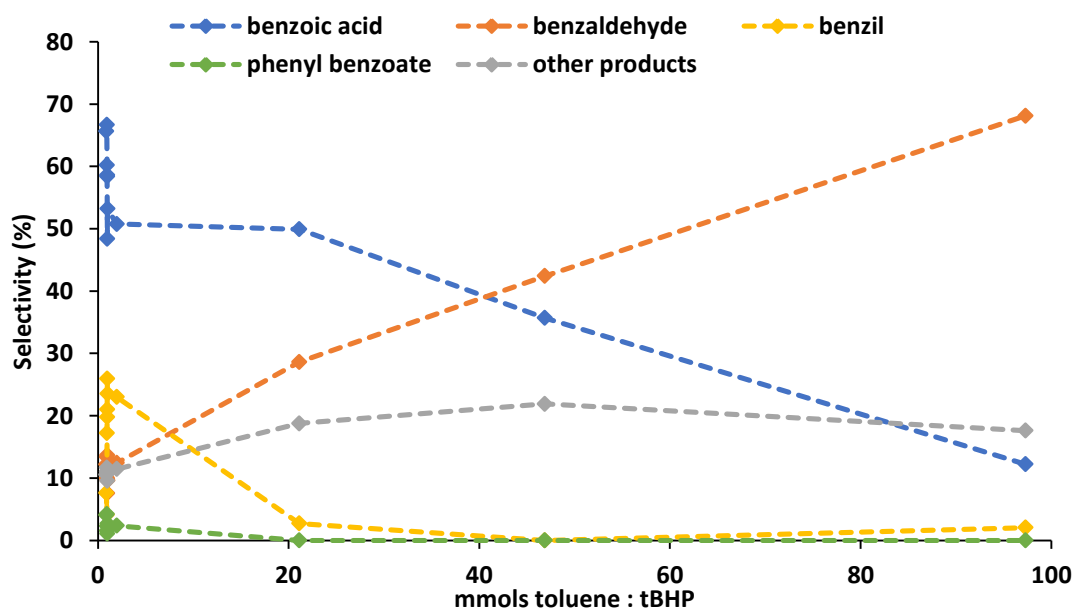


Figure 22c. The effect of varying substrate:tBHP molar ratio on product selectivity

Reaction conditions: *Molar ratio substrate:metal 6500:1, 24 mmol toluene, tBHP supplied as 70 wt.% solution in water, 80 °C, 24 h, 1000 rpm stirring.*

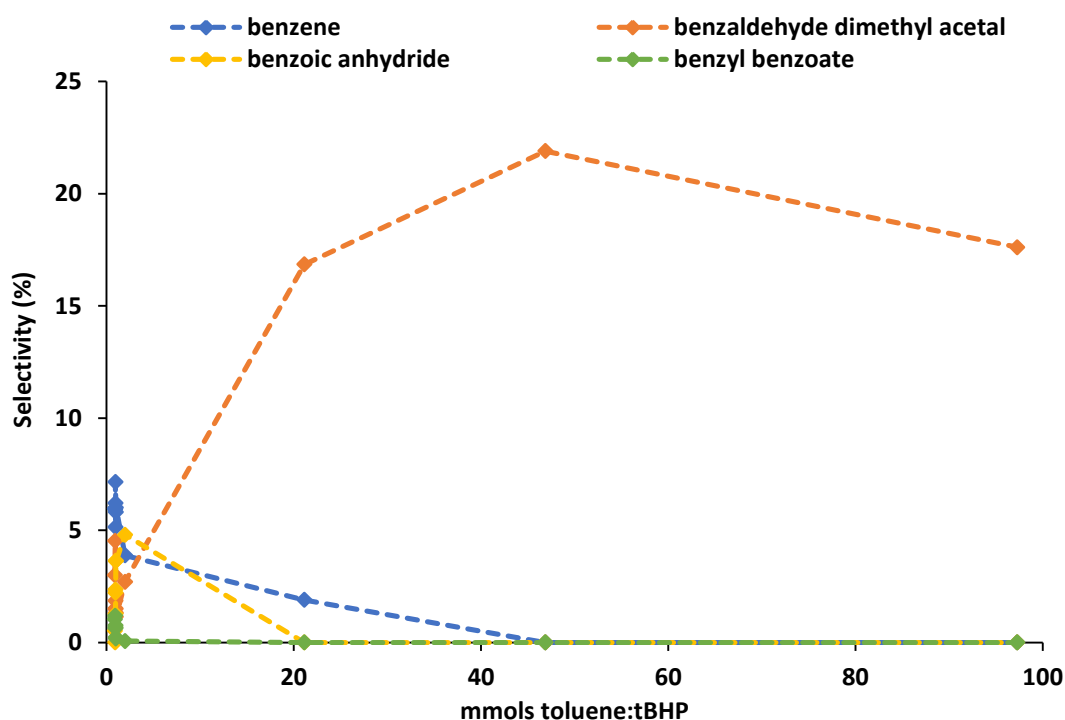


Figure 22d. The effect of varying substrate:tBHP molar ratio on product selectivity

Reaction conditions: *Molar ratio substrate:metal 6500:1, 24 mmol toluene, tBHP supplied as 70 wt.% solution in water, 80 °C, 24 h, 1000 rpm stirring.*

3.3.13. Influence of reaction temperature

Increasing reaction temperature increases the proportion of reactant molecules with sufficient energy for reaction, and therefore increases the rate. This should in turn lead to increased conversion and product yield.

However, as discussed in Chapter One, section 1.5., increasing reaction temperature can also decrease selectivity, and may even lead to complete combustion of product species to CO₂ and water. Given the high carbon balances obtained for toluene oxidation reactions with this catalyst under these conditions, it is extremely unlikely that complete combustion is taking place. The temperature may be having an effect on selectivity, however, and so lower reaction temperatures were explored.

The 1 wt.% Ru_{0.5}Pd_{0.5}/TiO₂ modified impregnation catalyst was applied to the toluene oxidation reaction at 40°C and 60°C. The results for these reactions are compared to the reaction at 80°C in **Figure 23**.

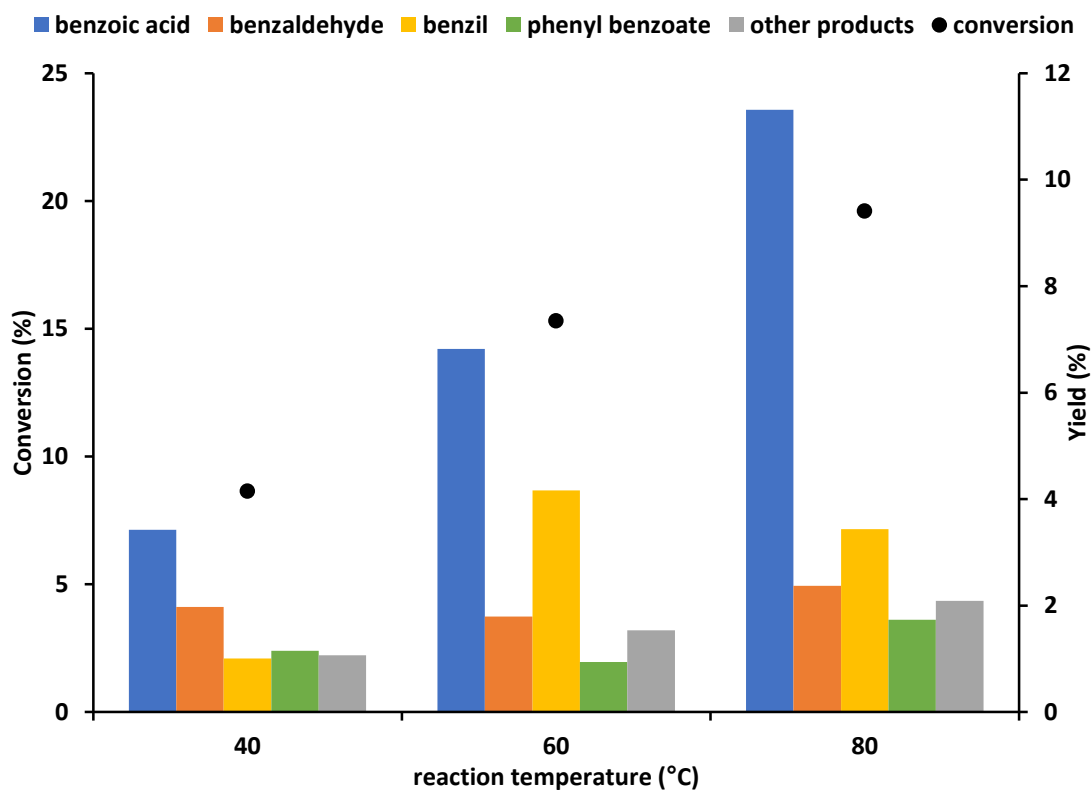


Figure 23. Influence of reaction temperature

Reaction conditions: *Molar ratio substrate:metal 6500:1, 24 mmol toluene, 24 mmol tBHP supplied as 70 wt.% solution in water, 24 h, 1000 rpm stirring.*

As expected, decreasing temperature leads to a significant decrease in conversion. This can be attributed to the reduced proportion of sufficiently energetic reactant molecules. When decreasing reaction temperature there is also a decrease in selectivity to benzoic acid: from 60% at 80°C to 45% at 60°C and 40% at 40°C. A 20°C decrease in temperature therefore approximately halves the benzoic acid yield.

It is possible that increasing temperature above 80°C would improve yield and conversion. This was not explored due to safety considerations regarding the use of tBHP.

3.3.14. Time-on-line studies

The product distribution throughout the reaction time was studied. Results are presented in **Figures 24a** through to **24d**.

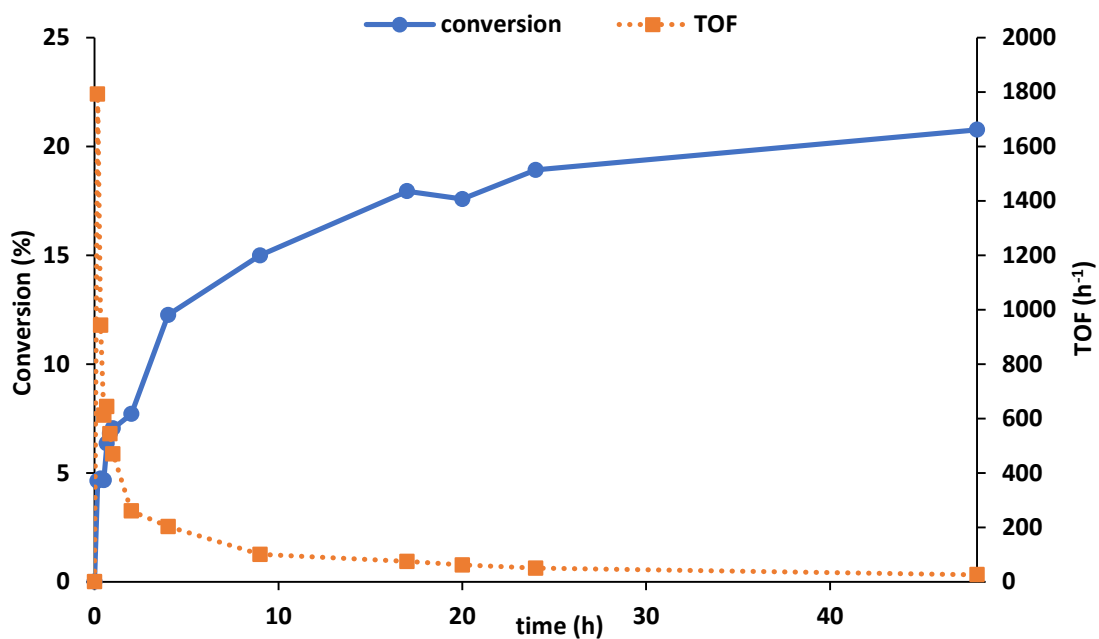


Figure 24a. The conversion and TOF achieved by reactions run for between 0 and 48 hours

Reaction conditions: *Molar ratio substrate:metal 6500:1, 24 mmol toluene, 24 mmol tBHP supplied as 70 wt.% solution in water, 80°C, 1000 rpm stirring.*

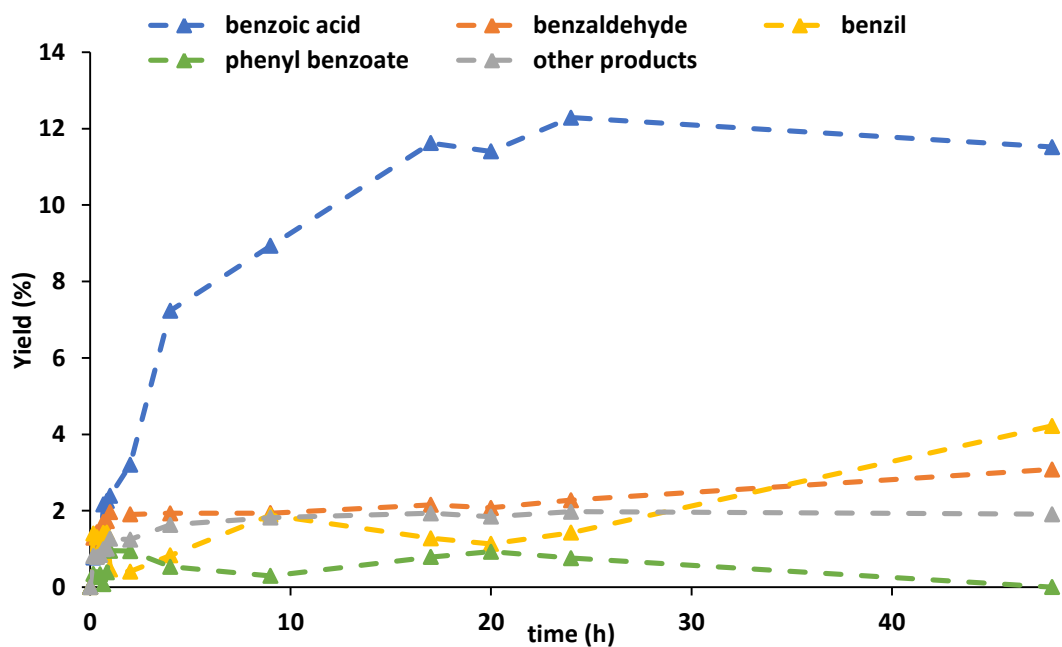


Figure 24b. The yield of product achieved by reactions run for between 0 and 48 hours

Reaction conditions: *Molar ratio substrate:metal 6500:1, 24 mmol toluene, 24 mmol tBHP supplied as 70 wt.% solution in water, 80°C, 1000 rpm stirring.*

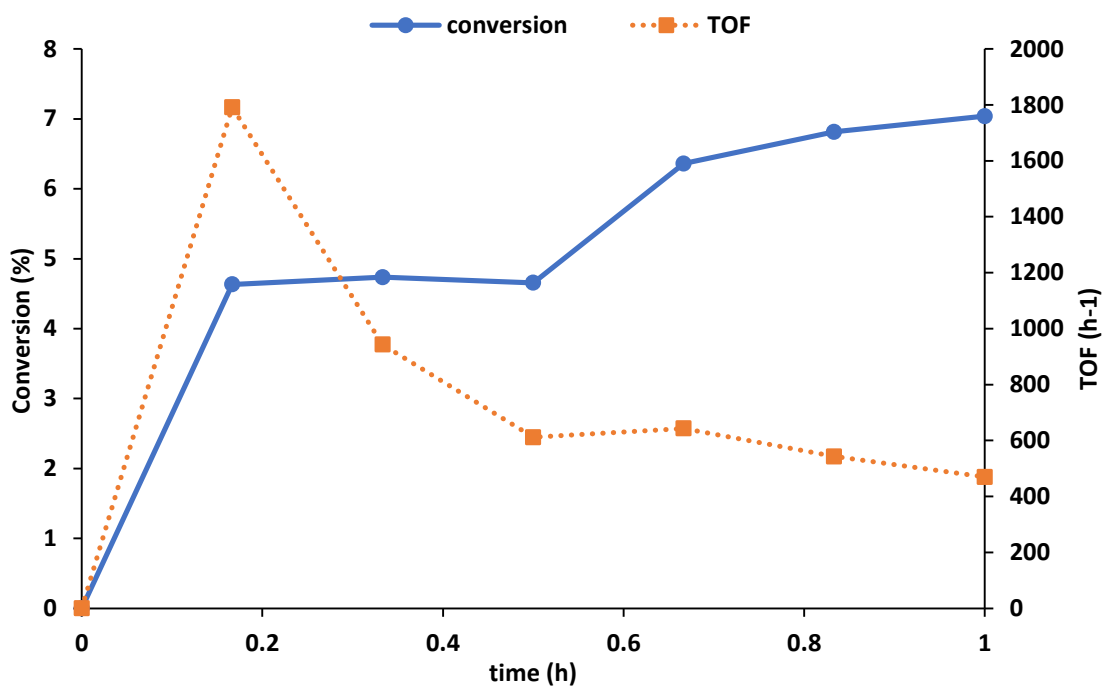


Figure 24c. The conversion and TOF(h⁻¹) achieved by reactions run for between 0 and 1 hour

Reaction conditions: *Molar ratio substrate:metal 6500:1, 24 mmol toluene, 24 mmol tBHP supplied as 70 wt.% solution in water, 80°C, 1000 rpm stirring.*

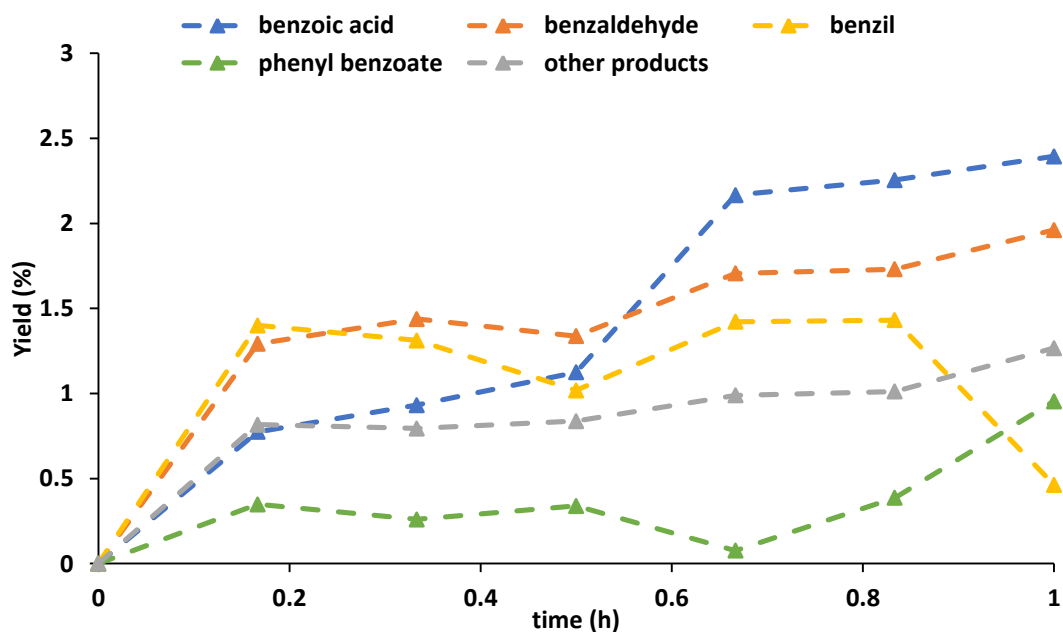


Figure 24d. The product yield achieved by reactions run for between 0 and 1 hour

Reaction conditions: *Molar ratio substrate:metal 6500:1, 24 mmol toluene, 24 mmol tBHP supplied as 70 wt.% solution in water, 80°C, 1000 rpm stirring.*

Figures 24a and 24b display data obtained at intervals over a 48 hour reaction period. After an initial rapid increase, the rate of reaction appears to decelerate, conversion increasing by only 2% in the last 24 hours of reaction. After 24 h, 62% of the tBHP has been converted into tertiary-butyl alcohol, the remainder split across the aqueous and organic layers. This suggests that the decrease in conversion is not the result of the unavailability of oxidant. Instead, it could be the result of catalyst deactivation.

Given the reusability of the catalyst demonstrated in section 3.3.10., it is unlikely the catalyst is undergoing sintering or any permanent change. It is possible that reaction sites are being blocked by product that does not leave the surface during the reaction, but can be removed by washing the catalyst between uses.

Figures 24c and 24d display data obtained within the first hour of reaction for greater clarity. These show that even during this shorter timeframe, the rate of reaction decreases. It also indicates that in the very early stages of the reaction, benzaldehyde is preferred over benzoic acid as product, though analysis at 24 hours reveals 58% selectivity to the acid product and 13% to the aldehyde. This is in agreement with the literature discussed in 1.5.1. which proposes that benzoic acid forms in a secondary reaction from the oxidation of benzaldehyde.

3.4. Conclusions

3.4.1. Comparing the glass and Radleys reactors

The influence of fumehood extraction rate on the mass balance of reactions carried out in the glass reactor system is discussed in section 3.2.3. This effect rendered further investigations in the glass reactor untenable. However, even when extraction rate was relatively constant, and considering only those reactions with a mass balance of 95% or higher, the glass reactor setup differs from the Radleys reactor in several significant ways. Therefore it cannot be assumed that the toluene oxidation reaction behaves in a consistent manner across both reactors.

The glass reactors were heated *via* an oil bath, and the Radleys reactor *via* an aluminium heating plate. In both cases, the thermocouple measuring and

controlling temperature is located in the heating medium, rather than the reaction vessel. Therefore the exact temperature of the reaction mixture may differ in each reactor. The effect of temperature on the reaction in the Radleys reactor was investigated in section 3.3.13.

Both reactors were set to stir at 1000 rpm, however due to the relative positioning of the stirrer bars, the stirring in the Radleys reactor is less efficient than in the glass. This may hinder conversion in the Radleys reactor if mass-transport limitations are in effect. This is further complicated by the fact the reaction is biphasic, with the oxidant in the aqueous phase.

The glass reactors are open to the atmosphere, whereas the Radleys are sealed in atmospheric pressure air prior to heating. If air acted as an oxidant, this would limit conversion in the Radleys reactor. However, it is more likely that tBHP serves as oxidant, as discussed in section 3.3.12.

The sealed vessels used in the Radleys reactor means the reactions in the Radleys system are carried out at slightly elevated pressure, due to the expansion of gas as it heats up.

Reactions in the Radleys reactor were carried out at half the scale of those in the glass, though all ratios (substrate:metal and substrate:tBHP) were kept the same.

Considering the factors described above, it seems appropriate to treat the glass and Radleys reactors separately; as distinct systems rather than complementary ones.

3.4.2. Catalyst investigation and optimisation

In sections 3.2.2. and 3.3.2. it was established that a 1 wt.% Ru_{0.50}Pd_{0.50}/TiO₂ catalyst prepared by the modified impregnation method offered superior activity to a 1 wt.% Au_{0.50}Pd_{0.50}/TiO₂ catalyst prepared the same way. This satisfied a key criterion for this investigation; to find an alternative metal to gold; the greater cost of ruthenium somewhat offset by the enhanced activity.

Further investigation revealed that the bimetallic 1 wt.% Ru_{0.50}Pd_{0.50}/TiO₂ catalyst prepared by modified impregnation offered superior activity to either monometallic 1 wt.% Ru/TiO₂ or 1 wt.% Pd/TiO₂ made by the same method. This indicated a

synergistic effect between the two metals; a beneficial consequence of alloying within the nanoparticle. Ruthenium was found to be inherently active for this oxidation, but this could be significantly improved by addition of palladium. Selectivity to benzoic acid increases at higher conversions; thus the ruthenium palladium catalyst was also more selective to this product.

Investigating 1 wt.% $\text{Ru}_{0.75}\text{Pd}_{0.25}/\text{TiO}_2$ and $\text{Ru}_{0.25}\text{Pd}_{0.75}/\text{TiO}_2$ indicated that an equimolar ratio of metals was most active. Experiments supporting a 1 wt.% $\text{Ru}_{0.50}\text{Pd}_{0.50}$ catalyst on ceria and carbon by modified impregnation indicated that TiO_2 was the more effective support material. 1 wt.% $\text{Ru}_{0.50}\text{Pd}_{0.50}/\text{TiO}_2$ catalysts reduced at 400 °C were more effective than those reduced at 200, 300 or 500 °C, and reducing the reaction temperature from 80 °C caused a substantial drop in conversion.

The 1 wt.% $\text{Ru}_{0.50}\text{Pd}_{0.50}/\text{TiO}_2$ catalyst was found to be reusable with little change in conversion, though selectivity to benzoic acid decreased with each use. This reusability was observed despite significant leaching of palladium into solution indicated by MP-AES and ICP-AES analysis. Ruthenium was found to be stable.

When decreasing the metal loading of the equimolar bimetallic catalyst, an interesting phenomenon was observed. Conversion does not decrease linearly with metal loading, as might be expected. Instead, a decrease in metal loading by a factor of ten – from 1.0 wt.% to only 0.1 wt.% - results in only a small decrease in conversion and a greatly enhanced TOF for the catalyst. This is extremely unusual, but may be explained by differences in particle size or morphology. Both catalysts were prepared by the same method, however the resulting nanoparticles are significantly different, as shown in **Table 5** in section 3.3.8.

Further unusual behaviour was observed when increasing the catalyst mass applied to the reaction, thus decreasing substrate:metal ratio. Rather than the predicted increase in activity, conversion actually decreased when molar ratios of substrate:metal decreased from 15000. This is potentially linked to mass transport limitations relating to agglomeration of catalyst, effectively decreasing the available surface area.

Nevertheless, this investigation was successful in its principal aims. A catalyst was developed that was more active than similar gold containing catalysts for oxidation of toluene in mild conditions. In future, more work should be undertaken to improve the stability of the catalyst by preventing the observed metal leaching, and to investigate the cause the loss of selectivity on catalyst reuse.

3.5. References

1. V. R. Choudhary, D. K. Dumbre and S. K. Bhargava, *Industrial & Engineering Chemistry Research*, 2009, **48**, 9471-9478.
2. I. Hermans, E. S. Spier, U. Neuenschwander, N. Turra and A. Baiker, *Topics in Catalysis*, 2009, **52**, 1162-1174.
3. R. A. Sheldon, *Chemtech*, 1991, **21**, 566-576.
4. M. I. bin Saiman, G. L. Brett, R. Tiruvalam, M. M. Forde, K. Sharples, A. Thetford, R. L. Jenkins, N. Dimitratos, J. A. Lopez-Sanchez, D. M. Murphy, D. Bethell, D. J. Willock, S. H. Taylor, D. W. Knight, C. J. Kiely and G. J. Hutchings, *Angewandte Chemie-International Edition*, 2012, **51**, 5981-5985.
5. V. Peneau, Q. He, G. Shaw, S. A. Kondrat, T. E. Davies, P. Miedziak, M. Forde, N. Dimitratos, C. J. Kiely and G. J. Hutchings, *Physical Chemistry Chemical Physics*, 2013, **15**, 10636-10644.
6. V. Peneau, Doctor of Philosophy, Cardiff University, 2014.
7. G. J. Hutchings and C. J. Kiely, *Accounts of Chemical Research*, 2013, **46**, 1759-1772.
8. M. Sankar, Q. He, M. Morad, J. Pritchard, S. J. Freakley, J. K. Edwards, S. H. Taylor, D. J. Morgan, A. F. Carley, D. W. Knight, C. J. Kiely and G. J. Hutchings, *Acs Nano*, 2012, **6**, 6600-6613.
9. W. Luo, M. Sankar, A. M. Beale, Q. He, C. J. Kiely, P. C. A. Bruijninx and B. M. Weckhuysen, *Nature communications*, 2015, **6**, 6540-6540.

10. F. Jiang, X. Zhu, B. Fu, J. Huang and G. Xiao, *Chinese Journal of Catalysis*, 2013, **34**, 1683-1689.
11. L. Kesavan, R. Tiruvalam, M. H. Ab Rahim, M. I. bin Saiman, D. I. Enache, R. L. Jenkins, N. Dimitratos, J. A. Lopez-Sanchez, S. H. Taylor, D. W. Knight, C. J. Kiely and G. J. Hutchings, *Science*, 2011, **331**, 195-199.
12. A. n. Martínez, C. López, F. Márquez and I. Díaz, 2003, **220**, 486-499.
13. G. Jacobs, T. K. Das, Y. Zhang, J. Li, G. Racoillet and B. H. Davis, 2002, **233**, 263-281.
14. J. Long, H. Liu, S. Wu, S. Liao and Y. Li, *Acs Catalysis*, 2013, **3**, 647-654.
15. M. D. Argyle and C. H. Bartholomew, *Catalysts*, 2015, **5**, 145-269.
16. E. Carter, A. F. Carley and D. M. Murphy, *The Journal of Physical Chemistry C*, 2007, **111**, 10630-10638.
17. M. J. Beier, B. Schimmoeller, T. W. Hansen, J. E. T. Andersen, S. E. Pratsinis and J.-D. Grunwaldt, *Journal of Molecular Catalysis a-Chemical*, 2010, **331**, 40-49.

Chapter Four – 2-ethylnaphthalene Oxidation

4.1. Introduction

Results of the investigation into the partial oxidation of 2-ethylnaphthalene oxidation are presented in this chapter. A scheme for this is presented in **Figure 1**.

The purpose of the work was to investigate the selective, partial oxidation of 2-ethylnaphthalene under mild conditions, ideally with a non-gold catalyst. To build on the work presented in Chapter Three, a bimetallic RuPd/TiO₂ catalyst was investigated, closely compared to a AuPd/TiO₂ catalyst which is known to be active for a number of reactions. Experimental conditions were chosen based on results obtained with toluene and those reported in the literature^{99, 100}. tBHP was used as an oxidant due to its strong oxidising properties.

Catalyst evaluation was carried out in the Radleys reactor. This reactor system allows control of temperature, stirring speed and atmosphere. The closed system prevents material loss from reaction vessels as previously identified and discussed in Chapter Three, section 3.3.2.

Preliminary work established the viability of the AuPd/TiO₂ and RuPd/TiO₂ catalysts for this reaction under the chosen conditions. Different catalyst preparation methods were explored.

All results reported are an averaged value of three or more runs with mass balances $\geq 92\%$.

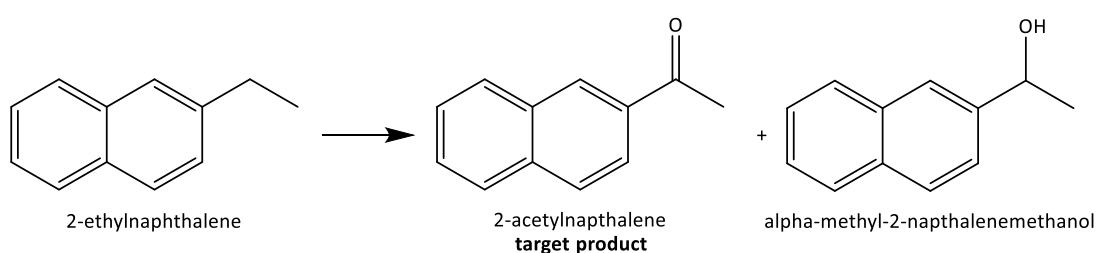


Figure 1. 2-ethylnaphthalene reaction scheme

4.2. Oxidation reactions in the Radleys reactor

4.2.1. Blank reactions

Reactions were carried out in the Radleys reactor without catalyst to ensure no auto-oxidation takes place under these conditions. Experimental data is presented in **Figure 2**. Carbon balances were >99% for these reactions.

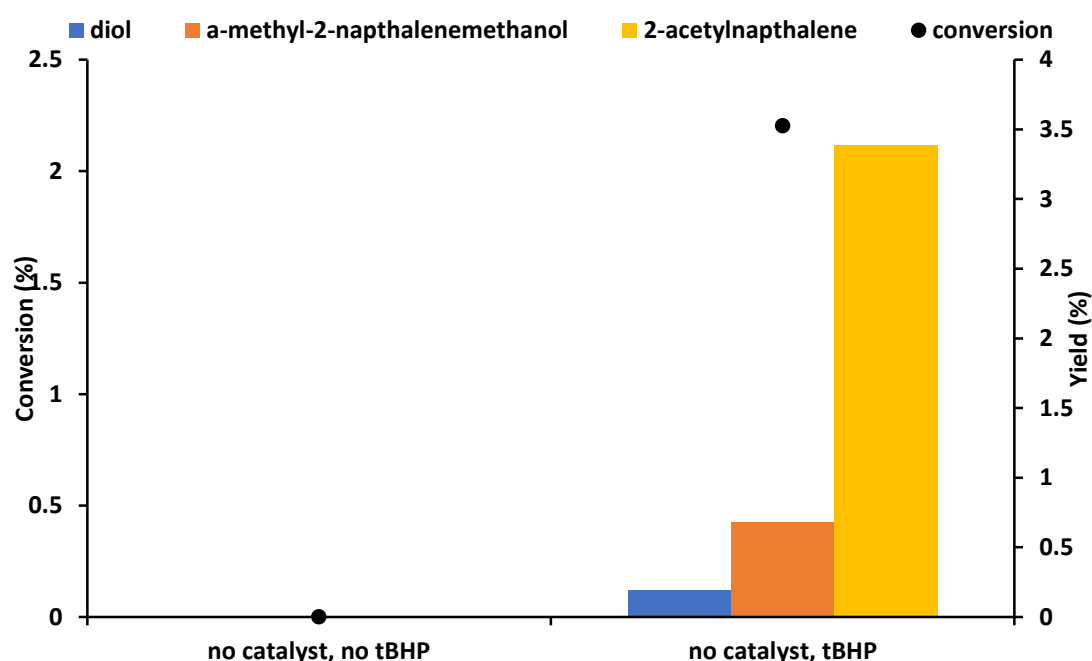


Figure 2. Reactions under standard conditions with no catalyst

Reaction conditions: 12.8 mmol 2-ethylnaphthalene, 12.8 mmol tBHP supplied as 70 wt.% solution in water (where applicable), 80°C, 24 h, 1000 rpm stirring.

In the absence of catalyst or tBHP, no product forms. This indicates that there is negligible auto-oxidation of 2-ethylnaphthalene under these conditions. When tBHP is present, slight conversion of just over 2% is observed. Under the reaction temperatures, tBHP will break down to form oxygen based radical species which can then catalyse the auto-oxidation mechanism³⁶. The low conversion achieved by auto-oxidation is likely the result of frequent termination, given the relative abundance of tBHP. The activity achieved demonstrates a clear selectivity to 2-

acetylnaphthalene as product. Additionally, small amounts of 1-(naphthalen-2-yl)ethane-1,1-diol, shown in **Figure 3**, were produced.

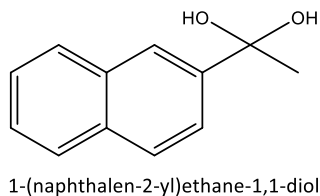


Figure 3. Structure of 1-(naphthalen-2-yl)ethane-1,1-diol

4.2.2. Oxidation reactions with RuPd/TiO₂ and AuPd/TiO₂

Having previously established that palladium alloys are effective for the partial oxidation of toluene, described in Chapter Three, it was predicted that these palladium alloys would also be active for the oxidation of 2-ethylnaphthalene. The additional aromatic ring on the molecule increases the number of possible products, but the stability of aromatic systems means the most likely target for the reaction lies on the alkyl chain, as it does for toluene. As the C-H bond strength is higher in the CH₃ group of the chain than in the CH₂, oxidation at the secondary carbon is more likely than at the primary carbon.

However, electronic effects due to the presence of the additional ring may have consequences for reactivity and therefore for the choice of catalyst. Two catalysts prepared by different methods were investigated, as the different preparations may result in nanoparticles of different size, distribution and composition. 1 wt.% Au_{0.50}Pd_{0.50}/TiO₂ catalysts were prepared by the sol immobilisation, modified impregnation and conventional impregnation methods described in Chapter Two, part 2.4., and tested for 2-ethylnaphthalene oxidation under standard conditions. Results are presented in **Figure 4**. All reactions had carbon balances of >92%.

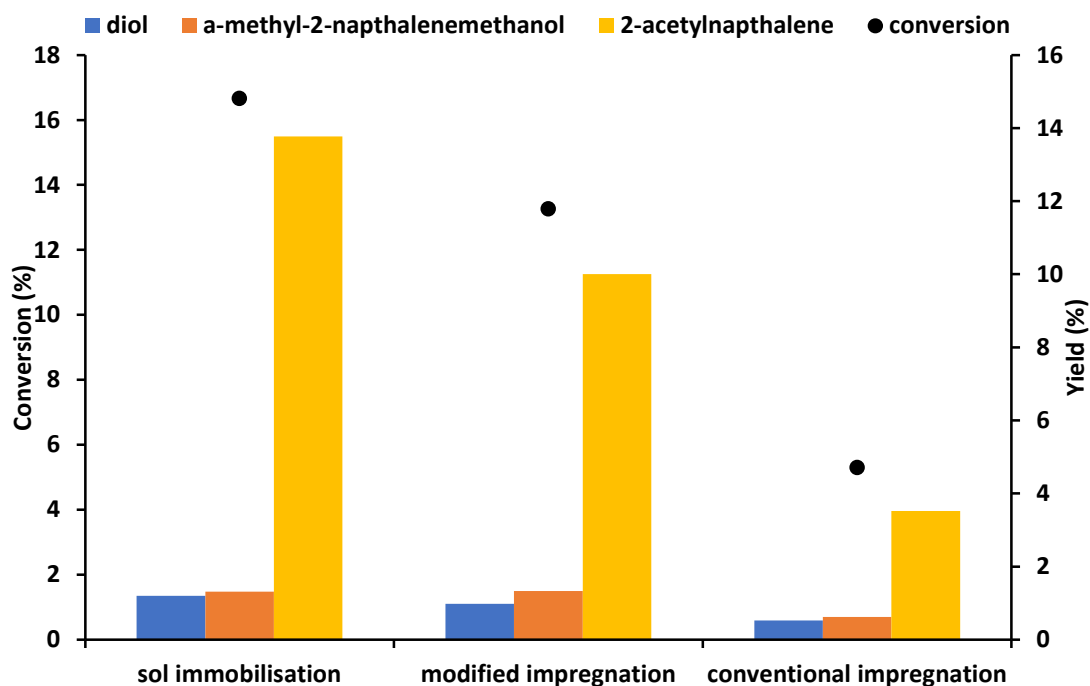


Figure 4. Comparison of 1 wt.% Au_{0.5}Pd_{0.5}/TiO₂ catalysts prepared by different methods

Reaction conditions: *Molar ratio substrate:metal 6500:1, 12.8 mmol 2-ethylnaphthalene, 12.8 mmol tBHP supplied as 70 wt.% solution in water, 80°C, 24 h, 1000 rpm stirring.*

In all cases, the AuPd catalysts are selective towards 2-acetylnaphthalene as product; the sol immobilised catalyst achieving >80% selectivity. However, there is a marked difference in the conversions achieved in each case.

The sol immobilised AuPd catalyst achieves the highest conversion, 17%, followed by the modified impregnation catalyst, 13%. The catalyst prepared by conventional impregnation achieves the lowest conversion, 5%. The greater activity of the modified impregnation catalyst over the conventional impregnation catalyst is consistent with previous findings for toluene oxidation, and in particular with previous literature reports on benzyl alcohol oxidation. The improvement in activity is possibly related to a greater degree of alloying in this catalyst³³. The superior activity of the sol immobilised catalyst has been shown to be related to improved alloying, to a smaller and more consistent particle size, and differences in dispersion^{57,106,34} in studies with other substrates.

The particle size and dispersion of the AuPd catalysts was examined by CO chemisorption, as described in Chapter Two, section 2.8.5. CO binds only weakly to gold, and less strongly to AuPd alloys than monometallic palladium. It is also thought that CO adsorbs only to low-coordinate sites on the nanoparticle. Therefore the results presented in **Table 1** must be considered with these factors in mind.

Table 1. Nanoparticle size and dispersion of 1 wt.% $Au_{0.50}Pd_{0.50}/TiO_2$ catalysts

	preparation method		
	<i>sol immobilisation</i>	<i>modified impregnation</i>	<i>conventional impregnation</i>
dispersion (%)	78.66	43.25	44.33
average particle size (Å)	4.67	8.63	2.78
metal surface area (m ² /g)	9.94	1.93	5.99

The sol immobilisation catalyst has the highest calculated nanoparticle particle dispersion and the second lowest average nanoparticle size by this analysis. This is likely to contribute significantly to the high activity observed with this catalyst. It is interesting to compare the modified impregnation and conventional impregnation catalysts. These have similar dispersion values, but the average nanoparticle size on the modified impregnation catalyst is far larger than that on the conventional impregnation catalyst. Despite this, the modified impregnation catalyst achieves far greater conversion. This may be indicative of a beneficial effect such as promotion of a particular kind of metal site or superior alloying when using this preparation technique. Alternatively, it may arise from inaccuracies caused by the gold component only slightly binding CO.

Like gold, ruthenium alloys with palladium^{107,108}. In Chapter Three, it was found that a RuPd/TiO₂ catalyst prepared by modified impregnation and reported for oxidation of levulinic acid¹⁰¹ was also active for the oxidation of toluene. Therefore, this catalyst was tested for the oxidation of 2-ethylnaphthalene. To further investigate the role of preparation method, 1 wt.% Ru_{0.50}Pd_{0.50}/TiO₂ catalysts were prepared by sol immobilisation and conventional impregnation as well as modified

impregnation. All three catalysts were tested under the same standard conditions and the results are presented in **Figure 5**. Carbon balances for these reactions were >97%.

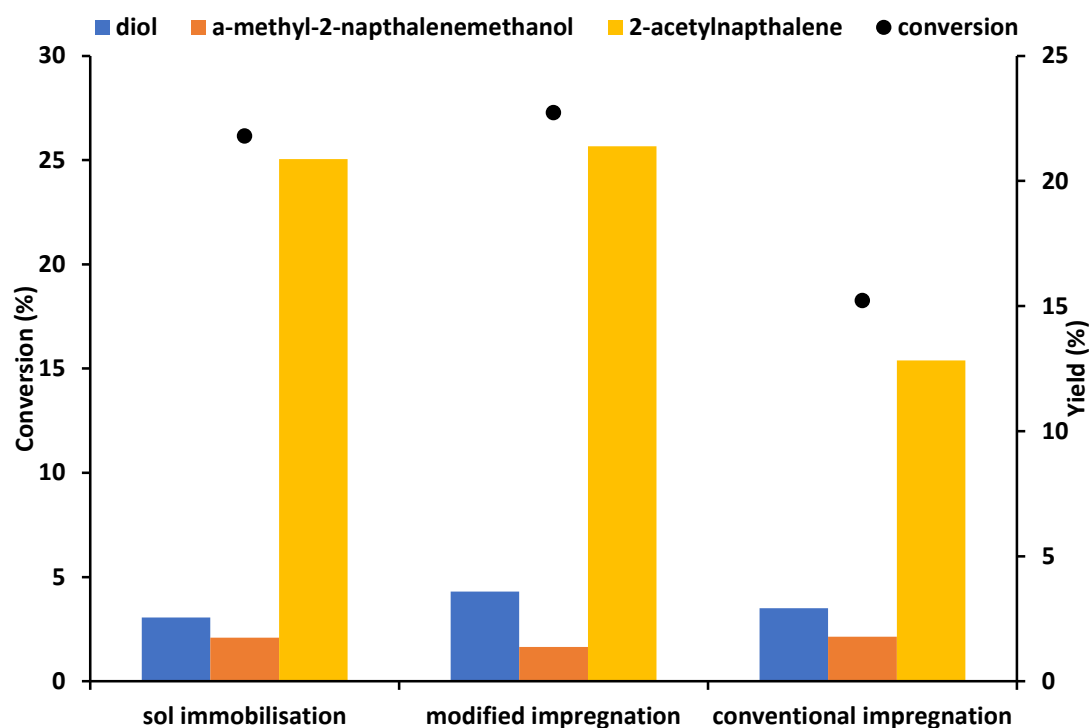


Figure 5. Comparison of 1 wt.% Ru_{0.5}Pd_{0.5}/TiO₂ catalysts prepared by different methods

Reaction conditions: *Molar ratio substrate:metal 6500:1, 12.8 mmol 2-ethylnaphthalene, 12.8 mmol tBHP supplied as 70 wt.% solution in water, 80 °C, 24 h, 1000 rpm stirring.*

The activity of the modified impregnation catalyst and the sol immobilised catalyst is similar, with both catalysts achieving approximately 79% selectivity to benzoic acid. The catalyst prepared by conventional impregnation is significantly less active, achieving a conversion of 18%. The modified impregnation catalyst also displays a slight decrease in selectivity to α-methyl-2-naphthalenemethanol and an increase in selectivity to the diol compared to the sol immobilised catalyst, hence the observed differences in yield. This is potentially the result of increased activity further oxidising the α-methyl-2-naphthalenemethanol to the diol. This may also be

explicable in terms of differences in the formed nanoparticles; size, degree of alloying or distribution across the surface.

The RuPd catalysts were examined by CO chemisorption to determine nanoparticle size and dispersion. Results are presented in **Table 2**.

	preparation method		
	<i>sol immobilisation</i>	<i>modified impregnation</i>	<i>conventional impregnation</i>
dispersion (%)	40.44	41.56	25.40
average particle size (Å)	9.23	8.98	14.70
metal surface area (m ² /g)	1.80	1.85	1.13

Unlike the results for the AuPd catalysts displayed in **Table 1**, the RuPd catalysts prepared by sol immobilisation and modified impregnation have similar dispersion values and average nanoparticle sizes, possibly explaining their similar activity.

The average nanoparticle size on the RuPd catalysts prepared by sol immobilisation and conventional impregnation is much larger than the average nanoparticle size on the equivalent AuPd catalysts. Comparable average nanoparticle size is obtained for both modified impregnation catalysts.

In all cases, the RuPd catalysts offer significantly higher conversion than their AuPd counterparts. This results in a higher yield of 2-acetylnaphthalene, though selectivity to this product is similar for RuPd and AuPd catalysts prepared in the same manner. The most apparent difference in behaviour is that the RuPd modified impregnation catalyst achieves highest conversion, whereas the AuPd sol immobilised catalyst is the most active.

4.2.3. Comparison of activity of bimetallic and monometallic catalysts

In section 4.2.2. it was shown that RuPd catalysts produced higher activity than AuPd counterparts in the oxidation of 2-ethylnaphthalene; suggesting Ru is intrinsically more active than Au for this reaction. To confirm this, monometallic 1 wt.% catalysts of Ru, Au and Pd supported on TiO₂ were prepared *via* the modified impregnation method described in Chapter Two, section 2.4.3. This method was

chosen because it produced the ruthenium-containing bimetallic catalyst with the highest conversion. The monometallic catalysts were all tested under reaction conditions, total mmols metal equivalent to the reactions with bimetallic catalysts. Results are shown in **Figure 6**. Carbon balances for these reactions were >99%.

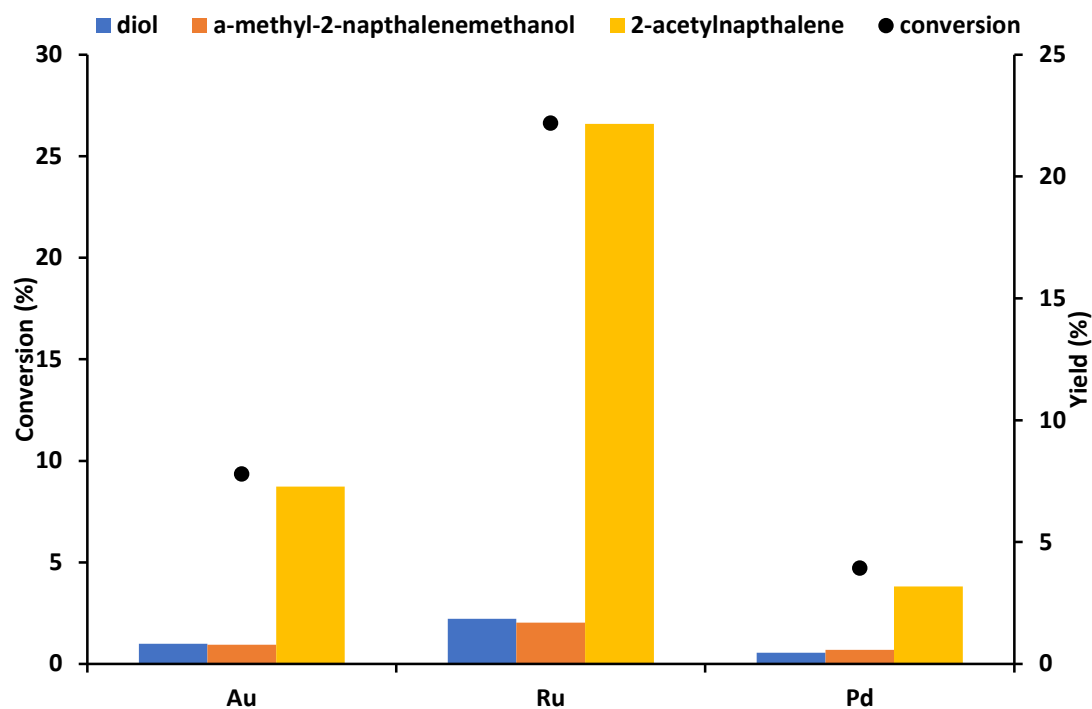


Figure 6. Comparison of monometallic modified impregnation catalysts

Reaction conditions: *Molar ratio substrate:metal 6500:1, 12.8 mmol 2-ethylnaphthalene, 12.8 mmol tBHP supplied as 70 wt.% solution in water, 80°C, 24 h, 1000 rpm stirring.*

The activity of the monometallic Ru catalyst far exceeds that of either the Au or the Pd monometallic, confirming the hypothesis drawn from earlier data: Ru is intrinsically more active than Au for this reaction. The lack of activity displayed by the Pd catalyst indicates that it is likely the Ru component of the RuPd bimetallic catalyst that is responsible for the observed activity. This is consistent with findings for toluene oxidation.

However, as total mmols metal remains constant under experimental conditions, in the case of the 1 wt.% Ru/TiO₂ catalyst there are approximately twice as many

mmols of ruthenium present as in the experiments with 1 wt.% Ru_{0.50}Pd_{0.50}/TiO₂. Despite this, the total conversion in these cases is similar, as are the TOF values obtained (~7200 h⁻¹ for 1 wt.% Ru/TiO₂ and ~7400 h⁻¹ for 1 wt.% Ru_{0.50}Pd_{0.50}/TiO₂). If ruthenium loading solely decided activity, the bimetallic catalyst would be expected to perform less well than the ruthenium monometallic. This suggests that only some of the ruthenium loaded on the monometallic is active, or that alloying ruthenium with palladium drastically enhances activity in some way.

To investigate this further, a 0.5 wt.% Ru/TiO₂ catalyst was prepared by the same modified impregnation method and applied for 2-ethylnaphthalene oxidation. The mass of catalyst used was equivalent to that of the 1 wt.% Ru/TiO₂ catalyst tested. Therefore the number of mmols ruthenium present is effectively halved, but all other conditions remained the same. A comparison of reaction results for these catalysts is shown in **Figure 7**. The reactions have carbon balances of >96%.

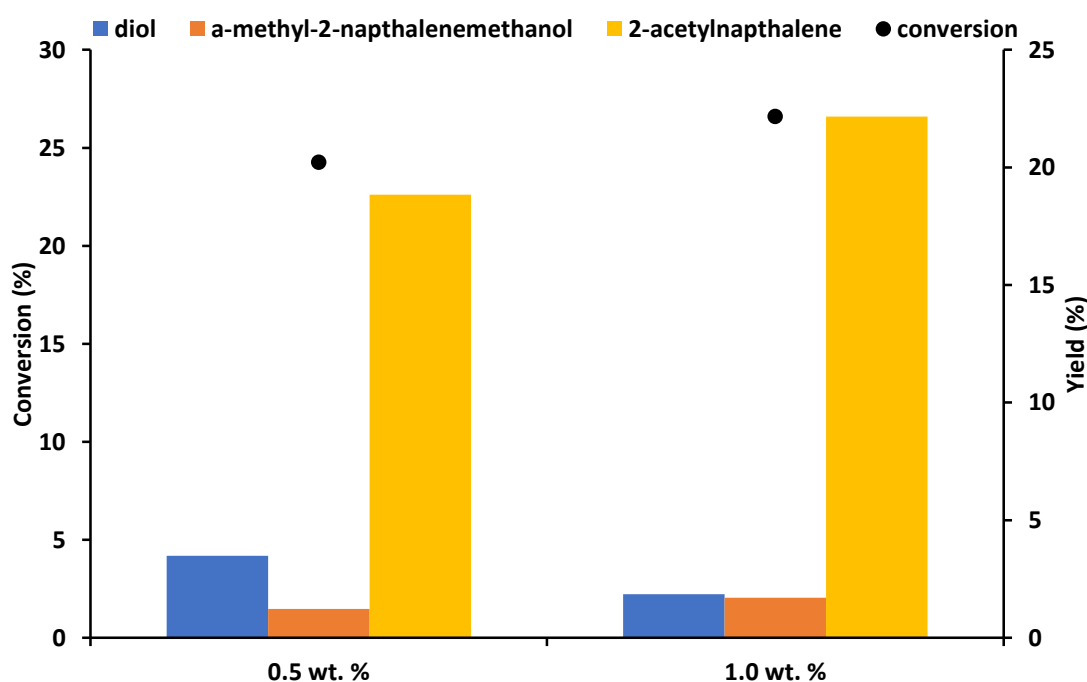


Figure 7. Comparison of monometallic Ru catalysts with different wt. % loading

Reaction conditions: 20 mg catalyst, 12.8 mmol 2-ethylnaphthalene, 12.8 mmol tBHP supplied as 70 wt.% solution in water, 80°C, 24 h, 1000 rpm stirring.

Doubling the weight loading of the catalyst from 0.5 wt.% to 1 wt.% Ru might be expected to double the conversion. Instead, it resulted in a conversion increase of 3%. This corresponds to TOF values of 7200 h^{-1} for the 1 wt.% catalyst and 13360 h^{-1} for the 0.5 wt.% catalyst. This strongly suggests that not all the metal present on the 1 wt.% Ru catalyst is active, or diffusion away from certain metal sites is poor, reducing the number of available sites. This is potentially due to ruthenium forming larger nanoparticles on the 1 wt.% catalyst than the 0.5 wt.% catalyst; effectively meaning the surface area of ruthenium available for reaction does not increase linearly with metal loading. Alternatively, at higher metal loadings, radicals formed near active sites may terminate prior to further reaction.

The total mmols ruthenium present in the above reaction with the 0.5 wt. % Ru/TiO₂ catalyst is equivalent to the total mmols ruthenium in the standard reaction with the 1 wt.% Ru_{0.50}Pd_{0.50}/TiO₂ catalyst. Therefore if ruthenium is solely responsible for the activity of the bimetallic catalyst, with the palladium playing no role, we might expect the conversion of the two catalysts under the same conditions to be similar. In **Figure 8**, results for these two catalysts are compared. Carbon balances were >96%.

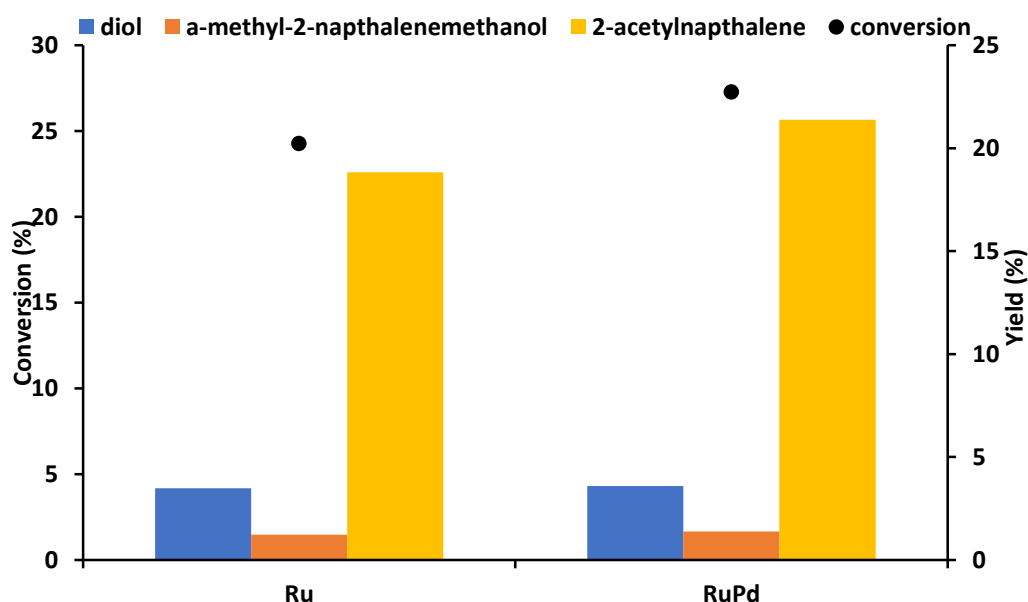


Figure 8. Comparison of bimetallic and monometallic catalyst: same total mols Ru

Reaction conditions: 20 mg catalyst, 12.8 mmol 2-ethylnaphthalene, 12.8 mmol tBHP supplied as 70 wt.% solution in water, 80°C, 24 h, 1000 rpm stirring.

The bimetallic catalyst achieves 27% conversion, and the monometallic 24% conversion. The addition of palladium, effectively doubling the mmols metal present, improves conversion by only 3%; an increase equivalent to that observed when metal loading of the monometallic catalyst was doubled from 0.5 wt.%.

This strongly supports the premise that ruthenium is responsible for the activity of the catalyst, but not all ruthenium sites are active. The 3% increase on addition of palladium may be the result of a beneficial effect such as increased metal-support interaction or promotion of active sites, but this requires further investigation to prove.

4.2.4. Influence of metal molar ratio

The toluene oxidation experiments described in Chapter Three, sections 3.3.4. and 3.3.5. and the 2-ethylnaphthalene results discussed in section 4.2.3. suggest that the activity of the bimetallic RuPd catalyst is primarily attributable to ruthenium. The palladium content instead acts similarly to a promoter; enhancing activity by modifying the electronic structure of the nanoparticle, diluting the Ru content to produce more active sites, or increasing metal support-interaction. If this is the case, the molar ratio of Pd to Ru should have a significant effect on catalyst activity.

Bimetallic 1 wt.% RuPd/TiO₂ catalysts were prepared using a range of Pd to Ru molar ratios. Each of these catalysts was tested under the same conditions. The molar ratio of total metal to substrate was kept constant throughout. Results are shown in **Figure 9**. Carbon balances for these reactions were >93%.

As the Pd content of the catalyst is increased from 50% of the total metal mols through to 75%, the total conversion decreases significantly. This is consistent with the hypothesis that it is ruthenium rather than palladium that is chiefly responsible for conversion; the increase in Pd content being concurrent with a decrease in Ru. However, conversion also decreases when increasing Ru content from an equimolar ratio to 75% of metal mols. This is reflected in TOF (h⁻¹) values for these catalysts, shown in **Table 3**.

Again, this suggests that there is an optimum loading of ruthenium, and at high loadings not all the metal present is active. It does not, however, explain why an increased ruthenium loading should lead to a decrease in conversion. There is potentially a dual effect to consider, in terms of how metal ratio and loading effects the overall particle morphology.

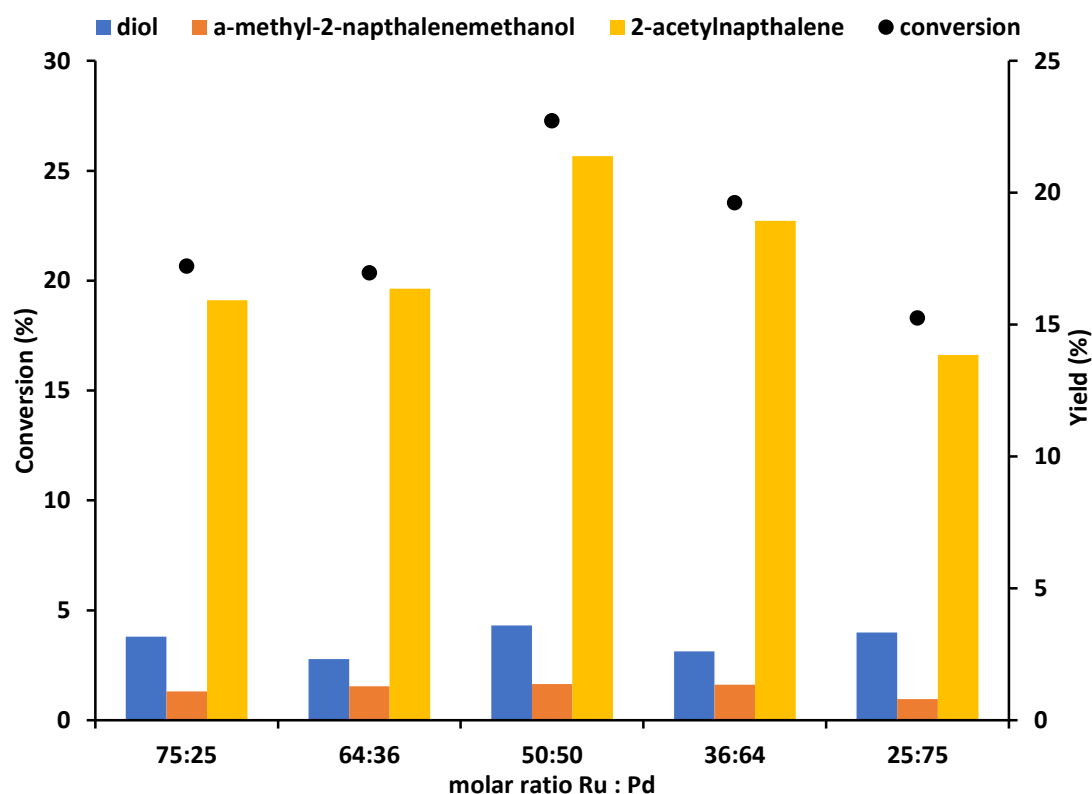


Figure 9. Effect of altering metal molar ratio

Reaction conditions: *Molar ratio substrate:metal 6500:1, 12.8 mmol 2-ethylnaphthalene, 12.8 mmol tBHP supplied as 70 wt.% solution in water, 80°C, 24 h, 1000 rpm stirring.*

Molar ratio Ru:Pd	conversion (%)	selectivity to acetylnaphthalene (%)	TOF (h ⁻¹)
25:75	18.3	75.7	5006
35:65	23.5	80.4	6425
50:50	27.3	78.4	7395
65:35	20.3	80.4	5558
75:25	20.7	77.1	5587

1 wt.% RuPd/TiO₂ catalysts prepared by modified impregnation.

To investigate this further, CO chemisorption was used to determine nanoparticle dispersion and average nanoparticle size of the catalysts with different metal molar ratios. Results are shown in **Table 4**.

Table 4. Dispersion and average nanoparticle size of RuPd catalysts with different molar metal ratios

molar ratio Ru:Pd	dispersion (%)	average particle size (Å)	metal surface area (m²/g)
25:75	6.52	41.10	0.38
35:65	9.75	43.43	0.43
50:50	41.56	8.98	1.85
65:35	21.89	20.32	0.80
75:25	30.47	14.60	1.11

1 wt.% RuPd/TiO₂ catalysts prepared by modified impregnation.

The equimolar metal ratio produces the smallest nanoparticles and the highest dispersion. Ru-rich or Pd-rich ratios form larger particles, which may in turn lead to a decrease in the number of active sites available and therefore the decrease in conversion.

In **Figure 10**, the 0.5 wt.% Ru/TiO₂ monometallic catalyst is compared with the 1 wt.% Ru_{0.36}Pd_{0.64}/TiO₂ and 1 wt.% Ru_{0.25}Pd_{0.75}/TiO₂ catalysts, both of which have a higher total metal loading but lower ruthenium content than the monometallic. The 0.5 wt.% Ru/TiO₂ catalyst and the 1 wt.% Ru_{0.36}Pd_{0.64}/TiO₂ catalyst achieve broadly similar conversion and yield, despite the fact the bimetallic contains less ruthenium; the component responsible for conversion to products. This is strong evidence that the presence of Pd is beneficial.

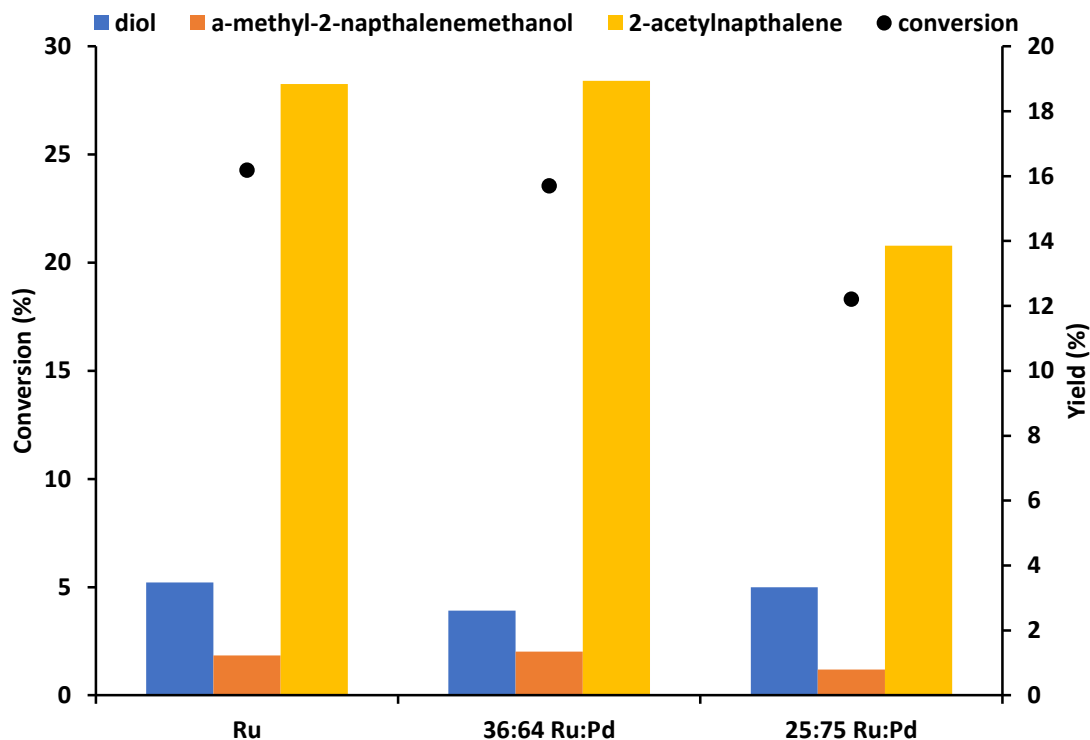


Figure 10. Comparing 0.5 wt.% Ru/TiO₂ to 1 wt.% RuPd/TiO₂ with different Ru:Pd ratios

Reaction conditions: 20 mg catalyst, 12.8 mmol 2-ethylnaphthalene, 12.8 mmol tBHP supplied as 70 wt.% solution in water, 80 °C, 24 h, 1000 rpm stirring.

4.2.5. Influence of substrate:metal ratio

Sections 4.2.3. and 4.24. suggest a complex relationship between metal ratio, nanoparticle size and metal loading. To examine this behaviour in greater detail, varying amounts of the same catalyst was used to produce different molar ratios of 2-ethylnaphthalene to metal. Similar studies with toluene, described in Chapter Three, section 3.3.9., found that decreasing mass catalyst used (and therefore increasing molar ratio of substrate:metal) resulted in increased conversion, contrary to expectations.

Results for experiments with 2-ethylnaphthalene are shown in **Figure 11**. Carbon balances for these reactions >92%.

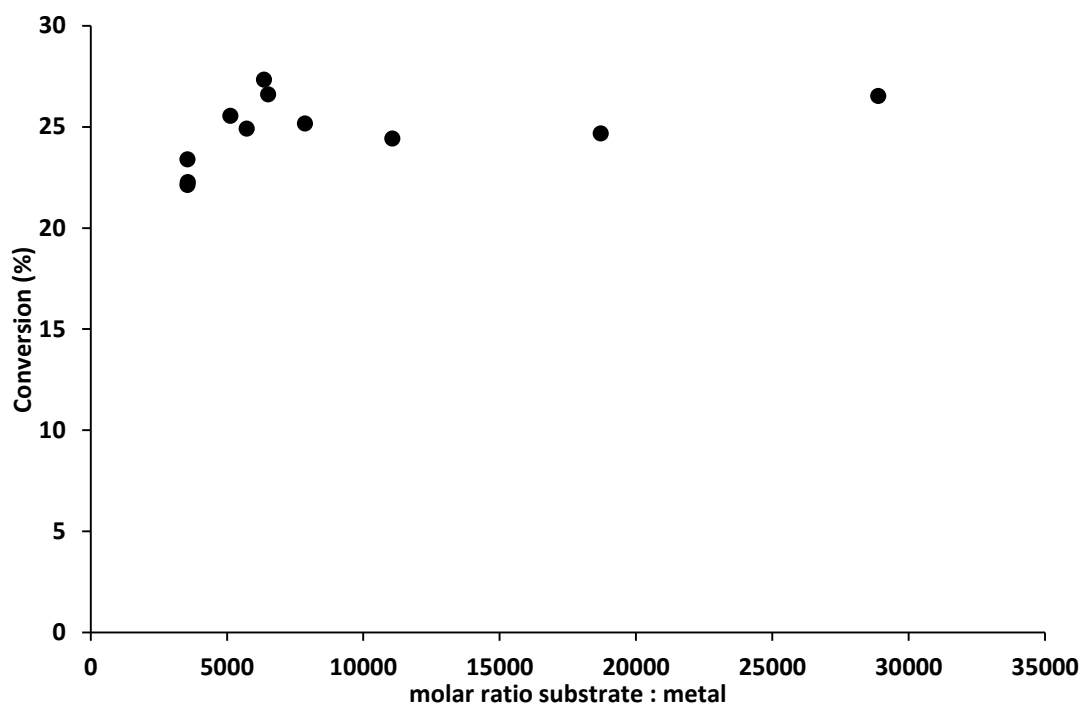


Figure 11. Effect of altering molar ratio of substrate to metal

Reaction conditions: *12.8 mmol 2-ethylnaphthalene, 12.8 mmol tBHP supplied as 70 wt.% solution in water, 80°C, 24 h, 1000 rpm stirring.*

In the previous experiments with toluene as substrate, the change in molar ratio of substrate to metal produced a clear trend. That is not the case here, when investigating 2-ethylnaphthalene. It is evident that multiple effects must be considered, but given the complexity of the system it is unlikely that the influence of each can be separated.

For instance, we must consider that this is a biphasic solvent system. 2-ethylnaphthalene and water are clearly immiscible, and so for the reaction with tBHP to take place, the oxygen-containing products of tBHP decomposition must come into contact with and be transferred into the reactant 2-ethylnaphthalene. This is confirmed by the presence of tertiary-butylalcohol in the organic layer, confirmed by GC analysis.

The variable amount of powder catalyst applied to achieve the changing ratio increases the complexity of the system. Larger quantities of catalyst may lead to agglomeration, effectively reducing the surface area. To try and prevent this, the

solid powder catalyst was added to the system after the liquid components and the mixture thoroughly stirred. Visual inspection revealed no build-up of catalyst on either the vessel or stirrer bar. Even so, should undetected agglomeration of catalyst occur, resulting mass transport limitations could substantially hinder conversion.

4.2.6. Influence of tBHP:metal ratio

The complicated relationship between nanoparticle size and conformation, metal ratio and loading, mass transport limitations and conversion can be investigated from another angle; examining the effect of changing the molar ratio of tBHP:metal.

Experiments were performed in which the total mass of 1wt.% Ru_{0.50}Pd_{0.50}/TiO₂ catalyst was kept constant and the volume of tBHP supplied was changed. Results from this experiment shown in **Figure 12**.

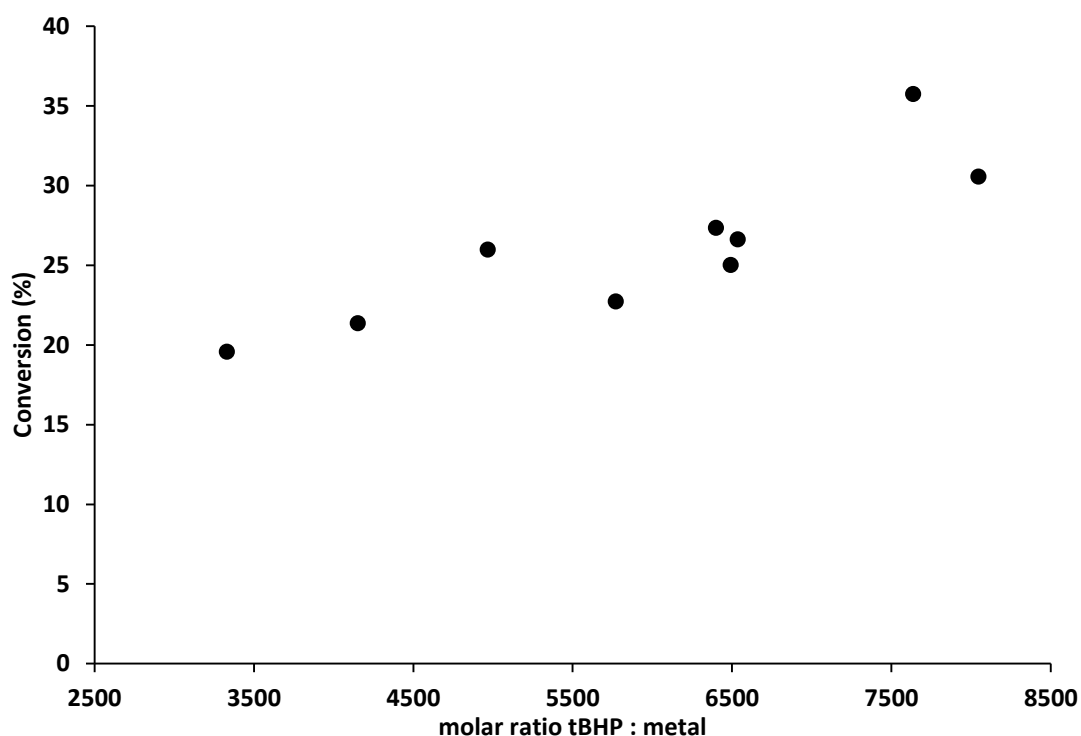


Figure 12. Altering molar ratio of tBHP to metal by varying mmols tBHP supplied

Reaction conditions: *Molar ratio substrate:metal 6500:1, 12.8 mmol 2-ethylnaphthalene, tBHP supplied as 70 wt.% solution in water, 80°C, 24 h, 1000 rpm stirring.*

Broadly, as the volume of tBHP increases, the total conversion increases. This is the expected result if tBHP is acting as the oxidant, as it was shown to do for toluene oxidation in Chapter Three, section 3.3.12...

The effect of changing molar ratio of tBHP to metal on the selectivity of the reaction is shown in **Figure 13**. The selectivity to 2-acetylnaphthalene, the major product, is largely unaffected by the change. However, at molar ratios of tBHP:metal of under 5400, the reaction is more selective to α -methyl-2-naphthalenemethanol than the diol product. At molar ratios of tBHP:metal of over 5400, the reverse is the case. This is likely due to the increased availability of tBHP making a secondary oxidation of α -methyl-2-naphthalenemethanol to the diol more feasible.

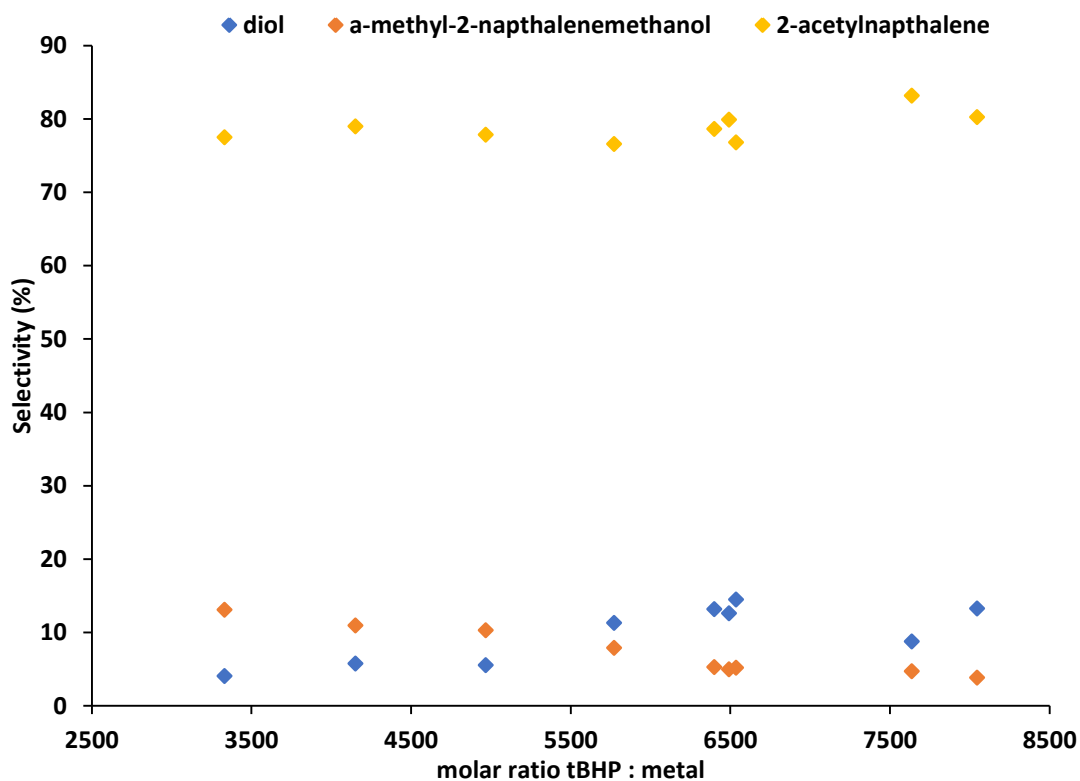


Figure 13. Selectivity when altering molar ratio of tBHP to metal by varying mmols tBHP supplied

Reaction conditions: *Molar ratio substrate:metal 6500:1, 12.8 mmol 2-ethylnaphthalene, tBHP supplied as 70 wt.% solution in water, 80°C, 24 h, 1000 rpm stirring.*

In section 4.2.5., it was suggested that agglomeration of the powder catalyst could effectively decrease the available surface area for reaction, and mass transport limitations would therefore reduce conversion. If this is the case, performing similar experiments to those above, altering the tBHP:metal ratio by keeping tBHP constant and varying mass 1 wt.% Ru_{0.50}Pd_{0.50}/TiO₂ catalyst, may give an indication as to whether this is taking place. Results for these experiments are shown in **Figure 14**.

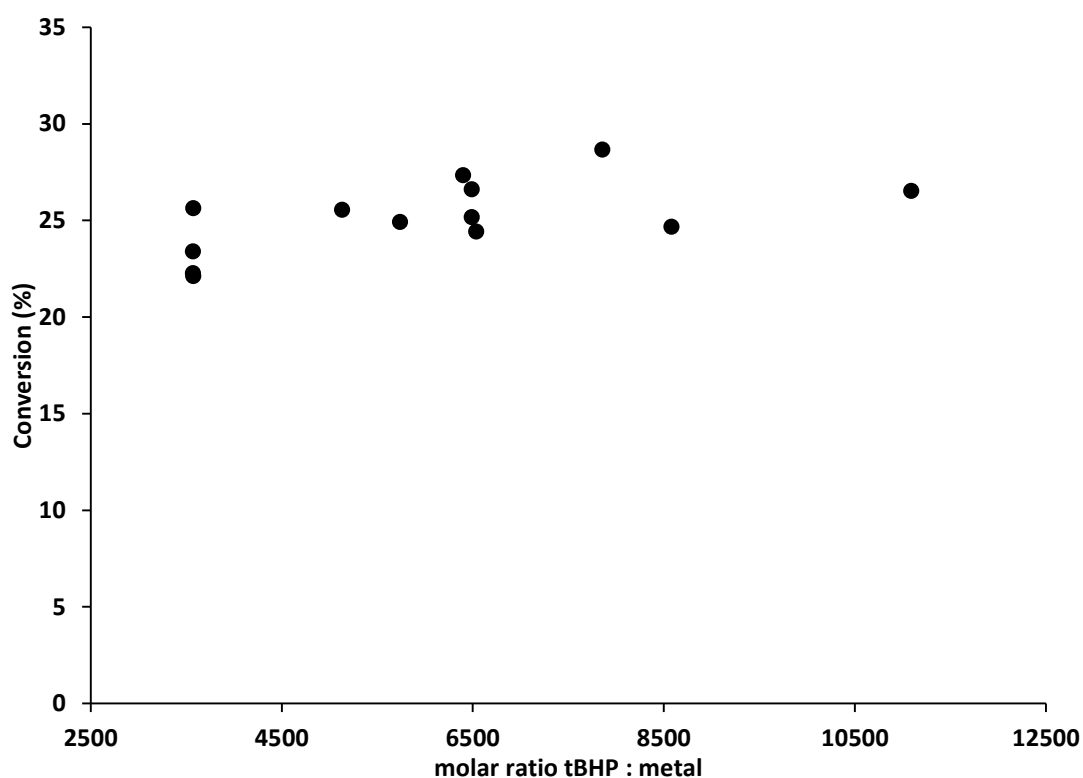


Figure 14. Altering molar ratio of tBHP to metal by varying mass catalyst supplied

Reaction conditions: *Molar ratio substrate:metal 6500:1, 12.8 mmol tBHP supplied as 70 wt.% solution in water, 80°C, 24 h, 1000 rpm stirring.*

The data shown in **Figure 14** displays no obvious trend, except a very slight increase in conversion when the molar ratio tBHP:metal increases, a.k.a. when the mass catalyst supplied is decreased. This supports the idea that mass transport issues relating to the catalyst plays a role in determining conversion. At very high mass loadings of catalyst, corresponding to molar ratios of tBHP:metal of <2500, catalyst is visibly deposited on the walls of the reaction flask due to insufficient stirring.

The effect of changing mass loading catalyst on selectivity is shown in **Figure 15**. Once again, the selectivity to acetylnaphthalene as the major product is unaffected. Significantly, the change in selectivity to diol and α -methyl-2-naphthalenemethanol previously observed at molar ratios tBHP:metal of 5400, shown in **Figure 13**, is not observed in this case. This supports the hypothesis that this is related specifically to availability of tBHP, as proposed, rather than mass transport limitations.

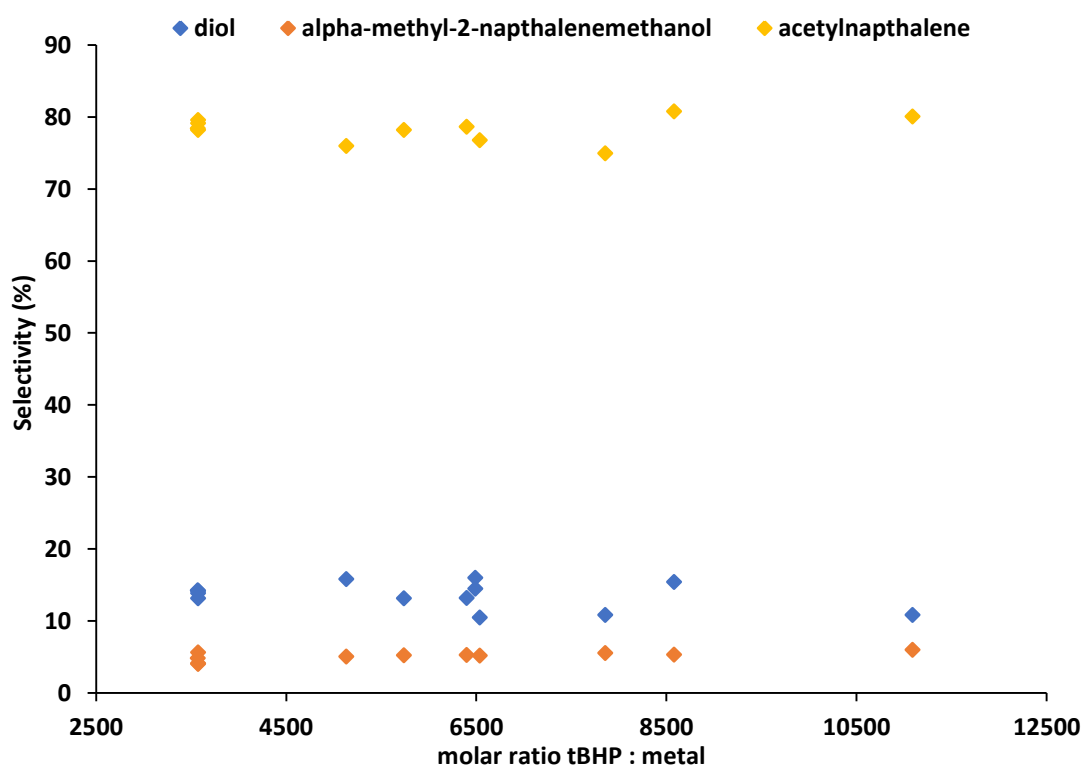


Figure 15. Selectivity when altering molar ratio of tBHP to metal by varying mass catalyst supplied

Reaction conditions: *Molar ratio substrate:metal 6500:1, 12.8 mmol tBHP supplied as 70 wt.% solution in water, 80°C, 24 h, 1000 rpm stirring.*

4.2.7. Influence of tBHP:substrate ratio

Tertiary-butylhydroperoxide is a powerful radical initiator. However, it may also act as an oxygen source. In Chapter Three, section 3.3.12., it was established that in reactions under similar conditions with 1 wt.% Ru_{0.50}Pd_{0.50}/TiO₂ as catalyst and toluene as substrate, the tBHP supplied acts as an oxidant. Given the similarities

between toluene and 2-ethylnaphthalene, and extensive use of tBHP as oxidant in the literature^{96, 99, 100, 109}, it was suspected that tBHP also acts as the oxidant in this case, being more easily utilised than O₂ in the atmosphere.

If tBHP is serving as an oxidant, decreasing the volume of tBHP supplied (increasing the mmol ratio of substrate/tBHP) should result in a loss of conversion. Experiments were carried out in which the mmols tBHP supplied was varied. Results are shown in **Figure 16**.

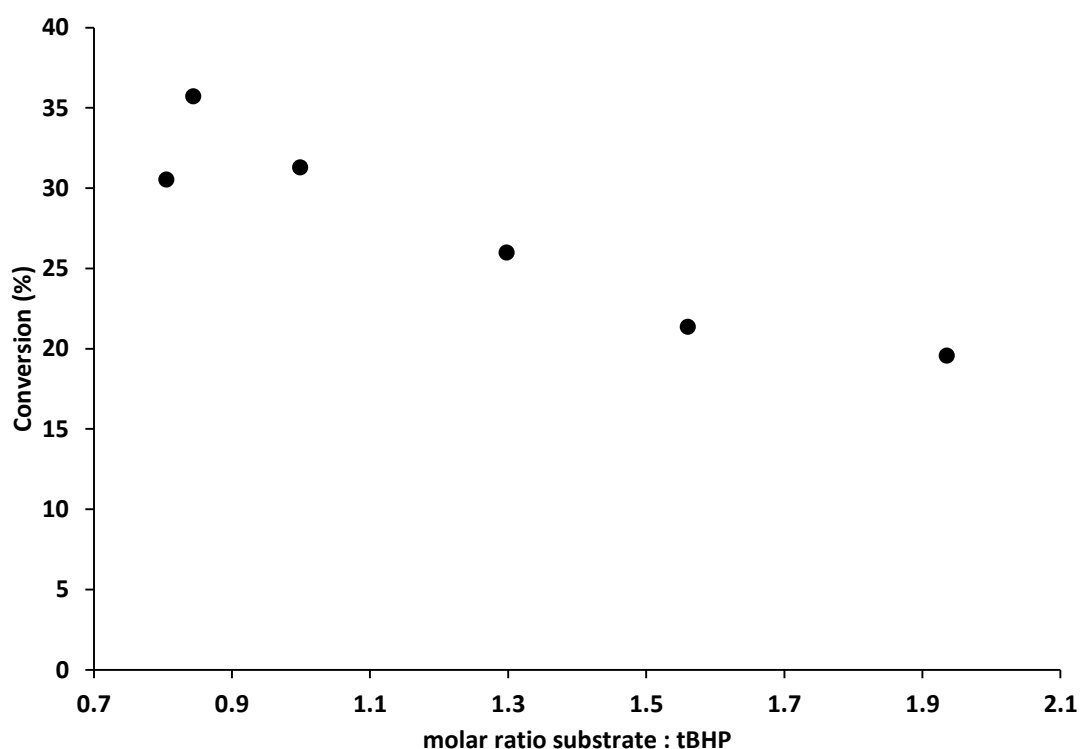


Figure 16. Altering ratio of substrate to tBHP

Reaction conditions: *Molar ratio substrate:metal 6500:1, 12.8 mmol 2-ethylnaphthalene, tBHP supplied as 70 wt.% solution in water, 80°C, 24 h, 1000 rpm stirring.*

Broadly, the data follows a similar trend to that observed in experiments with toluene as substrate. In both cases, conversion peaks just before the 1:1 point, at a ratio of 0.84:1 for 2-ethylnaphthalene and 0.87:1 for toluene. After this point, conversion decreases as mmols tBHP is decreased; as expected for tBHP acting as oxidant. The decrease in conversion is comparatively large for a small decrease in tBHP.

4.2.8. Influence of oxidant solvent

In the standard experimental conditions, an aqueous tBHP solution was used in the experiments. The reactions are therefore biphasic; water and 2-ethylnaphthalene are immiscible. Because of this, the interaction of tBHP and substrate may be hindered. This would in turn have a negative effect on the reaction, decreasing conversion and yield.

To establish if the biphasic nature of the system is detrimental, tBHP was instead supplied as part of an organic solution; in this case as 5.6 M tBHP in n-decane. Decane is stable under the reaction conditions; with no conversion observed after 24 h. 1 wt.% Ru_{0.50}Pd_{0.50}/TiO₂ was used as a catalyst and the same molar ratio of tBHP to substrate used in both cases. All other conditions were as described in Chapter Two, 2.6.3. Results are shown in **Figure 17**.

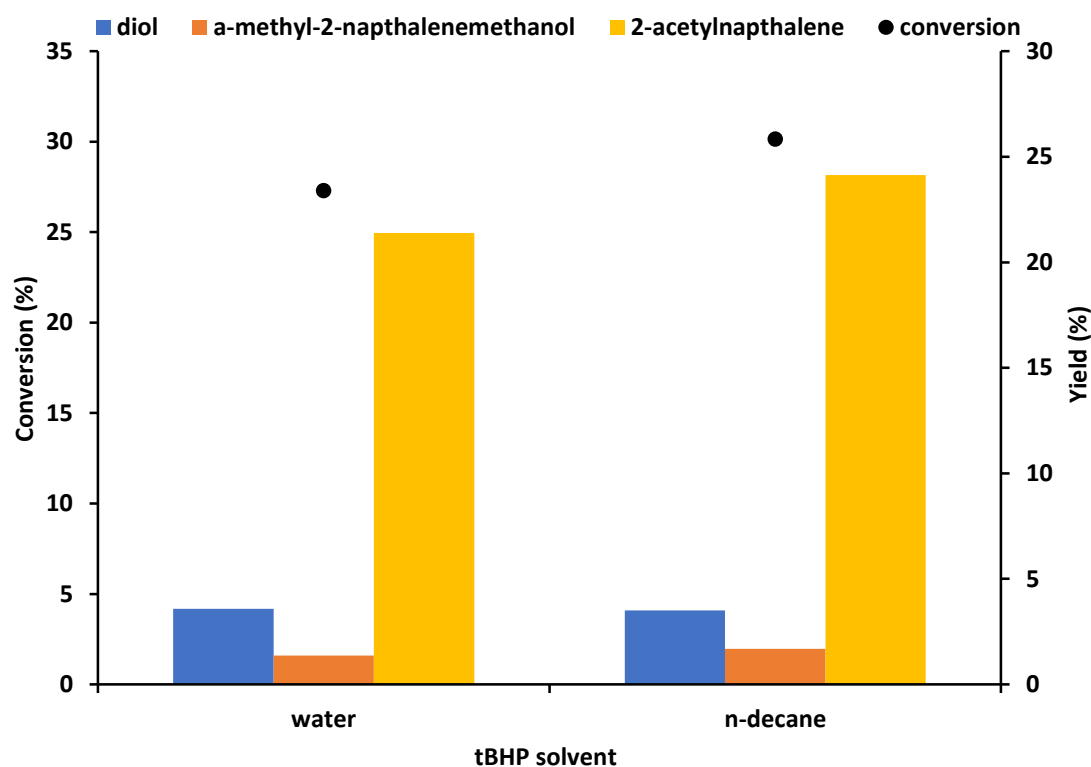


Figure 17. Influence of choice of tBHP solvent solution

Reaction conditions: *Molar ratio substrate:metal 6500:1, 12.8 mmol 2-ethylnaphthalene, tBHP supplied as 5.6M solution in n-decane or 70 wt% solution in water, 80°C, 24 h, 1000 rpm stirring.*

Changing the solvent from water to decane results in a 3% increase in conversion. While this represents an improvement, it is less significant than might have been expected. This may suggest that the biphasic nature of the reaction is not a problem. It is possible that the 24 h reaction time is sufficient for tBHP to diffuse into the organic phase. This would be consistent with the decrease in the volume of the aqueous layer observed post-reaction. Chromatograms of each layer post-reaction indicate that only trace amounts of tBHP remain in either; and the expected products of the breakdown of tBHP (primarily tertiary-butylalcohol) are found in the organic portion. This supports the idea that the reaction time is sufficient and may help to explain why the choice of solvent does not produce a more dramatic change.

4.2.9. Influence of temperature

Under the standard conditions chosen for this work, reactions are carried out at 80°C. This low temperature was selected in keeping with the project objective to achieve oxidation in mild conditions, and also as a safety precaution, given the nature of tBHP¹¹⁰ and the flammable nature of the reactant¹¹¹.

Decreasing the reaction temperature reduces costs and, in many cases, improves product selectivity. However, it also reduces the rate of reaction and ultimately the total conversion. To investigate this, reactions with 1 wt.% Ru_{0.50}Pd_{0.50}/TiO₂ were carried out at 40°C and 60°C. Results are shown in **Figure 18**. Carbon balances were >98% for these reactions.

As predicted, a decrease in reaction temperature leads to a corresponding decrease in conversion. Product selectivity was also affected by the temperature change. At lower temperatures, yields of the diol and α -methyl-2-naphthalenemethanol are similar. At higher temperatures, however, the diol is preferred over α -methyl-2-naphthalenemethanol, though both represent less than 20% of the products formed.

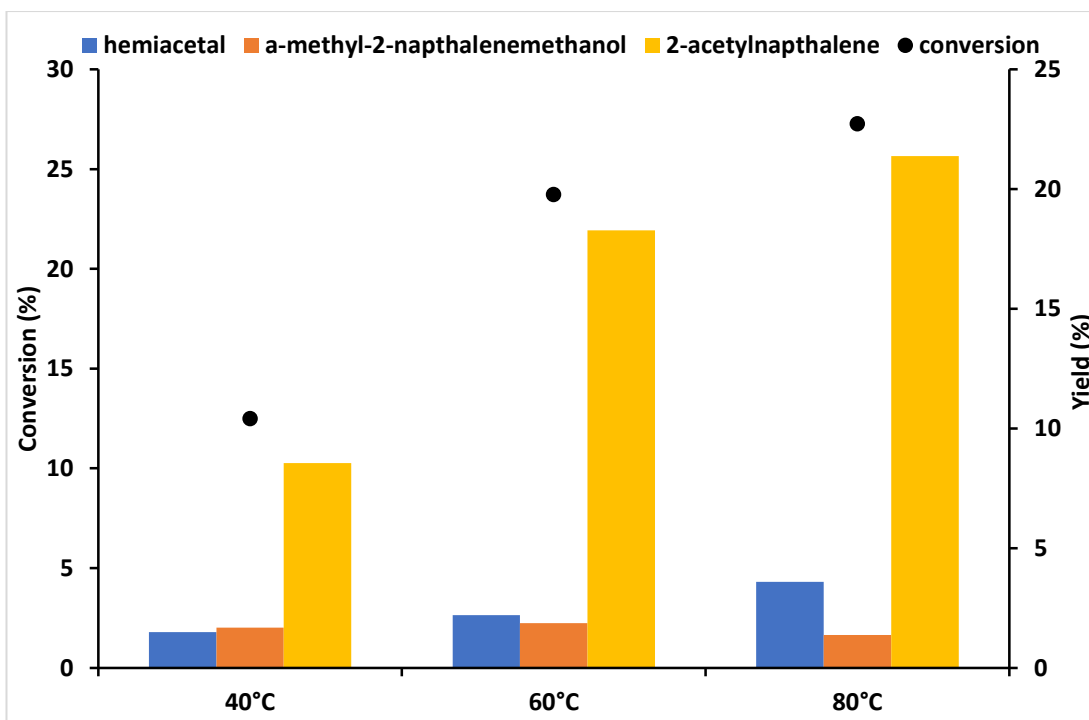


Figure 18. Effect of reaction temperature

Reaction conditions: *Molar ratio substrate:metal 6500:1, 12.8 mmol 2-ethylnaphthalene, 12.8 mmol tBHP supplied as 70 wt.% solution in water, 24 h, 1000 rpm stirring.*

4.3. Conclusions

Throughout this chapter, RuPd/TiO₂ catalysts found to be active for toluene oxidation (as discussed in Chapter Three) were applied to the oxidation of 2-ethylnaphthalene. These catalysts were extensively compared with the activity of gold-containing equivalents.

Firstly, the effectiveness of the sol immobilisation, conventional impregnation and modified impregnation techniques for the synthesis of both 1 wt.% Au_{0.50}Pd_{0.50}/TiO₂ and 1 wt.% Ru_{0.50}Pd_{0.50}/TiO₂ was explored. The average nanoparticle size and dispersion on catalysts prepared by these methods were examined by CO chemisorption. Unfortunately, the weakly binding nature of gold decreases the reliability of results for the 1 wt.% Au_{0.50}Pd_{0.50}/TiO₂ catalysts.

The 1 wt.% Au_{0.50}Pd_{0.50}/TiO₂ catalyst prepared by sol immobilisation achieved the highest conversion. This is consistent with results obtained with toluene. ChemBET

results suggest this may be linked to high nanoparticle dispersion, though this must be confirmed by a more appropriate and reliable form of analysis. The conventional impregnation technique produced the least active catalyst. This was also the case for 1 wt.% Ru_{0.50}Pd_{0.50}/TiO₂.

The 1 wt.% Ru_{0.50}Pd_{0.50}/TiO₂ catalysts prepared by sol immobilisation and modified impregnation achieved similar results, with the modified impregnation catalyst being slightly superior. The calculated average nanoparticle size, dispersion and metal surface area of these catalysts was found to be similar; with the modified impregnation catalyst boasting marginally smaller average nanoparticle size. (This data was also similar to that obtained for the 1 wt.% Au_{0.50}Pd_{0.50}/TiO₂ modified impregnation catalyst). This helps to explain the observed similar activity.

Comparison of 1 wt.% monometallic Au, Pd and Ru catalysts revealed that 1 wt.% Ru/TiO₂ was the most active and selective monometallic catalyst, supporting the hypothesis that ruthenium is particularly active for oxidation chemistry of this kind. However, a 0.5 wt.% Ru/TiO₂ modified impregnation catalyst was found to be almost as active as the 1 wt.%, despite the reduced metal loading. This is potentially due to differences in nanoparticle morphology. If, for example, only certain types of ruthenium site are active, it is possible the 1 wt.% catalyst contains a higher proportion of inactive sites; the result of larger nanoparticles or decreased dispersion. Alternatively, the similar activity could be explained by more frequent radical termination when using the 1 wt.% catalyst; perhaps driven by proximity at active sites. Further characterisation of the catalyst surface is required before this can be explained.

Neither the 0.5 wt.% or 1 wt.% Ru/TiO₂ catalyst exceeded the activity of 1 wt.% Ru_{0.50}Pd_{0.50}/TiO₂ bimetallic, presenting a strong argument for palladium alloying promoting activity. The molar ratio of Ru : Pd in the catalyst was therefore explored, and the equimolar bimetallic found to give the highest conversion, TOF and selectivity to 2-acetylnaphthalene. High selectivity to 2-acetylnaphthalene closely correlates to higher activity, as did selectivity to benzoic acid when oxidising toluene in Chapter Three, and as discussed in Chapter One, section 1.5.1.

Selectivity to 2-acetylnaphthalene remained almost constant when exploring different molar ratios of tBHP : metal, in section 4.2.6. At higher ratios, when more tBHP was supplied, selectivity to α -methyl-2-naphthalene methanol was reduced, and the diol product favoured. This is likely related to the greater availability of oxidant promoting a secondary oxidation step. The same change in selectivity was not observed when increasing the molar ratio of tBHP : metal by decreasing the amount of catalyst supplied. This suggests that in this case the availability of the catalyst is the limiting factor.

When the molar ratio of substrate : tBHP was decreased by decreasing the amount of tBHP supplied, conversion drastically decreased. This is consistent with tBHP serving as an oxidant, as was the case in reactions with toluene.

Given the importance of tBHP, an alternate source was explored: tBHP supplied in organic solution rather than aqueous, as was standard for all previous reactions. Using tBHP in decane eliminated the aqueous phase and improved conversion by 3%.

In conclusion, the 1 wt.% $\text{Ru}_{0.50}\text{Pd}_{0.50}/\text{TiO}_2$ catalyst was found to be a good alternative to 1 wt.% $\text{Au}_{0.50}\text{Pd}_{0.50}/\text{TiO}_2$, consistently outperforming these gold catalysts prepared by the same technique. High conversion of 2-ethylnaphthalene by 1 wt.% $\text{Ru}_{0.50}\text{Pd}_{0.50}/\text{TiO}_2$ was found to correlate with high average nanoparticle dispersion and small average nanoparticle sizes, determined by CO chemisorption. High conversion also appears to directly correlate with high selectivity to the target product 2-acetylnaphthalene.

In general, conversions observed when 2-ethylbenzene was substrate exceed those obtained in similar conditions when toluene was substrate. This is potentially due to the extension of the conjugated system across another aromatic ring improving the stability of reaction intermediates.

4.4. References

1. V. Peneau, Q. He, G. Shaw, S. A. Kondrat, T. E. Davies, P. Miedziak, M. Forde, N. Dimitratos, C. J. Kiely and G. J. Hutchings, *Physical Chemistry Chemical Physics*, 2013, **15**, 10636-10644.
2. V. Peneau, Doctor of Philosophy, Cardiff University, 2014.
3. R. A. Sheldon, *Chemtech*, 1991, **21**, 566-576.
4. M. Sankar, Q. He, M. Morad, J. Pritchard, S. J. Freakley, J. K. Edwards, S. H. Taylor, D. J. Morgan, A. F. Carley, D. W. Knight, C. J. Kiely and G. J. Hutchings, *Acs Nano*, 2012, **6**, 6600-6613.
5. N. Dimitratos, J. A. Lopez-Sanchez, D. Morgan, A. F. Carley, R. Tiruvalam, C. J. Kiely, D. Bethell and G. J. Hutchings, *Physical Chemistry Chemical Physics*, 2009, **11**, 5142-5153.
6. J. A. Lopez-Sanchez, N. Dimitratos, P. Miedziak, E. Ntainjua, J. K. Edwards, D. Morgan, A. F. Carley, R. Tiruvalam, C. J. Kiely and G. J. Hutchings, *Physical Chemistry Chemical Physics*, 2008, **10**, 1921-1930.
7. G. J. Hutchings and C. J. Kiely, *Accounts of Chemical Research*, 2013, **46**, 1759-1772.
8. S. N. Tripathi, S. R. Bharadwaj and S. R. Dharwadkar, *Journal of Phase Equilibria*, 1993, **14**, 638-642.
9. D. Wu, K. Kusada and H. Kitagawa, *Science and Technology of Advanced Materials*, 2016, **17**, 583-596.
10. W. Luo, M. Sankar, A. M. Beale, Q. He, C. J. Kiely, P. C. A. Bruijninx and B. M. Weckhuysen, *Nature communications*, 2015, **6**, 6540-6540.
11. S. Chen, Z. Liu, E. Shi, L. Chen, W. Wei, H. Li, Y. Cheng and X. Wan, *Organic Letters*, 2011, **13**, 2274-2277.
12. V. R. Choudhary, D. K. Dumbre and S. K. Bhargava, *Industrial & Engineering Chemistry Research*, 2009, **48**, 9471-9478.

13. *Luperox TBH70X, tert-Butyl hydroperoxide solution Safety Data Sheet, Sigma Aldrich, 2018.*
14. *2-Ethyl-naphthalene Safety Data Sheet, Sigma Aldrich, 2018.*

Chapter Five – Ethylbenzene Oxidation

5.1. Introduction

In this chapter, results for the oxidation of ethylbenzene under mild conditions are presented.

Chapters Three and Four focussed particularly on RuPd and AuPd bimetallic catalysts supported on TiO₂ and a variety of closely related catalysts produced via the conventional impregnation, modified impregnation or sol immobilisation methods. Mild reaction conditions were used throughout and similar behaviour was observed for both substrates.

The investigation into ethylbenzene oxidation continued to utilise mild reaction conditions, as per the project aims outlined in Chapter One. Experiments were carried out in the Radleys Reactor. However, in this Chapter a new catalyst was explored: an FePd bimetallic. This catalyst has the advantage of being significantly cheaper than its ruthenium or gold containing counterparts, and displays very different behaviour that may be the result of a radical-based mechanism.

Previous investigations into the ethylbenzene oxidation have also focused on possible radical reactions. Several mechanisms have been proposed^{73, 112}, each endeavouring to explain the unique number and variety of products observed under different experimental conditions.

All reported results are an average of three or more repeats with mass balances > 94 %.

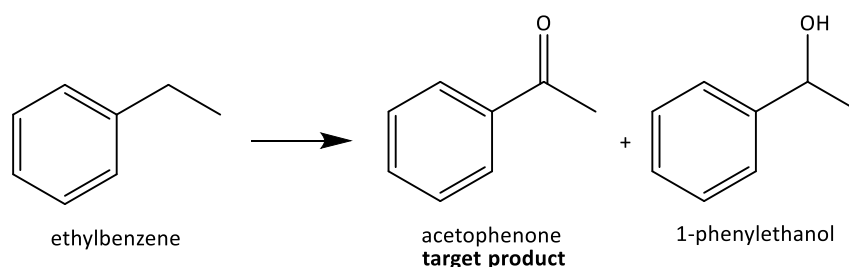


Figure 1. Expected products of ethylbenzene oxidation

5.2. Oxidation reactions in the Radleys reactor

5.2.1. Blank reactions

Auto-oxidation can result in the formation of product species. Reactions were carried out in the absence of catalyst to establish if auto-oxidation takes place under the selected conditions, described in Chapter Two, section 2.6.1. The support material of interest, TiO_2 , was also tested for activity. This TiO_2 first underwent the modified impregnation procedure described in Chapter Two, section 2.4.3., without the addition of metal. Results are shown in **Figure 2**. Carbon balances for these reactions were >97%.

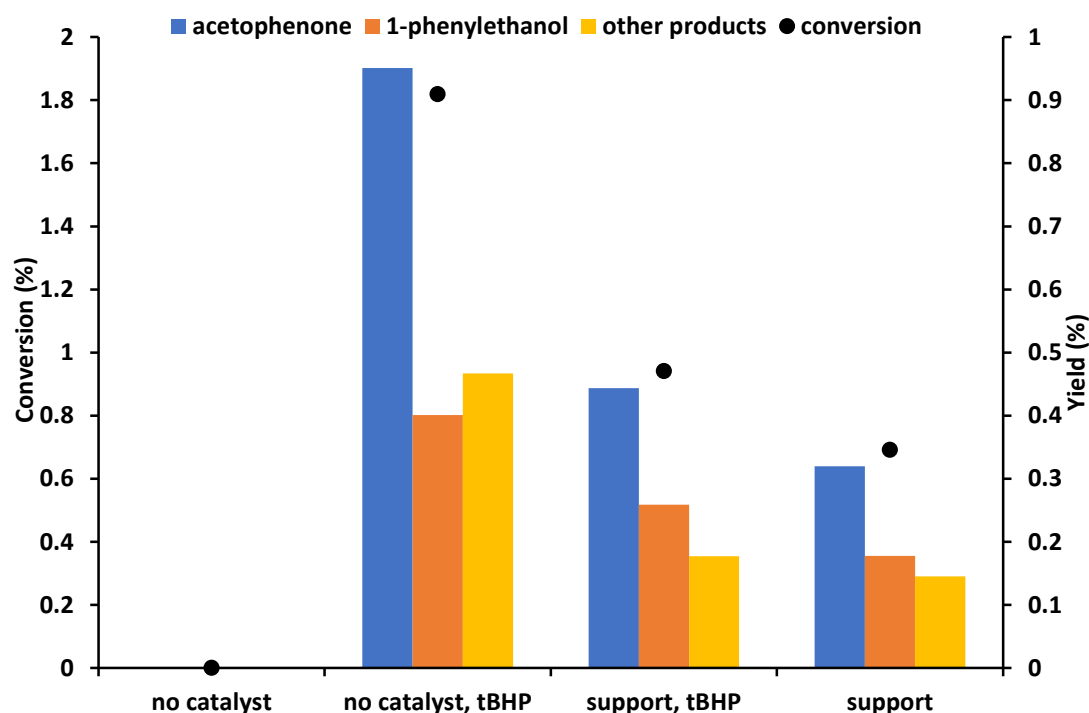


Figure 2. Reactions under standard conditions with no catalyst

Reaction conditions: 8.00 g ethylbenzene, 0.7 mmol tBHP supplied as 70 wt% solution in water (where applicable), 4 mg TiO_2 support material (where applicable), 3 bar O_2 , 140°C, 17 h, 1000 rpm stirring.

No auto-oxidation takes place in the absence of catalyst, TiO_2 or tBHP. When tBHP is present, there is some activity in these conditions. The conversion of <2% is likely the result of auto-oxidation catalysed by the breakdown of tBHP, which forms

oxygen based radicals. However, the experiments conducted with TiO_2 alone suggest that the initiator is not required for some auto-oxidation to take place, as a limited conversion of <1% was detected even in this case. When both initiator and TiO_2 are present, total conversion is lower than that observed when TiO_2 is absent. This suggests that the support material is limiting the conversion in some way; perhaps by allowing more frequent radical termination due to proximity on the surface. TiO_2 is known to support oxygen-based radical species¹⁰⁵.

In all cases, acetophenone is the preferred product, as was the case for the catalyst reported by Ma *et al.*⁶⁴. Both acetophenone and 1-phenylethanol, the next most abundant product, are oxidised at the alpha carbon; the preferred point for oxidation due to the lower bond strength of CH_2 over CH_3 groups. The other products observed were styrene, styrene oxide, benzyl alcohol, 2-phenylethanol and a dimer species: (oxybis(ethane-1,1-diyl))dibenzene. These are shown in **Figure 3**.

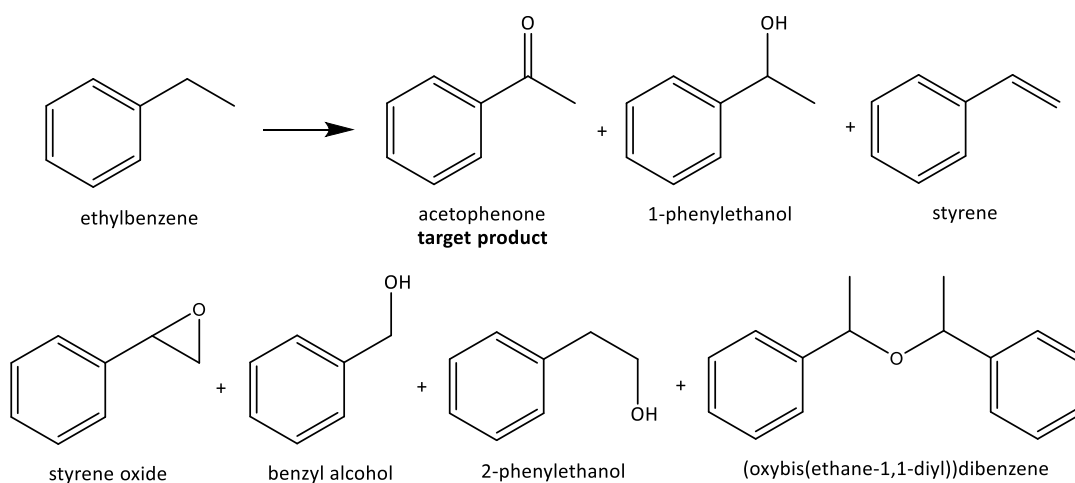


Figure 2. Reactions under standard conditions with no catalyst

5.2.2. AuPd catalysts

1 wt.% $\text{Au}_{0.5}\text{Pd}_{0.5}/\text{TiO}_2$ catalysts prepared by sol immobilisation and modified impregnation have been shown to be active for the oxidation of benzyl alcohol^{33, 57, 106, 113}, toluene^{24, 60, 98, 99} and 2-ethylnaphthalene. Given the similarity of these substrates, it was deemed likely that catalysts of this kind would be active for oxidation of ethylbenzene. Therefore these catalysts were utilized for ethylbenzene oxidation under the conditions described in Chapter Two, section 2.6.1.

Different mass loadings of catalyst were tested, with the intention of closely studying the complex relationship between conversion, molar ratio of substrate:metal and mass transport found in earlier work. Results for the sol immobilised catalyst are displayed in **Figure 4**, for the modified impregnation catalyst in **Figure 5**, and the catalysts and their respective TOF are compared in **Figure 6**. Carbon balances for these reactions were >98%.

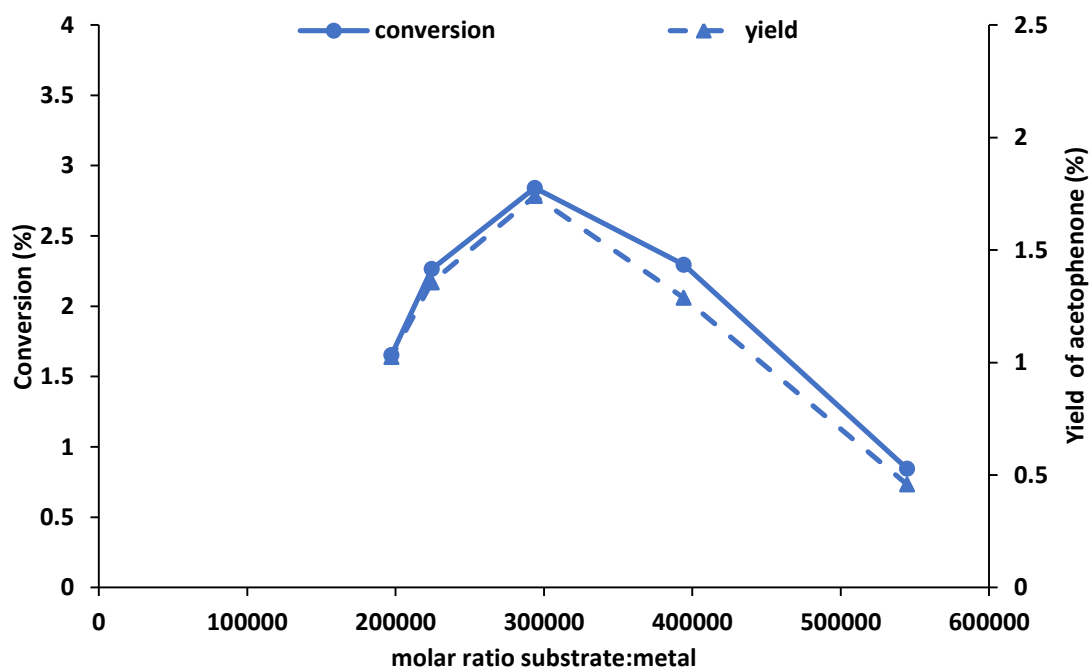


Figure 4. Effect of varying mass 1 wt.% $\text{Au}_{0.5}\text{Pd}_{0.5}/\text{TiO}_2$ sol immobilised catalyst to produce different molar ratios substrate:metal

Reaction conditions: 8.00 g ethylbenzene, 2 – 6 mg catalyst, 3 bar O_2 , 140°C, 17 h, 1000 rpm stirring.

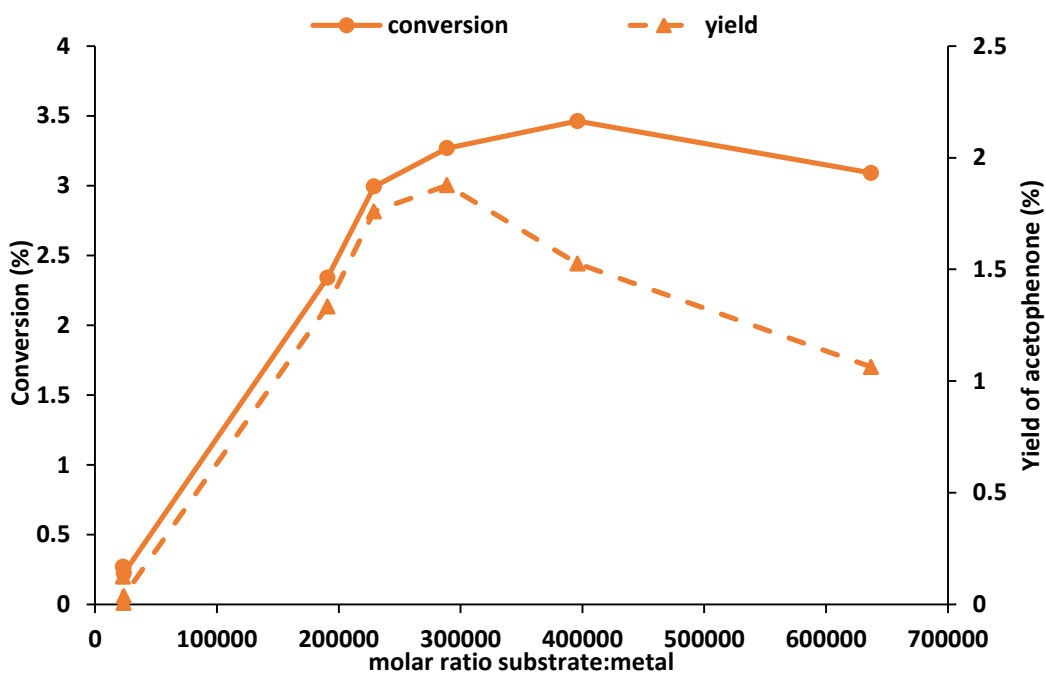


Figure 5. Effect of varying mass 1 wt.% $\text{Au}_{0.5}\text{Pd}_{0.5}/\text{TiO}_2$ modified impregnation catalyst to produce different molar ratios substrate:metal

Reaction conditions: 8.00 g ethylbenzene, 2 – 9 mg catalyst, 3 bar O_2 , 140°C, 17 h, 1000 rpm stirring.

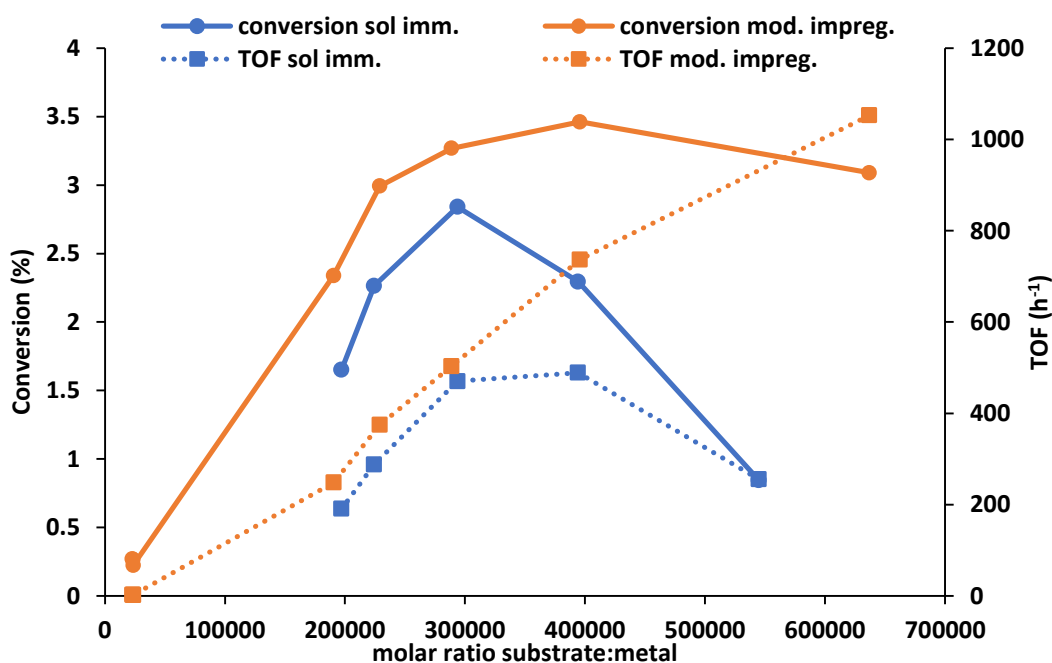


Figure 6. Comparing 1 wt.% $\text{Au}_{0.5}\text{Pd}_{0.5}/\text{TiO}_2$ catalysts prepared by sol immobilisation and modified impregnation

Reaction conditions: 8.00 g ethylbenzene, 2 – 9 mg catalyst, 3 bar O_2 , 140°C, 17 h, 1000 rpm stirring.

An increase in molar ratio substrate:metal corresponds to a decrease in mass catalyst supplied to the reaction. Typically, this is expected to cause a decrease in overall conversion, because as mass catalyst decreases so does the number of available active sites. Therefore the lowest conversions are expected at the highest molar ratios of substrate:metal, and the highest conversions at the lowest molar ratios of substrate:metal. This trend should be linear until mass transport limitations come into effect.

However, this is not the case for the catalysts examined in **Figures 4 to 6**. The activity of the 1 wt.% Au_{0.5}Pd_{0.5}/TiO₂ catalyst prepared by sol immobilisation actually increases when the substrate:metal ratio is increased from 200000 to 300000, (mass catalyst reduced from ~6mg to ~4mg), as opposed to the predicted decrease. After this point, (as catalyst mass is reduced from ~4mg to ~2mg) the conversion does decrease with increasing molar ratio substrate:metal, effectively causing a peak in activity at a ratio of approximately 300000.

The 1 wt.% Au_{0.5}Pd_{0.5}/TiO₂ catalyst prepared by modified impregnation displays similar behaviour, though activity peaks later, at a molar ratio of substrate:metal of approximately 400000. Increasing the molar ratio of substrate:metal to over 600000 decreases conversion by only ~0.5%, and as such produces the highest TOF value, in excess of 1050 h⁻¹. (TOF calculated using equations listed in Chapter Two, section 2.3.).

At all the ratios studied, the modified impregnation catalyst outperforms that prepared by sol immobilisation in terms of conversion and yield of the target product, acetophenone. In general, for both catalysts and all molar ratios of substrate:metal studied, the overall activity is low. Given the extremely small quantities of catalyst being applied, this is not unexpected.

5.2.3. FePd catalysts

The high activity and selectivity of nanoparticulate gold is well known, particularly for reactions involving radicals^{54, 56}. According to the project aims described in Chapter One, section 1.6., expanding the investigation to include an alternative to

gold was of interest. Work described in Chapters Three and Four focused on alternate catalysts containing ruthenium, which is very active but also expensive.

FePd/TiO₂ catalysts have previously been prepared by the sol immobilisation and modified impregnation methods utilised in section 5.2.2., as described in Chapter Two, sections 2.4.1. and 2.4.3. respectively. 1 wt.% Fe_{0.5}Pd_{0.5}/TiO₂ catalysts were synthesised using these techniques and were tested for ethylbenzene oxidation. Results for the sol immobilised catalyst are shown in **Figure 7**, for the modified impregnation catalyst in **Figure 8**, and the catalysts and their respective TOF are compared in **Figure 9**. Carbon balances for these reactions were >98%.

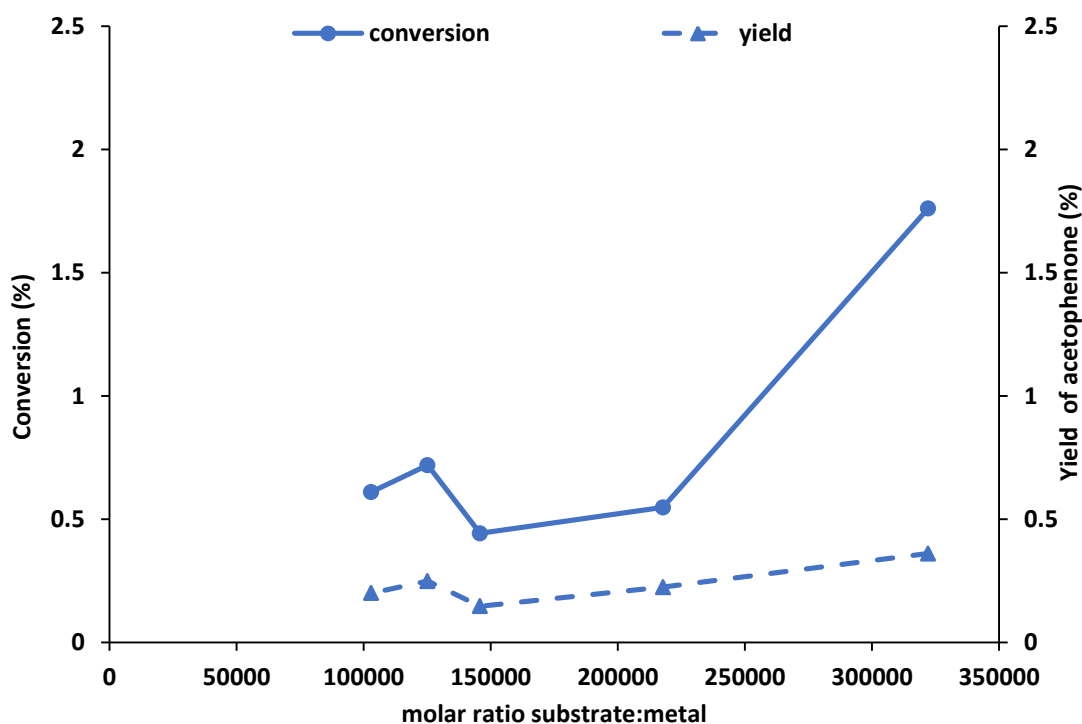


Figure 7. Effect of varying mass 1 wt.% Fe_{0.5}Pd_{0.5}/TiO₂ sol immobilised catalyst to produce different molar ratios substrate:metal

Reaction conditions: 8.00 g ethylbenzene, 2 – 6 mg catalyst, 3 bar O₂, 140°C, 17 h, 1000 rpm stirring.

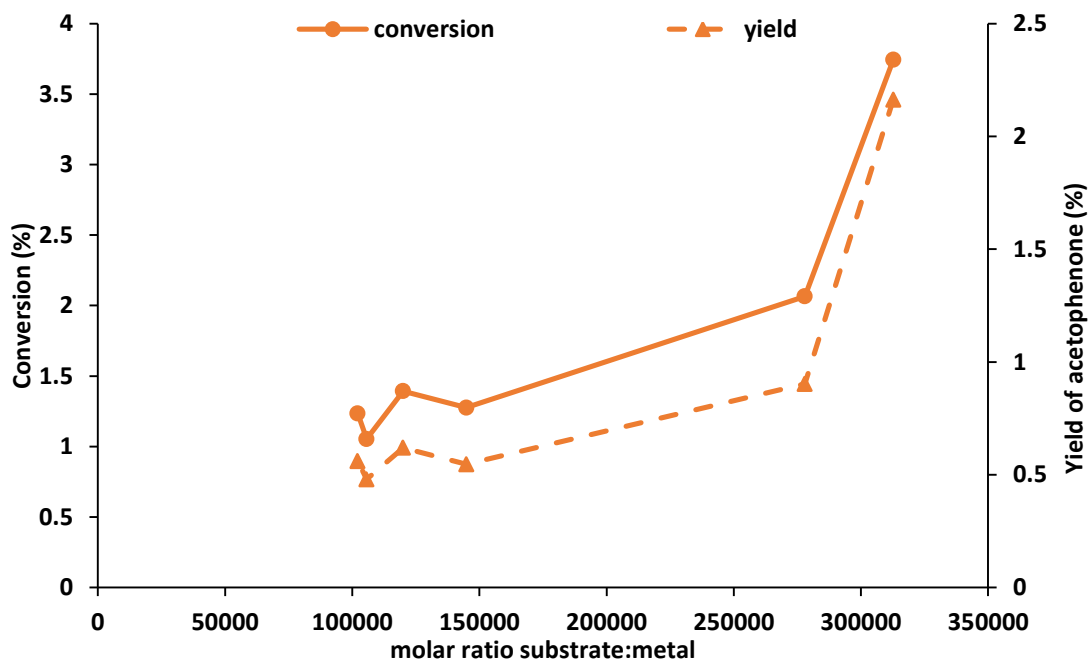


Figure 8. Effect of varying mass 1 wt.% $\text{Fe}_{0.5}\text{Pd}_{0.5}/\text{TiO}_2$ modified impregnation catalyst to produce different molar ratios substrate:metal

Reaction conditions: 8.00 g ethylbenzene, 2 – 6 mg catalyst, 3 bar O_2 , 140°C, 17 h, 1000 rpm stirring.

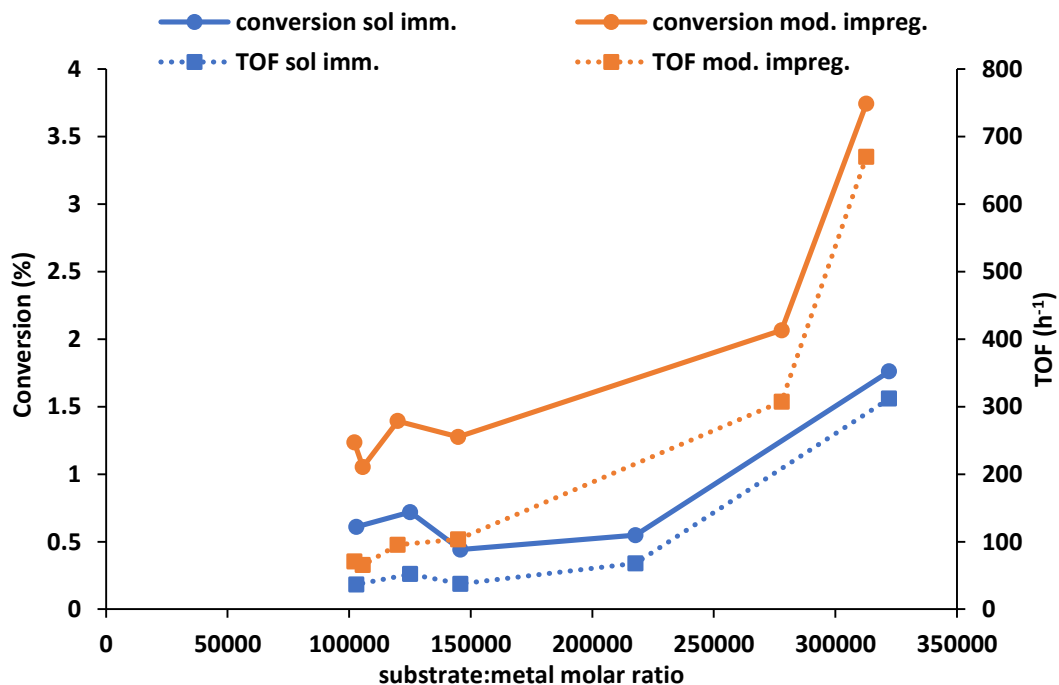


Figure 9. Comparing 1 wt.% $\text{Fe}_{0.5}\text{Pd}_{0.5}/\text{TiO}_2$ catalysts prepared by sol immobilisation and modified impregnation

Reaction conditions: 8.00 g ethylbenzene, 2 – 6 mg catalyst, 3 bar O_2 , 140°C, 17 h, 1000 rpm stirring.

As was the case for AuPd/TiO₂, the FePd/TiO₂ catalyst prepared by modified impregnation achieves higher activity than the equivalent prepared by the sol immobilisation method. This is likely due to differences in nanoparticle size and morphology resulting from the two preparation techniques. The modified impregnation method may, for instance, help to promote mixing and therefore alloying of the metals.

The 1 wt.% Au_{0.5}Pd_{0.5}/TiO₂ and 1 wt.% Fe_{0.5}Pd_{0.5}/TiO₂ catalysts prepared by modified impregnation are compared directly in **Figure 10**. Carbon balances for these reactions were >98%.

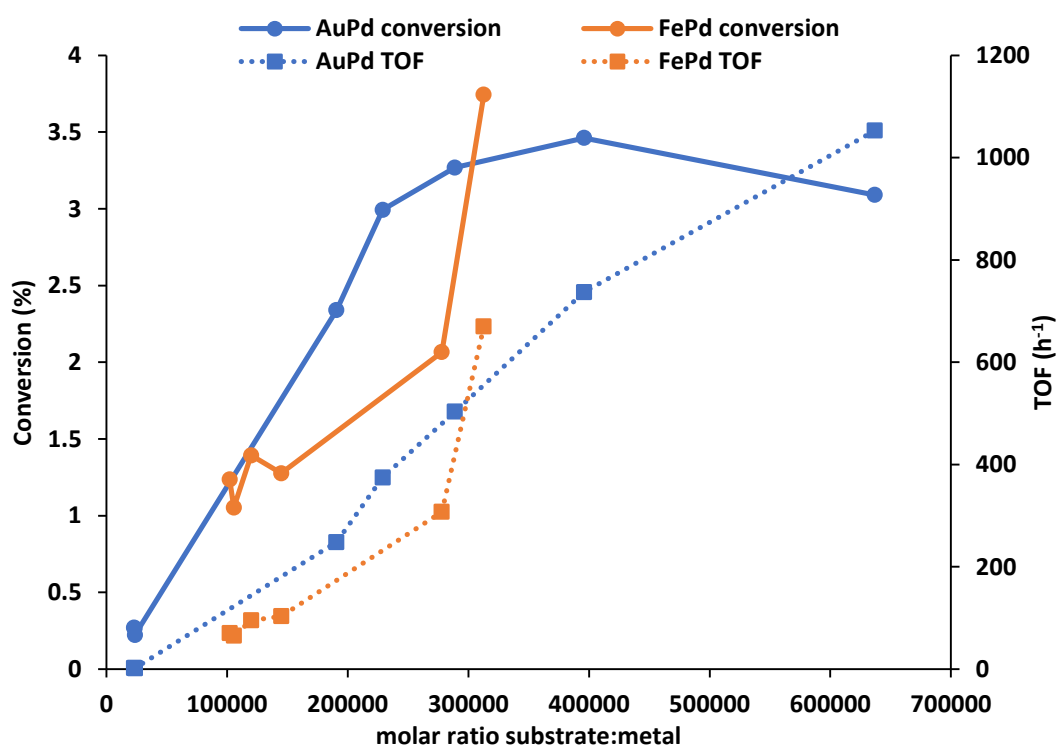


Figure 10. Comparing 1 wt.% Au_{0.5}Pd_{0.5}/TiO₂ and 1 wt.% Fe_{0.5}Pd_{0.5}/TiO₂ catalysts prepared by modified impregnation

Reaction conditions: 8.00 g ethylbenzene, 2 – 6 mg catalyst, 3 bar O₂, 140°C, 17 h, 1000 rpm stirring.

In general, the AuPd catalyst is more active than the FePd. The performance of the FePd catalyst exceeds that of the AuPd catalyst only at a molar ratio of

substrate:metal of >300000, and unfortunately it was not possible to extend the investigation to higher ratios with this catalyst due to the difficulties in accurately measuring such a small mass of catalyst. However, this result indicates that it is possible to replace gold with the much cheaper iron without compromising conversion or TOF under these conditions.

5.2.4. Comparison of bimetallic and monometallic catalysts

In section 5.2.3. it was established that a 1 wt.% Fe_{0.5}Pd_{0.5}/TiO₂ catalyst shows some activity for ethylbenzene oxidation under these conditions, and can even exceed the activity of the equivalent AuPd catalyst. The FePd catalyst was therefore investigated further. To explore the activity of each metal separately, a 0.66 wt.% Pd/TiO₂ catalyst and a 0.34 wt.% Fe/TiO₂ catalyst were prepared by modified impregnation. These weight loadings are equivalent to the quantities on the 1 wt.% Fe_{0.5}Pd_{0.5}/TiO₂ catalyst.

Modified impregnation may not be the most suitable preparation method for these monometallic catalysts, given that there is no enhanced alloying benefit to be considered in this case. The catalysts were prepared by this method to try and rule out the effect of different preparation techniques; as illustrated in section 5.2.3.

The monometallic catalysts were tested under standard conditions. Results are presented in **Figure 11**. Carbon balances for these reactions were >97%.

Under these conditions and at this molar ratio of substrate:metal neither monometallic catalyst is active. However, given the relationship between activity and molar ratio of substrate:metal found throughout the investigation, it is possible that the monometallic catalysts are active when supplied in a different quantity, thus changing the substrate:metal ratio. To test this, 2 – 6 mg of each catalyst was applied for the same reaction. Results are shown in **Figure 12**. Carbon balances for these reactions were >99%.

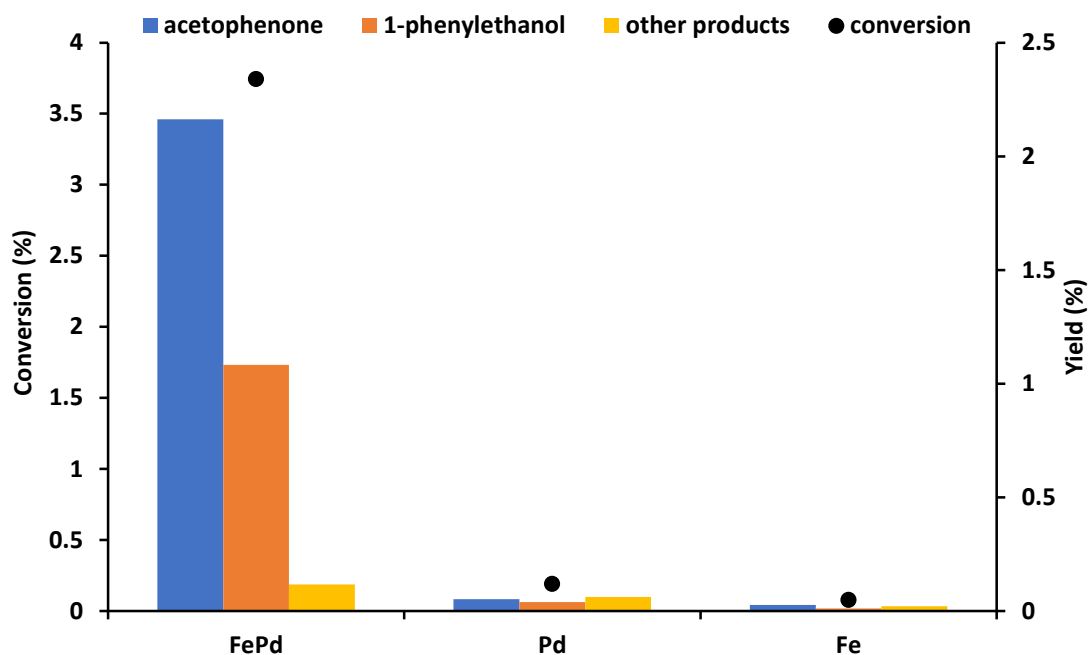


Figure 11. Comparing 1 wt.% Fe_{0.50}Pd_{0.50}/TiO₂ to 0.66 wt.% Pd/TiO₂ and 0.34 wt.% Fe/TiO₂

Reaction conditions: 8.00 g ethylbenzene, catalyst supplied so molar ratio substrate:metal 330000:1, 3 bar O₂, 140°C, 17 h, 1000 rpm stirring.

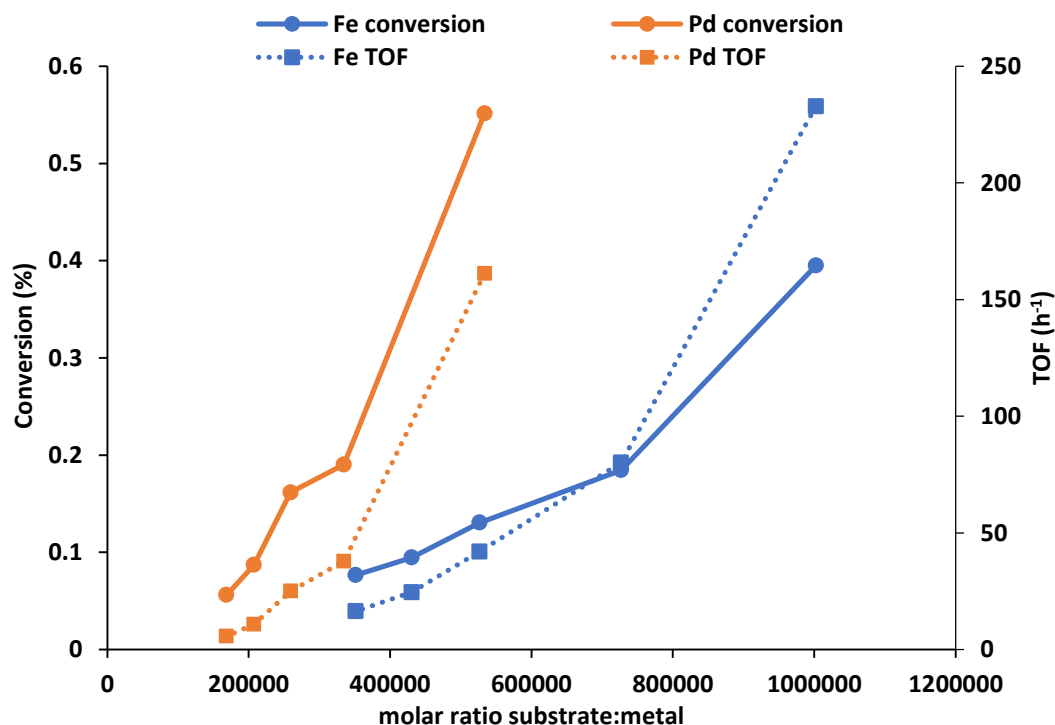


Figure 12. Comparing 0.34 wt.% Fe/TiO₂ and 0.66 wt.% Pd/TiO₂ catalysts

Reaction conditions: 8.00 g ethylbenzene, 2 – 6 mg catalyst, 3 bar O₂, 140°C, 17 h, 1000 rpm stirring.

Both monometallic catalysts achieve higher conversions at higher molar ratios of substrate:metal, but none of the results obtained exceed that of the bimetallic catalyst. Conversion remains low throughout, comparable to blank reactions. This suggests the activity of the bimetallic catalyst arises from superior metal dispersion on the bimetallic catalyst, or from alloy or mixed metal nanoparticles, rather than any monometallic nanoparticles on the surface.

5.2.5. Influence of metal molar ratio

As section 5.2.3. clearly shows that the bimetallic catalyst achieves better results than either monometallic, and can even exceed the activity of an equivalent AuPd bimetallic under certain conditions, the molar ratio of iron and palladium was explored. It was hoped that increased optimisation could further improve on results and produce catalysts more active than 1 wt.% $\text{Au}_{0.50}\text{Pd}_{0.50}/\text{TiO}_2$ prepared by modified impregnation.

1 wt.% $\text{Fe}_{0.35}\text{Pd}_{0.65}/\text{TiO}_2$ and 1 wt.% $\text{Fe}_{0.65}\text{Pd}_{0.35}/\text{TiO}_2$ were prepared by modified impregnation and compared against the 1 wt.% $\text{Fe}_{0.50}\text{Pd}_{0.50}/\text{TiO}_2$ catalyst synthesised by the same process. Results are compared in **Figures 13a, 13b and 13c.**

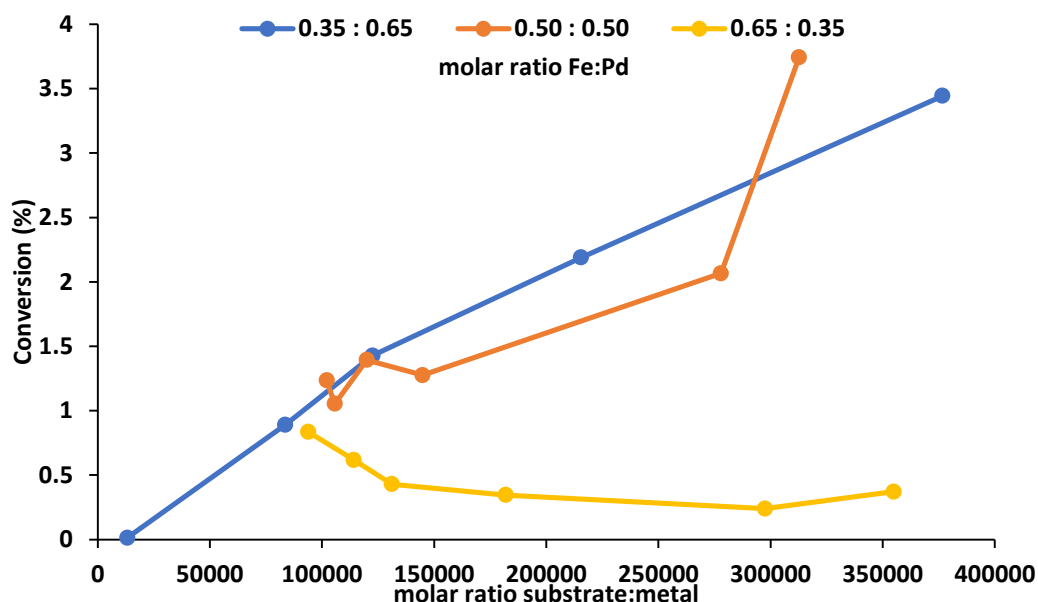


Figure 13a. Effect of varying metal ratio in 1 wt.% FePd/TiO₂ modified impregnation catalysts on conversion

Reaction conditions: 8.00 g ethylbenzene, 2 – 8 mg catalyst, 3 bar O₂, 140°C, 17 h, 1000 rpm stirring.

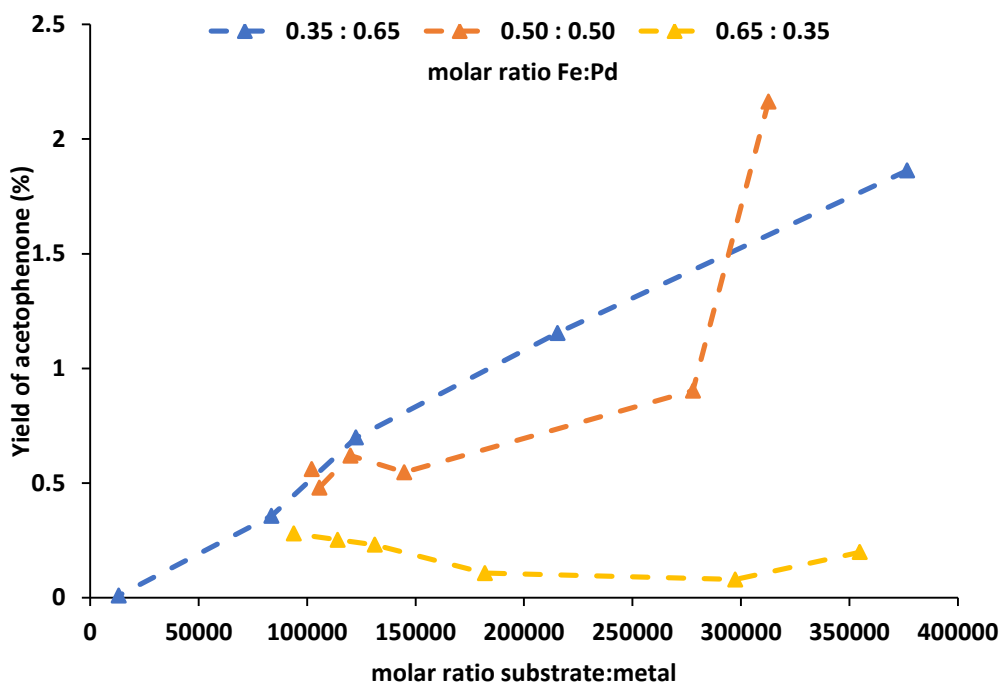


Figure 13b. Effect of varying metal ratio in 1 wt.% FePd/TiO₂ modified impregnation catalysts on yield of acetophenone

Reaction conditions: 8.00 g ethylbenzene, 2 – 8 mg catalyst, 3 bar O₂, 140°C, 17 h, 1000 rpm stirring.

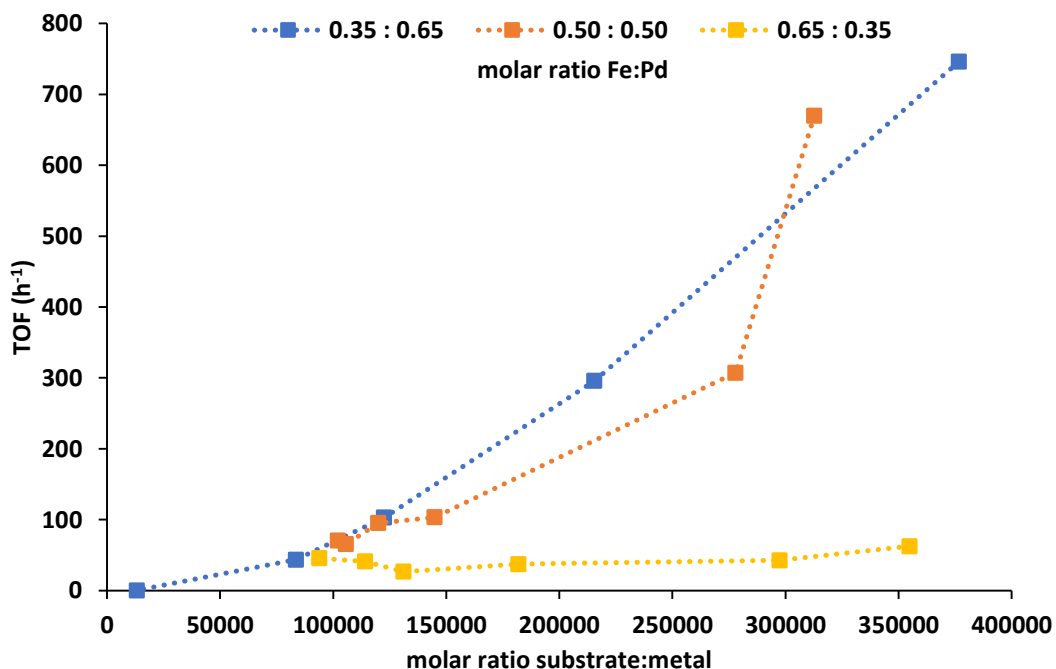


Figure 13c. Effect of varying metal ratio in 1 wt.% FePd/TiO₂ modified impregnation catalysts on TOF

Reaction conditions: 8.00 g ethylbenzene, 2 – 8 mg catalyst, 3 bar O₂, 140°C, 17 h, 1000 rpm stirring.

The molar ratio of iron to palladium clearly plays a significant role in determining catalyst activity. When using extremely low mass catalyst, (molar ratios of substrate:metal >277000), the 1 wt.% Fe_{0.50}Pd_{0.50}/TiO₂ catalyst is the most effective. At higher mass catalyst, (substrate:metal ratios <277000), the 1 wt.% Fe_{0.35}Pd_{0.65}/TiO₂ is more effective. In **Figure 14**, it can be seen that the 1 wt.% Fe_{0.35}Pd_{0.65}/TiO₂ catalyst achieves activity comparable to that of 1 wt.% Au_{0.50}Pd_{0.50}/TiO₂.

The differences in activity observed for catalysts with different molar ratios of iron and palladium are likely due to differences in nanoparticle composition and morphology. In **Figure 15**, a phase diagram for FePd alloys is reproduced¹¹⁴, the key is given in **Table 1**. From this, it can be seen that at 400 °C there are three different possible phases, depending on the weight % of palladium¹¹⁵.

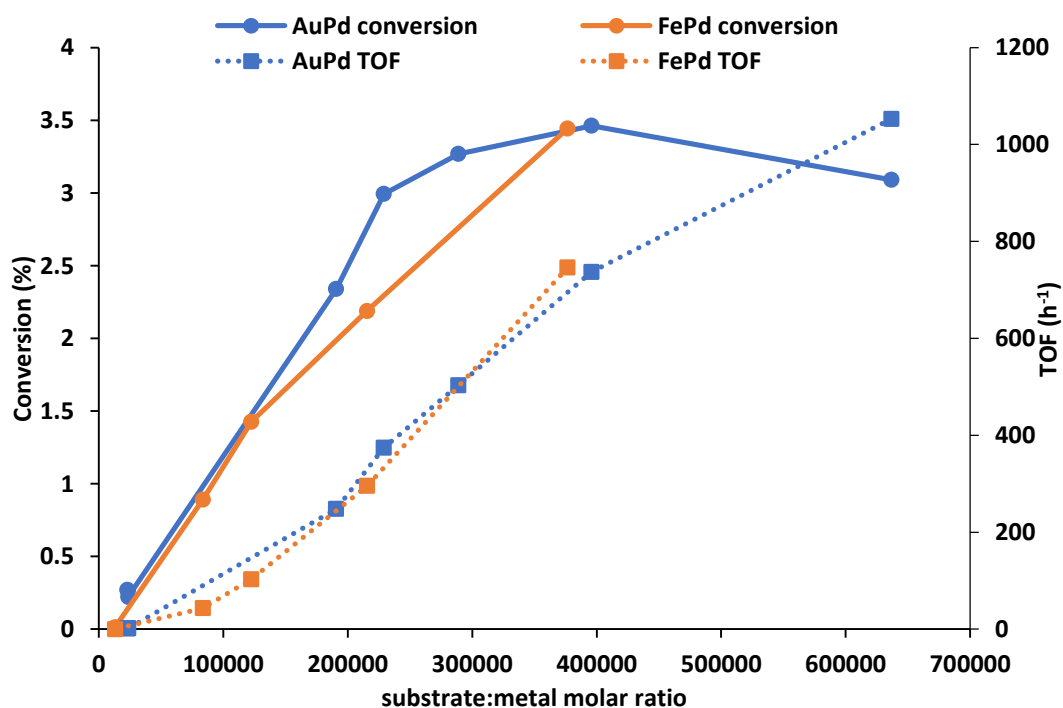


Figure 14. Comparing 1 wt.% Au_{0.50}Pd_{0.50}/TiO₂ and 1 wt.% Fe_{0.35}Pd_{0.65}/TiO₂ prepared by modified impregnation

Reaction conditions: 8.00 g ethylbenzene, 2 – 8 mg catalyst, 3 bar O₂, 140 °C, 17 h, 1000 rpm stirring.

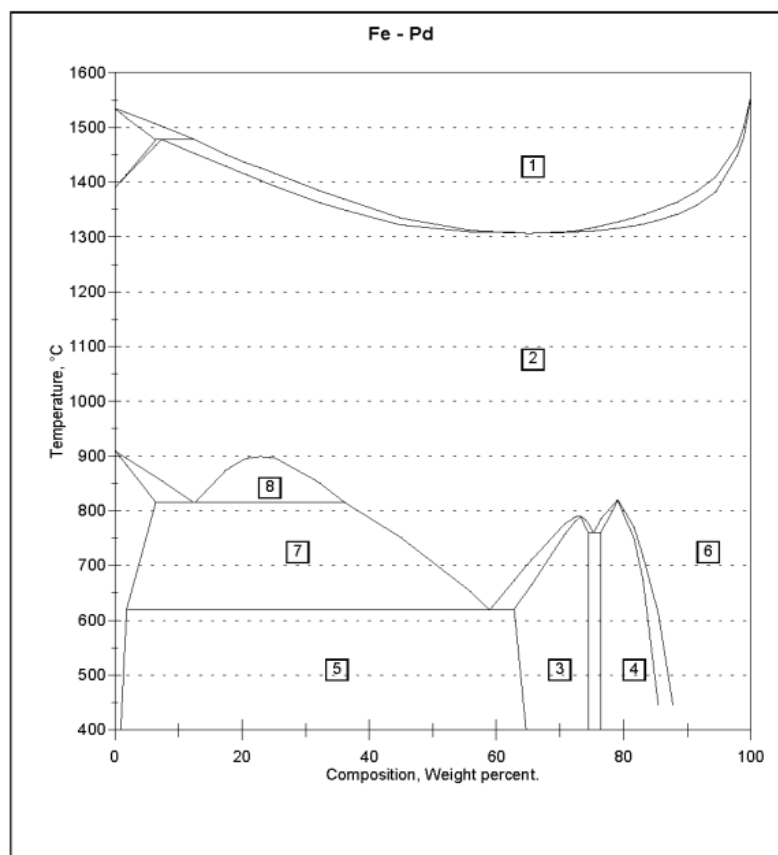


Figure 15. Phase Diagram of FePd alloys

Table 1. Phase diagram key	
section	composition or state
1	Liquid
2	Gamma (Fe,Pd)
3	(FePd)
4	(FePd ₃)
5	α Fe + (FePd)
6	(Pd)
7	α Fe + Gamma
8	Gamma 1 + Gamma 2

In the 1 wt.% Fe_{0.35}Pd_{0.65}/TiO₂ catalyst, the metal content is 22% Fe, 78% Pd. At 400 °C, this falls within the range for FePd₃ alloys. The metal content of the 1 wt.% Fe_{0.50}Pd_{0.50}/TiO₂ catalyst equates to 34% Fe and 66% Pd, and the metal content of the 1 wt.% Fe_{0.65}Pd_{0.35}/TiO₂ catalyst corresponds to 49% Fe and 51% Pd. Therefore at 400 °C the 1 wt.% Fe_{0.65}Pd_{0.35}/TiO₂ catalyst falls within the expected range of α Fe + (FePd), and the 1 wt.% Fe_{0.50}Pd_{0.50}/TiO₂ within on the borderline between this and (FePd).

It was established in section 5.2.4. that the monometallic catalysts are inactive. Assuming, therefore, that catalyst activity arises solely from alloy nanoparticles, the extremely low activity of the 1 wt.% $\text{Fe}_{0.65}\text{Pd}_{0.35}/\text{TiO}_2$ catalyst is attributable to the low loading of FePd, the α Fe being inactive. The 1 wt.% $\text{Fe}_{0.50}\text{Pd}_{0.50}/\text{TiO}_2$ catalyst, with proportionally higher loading of FePd, achieves higher activity, but less than the 1 wt.% $\text{Fe}_{0.35}\text{Pd}_{0.65}/\text{TiO}_2$ catalyst, loaded with FePd_3 . As the total weight loading of metal is the same for all catalysts, this suggests that FePd_3 is more active than FePd, or else forms nanoparticles of a more active size and dispersion.

However, we must also consider that the morphology of the nanoparticles present is likely to be different for the two catalysts, and this will also play a role in determining catalyst behaviour.

Further investigations were carried out using the 1 wt.% $\text{Fe}_{0.35}\text{Pd}_{0.65}/\text{TiO}_2$ catalyst.

5.2.6. Influence of metal loading

The metal loading of a catalyst plays a significant part in its activity and cost-effectiveness. Reducing metal loadings can reduce costs, but typically reduces activity. In Chapters Three and Four, it was found that the metal loading of RuPd/TiO_2 catalysts was a very important factor.

The degree of metal loading also influences nanoparticle composition, morphology and dispersion, and therefore also metal-support interaction and the degree of leaching, if any.

To determine how metal loading effected catalyst activity, 2.5 wt.% $\text{Fe}_{0.35}\text{Pd}_{0.65}/\text{TiO}_2$ and 5.0 wt.% $\text{Fe}_{0.35}\text{Pd}_{0.65}/\text{TiO}_2$ were prepared by modified impregnation and tested at a variety of molar ratios of substrate:metal. The results, compared to those obtained with the 1.0 wt.% $\text{Fe}_{0.35}\text{Pd}_{0.65}/\text{TiO}_2$ catalyst prepared by the same means, are shown in **Figures 16a, 16b and 16c**. Carbon balances for these reactions were >97%.

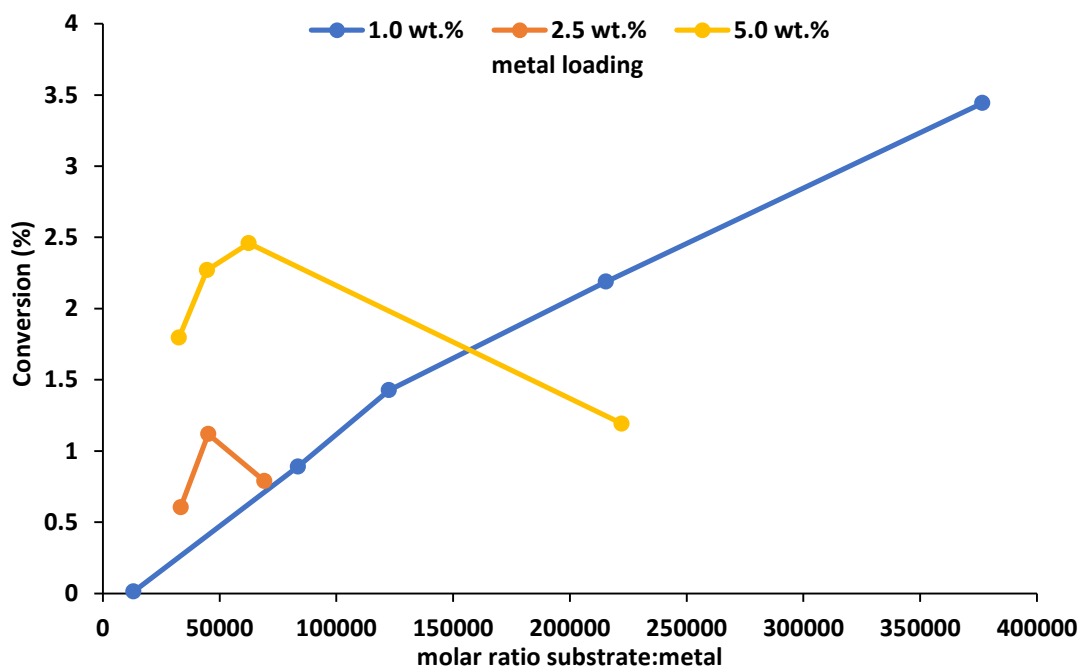


Figure 16a. Comparing conversions obtained with $\text{Fe}_{0.35}\text{Pd}_{0.65}/\text{TiO}_2$ modified impregnation catalysts with different wt.% metal loadings

Reaction conditions: *8.00 g ethylbenzene, 2 – 8 mg catalyst, 3 bar O_2 , 140°C, 17 h, 1000 rpm stirring.*

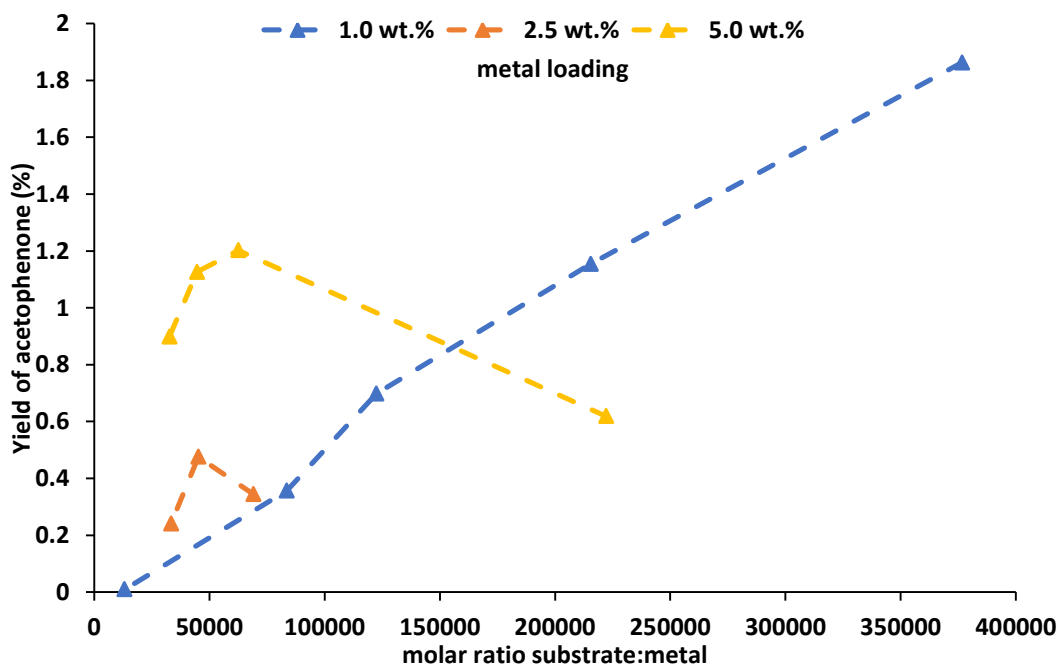


Figure 16b. Comparing yields of acetophenone obtained with $\text{Fe}_{0.35}\text{Pd}_{0.65}/\text{TiO}_2$ modified impregnation catalysts with different wt.% metal loadings

Reaction conditions: *8.00 g ethylbenzene, 2 – 8 mg catalyst, 3 bar O_2 , 140°C, 17 h, 1000 rpm stirring.*

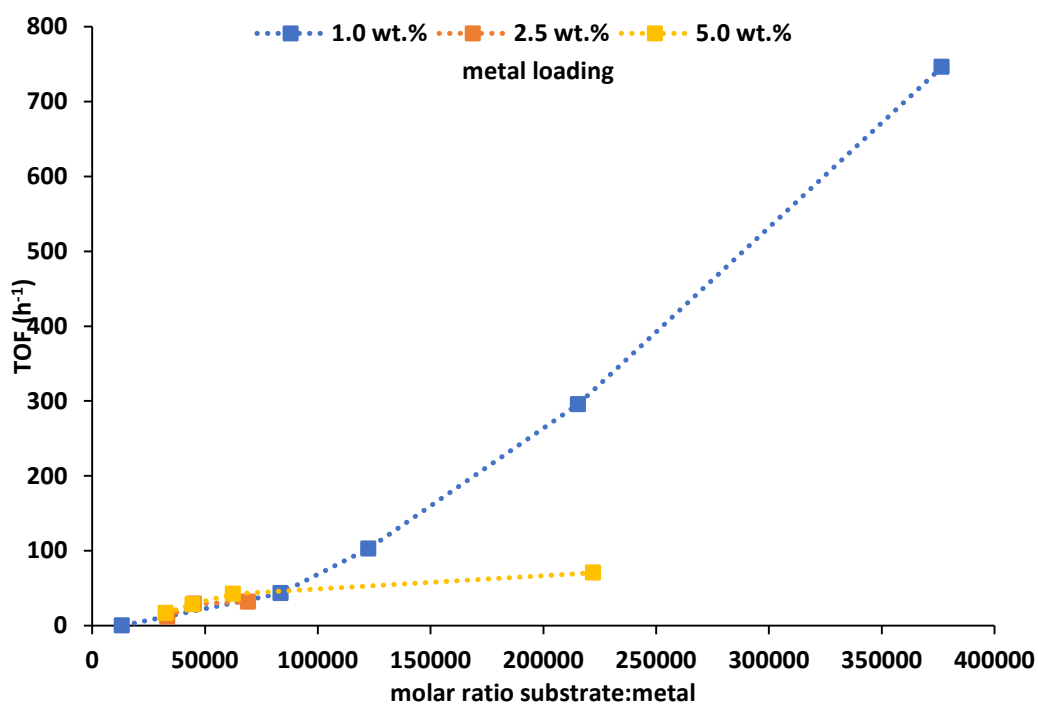


Figure 16c. Comparing TOF obtained with Fe_{0.35}Pd_{0.65}/TiO₂ modified impregnation catalysts with different wt.% metal loadings

Reaction conditions: 8.00 g ethylbenzene, 2 – 8 mg catalyst, 3 bar O₂, 140 °C, 17 h, 1000 rpm stirring.

It is clear from this data that the 2.5 wt.% and 5.0 wt.% catalysts achieve higher conversion and yield of acetophenone than the 1.0 wt.% catalyst at substrate:metal molar ratios of <70000 (for the 2.5 wt.% catalyst) and <155000 (for the 5.0 wt.% catalyst). This does not, however, correspond to a significant improvement in terms of TOF, given the greatly increased metal loading. Additionally, it is difficult to investigate high molar ratios of substrate:metal when using catalyst with increased metal loading.

5.2.7. Influence of reducing temperature

The reduction step of the modified impregnation procedure described in Chapter Two, section 2.4.3. serves a dual purpose: to reduce the metal present on the surface to the metallic state, and to remove chloride species on the catalyst which may act as poisons.

The temperature of reduction may also affect the morphology of the nanoparticles and the degree of metal-support interaction. Sufficiently high temperatures may

cause sintering, leading to a larger average nanoparticle size and lower overall dispersion. Therefore the reduction step can impact on catalyst activity.

A 1 wt.% $\text{Fe}_{0.35}\text{Pd}_{0.65}/\text{TiO}_2$ catalyst was prepared by the standard modified impregnation procedure and divided into three portions. One was reduced at the standard reducing temperature of 400 °C, and the other two at 300 °C and 500 °C respectively, all under flowing 5% H_2 in N_2 with a heating rate of 15 °C/min. The resulting catalysts were then tested at a range of molar ratios of substrate:metal and the results compared. Results are shown in **Figures 17a, 17b and 17c**, with carbon balances in all cases >97%.

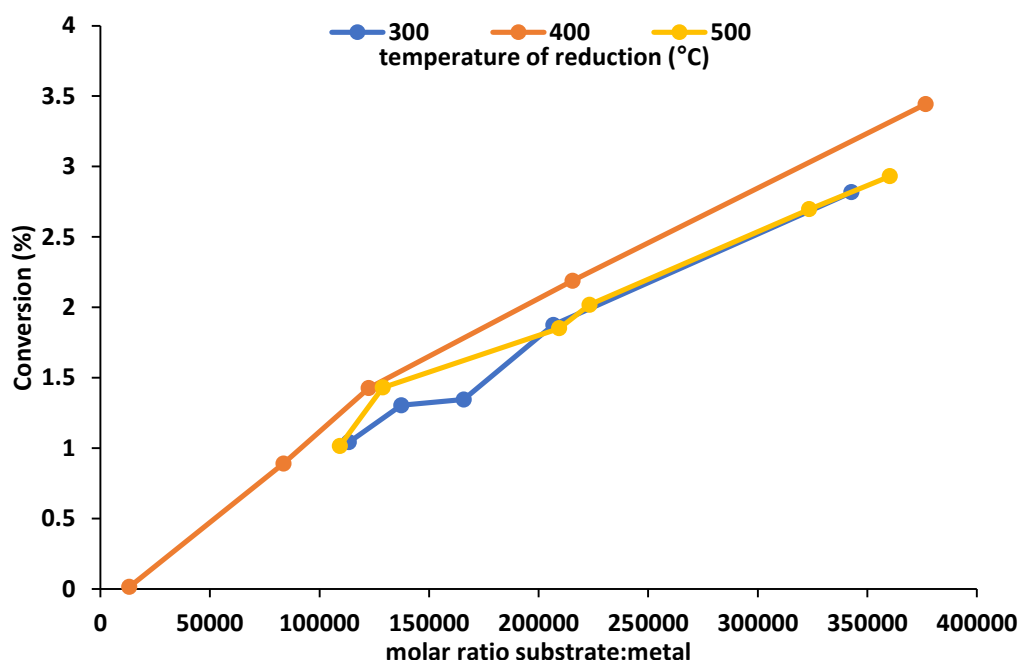


Figure 17a. Comparing conversions obtained with 1 wt.% $\text{Fe}_{0.35}\text{Pd}_{0.65}/\text{TiO}_2$ modified impregnation catalysts reduced at different temperatures

Reaction conditions: 8.00 g ethylbenzene, 2 – 8 mg catalyst, 3 bar O_2 , 140 °C, 17 h, 1000 rpm stirring.

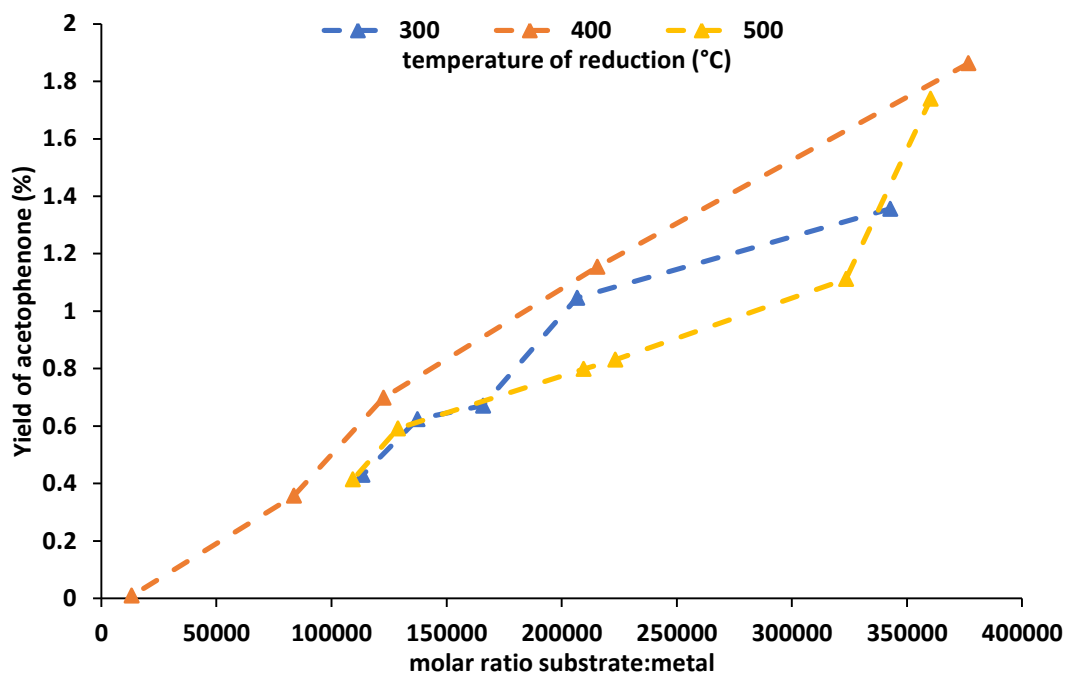


Figure 17b. Comparing yield of acetophenone obtained with 1 wt.% Fe_{0.35}Pd_{0.65}/TiO₂ modified impregnation catalysts reduced at different temperatures

Reaction conditions: 8.00 g ethylbenzene, 2 – 8 mg catalyst, 3 bar O₂, 140°C, 17 h, 1000 rpm stirring.

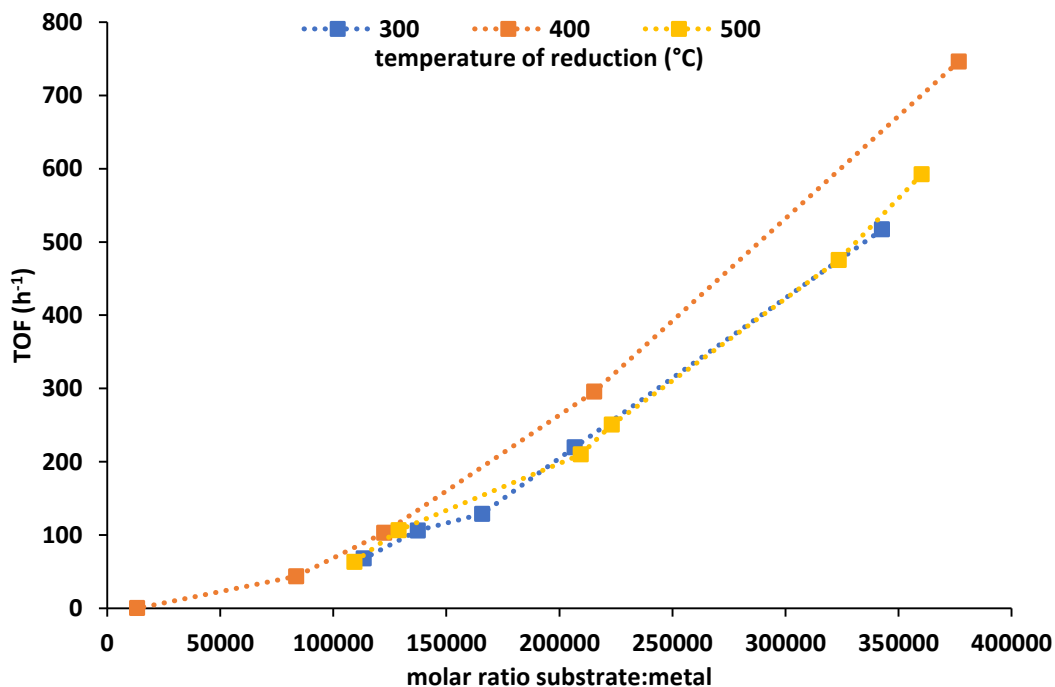


Figure 17c. Comparing TOF obtained with 1 wt.% Fe_{0.35}Pd_{0.65}/TiO₂ modified impregnation catalysts reduced at different temperatures

Reaction conditions: 8.00 g ethylbenzene, 2 – 8 mg catalyst, 3 bar O₂, 140°C, 17 h, 1000 rpm stirring.

The activity of the three catalysts reduced at different temperatures is very similar. This suggests that the metal was reduced and the chloride removed in every case without significant changes to the nature of the metal nanoparticle.

This can be corroborated by TPR analysis. Unreduced catalyst was reduced in situ using 5% H₂ in N₂ to produce a TPR graph shown in **Figure 18**.

The catalysts reduced at different temperatures were also analysed by CO chemisorption, to determine dispersion and average particle size. Results for this analysis are presented in **Table 2**.

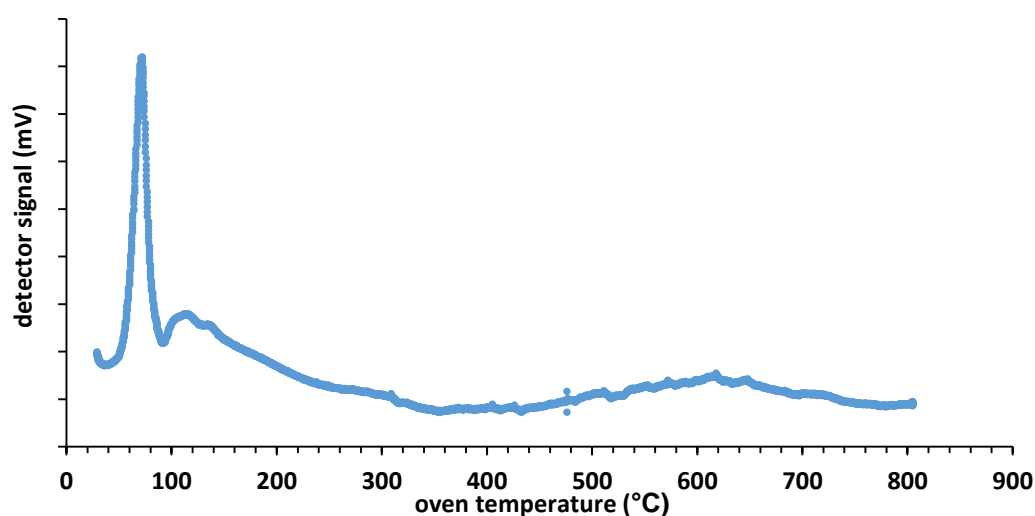


Figure 18. TPR of 1 wt.% Fe_{0.35}Pd_{0.65}/TiO₂ catalyst

The negative peak observed in the 35 – 50 °C range corresponds to desorption of hydrogen from Pd⁰ species already present (9% of loaded palladium, determined by XPS analysis of untreated catalyst). The bulk of the palladium content is present as PdO, (91% of palladium content) and the reduction peak of PdO to Pd²⁺ is visible at 72 °C.

Table 2. Nanoparticle size and dispersion of FePd catalysts

	preparation method		
	300	400	500
dispersion (%)	25.96	41.97	17.25
average particle size (Å)	14.39	8.90	21.64
metal surface area (m ² /g)	0.93	1.50	0.62

1 wt.% Fe_{0.35}Pd_{0.65}/TiO₂ catalysts prepared by modified impregnation.

The analysis presented in **Table 2** indicates that the catalyst reduced at 400 °C bears the smallest and most disperse metal nanoparticles, and therefore the highest metal surface area. This is consistent with this catalyst being the most active. However, the differences in activity observed with each catalyst are very slight, implying that the differences in nanoparticle size and dispersion do not impact the catalyst's activity severely.

5.2.8. Influence of preparation method and catalyst precursors

The bimetallic FePd/TiO₂ catalyst achieves significantly higher activity than the monometallic catalysts investigated in section 5.2.4. It was shown that the molar ratio of metals in the bimetallic material plays a significant role in determining its activity in section 5.2.5. Therefore it can be assumed that the degree of metal mixing and alloying plays an important part in the catalyst's activity. The composition of metal nanoparticles is often determined by the catalyst preparation method.

The sol immobilisation method is advantageous because the use of a polymer restricts nanoparticles to a particular size, creating a very narrow size distribution⁵⁷. The modified impregnation method is advantageous because it promotes mixing of the metals involved and typically results in a higher degree of alloying than other preparation techniques³³. This is achieved by acidifying the palladium solution with HCl and using chlorides as the metal precursors. The Cl⁻ ions in solution encourage mixing of the metals. Using alternate precursors, such as nitrates, should eliminate or reduce this effect.

1 wt.% Fe_{0.35}Pd_{0.65}/TiO₂ was prepared using the modified impregnation method with PdCl₂ and Fe(NO₂)₃ as precursors. The resulting catalyst was tested under the standard conditions. Results are shown in **Figures 19a and 19b**, compared to the results for the equivalent catalyst prepared from PdCl₂ and FeCl₃. Carbon balances were >99% for these reactions.

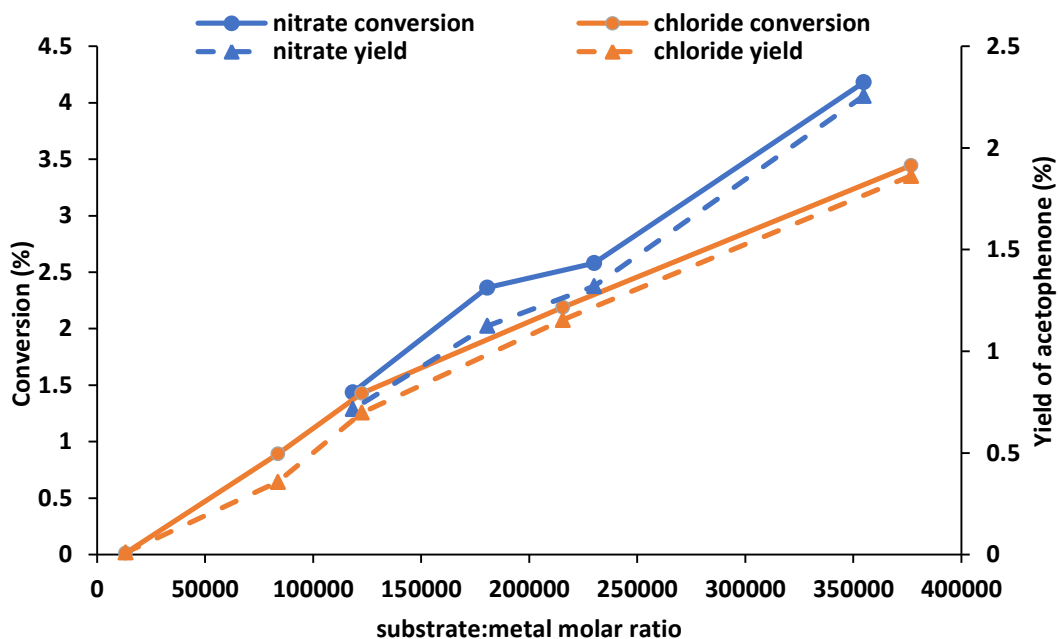


Figure 19a. Comparing 1 wt.% $\text{Fe}_{0.35}\text{Pd}_{0.65}/\text{TiO}_2$ modified impregnation catalysts prepared with $\text{Fe}(\text{NO}_2)_3$ or FeCl_3

Reaction conditions: 8.00 g ethylbenzene, 2 – 6 mg catalyst, 3 bar O_2 , 140°C, 17 h, 1000 rpm stirring.

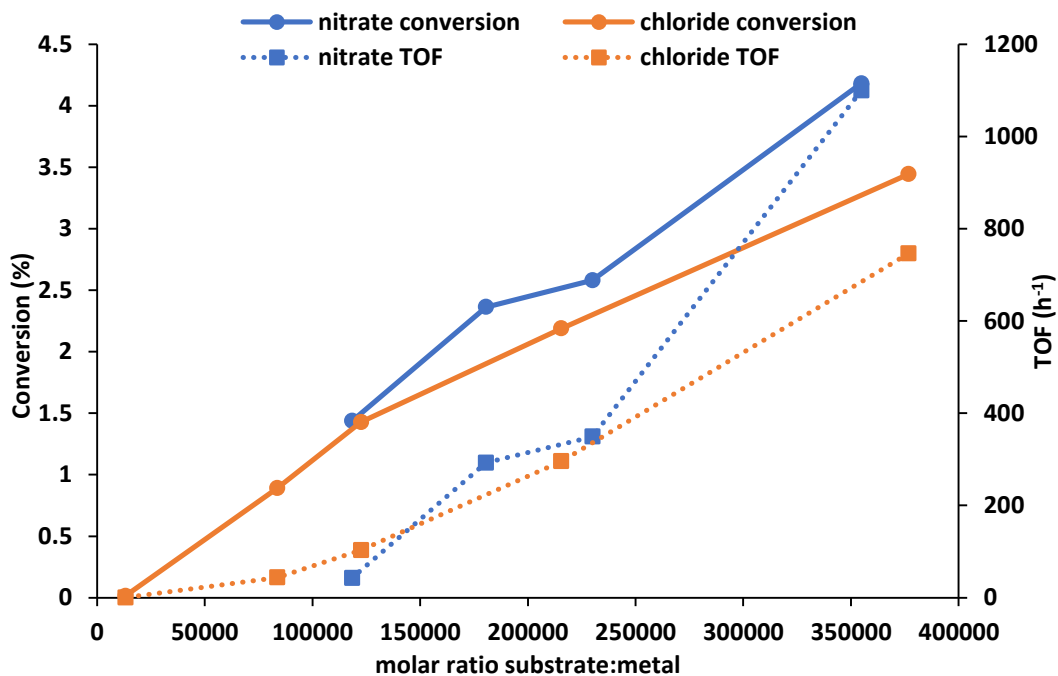


Figure 19b. Comparing 1 wt.% $\text{Fe}_{0.35}\text{Pd}_{0.65}/\text{TiO}_2$ modified impregnation catalysts prepared with $\text{Fe}(\text{NO}_2)_3$ or FeCl_3

Reaction conditions: 8.00 g ethylbenzene, 2 – 6 mg catalyst, 3 bar O_2 , 140°C, 17 h, 1000 rpm stirring.

If the activity of the 1 wt.% $\text{Fe}_{0.35}\text{Pd}_{0.65}/\text{TiO}_2$ catalyst arose from the enhanced mixing due to the use of chloride precursors and the modified impregnation method, the catalyst prepared using $\text{Fe}(\text{NO}_2)_3$ as a precursor would be expected to be less active. However, this is not the case. The catalyst prepared from $\text{Fe}(\text{NO}_2)_3$ offers higher conversion and yield than that prepared from FeCl_3 . The observed TOF for the catalyst prepared with the nitrate salt is considerably higher than that of its counterpart when used at a high molar ratio of substrate:metal. The TOF of the catalyst prepared from $\text{Fe}(\text{NO}_2)_3$ actually exceeds that of the 1 wt.% $\text{Au}_{0.50}\text{Pd}_{0.50}/\text{TiO}_2$ catalyst at a molar ratio of substrate:metal of ~ 350000 .

As the standard modified impregnation catalyst is less active than that prepared with the iron nitrate precursor, it can be concluded that the typical advantages of the modified impregnation procedure are not beneficial in this case. Therefore it was deemed appropriate to investigate the activity of the same catalyst made by conventional impregnation. 1 wt.% $\text{Fe}_{0.35}\text{Pd}_{0.65}/\text{TiO}_2$ catalysts were prepared from PdCl_2 and FeCl_3 and PdCl_2 and $\text{Fe}(\text{NO}_2)_3$ by the conventional impregnation method and tested under standard conditions. Results are shown in **Figures 20a and 20b**. Carbon balances for these reactions were $>97\%$.

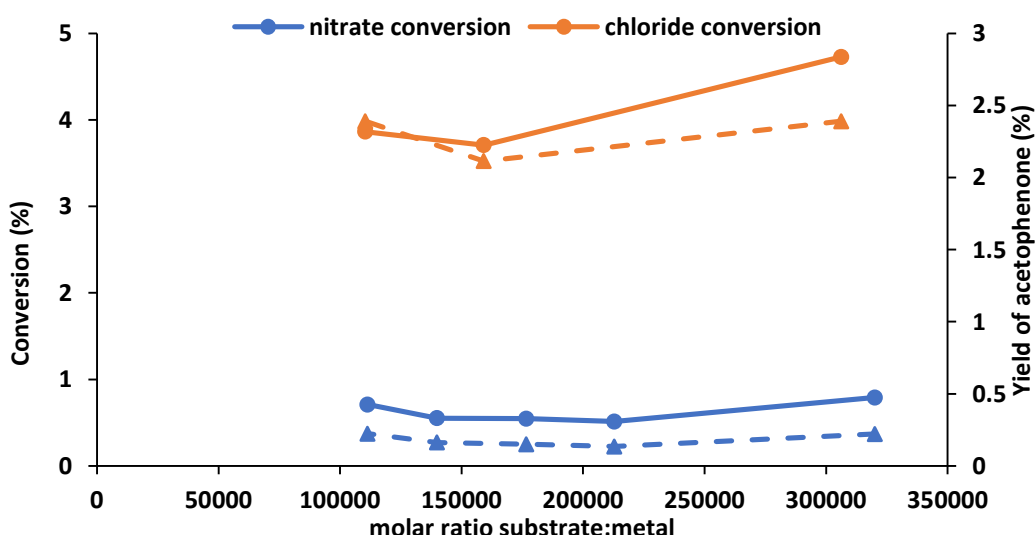


Figure 20a. Comparing 1 wt.% $\text{Fe}_{0.35}\text{Pd}_{0.65}/\text{TiO}_2$ conventional impregnation catalysts prepared with $\text{Fe}(\text{NO}_2)_3$ or FeCl_3

Reaction conditions: 8.00 g ethylbenzene, 2 – 6 mg catalyst, 3 bar O_2 , 140°C, 17 h, 1000 rpm stirring.

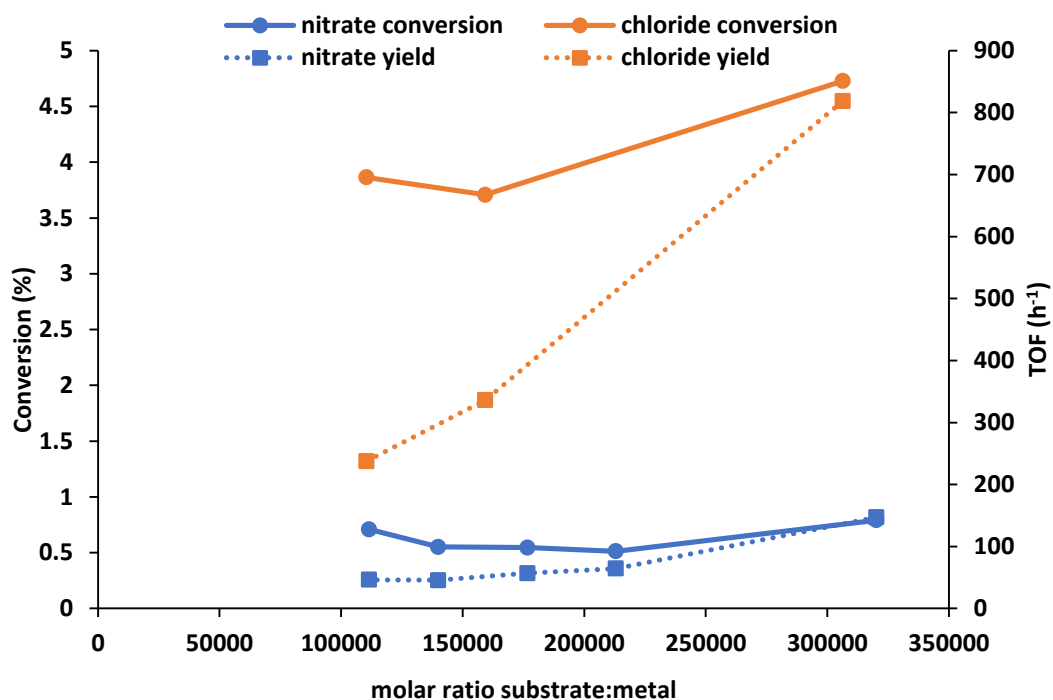


Figure 20b. Comparing 1 wt.% $\text{Fe}_{0.35}\text{Pd}_{0.65}/\text{TiO}_2$ conventional impregnation catalysts prepared with $\text{Fe}(\text{NO}_2)_3$ or FeCl_3

Reaction conditions: 8.00 g ethylbenzene, 2 – 6 mg catalyst, 3 bar O_2 , 140°C, 17 h, 1000 rpm stirring.

In this case, unlike the modified impregnation catalysts, the 1 wt.% $\text{Fe}_{0.35}\text{Pd}_{0.65}/\text{TiO}_2$ catalyst prepared with the chloride precursor is substantially more active than the equivalent prepared from the nitrate at all the different molar ratios of substrate:metal investigated, highlighting the importance of this choice. It may be that the additional acidity of the chloride precursor has a beneficial effect during catalyst preparation, reflected in the nanoparticle morphology, the nature of the support, or metal-support interaction.

Figure 21 and Table 2 compare the activities of the modified impregnation and conventional impregnation catalysts made with each precursor at a molar ratio of substrate:metal of ~ 110000 .

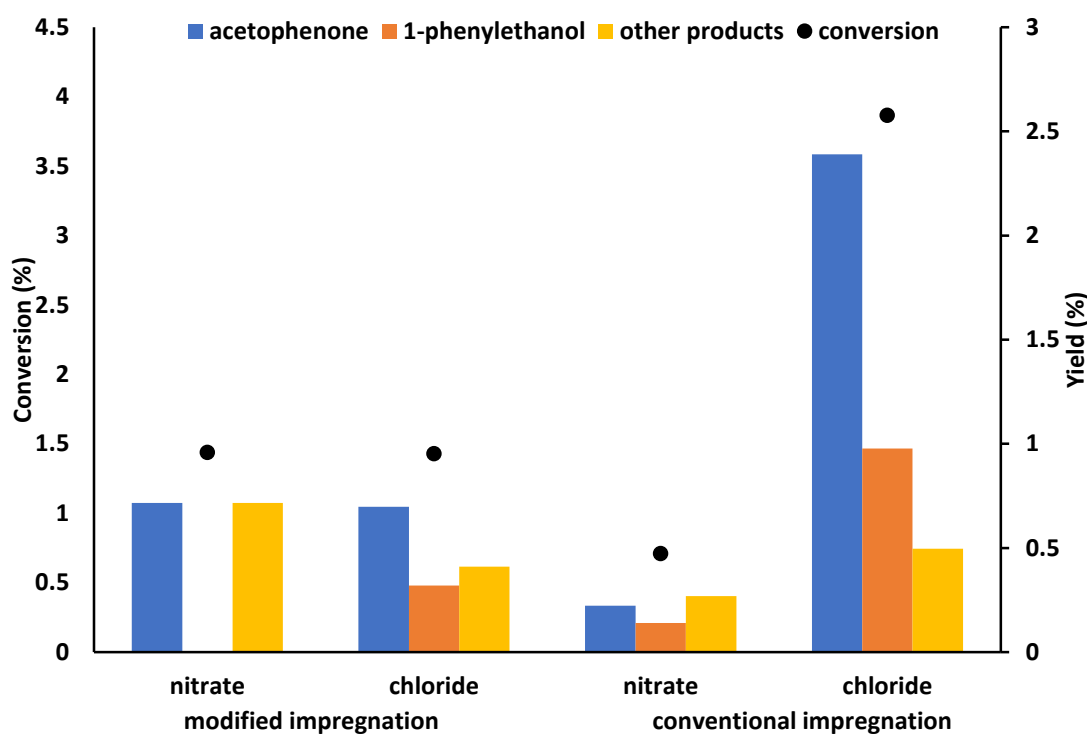


Figure 21. Comparing 1 wt.% $\text{Fe}_{0.35}\text{Pd}_{0.65}/\text{TiO}_2$ catalysts prepared with $\text{Fe}(\text{NO}_2)_3$ or FeCl_3 by modified or conventional impregnation methods

Reaction conditions: 8.00 g ethylbenzene, 6 mg catalyst, molar ratio substrate:metal 110000, 3 bar O_2 , 140°C, 17 h, 1000 rpm stirring.

Table 2. Comparing catalysts prepared from different precursors and methods

preparation method	iron precursor	conversion (%)	TOF (h^{-1})
modified impregnation	$\text{Fe}(\text{NO}_2)_3$	1.44	43
	FeCl_3	1.43	103
conventional impregnation	$\text{Fe}(\text{NO}_2)_3$	0.71	46
	FeCl_3	3.86	238

1 wt.% $\text{Fe}_{0.35}\text{Pd}_{0.65}/\text{TiO}_2$ catalysts prepared with PdCl_2 precursor. Tested under the following conditions: 8.00 g ethylbenzene, 6 mg catalyst, molar ratio substrate:metal 110000, 3 bar O_2 , 140°C, 17 h, 1000 rpm stirring.

The data displayed in **Figure 21** and **Table 2** illustrates the substantial improvement offered by 1 wt.% $\text{Fe}_{0.35}\text{Pd}_{0.65}/\text{TiO}_2$ catalysts prepared from PdCl_2 and FeCl_3 by modified impregnation at a 110000 molar ratio of substrate:metal. This catalyst is the most active tested thus far, exceeding the activity of the benchmark 1 wt.% $\text{Au}_{0.50}\text{Pd}_{0.50}/\text{TiO}_2$ modified impregnation catalyst when used in a similar molar ratio of substrate:metal, as shown in **Figures 22a and 22b**.

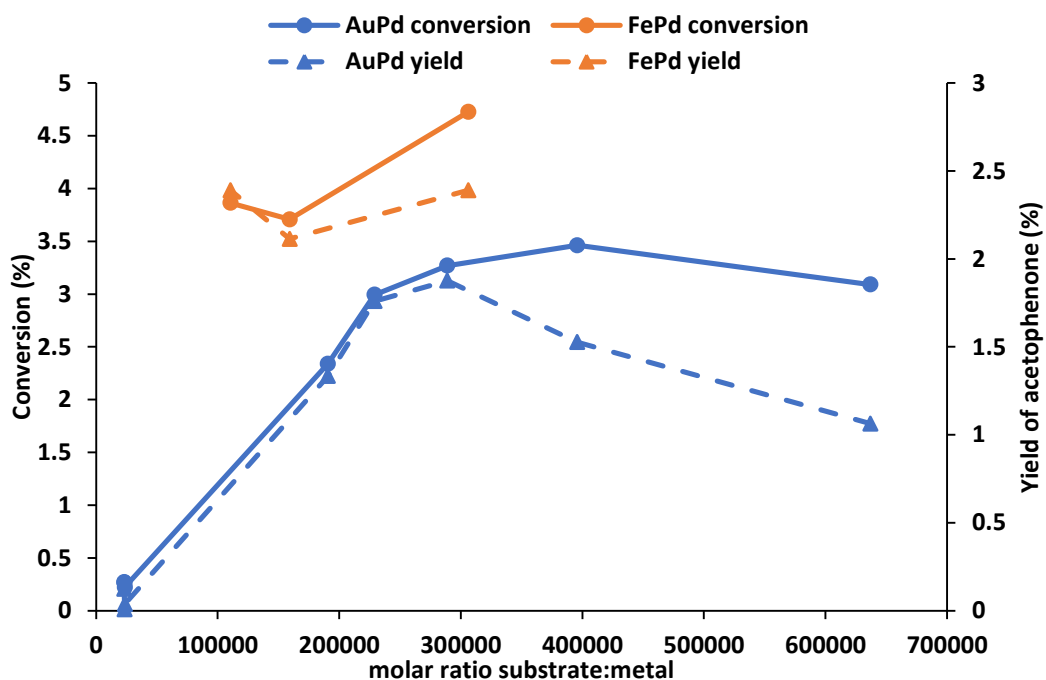


Figure 22a. Comparing 1 wt.% $\text{Au}_{0.50}\text{Pd}_{0.50}/\text{TiO}_2$ modified impregnation catalyst to 1 wt.% $\text{Fe}_{0.35}\text{Pd}_{0.65}/\text{TiO}_2$ conventional impregnation catalyst prepared from FeCl_3

Reaction conditions: 8.00 g ethylbenzene, 2 – 8 mg catalyst, 3 bar O_2 , 140°C, 17 h, 1000 rpm stirring.

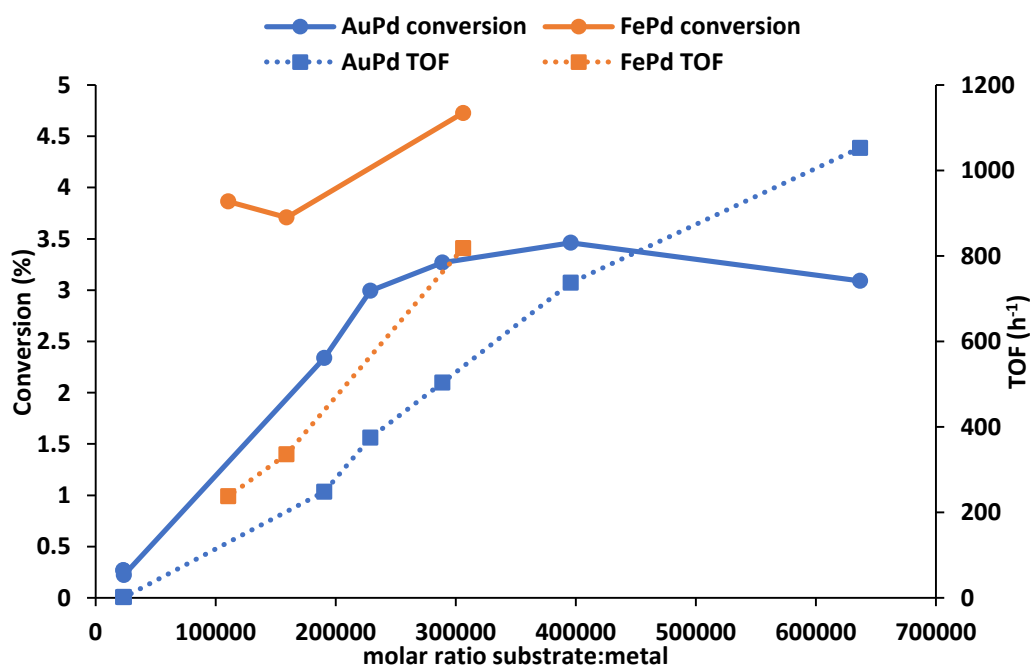


Figure 22b. Comparing 1 wt.% $\text{Au}_{0.50}\text{Pd}_{0.50}/\text{TiO}_2$ modified impregnation catalyst to 1 wt.% $\text{Fe}_{0.35}\text{Pd}_{0.65}/\text{TiO}_2$ conventional impregnation catalyst prepared from FeCl_3

Reaction conditions: 8.00 g ethylbenzene, 2 – 8 mg catalyst, 3 bar O_2 , 140°C, 17 h, 1000 rpm stirring.

While more characterisation is required to elucidate exactly why the catalysts investigated are active, it has been shown that gold can be successfully replaced with the far cheaper iron without suffering a loss of activity, and with optimisation these cheaper catalysts may exhibit superior activity.

5.2.9. Influence of radical initiators

Radical initiators produce radical species that can then initiate reactions, as described in Chapter One, section 4.1. Addition of a radical initiator to a catalytic reaction can lead to a drastic improvement in conversion and yield of any products that form as a result of a radical mechanism.

To investigate the role of radicals in the oxidation of ethylbenzene with 1 wt.% Fe_{0.35}Pd_{0.65}/TiO₂ as catalyst, experiments were carried out in the presence of initiators. **Figures 23a and 23b** display results obtained in the presence of tBHP, which produces oxygen-based radicals. Figures **24a and 24b** display results obtained in the presence of azobisisobutyronitrile (AIBN), which produces carbon-based radicals.

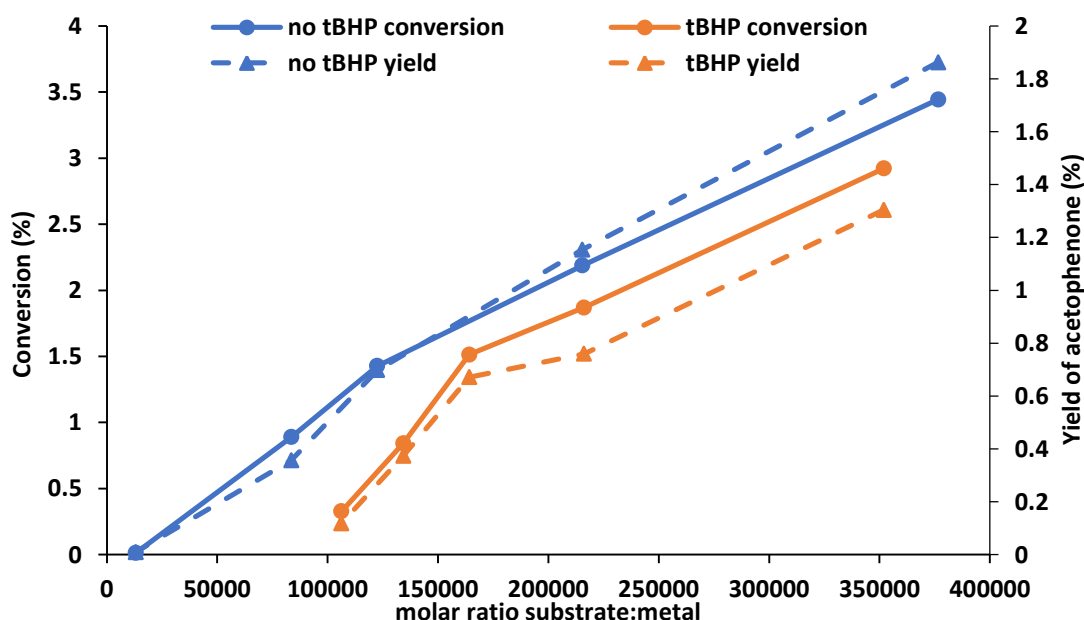


Figure 23a. Comparing conversion and yield with and without addition of tBHP initiator

Reaction conditions: 8.00 g ethylbenzene, 2 – 8 mg catalyst, 0.7 mmol tBHP supplied as 70 wt% solution in water (where applicable), 3 bar O₂, 140 °C, 17 h, 1000 rpm stirring.

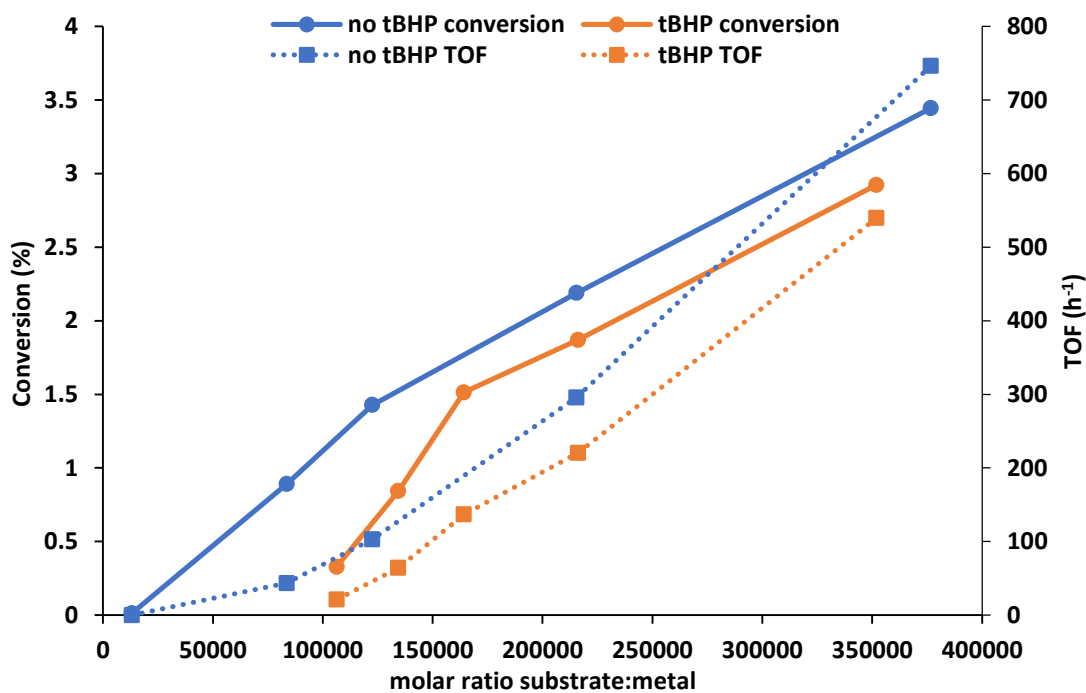


Figure 23b. Comparing conversion and TOF with and without addition of tBHP initiator

Reaction conditions: 8.00 g ethylbenzene, 2 – 8 mg catalyst, 0.7 mmol tBHP supplied as 70 wt% solution in water (where applicable), 3 bar O₂, 140°C, 17 h, 1000 rpm stirring.

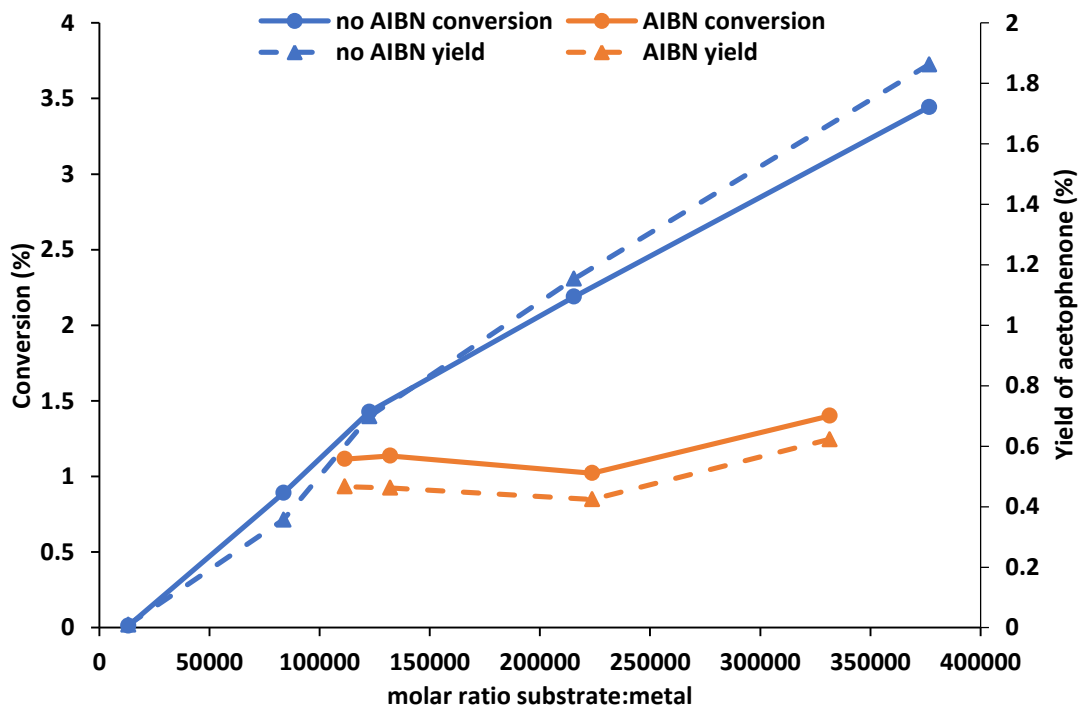


Figure 24a. Comparing conversion and yield with and without addition of AIBN initiator

Reaction conditions: 8.00 g ethylbenzene, 2 – 8 mg catalyst, 5 mg AIBN, 3 bar O₂, 140°C, 17 h, 1000 rpm stirring.

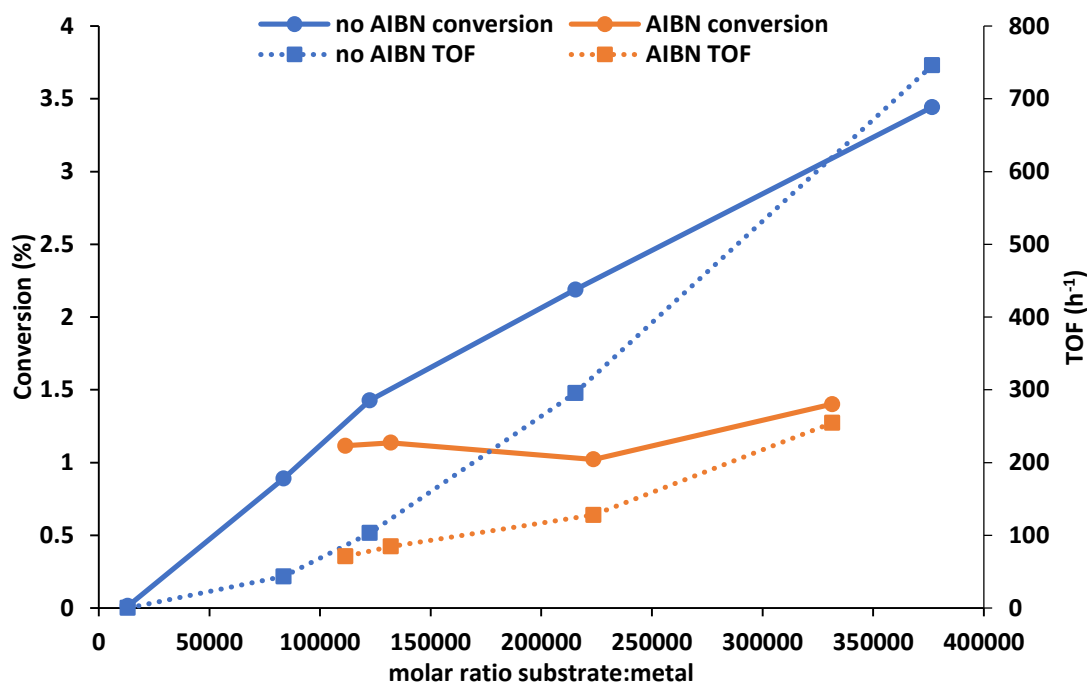


Figure 24b. Comparing conversion and TOF with and without addition of AIBN initiator

Reaction conditions: 8.00 g ethylbenzene, 2 – 8 mg catalyst, 5 mg AIBN, 3 bar O₂, 140°C, 17 h, 1000 rpm stirring.

The addition of tBHP, which generates oxygen-based radicals, causes a slight decrease in catalyst activity at all the molar ratios of substrate:metal investigated. This suggests that the presence of oxygen-radicals is not beneficial, though it is possible that the potential effects are hindered by the fact that tBHP was supplied as an aqueous solution, with which ethylbenzene is immiscible. Alternatively, given the extremely high ratio of substrate to catalyst, it is possible that the reaction is mass transfer limited, and the addition of tBHP provides no benefit for this reason.

The addition of AIBN, which produces 2-cyanoprop-2-yl radicals, substantially decreases activity at molar ratios of substrate:metal of >150000. AIBN is miscible with ethylbenzene, and so mass transport limitations are not likely. The observed decrease is contrary to expectations if the reaction mechanism utilised carbon based radicals; thus it can be safely concluded that it does not. The reasons for the decrease in activity are unclear, but could be related to AIBN blocking active sites on the catalyst surface.

5.2.10. Influence of radical scavengers

Radical scavengers depress or nullify radical mechanisms by reacting with radical species instead of the reactants. One example of this is described in the termination step given in Chapter One, section 1.4.

Hydroquinone scavenges oxygen-based radicals, the most likely candidate for any radical activity in the ethylbenzene oxidation reaction. To investigate the role of radicals, hydroquinone was applied to the reaction with ethylbenzene under standard conditions.

Figures 25a and 25b display results of the ethylbenzene oxidation reaction catalysed by 1 wt.% $\text{Fe}_{0.35}\text{Pd}_{0.65}/\text{TiO}_2$ when hydroquinone was supplied as a solid.

Figures 26a and 26b display results obtained when hydroquinone was supplied in an aqueous solution.

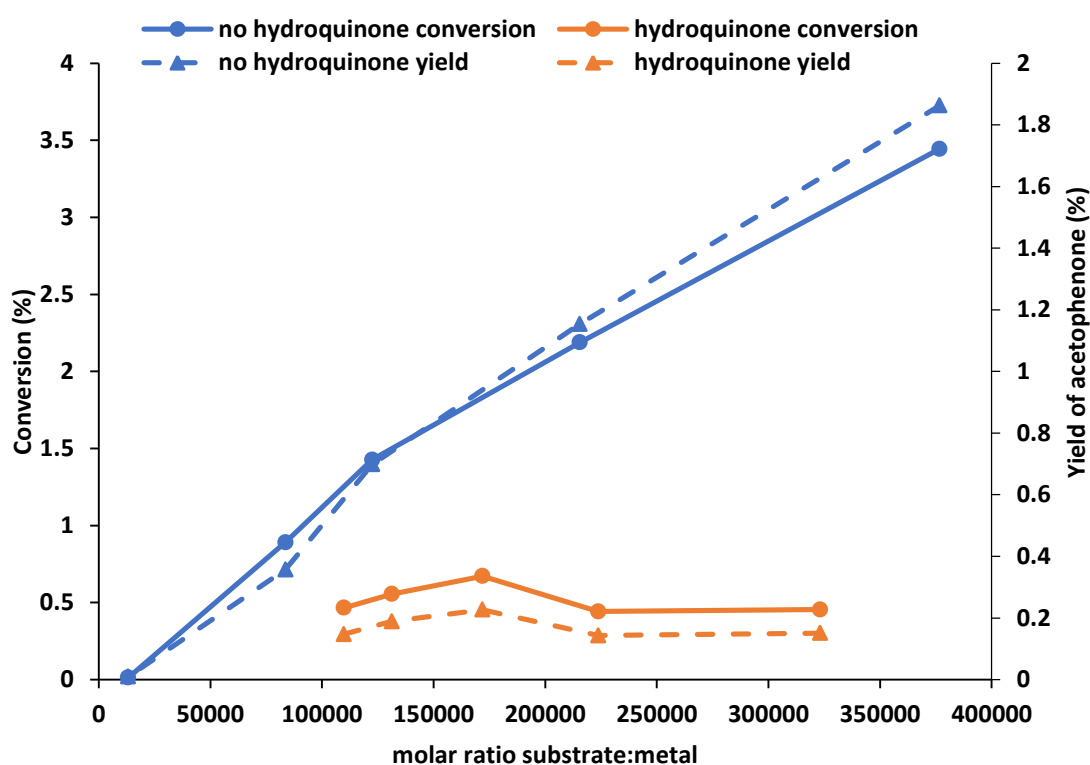


Figure 25a. Comparing conversion and yield with and without addition of hydroquinone scavenger as a solid

Reaction conditions: 8.00 g ethylbenzene, 2 – 8 mg catalyst, 5 mg hydroquinone, 3 bar O_2 , 140°C, 17 h, 1000 rpm stirring.

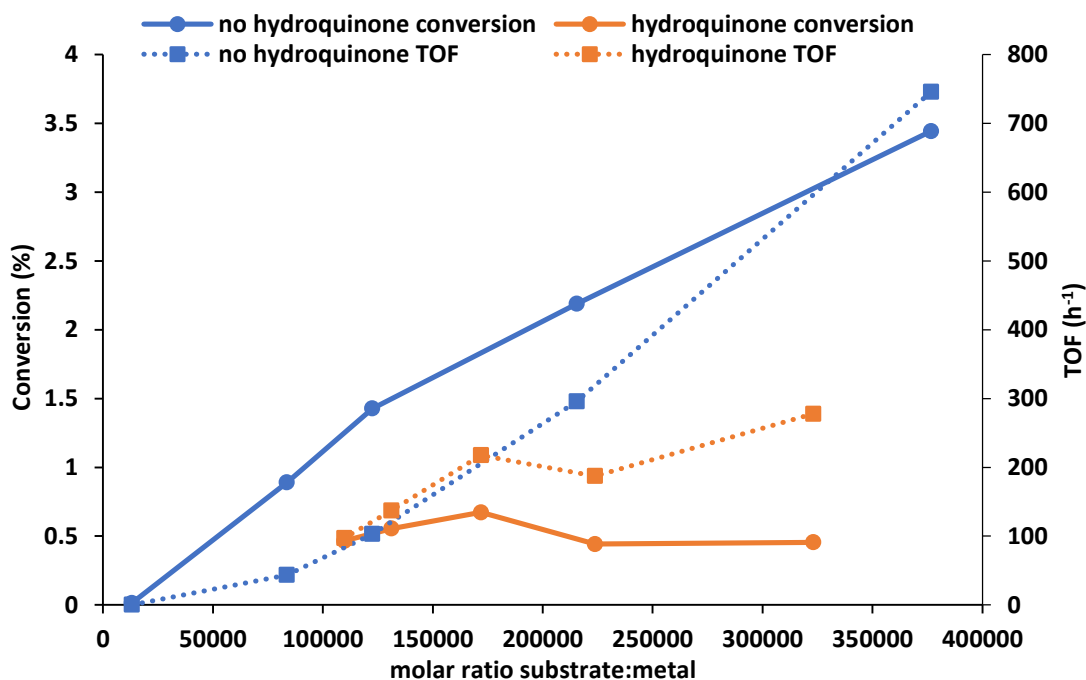


Figure 25b. Comparing conversion and TOF with and without addition of hydroquinone scavenger as a solid

Reaction conditions: 8.00 g ethylbenzene, 2 – 8 mg catalyst, 5 mg hydroquinone, 3 bar O₂, 140°C, 17 h, 1000 rpm stirring.

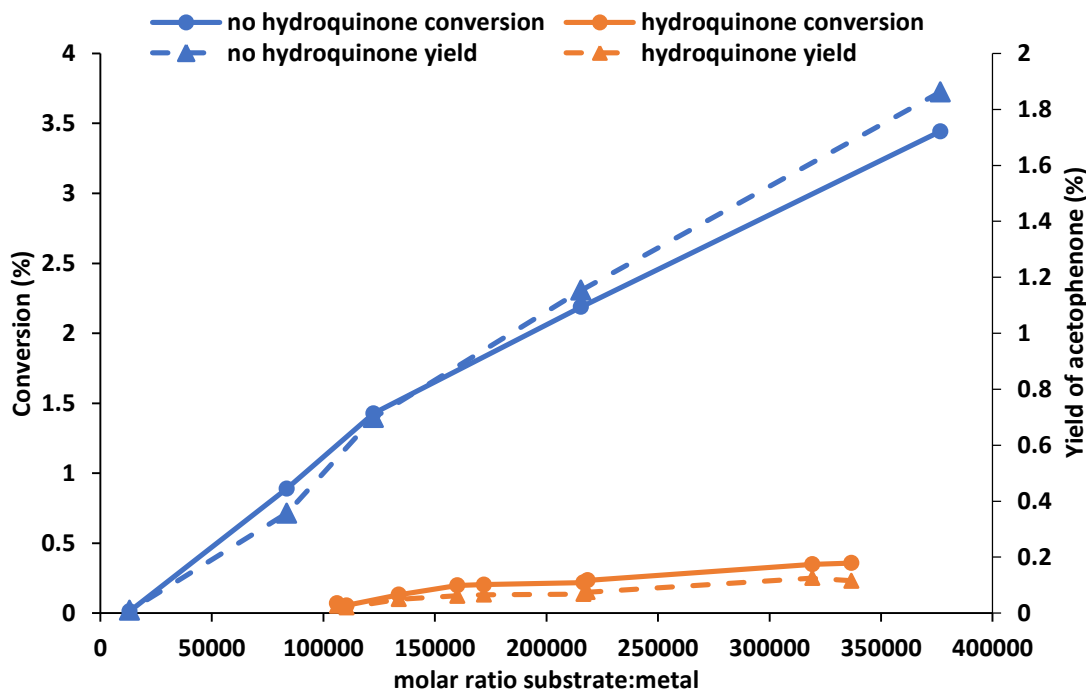


Figure 26a. Comparing conversion and yield with and without addition of hydroquinone scavenger as a liquid

Reaction conditions: 8.00 g ethylbenzene, 2 – 8 mg catalyst, 0.2 mL hydroquinone supplied as 3.5 M solution, 3 bar O₂, 140°C, 17 h, 1000 rpm stirring.

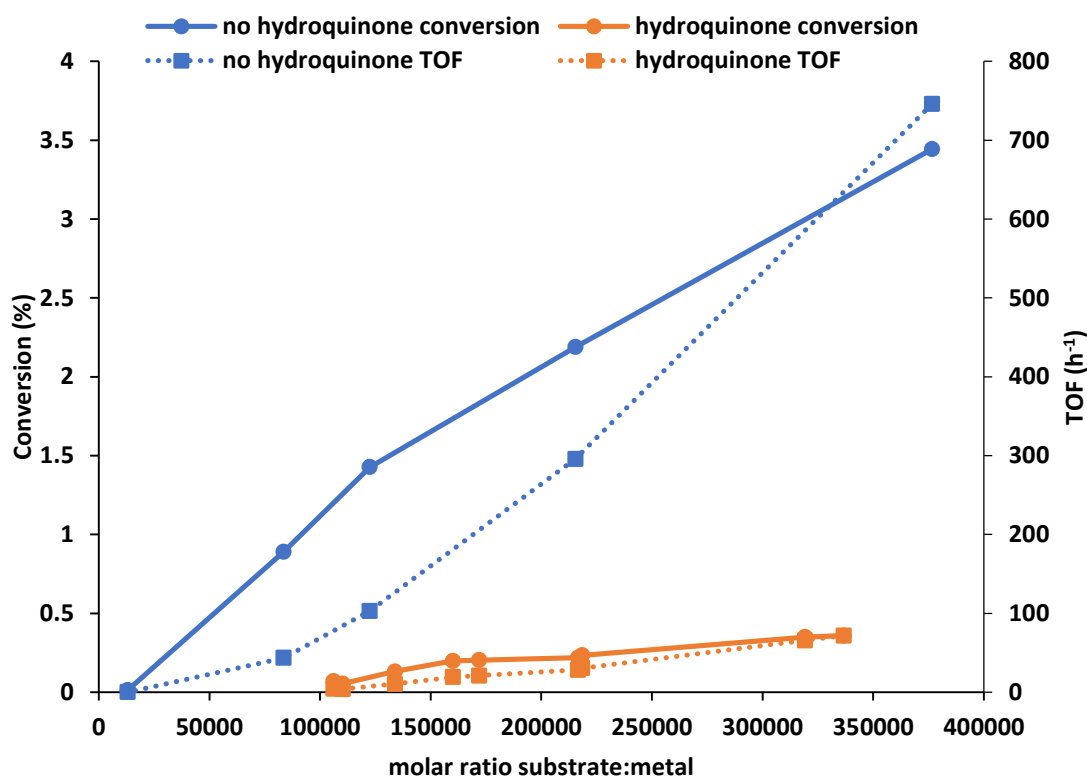


Figure 26b. Comparing conversion and TOF with and without addition of hydroquinone scavenger as a liquid

Reaction conditions: 8.00 g ethylbenzene, 2 – 8 mg catalyst, 0.2 mL hydroquinone supplied as 3.5 M solution, 3 bar O₂, 140°C, 17 h, 1000 rpm stirring.

The presence of hydroquinone significantly hinders the reaction. When supplied in solution, activity is restricted to levels comparable with the blank. This is likely due to better mixing of the hydroquinone when compared with the reactions where it was supplied as a solid.

The lack of activity in the presence of hydroquinone is strong evidence that the reaction mechanism proceeds *via* the action of oxygen-based radicals. To ensure this was indeed the case, and the observed activity not a unique effect when using hydroquinone, an alternate scavenger, diphenylamine, was studied. Diphenylamine also scavenges oxygen-based radicals, but unlike hydroquinone is miscible with ethylbenzene.

Figures 27a and 27b display results obtained when using the 1 wt.% Fe_{0.35}Pd_{0.65}/TiO₂ catalyst in the presence of diphenylamine.

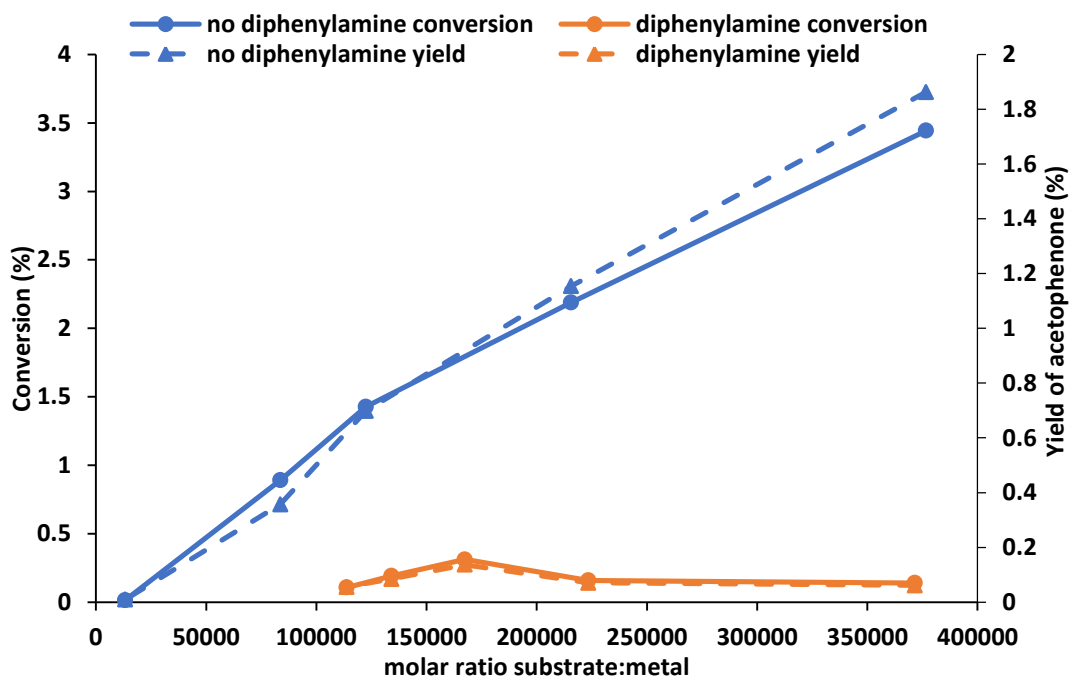


Figure 27a. Comparing conversion and yield with and without addition of diphenylamine scavenger

Reaction conditions: 8.00 g ethylbenzene, 2 – 8 mg catalyst, 5 mg diphenylamine, 3 bar O_2 , 140°C, 17 h, 1000 rpm stirring.

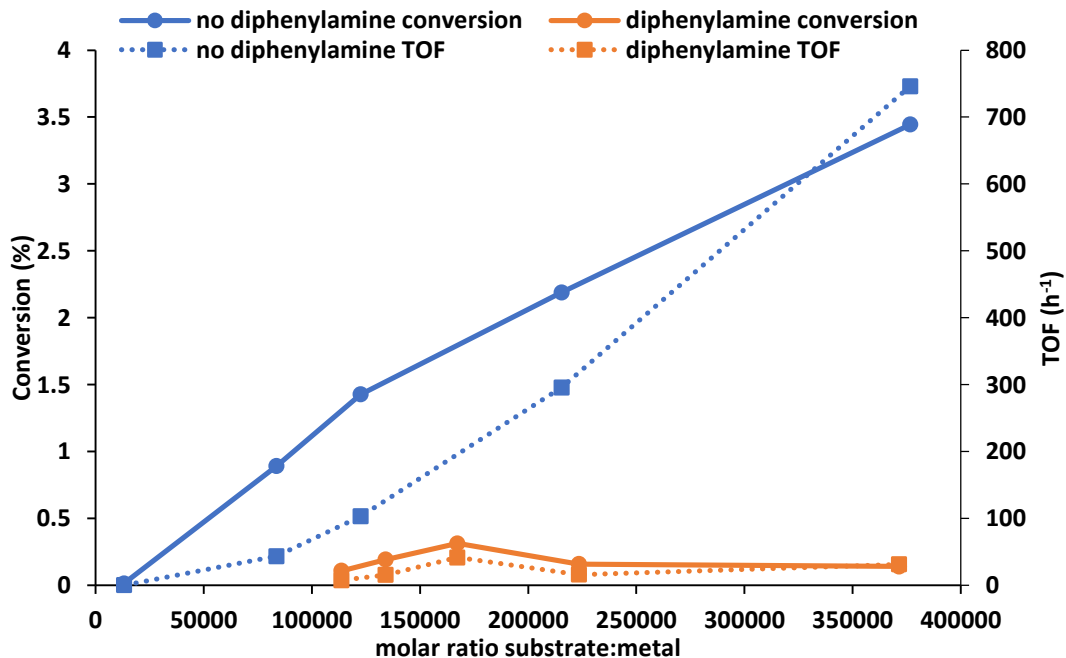


Figure 27b. Comparing conversion and TOF with and without addition of diphenylamine scavenger

Reaction conditions: 8.00 g ethylbenzene, 2 – 8 mg catalyst, 5 mg diphenylamine, 3 bar O_2 , 140°C, 17 h, 1000 rpm stirring.

As was the case when using hydroquinone, diphenylamine restricts conversion to levels obtained with the blank, further evidence that the reaction is reliant on oxygen radicals.

5.3. Conclusions

Chapters Three and Four focussed on a ruthenium-palladium catalyst for oxidation of toluene and 2-ethylnaphthalene. This chapter focussed instead on a similar but far cheaper iron palladium catalyst.

1 wt.% Fe_{0.50}Pd_{0.50}/TiO₂ was prepared by the modified impregnation and sol immobilisation methods. The modified impregnation catalyst was found to be superior, and achieved conversions comparable to that of an equivalent gold-palladium catalyst. This satisfies the project aim to find alternatives to gold in oxidation catalysts.

1 wt.% Fe_{0.50}Pd_{0.50}/TiO₂ was shown to be more active than 0.66 wt.% Pd/TiO₂ or 0.34 wt.% Fe/TiO₂. The molar ratio of metals in the bimetallic catalyst was explored, and 1 wt.% Fe_{0.35}Pd_{0.65}/TiO₂ found to be more active than the equimolar bimetallic prepared by the same means, suggesting that FePd₃ is more active for this reaction than FePd. The catalyst's activity exceeded that of 1 wt.% Au_{0.50}Pd_{0.50}/TiO₂ in the same conditions, and was therefore investigated further.

1 wt.% Fe_{0.35}Pd_{0.65}/TiO₂ was found to be most effective when reduced at 400 °C rather than 300 °C or 500 °C. This is potentially due to the smaller, more disperse nanoparticles detected on this catalyst. The catalyst was most active when prepared using chloride salts as precursors, rather than Fe(NO₃)₂ and PdCl₃. This is likely due to superior mixing, promoting alloying or the formation of mixed metal nanoparticles³³.

Throughout this investigation, catalysts were utilised in very small quantities: 2 – 8 mg in 8.00 g of substrate. In many cases, it was found that when using less catalyst, thus at increased molar ratios of substrate to metal, conversion actually improves. This is contrary to expectations, but consistent with results with ruthenium-palladium bimetallic catalysts in Chapters Three and Four. This behaviour was

particularly evident when testing $\text{Fe}_{0.35}\text{Pd}_{0.65}/\text{TiO}_2$ catalysts with different metal loadings: 1, 2.5 or 5 wt.%. At lower molar ratios of substrate to metal, when using 6 – 8 mg catalyst, increased weight loading corresponds to increased conversion. At molar ratios of substrate:metal of >165000 , the 1 wt.% catalyst achieved higher conversion than the 2.5 wt.% equivalent.

While this behaviour is interesting, it is difficult to study due to practical considerations. Further attempts to characterise the 1 wt.% $\text{Fe}_{0.35}\text{Pd}_{0.65}/\text{TiO}_2$ would be useful, as more information about the surface and the nanoparticles present may help to explain the catalysts behaviour.

5.4. References

1. S. K. Jana, P. Wu and T. Tatsumi, *Journal of Catalysis*, 2006.
2. B. Husson, M. Ferrari, O. Herbinet, S. S. Ahmed, P.-A. Glaude and F. Battin-Leclerc, *Proceedings of the Combustion Institute*, 2013, **34**, 325-333.
3. E. Carter, A. F. Carley and D. M. Murphy, *The Journal of Physical Chemistry C*, 2007, **111**, 10630-10638.
4. Y. Gao, G. Hu, J. Zhong, Z. Shi, Y. Zhu, D. S. Su, J. Wang, X. Bao and D. Ma, *Angewandte Chemie-International Edition*, 2013, **52**, 2109-2113.
5. J. A. Lopez-Sanchez, N. Dimitratos, P. Miedziak, E. Ntainjua, J. K. Edwards, D. Morgan, A. F. Carley, R. Tiruvalam, C. J. Kiely and G. J. Hutchings, *Physical Chemistry Chemical Physics*, 2008, **10**, 1921-1930.
6. N. Dimitratos, J. A. Lopez-Sanchez, D. Morgan, A. F. Carley, R. Tiruvalam, C. J. Kiely, D. Bethell and G. J. Hutchings, *Physical Chemistry Chemical Physics*, 2009, **11**, 5142-5153.
7. M. Sankar, E. Nowicka, R. Tiruvalam, Q. He, S. H. Taylor, C. J. Kiely, D. Bethell, D. W. Knight and G. J. Hutchings, *Chemistry-a European Journal*, 2011, **17**, 6524-6532.

8. M. Sankar, Q. He, M. Morad, J. Pritchard, S. J. Freakley, J. K. Edwards, S. H. Taylor, D. J. Morgan, A. F. Carley, D. W. Knight, C. J. Kiely and G. J. Hutchings, *Acs Nano*, 2012, **6**, 6600-6613.
9. L. Kesavan, R. Tiruvalam, M. H. Ab Rahim, M. I. bin Saiman, D. I. Enache, R. L. Jenkins, N. Dimitratos, J. A. Lopez-Sanchez, S. H. Taylor, D. W. Knight, C. J. Kiely and G. J. Hutchings, *Science*, 2011, **331**, 195-199.
10. M. I. bin Saiman, G. L. Brett, R. Tiruvalam, M. M. Forde, K. Sharples, A. Thetford, R. L. Jenkins, N. Dimitratos, J. A. Lopez-Sanchez, D. M. Murphy, D. Bethell, D. J. Willock, S. H. Taylor, D. W. Knight, C. J. Kiely and G. J. Hutchings, *Angewandte Chemie-International Edition*, 2012, **51**, 5981-5985.
11. V. Peneau, Q. He, G. Shaw, S. A. Kondrat, T. E. Davies, P. Miedziak, M. Forde, N. Dimitratos, C. J. Kiely and G. J. Hutchings, *Physical Chemistry Chemical Physics*, 2013, **15**, 10636-10644.
12. G. J. Hutchings, *Catalysis Today*, 2014, **238**, 69-73.
13. A. Corma and H. Garcia, *Chemical Society Reviews*, 2008, **37**, 2096-2126.
14. M.-C. Daniel and D. Astruc, *Chemical Reviews*, 2004, **104**, 293-346.
15. The Platinum Group Metal Database, www.pgmdatabase.com, accessed 12/08/16
16. B. Predel, Springer Berlin Heidelberg, Berlin, Heidelberg, 1995, pp. 1-7.

Chapter Six – Conclusions

6.1. Conclusions

The key objectives of this thesis, as outlined in Chapter One, section 1.6., were to develop stable and active gold-free catalysts for the oxidation of alkyl aromatics in mild conditions. These catalysts should achieve comparable or greater activity than benchmark gold catalysts, and elucidation of their mechanism help to inform future catalyst design.

Throughout this work, the commitment to mild or green conditions has been kept. All experiments were carried out at low temperatures and pressures in the absence of solvent. O₂ and tBHP were utilised as environmentally-friendly oxidants.

Two catalysts in particular achieved results exceeding those of gold-based catalysts in these conditions: 1 wt.% Ru_{0.50}Pd_{0.50}/TiO₂ for the oxidation of toluene and 2-ethylnaphthalene with tBHP, and 1 wt.% Fe_{0.35}Pd_{0.65}/TiO₂ for the oxidation of ethylbenzene with O₂. These are discussed in more detail in sections 6.1.1. and 6.1.2. respectively.

6.1.1. Ru_{0.50}Pd_{0.50}/TiO₂

Ruthenium-palladium bimetallic catalysts were applied to the oxidation of toluene and 2-ethylnaphthalene with great success. Ruthenium was found to be inherently active for these oxidations, even when present at only low metal loadings (Chapter Three, sections 3.3.5 and 3.3.8. and Chapter Four, sections 4.2.3. and 4.2.4.). Palladium achieved very poor results as a monometallic catalyst, but substantially enhanced the activity of bimetallic RuPd over that of monometallic ruthenium (Chapter Three, section 3.3.4. and Chapter Four section 4.2.3.). This indicates a synergistic effect, potentially linked to modulating the average nanoparticle size and dispersion on the bimetallic catalysts (Chapter Four, section 4.2.4.)

The ruthenium-palladium bimetallic catalyst was optimised in terms of molar ratio of Ru : Pd, wt.% metal loading, support material, preparation method and reducing

temperature (Chapter Three, sections 3.3.5., 3.3.8., 3.3.10. and 3.3.11. and Chapter Four, sections 4.2.2. and 4.2.4.).

The investigation into wt.% metal loading revealed particularly interesting data; conversion and yield do not decrease linearly with decreasing wt.% metal loading, as might be expected. This may be related to observed changes in average nanoparticle size and dispersion. For example, if only edge sites on the nanoparticle were active, a smaller average nanoparticle size and higher dispersion would correspond to a greater proportion of edge sites. This would enhance activity until the sites were saturated; site availability becoming rate limiting at very low loadings. This corroborates well with data obtained at different molar ratios of Ru : Pd. The most active catalyst, the equimolar bimetallic, possesses the smallest average nanoparticle size and highest dispersion (Chapter Four, section 4.2.4.).

To investigate this further, and examine the reaction mechanism as per the project aims, different molar ratios of substrate : metal were explored by varying the mass of catalyst applied to the reaction (Chapter Three, section 3.3.9 and Chapter Four, 4.2.5.). Ordinarily, conversion would be expected to increase with increasing mass of catalyst until mass transport limitations came into effect and conversion remained at a maximum. This was not the case. For both toluene and 2-ethylnaphthalene, increasing the total mass catalyst used in the reaction lead to a decrease in conversion. This was observed at molar ratios of substrate : metal of <14000, in the case of toluene, and <6500 for 2-ethylnaphthalene. However, for toluene, conversion also decreased when the mass of catalyst used corresponded to molar ratios of substrate : metal of >15000. For 2-ethylnaphthalene, conversion decreased in the substrate : metal range 6500>12000 as might be expected, but increased again in the >12000 region.

In short, the catalyst appears to exhibit a 'sweet spot' in conversion at a particular substrate : metal molar ratio. The exact reasons for this are not clear. At lower ratios, corresponding to a larger mass of catalyst, it is possible that the catalyst agglomerates, effectively reducing the surface area and therefore the availability of active sites. Alternatively, when increasing the amount of available catalyst, a

greater number of radicals may be generated from the oxidant tBHP, leading to increased termination.

It must also be considered that changing the ratio of substrate : metal also affects the tBHP : metal ratio. This was examined when varying mass catalyst applied for 2-ethylnaphthalene oxidation (Chapter Four, section 4.2.6.) but found to have little effect.

More insight into the reaction mechanism was obtained via time-on-line studies of toluene oxidation (Chapter Three, section 3.3.14.). These indicated an initial rapid rate of reaction that decreased steadily after the first hour. A more detailed study of the first hour of reaction indicated that this pattern was visible even in this time, with a decrease in rate of reaction after as little as ten minutes. Despite this, and despite substantial leaching of palladium metal established by MP-AES and ICP analysis (Chapter Three, section 3.3.6.) washed and dried catalyst was shown to be reusable with little change in conversion over four consecutive uses (Chapter Three, section 3.3.7.).

However, substantial differences in selectivity were observed over consecutive uses. This is of particular interest as throughout the rest of the work, and in much of the previously reported literature^{50, 51, 64}, selectivity was closely tied to conversion. Higher conversions of toluene encourage selectivity to benzoic acid as product. This is because benzoic acid is thought to form from the secondary oxidation of benzaldehyde. Over consecutive uses, the 1 wt.% Ru_{0.50}Pd_{0.50}/TiO₂ catalyst became increasingly less selective to benzoic acid and more so to a product tentatively identified as benzil. This presents an opportunity for developing active catalysts selective to products other than benzoic acid. This is discussed further in section 6.2.1.

In general, the development of the 1 wt.% Ru_{0.50}Pd_{0.50}/TiO₂ represents a significant success. This catalyst has been shown to achieve higher activity than gold-based equivalents in very mild, green conditions using tBHP as an eco-friendly oxidant. Furthermore, the high activity even at low metal loadings considerably mitigates the cost of the catalyst, one of the primary concerns when using gold or the

platinum group metals. A 0.10 wt.% Ru_{0.50}Pd_{0.50}/TiO₂ catalyst outperforms the most active gold-based catalyst tested (1 wt.% Au_{0.36}Pd_{0.64}/TiO₂ prepared by sol immobilisation) for toluene oxidation with a large improvement in turnover number: 480 h⁻¹ compared to 26 h⁻¹. This is also superior to several other reported catalysts^{58, 59, 98}.

6.1.2. Fe_{0.35}Pd_{0.65}/TiO₂

Iron-palladium bimetallic catalysts were investigated as an alternative to the more expensive ruthenium-palladium or gold-palladium for oxidation of ethylbenzene with O₂ as oxidant (Chapter Five). Prompted by literature reports¹¹⁶ and results obtained with ruthenium-palladium bimetallic catalysts, the mass of the iron-palladium catalyst applied to the reaction was varied throughout the investigation. At all times, the molar ratio of substrate:metal was relatively high.

Exploration of different masses of catalyst indicated unusual behaviour. When the molar ratio of substrate : metal was increased, corresponding to decreasing mass of catalyst applied, the conversion and TOF obtained increased. This is contrary to typical expectations, but consistent with similar findings with ruthenium-palladium (Chapter Three, section 3.3.9 and Chapter Four, 4.2.5.) and gold palladium (Chapter Five, section 5.2.2.) catalysts. This could potentially be explained by agglomeration of the catalyst, effectively decreasing surface area.

Alternatively, the explanation for this may relate to radical chemistry. In the absence of radical initiators, any radical generation must result from auto-oxidation or interaction with the catalyst. Auto-oxidation is unlikely, given that no conversion is observed under reaction conditions in the absence of catalyst (Chapter Five, section 5.2.1.). If radicals are generated by the catalyst, increasing the mass of catalyst applied to the reaction may lead to the formation of more radical species and increase the rate of termination and thus conversion.

If radical species are responsible for the activity observed with the iron-palladium catalyst, the presence of radical scavengers should hinder or prevent conversion. The presence of the scavengers hydroquinone and diphenylamine was shown to

reduce conversion significantly (Chapter Five, section 5.2.10.), strengthening this argument.

Conversely, if radicals are responsible for activity, the addition of radical initiators might be expected to increase conversion. However, addition of tBHP produced results similar and slightly inferior to the reaction without tBHP, and the addition of AIBN was shown to have a negative effect (Chapter 5.2.9.). This may be explicable if the presence of initiators accelerates the rate of termination, preventing further reaction, as proposed when the mass of catalyst used is increased.

This may also explain behaviour observed when investigating iron-palladium catalysts with different wt.% loadings of metal (Chapter Five, section 5.2.6.). Similarly to the gold-palladium and ruthenium-palladium catalysts, a 'sweet spot' was observed at particular molar ratios of substrate : metal, and increasing the mass of catalyst applied to decrease this ratio lead to decreased conversion.

In addition to wt.% metal loading, the catalyst was optimised in terms of molar ratio of Fe : Pd, reducing temperature, and preparation method and precursor choice (Chapter Five, sections 5.2.5., 5.2.7. and 5.2.8. respectively). 1 wt.% Fe_{0.35}Pd_{0.65}/TiO₂ was deemed the most effective catalyst. This is potentially due to the alloy expected to form at this ratio.

1 wt.% Fe_{0.35}Pd_{0.65}/TiO₂ prepared by modified impregnation successfully outperformed the most active gold-based catalyst tested, 1 wt.% Au_{0.50}Pd_{0.50}/TiO₂ prepared by the same method, under the same conditions. This represents a significant reduction in catalyst cost, and may be further exploited with future work (see section 6.2.2.).

6.2. Future work

6.2.1. Ru_{0.50}Pd_{0.50}/TiO₂

The high activity of 1 wt.% Ru_{0.50}Pd_{0.50}/TiO₂ prepared by modified impregnation makes it a good candidate for further investigation. In particular, the problem of metal leaching must be overcome. This may require screening of a larger range of preparation methods, support materials and treatment procedures.

Any future work undertaken with this catalyst would benefit greatly from further characterisation. An improved understanding of the nature and variety of nanoparticles present could significantly aid both optimisation and the understanding of the reaction mechanism. As such, TEM and SEM are of considerable interest.

6.2.2. $\text{Fe}_{0.35}\text{Pd}_{0.65}/\text{TiO}_2$

The iron-palladium bimetallic catalyst does not offer the substantial improvement over gold-based catalysts that the ruthenium-palladium catalysts explored represent. However, these catalysts do display unusual and complex radical chemistry that may be of considerable academic interest. This could potentially be elucidated by electron paramagnetic resonance spectroscopy.

As was the case for ruthenium-palladium, further characterisation of the catalyst would greatly enhance understanding of the reaction mechanism. TEM, SEM and temperature programmed reduction and desorption studies may prove useful. It is also necessary to establish the degree of metal leaching, if any, occurs during the reaction, as homogeneous metal will likely influence activity.

6.3. References

1. B. Lindstrom and L. J. Pettersson, *Cattech*, 2003, **7**, 130-138.
2. J. Wisniak, 2010, **21**, 60-69.
3. M. Boudart and T. Kwan, *Industrial and Engineering Chemistry*, 1956, **48**, 562-569.
4. P. B. Weisz, *Annual Review of Physical Chemistry*, 1970, **21**, 175-&.
5. R. L. Burwell, *Abstracts of Papers of the American Chemical Society*, 1982, **183**, 11-HIST.
6. R. Schlogl, *Angewandte Chemie-International Edition*, 2015, **54**, 3465-3520.
7. *Journal*.
8. S. Rebsdat and D. Mayer, in *Ullmann's Encyclopedia of Industrial Chemistry*, Wiley-VCH Verlag GmbH & Co. KGaA, 2000.
9. S. Rebsdat and D. Mayer, in *Ullmann's Encyclopedia of Industrial Chemistry*, Wiley-VCH Verlag GmbH & Co. KGaA, 2000.
10. M. A. Barakat, 2011, **4**, 361-377.
11. P. A. Kobielska, A. J. Howarth, O. K. Farha and S. Nayak, 2018, **358**, 92-107.
12. F. Haber and G. van Oordt, *Zeitschrift Fur Anorganische Chemie*, 1905, **44**, 341-378.
13. J. W. Erisman, M. A. Sutton, J. Galloway, Z. Klimont and W. Winiwarter, 2008, **1**, 636.
14. R. Schlögl, *Chemical Energy Storage*, 2012.
15. Z. Belohlav and P. Zamostny, 2000, **78**, 513-521.
16. W. H. Weinberg, *Accounts of Chemical Research*, 1996, **29**, 479-487.
17. *Chemical Engineering Science*, 1954, **3**, 41 - 59.
18. C. Doornkamp and V. Ponc, *Journal of Molecular Catalysis a-Chemical*, 2000, **162**, 19-32.
19. *Computational and Theoretical Chemistry*, 2017, **1100**, 28 - 33.
20. G. Bond, *Gold Bulletin*, 2008, **41**, 235-241.
21. H. Wu, L. Wang, J. Zhang, Z. Shen and J. Zhao, 2011, **12**, 859-865.
22. J. Kašpar, P. Fornasiero and N. Hickey, *Fundamentals of Catalysis and Applications to Environmental Problems*, 2003, **77**, 419-449.

23. J. A. Lupescu, J. W. Schwank, G. B. Fisher, J. Hangan, S. L. Peczonczyk and W. A. Paxton, *9th International Conference on Environmental Catalysis (ICEC2016), Newcastle, Australia, 2018*, **223**, 76-90.
24. G. J. Hutchings, *Catalysis Today*, 2014, **238**, 69-73.
25. R. Ferrando, J. Jellinek and R. L. Johnston, *Chemical Reviews*, 2008, **108**, 845-910.
26. B. Coq and F. Figueras, *Journal of Molecular Catalysis a-Chemical*, 2001, **173**, 117-134.
27. L. Ma, C. Y. Seo, X. Chen, K. Sun and J. W. Schwank, 2018, **222**, 44-58.
28. D. I. Enache, J. K. Edwards, P. Landon, B. Solsona-Espriu, A. F. Carley, A. A. Herzing, M. Watanabe, C. J. Kiely, D. W. Knight and G. J. Hutchings, *Science*, 2006, **311**, 362-365.
29. S. S. Li, D. D. Gong, H. G. Tang, Z. Ma, Z. T. Liu and Y. Liu, *Chemical Engineering Journal*, 2018, **334**, 2167-2178.
30. Z. Z. Yang, X. X. Lin, X. F. Zhang, A. J. Wang, X. Y. Zhu and J. J. Feng, *Journal of Alloys and Compounds*, 2018, **735**, 2123-2132.
31. F. Solymosi, *Catalysis Reviews*, 1968, **1**, 233-255.
32. G. Sastre, A. Chica and A. Corma, *Journal of Catalysis*, 2000, **195**, 227-236.
33. M. Sankar, Q. He, M. Morad, J. Pritchard, S. J. Freakley, J. K. Edwards, S. H. Taylor, D. J. Morgan, A. F. Carley, D. W. Knight, C. J. Kiely and G. J. Hutchings, *Acs Nano*, 2012, **6**, 6600-6613.
34. G. J. Hutchings and C. J. Kiely, *Accounts of Chemical Research*, 2013, **46**, 1759-1772.
35. C. He, X. Zhang, S. Gao, J. Chen and Z. Hao, *Journal of Industrial and Engineering Chemistry*, 2012, **18**, 1598-1605.
36. R. A. Sheldon, *Chemtech*, 1991, **21**, 566-576.
37. R. A. Sheldon, *HETEROGENEOUS CATALYTIC-OXIDATION AND FINE CHEMICALS*, 1991.
38. I. Arends and R. A. Sheldon, *Applied Catalysis a-General*, 2001, **212**, 175-187.
39. E. V. Gusevskaya, *Quimica Nova*, **26**, 242-248.
40. J. Xiao and X. Li, *Angewandte Chemie International Edition*, 2011, **50**, 7226-7236.

41. S. Perathoner and G. Centi, *Topics in Catalysis*, 2005, **33**, 207-224.
42. 1976.
43. C. Barckholtz, T. A. Barckholtz and C. M. Hadad, *Journal of the American Chemical Society*, 1999, **121**, 491-500.
44. X. Li, J. Xu, L. Zhou, F. Wang, J. Gao, C. Chen, J. Ning and H. Ma, *Catalysis Letters*, 2006, **110**, 255-260.
45. F. Wang, J. Xu, X. Q. Li, J. Gao, L. P. Zhou and R. Ohnishi, *Advanced Synthesis & Catalysis*, 2005, **347**, 1987-1992.
46. **1975**.
47. T. G. Carrell, S. Cohen and G. C. Dismukes, *Journal of Molecular Catalysis A: Chemical*, 2002, **187**, 3-15.
48. A. Aguadero, H. Falcon, J. M. Campos-Martin, S. M. Al-Zahrani, J. L. G. Fierro and J. A. Alonso, *Angewandte Chemie-International Edition*, 2011, **50**, 6557-6561.
49. Y. Ishii, S. Sakaguchi and T. Iwahama, *Advanced Synthesis & Catalysis*, 2001, **343**, 393-427.
50. T. W. Bastock, J. H. Clark, K. Martin and B. W. Trenbith, *Green Chemistry*, 2002, **4**, 615-617.
51. M. Ilyas and M. Sadiq, *Catalysis Letters*, 2009, **128**, 337-342.
52. K. R. Seddon and A. Stark, *Green Chemistry*, 2002, **4**, 119-123.
53. R. L. Brutchey, I. J. Drake, A. T. Bell and T. D. Tilley, *Chemical Communications*, 2005, 3736-3738.
54. A. Corma and H. Garcia, *Chemical Society Reviews*, 2008, **37**, 2096-2126.
55. N. Lopez and J. K. Nørskov, *Journal of the American Chemical Society*, 2002, **124**, 11262-11263.
56. M.-C. Daniel and D. Astruc, *Chemical Reviews*, 2004, **104**, 293-346.
57. N. Dimitratos, J. A. Lopez-Sanchez, D. Morgan, A. F. Carley, R. Tiruvalam, C. J. Kiely, D. Bethell and G. J. Hutchings, *Physical Chemistry Chemical Physics*, 2009, **11**, 5142-5153.
58. F. Jiang, X. Zhu, B. Fu, J. Huang and G. Xiao, *Chinese Journal of Catalysis*, 2013, **34**, 1683-1689.
59. J. Long, H. Liu, S. Wu, S. Liao and Y. Li, *Acs Catalysis*, 2013, **3**, 647-654.

60. L. Kesavan, R. Tiruvalam, M. H. Ab Rahim, M. I. bin Saiman, D. I. Enache, R. L. Jenkins, N. Dimitratos, J. A. Lopez-Sanchez, S. H. Taylor, D. W. Knight, C. J. Kiely and G. J. Hutchings, *Science*, 2011, **331**, 195-199.
61. X. Liu and L. Dai, 2016, **1**, 16064.
62. J. Luo, H. Yu, H. Wang and F. Peng, *Catalysis Communications*, 2014, **51**, 77-81.
63. K.-P. Lee, S.-H. Lee, K. S. Sundaram and G. A. Iyengar, *Radiation Physics and Chemistry*, 2012, **81**, 1422-1425.
64. Y. Gao, G. Hu, J. Zhong, Z. Shi, Y. Zhu, D. S. Su, J. Wang, X. Bao and D. Ma, *Angewandte Chemie-International Edition*, 2013, **52**, 2109-2113.
65. L. Červený, K. Mikulcová and J. Čejka, 2002, **223**, 65-72.
66. S. Kato, K. Nakagawa, N.-o. Ikenaga and T. Suzuki, 2001, **73**, 175-180.
67. B. Gutmann, P. Elsner, D. Roberge and C. O. K. Kappe, *Journal*, 2013, 2669-2676.
68. T. Liu, H. Cheng, L. Sun, F. Liang, C. Zhang, Z. Ying, W. Lin and F. Zhao, 2016, **512**, 9-14.
69. T. Mallat and A. Baiker, *Chemical Reviews*, 2004, **104**, 3037-3058.
70. A. Dhakshinamoorthy, M. Alvaro and H. Garcia, *Chemistry-a European Journal*, 2011, **17**, 6256-6262.
71. J. Gao, X. Tong, X. Li, H. Miao and J. Xu, *Journal of Chemical Technology and Biotechnology*, 2007, **82**, 620-625.
72. V. R. Choudhary, J. R. Indurkar, V. S. Narkhede and R. Jha, *Journal of Catalysis*, 2004, **227**, 257-261.
73. S. K. Jana, P. Wu and T. Tatsumi, *Journal of Catalysis*, 2006.
74. K. O. Xavier, J. Chacko and K. K. M. Yusuff, *Applied Catalysis a-General*, 2004, **258**, 251-259.
75. M. J. Beier, B. Schimmoeller, T. W. Hansen, J. E. T. Andersen, S. E. Pratsinis and J.-D. Grunwaldt, *Journal of Molecular Catalysis a-Chemical*, 2010, **331**, 40-49.
76. G. Raju, P. S. Reddy, J. Ashok, B. M. Reddy and A. Venugopal, *Journal of Natural Gas Chemistry*, 2008, **17**, 293-297.
77. Manufacturer's information, Alfa Aesar, <https://www.alfa.com/en/>.

78. Manufacturer's information, Sigma-Aldrich, <https://www.sigmaaldrich.com/united-kingdom.html>.
79. Gas Chromatography, <http://www.gas-chromatography.net/gas-chromatography.php>, (accessed 25/03/18).
80. Gas Chromatography, https://chem.libretexts.org/Core/Analytical_Chemistry/Instrumental_Analysis/Chromatography/Gas_Chromatography, 25/03/18).
81. Gas chromatography, <https://www.agilent.com/en-us/products/gas-chromatography>, (accessed 25/03/18).
82. Gas Chromatography Mass Spectrometry (GC/MS), <http://www.bris.ac.uk/nerclsmf/techniques/gcms.html>, (accessed 25/03/18).
83. Gas Chromatography Mass Spectrometry (GC/MS) Information, <https://www.thermofisher.com/uk/en/home/industrial/mass-spectrometry/mass-spectrometry-learning-center/gas-chromatography-mass-spectrometry-gc-ms-information.html>, (accessed 25/03/18).
84. Nuclear magnetic resonance, <https://www.cardiff.ac.uk/chemistry/research/facilities/nuclear-magnetic-resonance>.
85. Nuclear Magnetic Resonance, <https://www.bruker.com/products/mr/nmr.html>, (accessed 25/03/18).
86. J. D. Roberts, *Journal of Chemical Education*, 1961, **38**, 581.
87. *Journal*.
88. 4100 MP-AES, <https://www.agilent.com/en/products/mp-aes/mp-aes-systems/4100-mp-aes>, 25/03/18).
89. 7900 ICP-MS, <https://www.agilent.com/en/products/icp-ms/icp-ms-systems/7900-icp-ms>, (accessed 25/03/18).
90. N. W. Hurst, S. J. Gentry, A. Jones and B. D. McNicol, *Catalysis Reviews*, 1982, **24**, 233-309.
91. S. Subramanian, *Platinum Metals Review*, 1992.
92. Carrying Out Dispersion Measurements by CO Pulse Chemisorption, <https://www.azom.com/article.aspx?ArticleID=12246>, (accessed 25/03/18).

93. C.-H. Yang and J. G. Goodwin, 1982, **20**, 13-18.
94. Powder X-ray Diffraction,
https://chem.libretexts.org/Core/Analytical_Chemistry/Instrumental_Analysis/Diffraction_Scattering_Techniques/Powder_X-ray_Diffraction, (accessed 25/03/18).
95. What is X-ray Photoelectron Spectroscopy (XPS)?,
<https://xpssimplified.com/whatisxps.php>, (accessed 20/03/18).
96. V. R. Choudhary, D. K. Dumbre and S. K. Bhargava, *Industrial & Engineering Chemistry Research*, 2009, **48**, 9471-9478.
97. I. Hermans, E. S. Spier, U. Neuenschwander, N. Turra and A. Baiker, *Topics in Catalysis*, 2009, **52**, 1162-1174.
98. M. I. bin Saiman, G. L. Brett, R. Tiruvalam, M. M. Forde, K. Sharples, A. Thetford, R. L. Jenkins, N. Dimitratos, J. A. Lopez-Sanchez, D. M. Murphy, D. Bethell, D. J. Willock, S. H. Taylor, D. W. Knight, C. J. Kiely and G. J. Hutchings, *Angewandte Chemie-International Edition*, 2012, **51**, 5981-5985.
99. V. Peneau, Q. He, G. Shaw, S. A. Kondrat, T. E. Davies, P. Miedziak, M. Forde, N. Dimitratos, C. J. Kiely and G. J. Hutchings, *Physical Chemistry Chemical Physics*, 2013, **15**, 10636-10644.
100. V. Peneau, Doctor of Philosophy, Cardiff University, 2014.
101. W. Luo, M. Sankar, A. M. Beale, Q. He, C. J. Kiely, P. C. A. Bruijninx and B. M. Weckhuysen, *Nature communications*, 2015, **6**, 6540-6540.
102. A. n. Martínez, C. López, F. Márquez and I. Díaz, 2003, **220**, 486-499.
103. G. Jacobs, T. K. Das, Y. Zhang, J. Li, G. Racoillet and B. H. Davis, 2002, **233**, 263-281.
104. M. D. Argyle and C. H. Bartholomew, *Catalysts*, 2015, **5**, 145-269.
105. E. Carter, A. F. Carley and D. M. Murphy, *The Journal of Physical Chemistry C*, 2007, **111**, 10630-10638.
106. J. A. Lopez-Sanchez, N. Dimitratos, P. Miedziak, E. Ntainjua, J. K. Edwards, D. Morgan, A. F. Carley, R. Tiruvalam, C. J. Kiely and G. J. Hutchings, *Physical Chemistry Chemical Physics*, 2008, **10**, 1921-1930.
107. S. N. Tripathi, S. R. Bharadwaj and S. R. Dharwadkar, *Journal of Phase Equilibria*, 1993, **14**, 638-642.

108. D. Wu, K. Kusada and H. Kitagawa, *Science and Technology of Advanced Materials*, 2016, **17**, 583-596.
109. S. Chen, Z. Liu, E. Shi, L. Chen, W. Wei, H. Li, Y. Cheng and X. Wan, *Organic Letters*, 2011, **13**, 2274-2277.
110. *Luperox TBH70X, tert-Butyl hydroperoxide solution Safety Data Sheet*, Sigma Aldrich, 2018.
111. *2-Ethyl-naphthalene Safety Data Sheet*, Sigma Aldrich, 2018.
112. B. Husson, M. Ferrari, O. Herbinet, S. S. Ahmed, P.-A. Glaude and F. Battin-Leclerc, *Proceedings of the Combustion Institute*, 2013, **34**, 325-333.
113. M. Sankar, E. Nowicka, R. Tiruvalam, Q. He, S. H. Taylor, C. J. Kiely, D. Bethell, D. W. Knight and G. J. Hutchings, *Chemistry-a European Journal*, 2011, **17**, 6524-6532.
114. *Journal*.
115. B. Predel, Springer Berlin Heidelberg, Berlin, Heidelberg, 1995, pp. 1-7.
116. M. Conte, X. Liu, D. M. Murphy, K. Whiston and G. J. Hutchings, *Physical Chemistry Chemical Physics*, 2012, **14**, 16279-16285.